CHARACTERISATION OF NOVEL INSECTICIDAL ION CHANNEL TOXINS FROM ARANEOMORPH AND MYGALOMORPH SPIDER VENOMS

Youmie Chong
BMedSc (Honours)

Submitted in fulfilment of the requirements for the Degree of Doctor Philosophy (Science)

School of Medical and Molecular Biosciences, University of Technology, Sydney

ABSTRACT

The high potency and selectivity of various peptide neurotoxins within spider venoms means these toxins are being considered as leads for the development of new environmentally-benign biopesticides that target pest insects. Currently, the ω-HXTX family of 37-residue arthropod-selective peptide neurotoxins from Australian hexathelid spider venoms are considered a prime candidate for biopesticide development. ω-HXTX-Hv1a, a prototypic member of the ω-HXTX-1 family, was electrophysiologically characterised by voltage-clamp analysis using the whole-cell patch-clamp technique on cockroach dorsal unpaired median (DUM) neurons. ω-HXTX-Hv1a exerted a reversible, concentration-dependent, voltage-independent block of barium currents (I_{Ba}) through mid-low voltage-activated (M-LVA) and high voltage-activated (HVA) voltage-activated calcium (Ca_v) channels without alteration in the activation or inactivation kinetics of the Ca_v channel. To improve the structural stability of this disulfide-rich peptide under biologically reducing conditions, and thereby increase its commercial viability, a synthetic ω-HXTX-Hv1a mutant was produced with the replacement of one disulfide bond with a Sec[1,4] diselenide bridge. The selenocysteine mutant had comparable oral activity to the native toxin in blowflies and there was no significant difference between the native and diselenide toxin in terms of block of M-LVA and HVA Ca_V channels. This demonstrated that selenocysteine substitution had the potential to improve peptide stability without altering the biological activity of the toxin.

There is a continuous need to identify novel insecticidal peptide toxins for biopesticide development. By screening the venom of mygalomorph Sydney funnel-web (*Atrax robustus*) and Eastern mouse (*Missulena bradleyi*) spiders; two novel insect-selective peptide neurotoxins were isolated: ω-HXTX-Ar1a from *A. robustus* is a homolog of ω-HXTX-Hv1a, and ω-AOTX-Mb1a from *M. bradleyi* has up to 59% homology with the ω-HXTX family. In acute toxicity tests in house crickets, these neurotoxins induced potent neuroexcitatory symptoms followed by paralysis and death. Vertebrate nerve-muscle preparations showed that the toxins lacked overt vertebrate toxicity at

concentrations up to 1 μM. To further characterise the molecular target of ω-HXTX-Ar1a and ω-AOTX-Mb1a on insects, whole-cell patch-clamp experiments were undertaken on cockroach DUM neurons. ω-HXTX-Ar1a induced a reversible, and the ω-AOTX-Mb1a an irreversible, block of both M-LVA and HVA Ca_v channels. The level of block was concentration-dependent and occurred in the absence of alterations in the voltage-dependence of Ca_v channel activation. The block was voltage-independent, suggesting that these toxins are Ca_v channel pore blockers rather than channel gating modifiers. Both ω-HXTX-Ar1a and ω-AOTX-Mb1a are promising biopesticide candidates and their activity on M-LVA and HVA Ca_v channels validates insect Ca_v channels as a novel molecular target for insecticides.

Apart from their insecticidal properties, spider venom can cause serious envenomation and death in vertebrates and invertebrates. Male *M. bradleyi* spiders are clinically important, but the toxin primarily responsible for the envenomation syndrome in humans has not previously been identified. By separating whole male *M. bradleyi* venom and testing for activity, a 42-residue peptide (δ-AOTX-Mb1a) was isolated. In a chick biventer cervicis nerve-muscle preparation, 85 nM concentration of δ-AOTX-Mb1a caused an increase in resting tension, muscle fasciculation and a decrease in indirect twitch tension. These effects were neutralised by *A. robustus* antivenom. The toxic effects were attributed to inhibition of peak tetrodotoxin-sensitive sodium current, a slowing of sodium current inactivation and a hyperpolarising shift in the voltage at half-maximal activation as determined by whole-cell patch-clamp analysis on rat dorsal root ganglion neurons. In acute insect toxicity bioassays, δ-AOTX-Mb1a displayed only moderate insecticidal activity in house crickets (*Acheta domesticus*), with doses up to 2 nmol/g causing reversible neurotoxic symptoms including involuntary spasms and slight loss of coordination within 24 hours. At this dose, lethality was only observed in 60% of crickets after 48 hours. δ-AOTX-Mb1a is highly toxic to vertebrates through its action on sodium channels, but has relatively low biological activity against invertebrates.

Spider peptide toxins that display non-selective toxicity toward both vertebrates and invertebrates can be used as molecular tools to probe the function of, and phylogenetic differences in, receptors and ion channels. Accordingly, ω-CNTX-Cs1a, a 74-residue peptide toxin from the venom of the Central American hunting spider (*Cupiennius salei*) that displays high toxicity in mammalian and insect bioassays, was investigated. Whole-cell patch-clamp experiments showed that ω-CNTX-Cs1a caused a voltage-independent block of mammalian L-type HVA Ca_v channels in rat neurons and neuroendocrine GH3 and GH4 cells, but had no significant effect on other types of HVA, or LVA Ca_v channels. In contrast, ω-CNTX-Cs1a induced a slow voltage-independent, concentration-dependent block of both M-LVA and HVA Ca_v channels in whole-cell patch-clamp experiments performed on cockroach DUM neurons. ω-CNTX-Cs1a shows high selectivity for a subset of mammalian Ca_v channels, but indiscriminate activity on invertebrate Ca_v channels, which makes this toxin useful as a molecular tool for further investigation of mammalian and insect Ca_v channels.

The incredible diversity in the phylogenetic selectivity and ion channel specificity of spider neurotoxins means there is great potential for these toxins as molecular tools, and many may become the defining pharmacology for receptor or ion channel subtypes. As a result of such investigations we now also understand the underlying basis for clinical envenomation syndromes that develop following envenoming, and many are being investigated as environmentally-friendly biopesticides and therapeutic drugs.

ACKNOWLEDGEMENTS

PUBLICATIONS ARISING FROM THIS THESIS

1) Herzig, V., Khalife, A.A., Chong, Y., Isbister, G. K., Currie, B.J., Churchill, T.B., Horner, S., Escoubas, P., Nicholson, G.M. and Hodgson, W.C. 2008. Intersexual variations in Northern (*Missulena pruinosa*) and Eastern (*M. bradleyi*) mouse spider venom. *Toxicon*, 517, 1167-77.

2) Chong, Y., Hayes, J.L., Sollod, B., Wen, S., Wilson, D.T., Hains, P.G., Hodgson, W.C., Broady, K.W., King, G.F., Nicholson, G.M. 2007. The ω-atracotoxins: selective blockers of insect M-LVA and HVA calcium channels. *Biochemical Pharmacology*, 74, 623-38.

3) Kubista, H., Mafra, R.A., Chong, Y., Nicholson, G.M., Beirão, P.S., Cruz, J.S., Boehm, S., Nentwig, W., & Kuhn-Nentwig, L. 2007. CSTX-1, a toxin from the venom of the hunting spider *Cupiennius salei*, is a selective blocker of L-type calcium channels in mammalian neurons. *Neuropharmacology*, 52, 1650–62.

4) Gunning, S.J., Chong, Y., Khalife, A.A., Hains, P.G., Broady, K.W., Nicholson, G.M. 2003. Isolation of δ-missulenatoxin-Mb1a, the major vertebrate-active spider δ-toxin from the venom of *Missulena bradleyi* (Actinopodidae). *FEBS Letters*, 554, 211-18.

TABLE OF CONTENTS

LIST OF TABLES

LIST OF FIGURES

LIST OF ABBREVIATIONS AND ACRONYMS

$\tau_{on/off}$: time constants for onset of (on) and recovery from (off) current block

3D: three-dimensional

4-AP: 4-aminopyridine

4VP: 4-vinylpyridine

ACh: acetylcholine

AChE: acetylcholinesterase

ACN: acetonitrile

AOTX: actinopoditoxin

APAF: Australian Proteome Analysis Facility

Arg: arginine

Asn: asparagine

Asp: aspartic acid

ATP: adenosine triphosphate

BCA: bicinchoninic acid

BSA: bovine serum albumin

Bt: *Bacillus thuringiensis*

Ca_v: voltage-activated calcium

cDNA: complementary deoxyribonucleic acid

CMF-PBS: Calcium- and Magnesium-Free Phosphate-Buffered Saline

CNTX: ctenitoxin

Cys: cysteine

DDT: dichlorodiphenyltrichloroethane

DMEM: Dulbecco"s Modified Eagle Medium

DNA: deoxyribonucleic acid

DRG: dorsal root ganglion

DTT: dithiothreitol

DUM: dorsal unpaired median

E. coli: *Escherichia coli*

EDTA: ethylenediaminetetraacetic acid

EGTA: ethylene glycol tetraacetic acid

ESI-MS: electrospray ionisation mass spectrometry

FPLC: fast-perfusion liquid chromatography

GABA: gamma-amino butyric acid

Gln: glutamine

Glu: glutamic acid

G_{max}: maximum conductance

GNA: *Galanthus nivalis* agglutinin

GSSG: glutathione disulfide

GST: glutathione S-transferase

HEK: human embryonic kidney

HEPES: 4-(2-hydroxyethyl)piperazine-1-ethanesulfonic acid sodium salt

HF: hydrogen fluoride

HVA: high voltage-activated

HXTX : hexatoxin

I: current

I_{Ba}: barium currents

IC_{50}: half maximal inhibitory concentration

ICK: inhibitory cystine knot

KD_{50}: median knockdown dose

K_v: voltage-activated potassium

LD_{50}: median lethal dose

LJP: liquid junction potential

Lys: lysine

m/z: mass/charge

MALDI-TOF MS: matrix-assisted laser desorption/ionisation-time of flight mass spectrometry

MeOH: methanol

mLVA: maintained low voltage-activated

M-LVA: mid-low voltage-activated

Na_v: voltage-activated sodium

NIS: normal insect saline

POPs: persistent organic pollutants

Pro: proline

RNSH: Royal North Shore Hospital

Rp-HPLC: reverse phase high pressure liquid chromatography

S: slope factor

SAR: structure-activity relationship

Sec: selenocysteine

Ser: serine

TAG: terminal abdominal ganglion/ganglia

TEA-Br: tetraethylammonium bromide

TEA-Cl: tetraethylammonium chloride

TEA-OH: tetraethylammonium hydroxide

TFA: trifluoroacetic acid

Thr: threonine

tLVA: transient low voltage-activated

Tris: tris(hydroxymethyl)aminomethane

TTX: tetrodotoxin

Tyr: tyrosine

UNSW: University of New South Wales

USEPA: United States Environmental Protection Agency

UTS: University of Technology, Sydney

UV: ultraviolet

UV-VIS: ultraviolet-visible

V: voltage

$V_{1/2}$: voltage of half-maximal activation

V_h: membrane holding potential

V_{rev}: reversal voltage

WHO: World Health Organisation

1   Introduction

1.1 The Global Need for Insecticides

Around the world, more than 10,000 arthropod species are considered as pests that cause negative impacts on the economy, health and welfare of humans as well as domestic and farm animals (Whalon et al., 2008). The majority of pest arthropods are insects of agricultural and medical importance, which need to be controlled through the use of pesticides.

1.1.1 Insects and Food Security

Insects and their larvae consume fresh and stored foodgrains, legumes, fruits and vegetables, leading to reductions in agricultural yield, and they also damage and contaminate food with frass (insect excrement or castings), which render the food unsellable for farmers (Dent, 2000). The use of intensive mono-agricultural methods in the past few decades has allowed crops to be produced on a massive scale, but has also meant they are also highly vulnerable to attack by pests (Yudelman et al., 1998).

The use of insecticides is vital because pest insects such as the larvae of butterlies and moths (Order: Lepidoptera), beetles and weevils (Order: Coleoptera), grasshoppers and locusts (Order Orthoptera) and aphid species (Order Hemiptera; Superfamily Aphidoidea), together with pathogens and weeds, cause the destruction of approximately 20% of global annual crop production, and up to 40% in developing economies such as Latin America (Oerke and Dehne, 2004). Around 20% of stored foodgrains is lost to pests (Bergvinson and Garcia-Lara, 2004), which is significant given that three cereal crops (wheat, rice and corn) provide 60% of food for humans (Tilman et al., 2002). Understandably, the pesticide industry is big business; an estimated $US 1 billion is spent per annum just to control a single species of diamondback moth (*Plutella xylostella*) larvae, the world"s most destructive

pest of cruciferous plants such as cabbage, broccoli, and cauliflower (Talekar and Shelton, 1993). According to the United States National Research Council, removal of pesticides from the US agricultural sector would lead to a 50% decline in the production of certain crop species, resulting in a significant rise in food prices (NRC, 2000).

Pesticide use has genuine benefits for farmers, for example, the application of insecticides tripled cocoa production in Ghana and increased sugar production in Pakistan by one-third (Ware and Whitacre, 2004). It has been estimated that the farmer receives $3.00 - $6.50 in return for every dollar spent on pesticides (Zilberman et al., 1991).

Around one billion people are currently undernourished (Barrett, 2010), and this number is likely to increase with a projected world population of 9.1 billion by 2050 (UN, 2009). It has been speculated that there will be a three-fold increase in the demand for food over the next 50 years (McMichael, 2001, Godfray et al., 2010), which will outstrip the yield potential of farmland (Cassman, 1999). Effective management of arable land and pest insect will play an important role in safeguarding future food supplies.

1.1.2 Insects and Health

Insects are capable of transmitting pathogens that cause pernicious diseases to humans and animals (see Table 1.1) in developing and first-world countries, including Australia (Petersen and Roehrig, 2001). The classic example is malaria, which is currently endemic in over 100 countries and accounts for over a million deaths each year (WHO, 2007). Mosquitoes are vectors of many other emerging and resurging human diseases including Japanese encephalitis, West Nile virus (Solomon and Mallewa, 2001, Mackenzie et al., 2004) and dengue fever, which is spread by *Aedes* species mosquitoes (Gubler, 2002).

To prevent the spread of these diseases, synthetic insecticides are used to control and reduce the longevity of the mosquito vector (Nauen, 2007). This approach is effective because infective parasites usually develop near the end of a mosquito"s life span (Vernick and Waters, 2004). The annual death rate from malaria has progressively reduced since the introduction of insecticides, from 6 million in 1939, to 2.5 million in 1965, and around 1 million in 1991 (Ware and Whitacre, 2004). The use of insecticides has led to similar a reduction in the death rate for other vector-borne diseases such as yellow fever and sleeping sickness.

Table 1.1: Examples of vector-borne diseases in humans and/or animals.

Vector	Diseases
Mosquitoes	Malaria, Ross River virus, lymphatic filariasis, yellow fever, Dengue-dengue haemorrhagic fever, Japanese encephalitis, West Nile virus, Rift Valley fever, leishmaniasis, trypanosomiasis, Eastern and Western equine encephalitis, Murray Valley encephalitis, Barmah Forest virus, O"nyong-nyong fever, potasi virus, rocio virus
Ticks	Lyme disease, Rocky Mountain spotted fever, anaplasmosis, Kyasanar Forest disease, tick-borne encephalitis, Congo-Crimean haemorrhagic fever, human ehrlichiosis (monocytic and granulocytic), kyasanur forest disease, tularemia
Sandflies	Leishmaniasis, Sandfly fever
Biting Midges	Bluetongue virus, oropouche fever, african horse sickness
Fleas	Bubonic plague, murine typhus fever, tungiasis, cat flea typhus, cat-scratch disease
Black flies	Onchocerciasis

References: (Nicholson, 2007a, Sattenspiel, 2000, Gubler, 2002, Kedzierski et al., 2006, Lounibos, 2002, Wittmann and Baylis, 2000, Prentice and Rahalison, 2007, Gratz, 1999, Parola and Raoult, 2001, Zaim and Guillet, 2002, Gatton et al., 2005).

In the urban environment, nuisance pest insects include ants, flies, fleas, silverfish and cockroaches, which can cause health problems, especially for those with respiratory conditions. For example, cockroaches are associated

with increased incidences of bronchial asthma (particularly in children) and cockroach casts, egg shells and faecal matter are known to contain several major and minor allergens that can trigger asthma attack (Helm et al., 1996, Wu et al., 1996). In the case of tick bites, certain ticks (e.g. genus *Ixodes*) are known to secrete paralytic neurotoxins that can be debilitating and sometimes fatal to humans and animals (Nicholson et al., 2006, Jongejan and Uilenberg, 2004, Vedanarayanan et al., 2004).

Effective management of insect vectors will become increasingly important in the future if global temperatures continue to rise, because vector-borne pathogens spend the majority of its life inside an invertebrate host that is thermo-sensitive to ambient weather (Patz and Reisen, 2001, Patz et al., 2005). One potential effect is an increase in the rate of insect reproduction (Epstein, 2005) and a shift in the geographic distribution of vectors so that naïve populations become exposed to vector-borne diseases (Haines et al., 2006, Sutherst, 2004). Indeed there have already been documented cases of such events occurring, including the ferocious outbreak of bluetongue disease during the summer of 2006 in northern Europe that devastated wool, mutton and goat industries in at least five countries (Enserink, 2006, Carpenter et al., 2009). This haemorrhagic disease is caused by a viral serotype carried by *Culicoides* biting midges and outbreaks had previously only been seen in warmer countries of North Africa.

Billions of dollars are spent globally to control pests and mitigate the harm they cause, but modern day practices such as intensive farming and densely populated urban living can promote the lifecycle of nuisance insects. Pesticides have a proven track record; however growing scientific evidence about its toxicity, persistence in the environment and insect resistance has resulted in a paradigm shift in the attitude toward chemical insecticides.

The following section looks at the history of insecticide use, modern chemical insecticides and biological pesticides.

1.2 A Brief History of Insecticides

The use of chemicals to control pests dates back to when the Sumerians used sulfur to kill insects more than 4500 years ago (McKinney et al., 2007). Inorganic chemicals such as copper, arsenic and lead were also used extensively until the early twentieth century and worked by abrading or removing cuticle waxes, leading to desiccation and death of insects. Other chemicals used to kill common pests such as cockroaches and fleas included soap, kerosene, silica gels, turpentine, camphor and pepper (Hodgson and Kuhr, 1990). Natural plant extracts were also explored for their insecticidal properties, for example nicotine from crushed tobacco leaves was used in the 1700s to control aphids (Hodgson and Kuhr, 1990) and pyrethrins from the pyrethrum daisy *Chrysanthemum cinerariifolium* were useful anti-insect agents, albeit with limited use due to its rapid breakdown by ultraviolet (UV) radiation from sunlight (Khambay, 2002).

The discovery of DDT by Paul Hermann Müller and its effectiveness in controlling vector diseases such as malaria and typhus was viewed as a scientific breakthrough, and the Nobel Prize in Physiology or Medicine was awarded to the Swiss scientist in 1948 (Fenton, 2002). By the 1950s, DDT, organochlorines, organophosphates and carbamates were viewed as a „silver bullet" and used in vast quantities on a global scale (Wheeler, 2002).

In 1962, Rachel Carson"s *Silent Spring* exposed the detrimental effects of pesticides on the environment and animals. The author highlighted the toxic effects of organochlorines, pesticide residues in the food chain, and the demise of certain bird populations through the thinning of eggshells (Krebs et al., 1999). As a result, industry, government and community awareness of the hazards and risks of pesticides began to increase, and the public outcry was one of the driving forces behind the environmental movement of today.

In the 1960s and 70s, the first and second generations of UV-stable synthetic analogues of pyrethrins or pyrethroids, were developed and commercialized (Elliott, 1976). Pyrethroids were more active than the plant-derived pyrethrum

and viewed as a „safer" insecticide due to the relatively low mammalian toxicity and low potential for environmental persistence (Casida, 2009). Synthetic pyrethroids set a new standard for contact insecticides because they were photostable without compromising biodegradability and they were highly insecticidal but minimally toxic to fish and mammals (Casida and Quistad, 1998, Casida, 2009).

In 2001, heads of state and government leaders of over ninety nations met at a conference in Stockholm, Sweden, to sign a treaty that aimed to protect the environment and human health from the effects of persistent organic pollutants (POPs) (Lallas, 2001). The *Stockholm Convention* listed twelve toxic chemicals for gradual elimination from usage and production around the world and these chemicals became known as the „Dirty Dozen". Eight of the twelve chemicals were insecticides belonging to the organochlorine class of compounds: aldrin, chlordane, dieldrin, endrin, heptachlor, mirex, toxaphene and DDT (Karlaganis et al., 2001). These insecticides were chosen due to their hazardous properties which included high human toxicity, bioaccumulation in fatty tissue and environmental persistence (Kaiser and Enserink, 2000). These chemicals were considered especially dangerous in developing countries because they were often stored in unsafe conditions, sometimes with disastrous consequences. For example, hundreds of drinking wells in Mali were shut down due to contamination by dieldrin which was once used to control locusts (Pearce, 2003), leading to critical water shortages. As a result, there is increasing pressure to create safe insecticidal agents to replace chemical insecticides undergoing use-cancellation.

1.3 **Modern Insecticides**

Developing new insecticides has become more challenging than ever before because they must meet high standards for regulatory approval as well as market demands. Insecticides are expected to be fast-acting and toxic to pest species at low concentrations and yet be safe for beneficial insects such as pollinators. In particular, they cannot cause acute or chronic effects to humans and other vertebrate animals. Further, they should not bioaccumulate, but

must be biodegradable and not persistent in soil, air or groundwater. The insecticide should also be economical and remain effective after multiple applications over a relatively long period of time. Using conventional insecticide manufacturing methods, bringing a new insecticidal agent with these attributes onto the market is estimated to take more than a decade in research and development and cost over $200 million (Hemingway, 2009).

Modern day use of insecticides still revolves around liquid chemical-based insecticides but the landscape has evolved to include other types of pest insect management systems. Contemporary insecticides are broadly grouped into synthetic chemical insecticides and biological pesticides.

1.3.1 Chemical Insecticides

Broad-spectrum synthetic chemical insecticides are still the predominant method of insect pest control and they are used on a vast scale to improve crop yields and control insect vectors of disease (see Table 1.2). The major classes of insecticides are nervous system toxins that act on three target sites in insects:

(1) acetylcholinesterase (AChE) inhibition at the synapses and neuromuscular junctions (e.g. organophosphates, carbamates);
(2) alteration of voltage-gated sodium channel function (e.g. pyrethroids, DDT, indoxacarb); and
(3) alteration/agonists of ionotropic receptors such as nicotinic acetylcholine (e.g. imidacloprid, cartap, spinosyns), GABA (e.g. cyclodienes, phenylpyrazoles), and glutamate (e.g. avermectins, milbemycins).
(Raymond-Delpech et al., 2005).

Although they are incredibly powerful and useful, there are many limitations to traditional chemical insecticides, including:
- Poor species specificity leading to loss of beneficial insects;

- Toxicity to vertebrate species including birds, fish and mammals; and

- Negative perception in the community about adverse health and environmental effects.

Increasing evidence of the hazards of many insecticides has also meant that there are heavy regulatory restrictions or bans on usage. One such example is methyl bromide that was used to kill insects in grain mills and silos to the tune of 27 million kilograms per year in the US alone. Methyl bromide has been banned internationally since 2005 due to its ozone-depleting effects, although it was met with heavy opposition by industry which lobbied to continue using this agent (Pearce, 2002).

Due to international regulatory action on organochlorine insecticides, their use has progressively reduced along with organosphosphates, further increasing pressure to find new and safer insecticides as replacements.

Table 1.2: Major chemical classes of insecticides and their market share (Adapted from Nauen, 2006, Duke et al., 2010).

Class of insecticide	% global market share
Organophosphates	24.7
Pyrethroids	19.5
Neonicotinoids	15.7
Carbamates	10.5
Others (e.g. fipronil, imidacloprid)	7.7
Natural Products	7.6
Acaricides	6.4
Insect Growth Regulators	5.8
Organochlorines	2.1

1.3.2 Insecticide Resistance

Most insecticides are not sustainable in the long-term due to the development of resistance by insects following repeated exposure. Pesticide resistance is

defined by the World Health Organisation as an „inherited characteristic that imparts an increased tolerance to a pesticide, or group of pesticides, such that the resistant individuals survive a concentration of the compound(s) that would normally be lethal to the species" (WHO, 1992). The molecular basis for resistance in insects is mainly linked to target ion channel sites becoming insensitive to insecticides via point mutations in structural genes for ion channels, and increased ability of insects to metabolise and detoxify the chemical through the action of cytochrome P450s and glutathione transferases (Feyereisen, 1995, Ffrench-Constant et al., 2004, Brogdon and McAllister, 1998, Ranson et al., 2002).

Currently, there is widespread resistance to all major classes of chemical insecticides (Hemingway and Ranson, 2000) and at least 540 insect and other arthropod species of agricultural and public health importance are resistant to one or more insecticides or acaricides (Capinera, 2008). This problem is considered critical in the area of vector control for public health, where the number of cost-effective insecticides has diminished significantly due to resistance in mosquito populations (Pinto et al., 2006). The appearance of malaria parasites resistant to insecticides and insecticide-impregnated bed nets has meant that malaria infection rates are on the rise again in Africa (Holt et al., 2002). This problem is exacerbated by the non-registration of chemical agents by regulatory bodies due to safety concerns and lack of investment into research of new compounds to use against public health pests (Zaim and Guillet, 2002).

New insecticide design has largely been steered by chemists and chemical manufacturers using structure-activity relationship (SAR), molecular modelling and ligand-based methodologies for pesticide design in a manner similar to medical drug design. However, the number of well-characterised pharmacological targets for invertebrates is significantly smaller than that available in medicinal/pharmaceutical chemistry (Bordas et al., 2003). The fact that most of the commercially available insecticides act on a relatively small number of target sites has exacerbated the problem of insect resistance. The

four major classes of insecticides either act as nerve poisons causing disruption of nerve functions by interfering with neurotransmitter action (e.g. organophosphates, carbamates, neonicotinoids) or by disrupting specific ion channel functions (e.g. pyrethroids). Since the introduction of neonicotinoids, such as imidacloprid in 1991, no significantly new class of insecticides has been released onto the market (Nauen, 2006).

1.4 **Biopesticides**

Biopesticides are viewed as an attractive alternative to traditional chemical insecticides because they typically have fewer adverse effects and have a narrow target range, which help preserve non-target arthropod species (USEPA, 2011). Biopesticides are pest control agents derived from a natural source, usually from animals, plants, certain minerals and microorganisms (Gan-Mor and Matthews, 2003, USEPA, 2011). These have risen to take up a greater portion of the pest control market due to increased pressure on industry to reduce synthetic chemical insecticide use and its residues in the environment and food.

Bacteria and viruses that infect insects have proven to be particularly useful for this application, and of these, *Bacillus thuringiensis* and baculoviruses have the greatest potential for widespread commercial use.

1.4.1 Bacillus thuringiensis (*Bt*)

Bacillus thuringiensis (*Bt*) is undoubtedly the world‟s most successful biopesticide (Federici, 2005). *Bt* are widely occurring gram-positive, spore-forming soil bacteria that possess *cry* genes which express protein crystalline inclusion bodies that become toxic to insects upon ingestion (Bravo et al., 2007) Over 25 *cry* genes have been described and reported to have specific insect host ranges. For example, cry II genes produce proteins that are toxic to lepidopterous larvae and cry III genes produce toxins towards coleopterans (Copping and Menn, 2000). These genes have been incorporated into plants

that have been genetically modified to express the insecticidal toxins in the leaves, resulting in transgenic plants that „self-protect" against insect pests. *Bt* plants have been shown to provide long-term widespread control of pest insects affecting cotton and corn (Carriere et al., 2003).

Genetic modification of crops to include toxins has a distinct advantage over chemical pesticides because they specifically target crop-feeding insects rather than pollinators and predatory arthropods such as spiders. An added benefit of transgenic crops is that they reduce the need for repeated spray-on pesticide applications, which decreases financial burden on farmers and reduces the volume of pesticide run-off into waterways (Toenniessen et al., 2003). This effect has been demonstrated in China where *Bt* cotton producers were able to reduce their pesticide use by more than 44,000 tonnes or around US$138 million in the first four years of implementing the variety in 1996-1999, compared to non-*Bt* cotton producers whose level of pesticide use went up during the same period (Huang et al., 2003).

Bt plants have become increasingly popular, and in 2005, *Bt* crops were grown in 17 countries with the total area of *Bt* corn and cotton covering over 80 million ha worldwide (Bates et al., 2005). Given the widespread usage, there were many concerns about the ecological impact to non-target invertebrate species, particularly predators of pest insects that consume *Bt* plants. So far the reports have been favourable toward *Bt* plants, for example a study on carabid beetles and parasitoid wasps showed that the *Bt* toxin is readily excreted and not accumulated through different trophic levels (Christou et al., 2006). Moreover, a three-year study on the effect of *Bt* transgenic plants on spiders (an important pest predator in crop fields) revealed no consistent effect on individual numbers and species richness of spiders dwelling among transgenic crops in comparison to adjacent spiders in non-*Bt* fields (Ludy and Lang, 2006).

There are foreseeable issues with *Bt* plants in the long-term, including heightened negative public perception about safety of foods from genetically-

modified plants. This is despite robust risk assessments by regulatory authorities around the world which have concluded that the benefits of using biotechnology in food production outweighs the potential risks (Shelton et al., 2002). Another issue is that continuous expression of *Bt* toxins coupled with increased adoption of *Bt* plant varieties around the world may expedite the development of insect resistance to the toxin (Gould, 1998, Morin et al., 2003, Downes et al., 2007). Although widespread field resistance to *Bt* crops has not yet been documented, resistance to the toxin has been reported in isolated cases (Bagla, 2010, Tabashnik et al., 2009, Tabashnik et al., 2010, Kruger et al., 2009, Storer et al., 2010). Insect resistance to *Bt* sprays has been detected in several diamondback moth (*Plutella xylostella*) populations (Ferré and Van Rie, 2002) and many pest species have been successfully selected in the laboratory for *Bt* resistance (Tabashnik et al., 2003, Bates et al., 2005, Griffitts and Aroian, 2005).

To counter this, management strategies are being deployed to delay the onset of resistance, including planting of non-*Bt* plants in "refuges" to conserve susceptible alleles (Shelton et al., 2000). However the longevity of *Bt* may be in doubt, with the identification of a recessive gene that confers much of the resistance to *Bt* toxin in a resistant laboratory strain of tobacco budworm, *Heliothis virescens*, which could seriously threaten the future of *Bt* transgenic-based plants (Gahan et al., 2001).

Given this prospect, it is necessary to search for other sources of insecticidal toxins to replace *Bt* and hence create a new line of transgenic plants. Some of the proposed alternatives include toxins derived from animal venoms such as spiders and scorpions (Khan et al., 2006, Hernandez-Campuzano et al., 2009).

1.4.2 Recombinant Baculoviruses

The most successful pathogenic viruses for biopesticide application has been the family *Baculoviridae* (Hajek et al., 2007, Fauquet et al., 2005), which are a

major group of naturally-occurring viruses with circular, supercoiled, double-stranded DNA that specifically infect arthropods (Wood and Granados, 1991). Baculoviruses can produce large numbers of occlusion bodies in host cells until the death of an infected individual, upon which progeny virus particles are liberated into the environment where they may cause subsequent infections (Szewczyk et al., 2006, Richards et al., 1998).

Baculoviruses are advantageous because they are non-pathogenic to vertebrates and plants (Herniou et al., 2003), and have a restricted host range, being active on a single family or genus (Black et al., 1997), which is useful for targeting specific pest populations. More than 400 insect species, including economically and agriculturally important insect orders such as Lepidoptera and Hymenoptera, have been reported as viral hosts (Lacey et al., 2001). Baculoviruses have been successfully used to protect fields, orchard crops and forests in America, Europe and Asia (Whetstone and Hammock, 2007), including over two million hectares of soybean plantations in Brazil that were infested with velvet bean caterpillars (*Anticarsia gemmatalis*) (Moscardi, 1999). Despite this success, baculoviruses have never been widely adopted as a pesticide because of its inherently slow kill rate ranging from four days to two weeks between ingestion of virus particles and time of death (Miller, 1995). During this period, the insect continues to feed and cause damage to foliage of crops and plantations (Bonning and Hammock, 1996, Feng et al., 2001).

To overcome this limitation, recombinant baculoviruses were constructed with the aim of improving the time-to-kill of insects compared to wild-type baculoviruses (van Beek and Hughes, 1998). This was achieved through incorporation of a foreign gene into the baculoviral genome to express an enzyme, hormone or toxin (Cory et al., 1994). The most reported and successful recombinants are baculoviral constructs expressing insecticidal toxins from venomous animals, including mites (Tomalski and Miller, 1991, Popham et al., 1997, Burden et al., 2000), sea anemones (Prikhod'ko et al., 1996), scorpions (Chejanovsky et al., 1995, Gershburg et al., 1998,

McCutchen et al., 1991, Stewart et al., 1991) and spiders (Hughes et al., 1997, Prikhod'ko et al., 1996, Prikhod'ko et al., 1998). One of the best known examples is a recombinant baculovirus encoded with the gene for AaIT, an insect-specific neurotoxin from the North African scorpion *Androctonus australis* (Chen et al., 2000, Zlotkin et al., 2000). Lepidopterous larvae infected with an AaIT-expressing baculovirus showed symptoms of paralysis identical to that of larvae injected with the native toxin (Elazar et al., 2001), but with an increase in the speed-of-kill by up to 40%, and reduction in feeding damage by about 60% (McCutchen et al., 1991, Kunimi et al., 1996). Further improvements in baculoviral efficacy were observed after synergistic expression of a pair of toxins in a single recombinant baculoviral construct (Regev et al., 2003). Although there are currently no recombinant baculovirus insecticides registered for commercial use, these improvements greatly increase its commercial viability (Lord, 2005).

In terms of ecological impacts, experiments showed that AaIT-recombinant baculoviruses were non-pathogenic to bees, birds, fish and other vertebrates (Sun et al., 2002). Furthermore, recombinants showed reduced fitness in the environment and was not considered to have an ecological advantage over wild-type viruses (Inceoglu et al., 2001).

Biopesticides provide a distinct advantage over existing chemical insecticides because of its low hazard and low environmental risk profile. This technology is innovative because of its use of natural toxins as the basis for insecticidal activity, in particular toxins from animal venoms which until now have largely been overlooked in terms of their potential as insecticides. The next section looks at spider venom as a potentially abundant source of novel insecticidal compounds for biopesticide use.

1.5 Toxins in Spider Venom

1.5.1 Spider Venom

Spiders (Class: Arachnida, Order: Araneae) are an incredibly diverse and ancient group of invertebrates that dates back over 300 million years from the Carboniferous period (Platnick, 1993). They are the largest group of venomous animals with over 40,000 described species spanning more than 3,820 genera and 110 families (Platnick, 2011). Some have estimated that many more spider species have yet to be described (Platnick, 1995, Coddington and Levi, 1991).

The majority of spiders belong to two major sub-orders: Araneomorphae ("modern" spiders) and Mygalomorphae ("primitive" spiders). The distinguishing features are that araneomorphs have diagonally-pointing fangs that move like pincers and multiple spinnerets that produce an extremely fine sticky silk which easily entangle prey insects. Mygalomorphs have fangs that point straight down like the blade of a scythe and they possess a smaller number of spinnerets which produce silk that is used predominantly for lining burrows and making egg sacs (Coddington and Levi, 1991). Although araneomorph spiders represent more than 90% of the world"s spiders, mygalomorphs are of particular interest to toxinologists because of their large venom apparatus compared to modern spiders (King et al., 2002).

Spider venom is produced in specialised glands and although the volume of venom produced by spiders is relatively small, technological advances in analytical and proteomic techniques has led to greater resolution and accuracy, making it worthwhile to fully explore venom (Griffin and Aebersold, 2001, Pimenta and De Lima, 2005). An investigation of spider venom by mass spectrometry, chromatography and venom-gland cDNA libraries has revealed that venom represents an enormous library of millions of bioactive molecules (Escoubas et al., 2006, Escoubas et al., 2008), with potential uses in medicine

and agriculture (King et al., 2008b, Wood et al., 2009, Escoubas and King, 2009). Spider venom is a complex chemical mixture that contains enzymes, nucleic acids, free amino acids, monoamines and inorganic salts, but the main active components are neurotoxins composed of proteins, peptides and polyamines (Escoubas et al., 2008, Vassilevski et al., 2009).

Spider venom toxins predominantly have molecular masses of 3-8 kDa, and like peptide toxins from other venomous animals such as marine cone snails (*Conus*), they are structured by many cysteines and interlinking disulfide bridges relative to the backbone length (Escoubas et al., 2000). These disulfide bridges give the molecule rigidity and acts as a stabiliser for the three-dimensional globular folding pattern (Sevilla et al., 1993), which provides good resistance to denaturation (Mouhat et al., 2004) and is essential for its biological activity. The globular conformation created by disulfide bonds likely causes maximum presentation of the amino acid residues to the outside of the peptide, contributing to the overall charge distribution and interaction with the binding site (Escoubas et al., 2000).

Although the cysteine framework is a highly successful structure that has been maintained in the amino acid sequence of many peptide toxins, there is also a high degree of toxin diversity in terms of the composition of the amino acid residues and target specificity. This diversity occurs through an evolutionary process of structural hypervariability in the toxin gene (Mebs, 2001, Sollod et al., 2005). Analysis of prepropeptide precursor sequences have shown that the signal sequence is highly conserved, but there is extensive sequence variation within the propeptide and mature-toxin regions (Sollod et al, 2005). This combinatorial peptide library system has resulted in an extensive number of pharmacologically diverse toxins (Tedford et al., 2004b, Escoubas et al., 2000), particularly those that target ion channels in the nervous system.

1.5.2 Peptide Neurotoxins as Pharmacological Tools

Most early studies of arachnid toxins focused on peptides and polypeptides that were capable of causing systemic envenomation or even death in humans. As a geographically isolated continent, Australia is home to a distinct range of clinically important venomous spider species such as red-back (*Latrodectus hasselti)* (Vetter and Isbister, 2008), funnel-web (*Atrax* and *Hadronyche* spp.) (White, 2010) and *Missulena* spp. mouse spiders (Isbister, 2004) (see Chapter 7). Neurotoxin research in recent years has provided an understanding of how they cause toxicity in humans, with a particular focus on the development of species-specific antivenoms to treat bite victims (Nicholson et al., 2006).

Peptide neurotoxins in spider venoms display a high level of ion channel selectivity, which means they are useful pharmacological tools for understanding the molecular processes of ion channel structure-function relationships in the nervous system and investigating their role in human diseases. Indeed some peptide toxins have become the defining pharmacology for particular vertebrate ion channel classes. For example, ω-agatoxin-Aa4a and -Aa4b (formerly ω-agatoxin-IVA and -IVB) from the American funnel-web spider *Agelenopsis aperta* (Bindokas and Adams, 1989, Adams et al., 1990, Adams, 2004) and κ-theraphotoxins (formerly Hanatoxins) from the tarantula *Grammostola spatulata* (Swartz and MacKinnon, 1995, Swartz and MacKinnon, 1997a, Swartz and MacKinnon, 1997b) are used to distinguish vertebrate P/Q-type ($Ca_v2.1$) voltage-gated calcium channels and $K_v2.1$, $K_v4.2$ voltage-gated potassium channels, respectively.

Their small molecular mass, structural stability and relative ease of synthesis (Lewis and Garcia, 2003) means these peptide toxins can also be novel leads or structural templates from which new therapeutic agents might be developed (Adams and Olivera, 1994, Estrada et al., 2007, Escoubas and King, 2009, Vetter et al., 2011), in a manner similar to the cone snail peptide, ω-conotoxin-

MVIIA, which was recently developed into a therapeutic drug (SNX111/Ziconotide/Prialt; Elan) to treat chronic pain (Molinski et al., 2009).

1.5.3 Peptide Neurotoxins as Insecticides

Spiders are specialised predators that rely on venom to kill or paralyse prey arthropods, hence many spider venoms contain a large repertoire of insect-selective toxins (Nicholson, 2007b) that can kill, or induce rapid paralysis in insects at concentrations in the picomolar and nanomolar (10^{-12} – 10^{-9} M) ranges (Zlotkin, 1991). Interestingly, spider venoms can display differences in potency towards one arthropod species over another, for example, toxins from the venom of the ctenid spider, *Cupiennius salei* are much more lethal towards *dipterans* (LD_{50} < 0.25 nl/mg insect) than beetles or ants (LD_{50} > 3.0 nl/mg insect) (Kuhn-Nentwig et al., 1998). A study on the main constituent of *C. salei* venom is covered in Chapter 8 of this thesis.

Spider toxins that are selectively toxic to insects are promising candidates for novel insecticides because they have high specificity and a large range of target ion channels in insects (King et al., 2008a). In fact, the target range is greater than commercial insecticides which are currently effective on only a small subset of ion channels (Narahashi, 1996, Bloomquist, 1996, Raymond-Delpech et al., 2005). Pertinent examples are the ω-hexatoxin (ω-HXTX) family of insect-selective toxins from Australian funnel-web spiders (see Chapters 3 and 4) that display high specificity for insect voltage-gated calcium channels, which are not currently targeted by mainstream pesticides.

Spider venom can therefore be viewed as an extensive reservoir of preoptimised insecticidal molecules that may be useful as insecticide leads, or useful tools for validating novel insecticide targets for the design of new, highly selective and environmentally-friendly insecticides (Tedford et al., 2004b).

1.5.3.1 Neurotoxins as Leads for Chemical Insecticides

Recently, peptide neurotoxins have been investigated for their utility in the rational design of chemical insecticides due to their robust structure, in particular, a common structural feature of peptide toxins called the inhibitory cystine knot (ICK) motif (Pallaghy et al., 1994, Craik et al., 2001). The ICK is a ring formed by two disulfide bridges between Cys (I-IV) and Cys (II-V) and an interconnecting backbone segment that is threaded by a third disulfide bond, Cys (III-VI) (Isaacs, 1995). This ICK motif is a compact three-dimensional (3D) scaffold that could serve as a structural template for insecticide design. This could take the form of a small, non-peptidic molecule onto which insect-killing functional groups could be grafted (Norton and Pallaghy, 1998, Craik et al., 2001). These functional groups are considered critical for reproducing the same level of insecticidal activity and insect-specificity observed with the native toxin. Generally speaking, these could be obtained by mapping the key residues on the neurotoxin that binds to the insect target site (insectophore) (Norton and Pallaghy, 1998, Tedford et al., 2004b), as well as the 3D structure and exact spatial position of each insectophore. For this approach to be successful, a wide range of characterised insecticidal toxins are required, but to date there are still relatively few spider toxins that have been isolated and characterised.

1.5.3.2 Neurotoxins as Biopesticides

It is envisaged that certain spider neurotoxins could act as insecticides without any modification by delivery through existing technologies such as genetically-engineered baculoviruses and transgenic plants as discussed in section 1.4.

A promising new area of biopesticide technology is orally active insecticides based on the snow drop plant lectin, also known as GNA (*Galanthus nivalis* agglutinin). GNA is a protein that causes reduction in weight gain and slower developmental rate in insects such as tomato moth (*Lacanobia oleracea*)

larvae when incorporated into an artificial diet or expressed in transgenic plants (Gatehouse et al., 1997). Although the exact mechanism is not clear, GNA appears to bind to, and cross the gut epithelium after ingestion by the insect. GNA resists gut proteolysis, as evidenced by its presence in the hemolymph after oral administration to insects (Fitches et al., 2001). The ability of GNA to cross the gut epithelium means that it can act as a carrier to deliver fused insecticidal peptide toxins to the circulatory system of target insect species. This was demonstrated in several experiments, including oral toxicity assays of GNA fusion protein constructs encoding SFI1, an insecticidal toxin from the spider *Segestria florentina* that were fed to hemipteran and lepidopteran insects through incorporation into the diet. Significant effects on mortality were observed on insects fed the SFI/GNA fusion protein, but not on insects fed on a control diet (Fitches et al., 2004, Down et al., 2006). Similarly, GNA fused with ButaIT toxin from the scorpion *Mesobuthus tamulus* was highly lethal to lepidopteran, dipteran and coleopteran insects fed on a diet containing the fusion protein (Fitches et al., 2010). These studies show that fusion proteins have the potential to create a whole new range of orally active insecticides using spider venom toxins as the active ingredient.

Peptide neurotoxins from spider venom have never been formulated as an active ingredient of topical insecticidal sprays because of the assumption that peptides were not bioavailable through the oral route (Fitches et al., 2004). However, recent studies have confirmed that at least one insecticidal peptide from Australian funnel-web spider venom is inherently orally active in arthropods (Khan et al., 2006, Mukherjee et al., 2006), and is therefore of great interest for further investigation as a biopesticide.

1.6 Venom of Australian funnel-web spiders

The venoms of Australian funnel-web spiders such as the Sydney (*Atrax robustus*) and Blue Mountains (*Hadronyche versuta*) funnel-web spiders (Araneae: Mygalomorphae: Hexathelidae: Atracinae) are recognised as some of the most venomous spiders to humans world-wide (Graudins et al., 2002). Clinical cases of envenomation syndrome were linked to venom produced by

male *A. robustus* (Nicholson et al., 2006) and symptoms included fasciculations (particularly face, tongue and intercostals), hypertension, cardiac arrhythmias, vomiting, excessive salivation and pulmonary oedema (Miller et al., 2000). Fourteen casualties were recorded from 1927 until the development of antivenom for clinical use in 1980 (Sutherland, 1980).

By fractionating funnel-web spider venom and screening for activity, a major group of neurotoxins called δ-hexatoxins (formerly δ-atracotoxins) (King et al., 2008b), that was responsible for the envenomation syndrome was identified (Fisher et al., 1980, Hartman and Sutherland, 1984, Isbister et al., 2005). Patch-clamp studies on δ-hexatoxins from both *A. robustus* and *H. versuta* showed that these toxins target mammalian, and particularly primate voltage-gated sodium (Na_v) channels (Nicholson and Graudins, 2002, Duncan et al., 1980) and causes a reduction in peak sodium currents and alteration of channel kinetics (Nicholson et al., 1994, Nicholson et al., 1998, Alewood et al., 2003, Gunning et al., 2003). These effects result in the clinical picture of envenomation by causing massive neurotransmitter release at motor and autonomic nerve fibres (Nicholson et al., 2004). Despite this primate-specific activity, δ-hexatoxins are also neurotoxic to insects through modulation of Na_v channels on neurons (Little et al., 1998, Grolleau et al., 2001).

Given that spiders mostly prey on arthropods and in particular insects, recent attention has focused on insecticidal toxins within funnel-web venom, which has been speculated to be useful as an environmentally-friendly biopesticide agent as an alternative to traditional chemical pesticides.

1.6.1 Insecticidal toxins: ω-hexatoxins

Some of the earliest studies on the insecticidal properties of Australian funnel-web venom involved insect bioassays testing the effects of female *Hadronyche versuta* venom fractions on a number of economically important insect species including moth larvae (*Heliothis armigera*), beetle (*Tenebrio molitor*), cockroach (*Periplaneta Americana*), Australian plague locust

(*Chortoicetes terminifera*) and blowfly (*Lucilia cuprina*). All venom fractions caused some degree of toxicity including rapid paralysis (permanent or temporary), and continuous and uncontrolled movements leading to death (Atkinson et al., 1996).

Peptides belonging to the ω-hexatoxin-1 (formerly ω-atracotoxin-1) family were the first insect-specific toxins to be isolated from the venom of *Hadronyche* and *Atrax* spp. of Australian funnel-web spiders. There are six described toxins within this family (ω-HXTX-Hv1a to -Hv1f) and each are made up of 36-37 amino acid residues, including six cysteines paired to form three disulfide bonds (Fletcher et al., 1997). These toxins are lethal to a range of insects such as ticks, moths, beetles, cockroaches, mealworms, blowflies and locusts (Fletcher et al., 1997, Khan et al., 2006, Mukherjee et al., 2006). The ω-hexatoxin-1 (ω-HXTX-1) family is neurotoxic, causing irreversible paralysis and death within 10-48 hours in the affected insect, depending on the species (Fletcher et al., 1997, Wang et al., 1999). Vertebrate toxicity tests showed that ω-HXTX-1 has no adverse effects when high doses up to 2.5 mg/kg are subcutaneously injected into newborn mice (Atkinson et al., 1998).

1.6.2 ω-hexatoxin-Hv1a

ω-hexatoxin-Hv1a (formerly ω-atracotoxin-Hv1a) from the venom of *H. versuta* is a prototypic insect-selective neurotoxin from the ω-HXTX-1 toxin family. Insects injected with sufficient doses of ω-HXTX-Hv1a display neurophysiological effects such as high frequency twitching and extension of limbs, antennae and mandibles, loss of coordinated locomotion and righting reflexes, followed by spastic paralysis and death (Fletcher et al., 1997, Atkinson et al., 1998, Bloomquist, 2003).

An analysis of the 3D structure of ω-HXTX-Hv1a revealed a core rich in disulfides and a β-hairpin that protrudes from the core to form a classical ICK motif (Fletcher et al., 1997, Tedford et al., 2004b). The β-hairpin is highly conserved in the ω-HXTX-1 family of toxins (King et al., 2002) and was

hypothesised to be of functional significance. The N-terminal residues (residues 1-3) are also highly conserved across the entire family of ω-HXTXs (Wang et al, 1999). There were no homologs of these peptides in protein or DNA sequence databases (Tedford et al., 2004b), however the 3D structural fold of ω-HXTX-Hv1a is similar to that of the scorpion toxin, maurocalcin, from *Scorpio maurus palmatus* (Tedford et al., 2004b, King et al., 2002). Maurocalcin irreversibly modifies vertebrate ryanodine-sensitive calcium channel gating behaviour (Fajloun et al., 2000, Mosbah et al., 2000).

1.6.3 Pharmacophore of ω-HXTX-1

Structure-function studies have revealed that the N-terminal residues and β-hairpin of the ω-HXTX-1 molecular structure contribute significantly to the toxic activity. Wang et al. (1999) showed that synthesised ω-HXTX-Hv1a truncates lacking up to three N-terminal residues were found to be up to 16-fold less potent than the original molecule, and a mutant version of ω-HXTX-1 with the β-hairpin removed from the C-terminal end of the peptide was found to be devoid of insecticidal activity, even though the overall 3D structure was unchanged from the native molecule (Tedford et al., 2001).

By probing the hairpin for key functional residues using alanine-scanning mutagenesis, three residues, Pro^{10}, Asn^{27} and Arg^{35}, which forms a contiguous surface on the molecule, were found to be essential for insecticidal activity and thus formed a major part of the toxin pharmacophore/ insectophore (Tedford et al., 2004a). In terms of insecticide molecule design, ω-HXTX-1 may be a suitable candidate because the pharmacophore corresponds to a contiguous and relatively small surface area (~200 $Å^2$), which is comparable to the surface area of a small drug molecule (150-500 $Å^2$) (Gadek and Nicholas, 2003, Tedford et al., 2004a).

1.6.4 Ion channel target of ω-HXTX-1

Based on the results of electrophysiological experiments on insect neurons, the phylogenetic specificity of ω-HXTX-Hv1a towards arthropods was attributed to the toxin"s effects on insect voltage-gated calcium (Ca_v) channels (Fletcher et al., 1997), which is important because it represents a non-conventional target for pesticides. ω-HXTX-1 inhibited Ca_v channels in fruit fly and cockroach, as well as the lone star tick *Amblyomma americanum*, which showed signs of toxicity and mortality after exposure to < 500 pmol/g ω-HXTX-Hv1a (Fletcher et al., 1997). Moreover, there was no toxic effect to vertebrate Ca_v channels in rat, and Ca_v1.2, 2.1 and 2.2 channels expressed in human embryonic kidney (HEK) cells at very high concentrations up to 10 μM (Fletcher et al., 1997, Wang et al., 1999, Tedford et al., 2004a). The combination of arthropod-selectivity and novel insect target suggested that ω-HXTX-Hv1a was an attractive biopesticide lead. However, the specific subtype of Ca_v channel that was being targeted in arthropods by ω-HXTX-Hv1a was not determined.

1.6.5 Oral and Topical Activity of ω-HXTX-Hv1a

Several important studies have recently shown that ω-HXTX-Hv1a is toxic to acarines and Lepidoptera after ingestion or external application, which further confirms the potential of ω-HXTX-Hv1a as a biopesticide. In these studies:

1. ω-HXTX-Hv1a caused neurophysiological effects when fed orally to the lone star tick, *A. americanum*, and the oral LD_{50} was determined to be 716 ± 23 pmol/g, which was less than two-fold higher than the LD_{50} from direct injection of the toxin into ticks (447 ± 3 pmol/g). At high doses > 1000 pmol/g, the treated ticks became completely paralysed and 100% mortality occurred. (Mukherjee et al., 2006).

2. The potential of ω-HXTX-Hv1a as a topical insecticide was investigated via gene expression of ω-HXTX-Hv1a in *E. coli* as a fusion construct with thioredoxin (to enhance Hv1a peptide stability). The thioredoxin/Hv1a construct was applied externally in droplet form (2 µl) to the thoracic region of *Helicoverpa armigera* and *Spodoptera littoralis* larvae at doses up to 16 pmol. Larvae ceased feeding at 1 pmol and the LD_{50} at 12 hours after application was 4 and 2 pmol of toxin per gram of body weight of *H. armigera* and *S. littoralis* larvae, respectively. There was 100% mortality within 24 hours. Control larvae receiving an equivalent concentration of thioredoxin alone was not affected (Khan et al., 2006).

3. The effectiveness of ω-HXTX-Hv1a as an expressed toxin in the leaves of transgenic tobacco plants (*Nicotiana tabacum*) was explored. The plants were effectively protected from the lepidopteran larvae of *H. armigera* and *S. littoralis* with 100% mortality observed within 48 hours (Khan et al., 2006).

These studies provide strong evidence of the potential for ω-HXTX-Hv1a as a novel oral or topical insecticide, however there was still a lack of knowledge

around the mode of action of ω-HXTX-Hv1a on insects, particularly the specific Ca$_v$ channel components that were being targeted by ω-HXTX-Hv1a.

1.7 **Aims and Objectives of this Project**

The growing problem of insecticide-resistance in pest insects, as well as public awareness around chemical pesticides and the environment means there is an urgent need to isolate new and safe insecticidal lead compounds. Therefore, the major aim of this thesis was to isolate and characterise novel insecticidal toxins from the venom of Australian funnel-web spiders that could be used as biopesticides or leads for the design of new chemical insecticides. The specific aims were to:

- Electrophysiologically characterise the effect of ω-HXTX-Hv1a from the venom of *Hadronyche versuta* and determine the target specificity in insect Ca$_v$ channels in an effort to further explore the potential of ω-HXTX-Hv1a as an insecticide lead (Chapter 3); and
- Isolate and characterise a novel insect-specific toxin from the venom of *Atrax robustus*, determine the insect ion channel target, and characterise its effects on target channel subtypes (Chapter 4).

As a part of the search for novel insecticidal toxins, this thesis also examined the venom of the unique Australian Eastern mouse spider (*Missulena bradleyi*). The aims were to:
- Fractionate *M. bradleyi* venom and systematically screen venom components for insecticidal activity; and
- Isolate and characterise a novel insect-selective peptide neurotoxin that may be suitable for biopesticide design (Chapters 5 and 6).

The secondary aim was to investigate the differences and commonality between insect and vertebrate ion channels using peptide neurotoxins from mygalomorph and araneomorph spider venoms. The objectives were to pharmacologically and electrophysiologically characterise toxins from the

venom of the Central American hunting spider, *Cupiennius salei* (Chapter 7) and the male Eastern mouse spider, *M. bradleyi* (Chapter 8).

2 Materials and Methods

2.1 Supply of spider toxins

Native ω-hexatoxin-Hv1a from *H. versuta* and the diselenide-substituted ω-hexatoxin-Hv1a toxins described in Chapter 3 were provided by the Institute for Molecular Bioscience, The University of Queensland, Australia. The method of synthesis for these toxins is described in section 2.18.

ω-Hexatoxin-Ar1a described in Chapter 4 was purified from whole venom that was collected by milking female Sydney funnel-web (*Atrax robustus*) spiders that were maintained in a captive colony at UTS.

Venom from female Eastern mouse spiders (*Missulena bradleyi*) described in Chapter 5 was manually collected by milking spiders that were maintained in a captive colony at UTS. Pooled female *M. bradleyi* venom was fractionated to isolate ω-actinopoditoxin-Mb1a as described in Chapter 6.

Purified ω-ctenitoxin-Cs1a (formerly CSTX-1) described in Chapter 8 was provided by Prof Lucia Kuhn-Nentwig of the Zoological Institute at the University of Bern, Switzerland. Spider venom collection and purification procedures for ω-ctenitoxin-Cs1a are detailed in Kubista et al. (2007).

δ-actinopoditoxin-Mb1a described in Chapter 7, was purified from whole venom that was collected by milking male *M. bradleyi* spiders that were maintained in a captive colony at UTS.

2.2 Supply of Eastern mouse and Sydney funnel-web spiders

Missulena bradleyi and *Atrax robustus* spiders were donated by the Australian Reptile Park in Somersby, New South Wales. The spiders originated from metropolitan Sydney, Newcastle and Central Coast regions of NSW and were initially captured by members of the public.

A. robustus have readily adapted to urban environments and are frequently encountered in suburbs, with some colonies exceeding 150 spiders (Sutherland, 1983, White et al., 1995). Female *A. robustus* spiders used for this project were found in abundance and able to be collected regularly from members of the general public and the Australian Reptile Park. In contrast, *M. bradleyi* were elusive and hence the numbers were comparatively small, presumably due to their sedentary lifestyle in underground burrows where they live in cocoons made from silk. During the cooler months from mid-autumn (March) to early winter (July), there was a slight increase in the numbers of *M. bradleyi* spiders. Whilst the exact reason for this is unknown, one theory is that areas populated by *M. bradleyi* experience higher levels of rainfall during this season, which flood their burrows and force them aboveground where they are easily spotted. This may explain why in 2001, hundreds of Eastern mouse spiders began suddenly appearing in the yard of a suburban home in Newcastle over several nights following a period of torrential rain and garden hosing (Thomas, 2001).

The supply of *M. bradleyi* noticeably decreased during dry months from July onwards and is most likely due to the fact that these spiders prefer to live in semi-arid to humid environments (Main, 1984), therefore spend much of their time deep in the moist earth to avoid desiccation.

In the latter years of this project, for reasons unknown, the overall numbers of *M. bradleyi* spiders being captured sharply declined, even during wetter months. This led to a major shortage of spiders and subsequent decrease in the amount of venom available for experiments.

2.3 Spider identification

The sex and species of spiders were initially identified by staff at the Australian Reptile Park prior to arriving in the UTS laboratory, although it was necessary to confirm the identity of spiders due to similar morphology between funnel-web and mouse spiders.

2.3.1 Differentiation of *A. robustus* and *M. bradleyi* spiders

Accurate differentiation between funnel-web and mouse spiders was achieved by observing key morphological characteristics that were first described by Densey Clyne (Clyne, 1969) and Robert Raven (Raven et al., 2002).

Figure 2.1: Female *Atrax* and *Missulena* spiders. A typical female *A. robustus* (left) and female *M. bradleyi* (right).

Missulena and *Atrax* spiders share common characteristics such as a stocky, solid body with dark brown to black glossy carapace on the cephalothorax (front half of the body from which the legs and chelicerae originate) (Figure 2.1). The abdomen or opisthosoma is brown-black and covered in fine hairs. *Missulena* are medium-sized and grow to approximately 35 mm in length for females, and around 20 mm for male spiders (Rash et al., 2000). *Atrax* are medium to large sized and adults can reach almost twice the length of mouse spiders.

The shape of the posterior section of the caput (head region in which the eyes are located on the cephalothorax) is one of the key distinguishing features between *Atrax* and *Missulena*. *Missulena bradleyi* has a steeply raised (almost vertical) caput relative to the horizontal plane of the body (Figure 2.2A), which

positions the eyes at the highest point of the body and makes the chelicerae a prominent feature. The caput of *Atrax robustus* is gently sloped from the top of the caput to the base of the abdomen (Figure 2.2B).

A

B

Figure 2.2: Shape of *Atrax* and *Missulena* caput. Steep angle of elevation of the posterior caput is characteristic of the *M. bradleyi* (A). The caput is gently sloped in the *A. robustus* (B).

The shapes of the spinnerets (organs that extrude silk) are also physically different. The spinnerets of *Missulena* are smaller and dome-shaped compared to *Atrax*, which are longer and resemble digits at the apex (Figure 2.3).

Figure 2.3: Spinnerets of *Atrax* and *Missulena*. The spinnerets of *Atrax* are longer and have a pointy apex (left), but are shorter and dome-shaped in *Missulena* (right).

2.3.2 Identification of male and female *M. bradleyi* spiders

The genus *Missulena* (Araneae, Mygalomorphae, Actinopodidae) consists of 10 species from Australia and 1 from Chile (Platnick, 2011). Two species are known to inhabit the Sydney-Central Coast region of NSW - *M. bradleyi* and *M. occatoria*, hence it was necessary to discriminate between the two species to ensure that only *M. bradleyi* spiders were kept for venom collection.

The male of both species are easily distinguished from females by their unique and conspicuous colouring. Male *M. bradleyi* has a trapezium-shaped bright white-grey patch on the anterior dorsal surface of its abdomen (Rash et al., 2000)(Figure 2.4A). Male *M. occatoria* (red-headed mouse spider) has a vibrant red carapace and a rich blue-coloured abdomen (Figure 2.4B).

As *M. occatoria* was not the subject of this thesis, the male spiders were marked and removed from the colony and eventually returned to the Australian Reptile Park.

A **B**
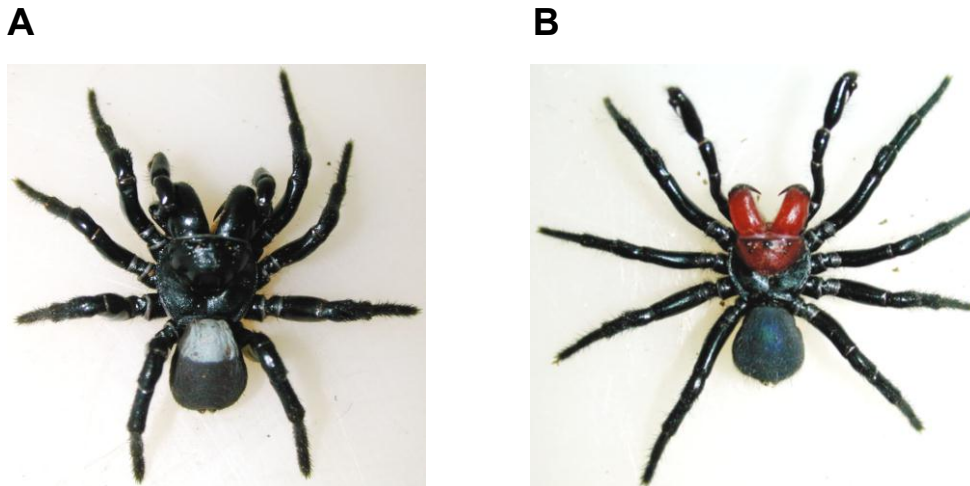
Figure 2.4: Male *Missulena* spiders. (A) male *M. bradleyi* and (B) male *M. occatoria*

In contrast to males, female *M. bradleyi* and female *M. occatoria* are virtually indistinguishable when viewed with the naked eye. Correct species identification of female mouse spiders was only possible by examining the ventral thoracic plate of individual spiders through a dissecting microscope. The major distinguishing feature separating the females is the arrangement of impressed spots on the anterior ventral plate that mark internal leg muscle attachment points known as sigilla (Figure 2.5). These indentations are characteristically different between the two species: female *M.bradleyi* has exactly three ordered pairs of oval shaped concave indentations on the ventral surface, whilst female *M. occatoria* have a greater number of these indented marks, which are irregular in size and shape (Faulder, 1995).

Around 5% of captured female spiders were determined to be female *M. occatoria* and these were marked and returned to the Australian Reptile Park.

Figure 2.5: Ventral view of female *Missulena bradleyi*. Red arrows indicate the location of three oval-shaped sigilla.

Around 15% of all spiders that arrived in the lab were immature spiders below 10 mm in length. These spiders were maintained in a separate colony and raised to maturity until such time when the sex and species could be accurately identified.

2.3.3 Identification of female *A. robustus*

Australasian funnel-web spiders (Araneae, Mygalomorphae, Hexathelidae) of the subfamily Atracinae consists of two genera; *Atrax* and *Hadronyche.* There are 15 known species of *Hadronyche*, 13 in Australia, one in New Guinea (*H. hirsuta*) and one in Solomon Islands (*H. insularis*) (Platnick, 2011). The *Atrax* genus consists of the clinically important *Atrax robustus* plus two other newly described species (Gray, 2010). All spiders used in this study were collected within the distribution area of *A. robustus*, which is limited to a relatively small area within a radius of around 160 km from the centre of Sydney city (Sutherland, 1983, Sutherland and Tibballs, 2001).

Only female *A. robustus* spiders were studied in this thesis, therefore all funnel-webs were sex-selected to identify and remove male *A. robustus* spiders from the colony. Males were easily distinguished from females by the presence of a spiny apophysis, otherwise known as a spur, on each of the second legs which are used to hold the female during mating.

2.4 Maintenance of spiders

Spiders were housed individually in aerated 13 cm-high plastic jars containing 3-4 cm of palm peat (Magic Soils Pty Ltd, Glen Waverley, Victoria) that were maintained at a temperature of 20-22°C. The palm peat was kept lightly moistened with water from a spray bottle. Spiders were fed once every fortnight with a live medium-sized house cricket (*Acheta domesticus*) (Pisces Enterprises Pty Ltd, Kenmore, Queensland) following venom collection.

2.5 Collection of spider venom

Venom from male *M. bradleyi* and female *A. robustus* spiders was obtained by „milking" on a fortnightly basis. Due to their sensitive and generally aggressive nature, the spiders often exuded venom from the fang tips immediately after being removed from their housing container or whenever air was blown over

the chelicera. The venom was then directly aspirated with a pipette and transferred to an eppendorf tube containing distilled water.

In preparation for milking female *M. bradleyi*, the spiders were removed from their housing jar with a pair of forceps, or, if they were beneath the palm peat inside a cocoon or burrow, two pairs of forceps were used to pull apart the cocoon and extract the spider. The spider was held down at the junction of the celaphalothorax and abdomen by hand and a piece of flexible plastic tubing (diameter ~ 5mm) was inserted between the chelicera. This triggered the spiders to clamp down in a pincer motion causing venom to be expressed from the fang tips (Figure 2.6). Venom was then aspirated using a pipette and washed into an eppendorf tube containing distilled water.

Initially, female *M. bradleyi* were milked by the application of pulsed electrical current to the chelicera, which causes contraction of the muscles that controls venom output and leads to the expulsion of venom from the fang tips (Rash et al., 2000). However this method of collection was abandoned due to the potential for contamination of venom with regurgitated material from the digestive tract (Wilson and Alewood, 2004). For similar reasons, the venom gland extraction method was not used, because gland extracts are known to be often contaminated with haemolymph, venom gland debris and digestive secretions, making it difficult to use (Jackson and Parks, 1989).

Figure 2.6: Collection of venom from female *M. bradleyi*. Venom was released from the fang tips when the chelicerae clamped down on the tube.

2.6 **Fractionation and purification of whole venom**

Whole venom was pooled and separated using reverse-phase high-performance liquid chromatography (rp-HPLC). This method was employed because of its ability to efficiently fractionate and selectively elute small disulfide-bridged peptides by binding of hydrophobic amino acid residues to the stationary phase (HPLC column). An acetonitrile/trifluoroacetic acid buffer system was used as the mobile phase as it is a water-miscible solution that solubilises peptides and has low viscosity and high transparency in the UV region (Imoto and Yamada, 1983, Stone and Williams, 1996).

2.6.1 Purification of venom fractions and ω-actinopoditoxin-Mb1a from *Missulena bradleyi*

M. bradleyi whole venom was dissolved in 0.5 ml solution containing 5% acetonitrile (ACN)/0.1% trifluoroacetic acid (TFA) and loaded onto an analytical C18 column (0.46 x 25 cm, 5 μm particle size, Vydac, CA, USA) on a Shimadzu Class-VP HPLC (Kyoto, Japan) connected to a FCV-10AL pump. Venom components were eluted using a linear concentration gradient of 5-60% ACN/0.085% TFA over a total period of 55 minutes (1%/min) at a flow rate of 1.0 ml/min. The UV absorbance was monitored at 215 nm using a SPD-10A dual wavelength UV-VIS detector. Peaks were collected and lyophilised using a freeze-drier to remove ACN, TFA and water. The samples were then stored at -80°C until required.

M. bradleyi venom fractions were further purified in preparation for biochemical analyses. Initially, bioactive fractions obtained from the purification of whole venom (see section 5.4) were subjected to rp-HPLC using a ACN/0.085% TFA buffer at a shallow gradient concentration increasing at 0.1%/min. If components could not be separated into individual peaks using this protocol, anion exchange fast-perfusion liquid chromatography (FPLC) was employed using either a Phenosphere SAX 5 μm particle size column

(Phenomenex, USA) or a Mono-Q HR5/5 anion exchange FPLC column (Pharmacia Biotech, Sweden) attached to an HPLC system with the UV absorbance set at 215 and 280 nm. Protein fractions were eluted using 20 mM NaCl/20 mM Tris-Base to 1.0 M NaCl/20 mM Tris-Base (pH 7.4) mobile phase, employing a linear NaCl gradient at a flow rate of 1 ml/ min. Given that salt buffers were used, the fraction that was collected from anion exchange purification contained toxin as well as a large amount of salt which required removal before further pharmacological experiments could be performed. Desalting was done using a Vydac analytical C18 rp-HPLC column with an ACN/TFA concentration gradient of either 1%/min or 0.1%/min at a flow rate of 1 ml/min.

2.6.2 Purification of ω-hexatoxin-Ar1a toxin from *Atrax robustus* venom

ω-HXTX-Ar1a was purified from the pooled whole venom of *A. robustus* using rp-HPLC employing a Vydac analytical column (C18, 4.6mm, 250 mm, 5 μm) on a Shimadzu HPLC system. Peptide peaks were monitored at an absorbance of 215 nm. Elution of venom peptide components was achieved using a linear gradient of 5-25% ACN/0.1% TFA over 20 min, then 25-50% ACN/0.1% TFA over 20 min at flow rate of 1.0 ml/ min. Selected fractions were subjected to acute toxicity bioassays using house crickets to determine insect toxicity (see Section 2.8). The major toxic fraction containing ω-HXTX-Ar1a (referred to as peak „f9" in Chapter 4) was further purified on an analytical C18 rp-HPLC column using a linear gradient of 5–14% ACN/0.1% TFA over 5 min, then 14–16% ACN/0.1% TFA over 20 min, at a flow rate of 1 ml/min. Purified toxin was collected, lyophilised, and stored at -80°C until required.

2.7 Bicinchoninic acid (BCA) protein assay

A BCA protein assay kit (Pierce Biotechnology, Illinois, USA) was used to quantify the amount of protein present in the fractions. This assay is based on the combination of two reactions, the first being the reduction of Cu^{2+} to Cu^+ by protein in an alkaline medium. The second is a sensitive colorimetric detection

using a reagent containing BCA that forms a purple-coloured product when two molecules of BCA chelate with one Cu^+ (Smith et al., 1985). The reactions were carried out in microwell plates (Microdish MC96FR, C.E.R., France) and incubated at 37°C for 30 minutes. The reaction products absorbed strongly at 562 nm that was linear with increasing protein concentrations over an optimum range of 20 µg/ml - 1500 µg/ml. A Titertek Multiscan Plus MKII absorbance scanner (Flow Laboratories, North Ryde, NSW) set at 560 nm was used to measure absorbance using bovine serum albumin (BSA) as a standard. Protein concentration was determined based on interpolation of the generated standard curve.

2.8   Insect toxicity assays

Venom fractions were tested for insecticidal activity on house crickets (*Acheta domesticus*) (Pisces Enterprises, Kenmore, Queensland). Crickets were chosen because they are normally highly active, making it easier than other insect species such as Sheep blowflies (*Lucilia cuprina*) or mealworms (*Tenebrio molitor*) to detect whether they are alive, paralysed or dead.

2.8.1 Maintenance of crickets

House crickets ranging from 50-180 mg were kept for the purpose of feeding the spiders and insect toxicity testing. Crickets were kept in plastic containers containing vermiculite or sand and egg carton harbourages. The crickets were given water and dog biscuits, carrots or „Gutload‟ invertebrate food (Pisces Enterprises, Queensland).

2.8.2 Insect toxicity test procedures

Female and male 3rd-4th instar nymph crickets weighing approximately 100 mg were placed into eight test groups with each group consisting of five crickets. The test solutions were prepared by dissolving venom fractions in insect saline (Table 2.1).

Table 2.1: Composition of insect saline for insect toxicity testing of venom fractions.

Chemical	mM
NaCl	200
KCl	3.1
HEPES*	10
$CaCl_2$	5
$MgCl_2$	4
Sucrose	50
Bovine serum albumin (BSA) added 0.1% w/v to reduce non-specific binding	
pH 7.4	

* 4-(2-Hydroxyethyl)piperazine-1-ethanesulfonic acid (HEPES).

Whole venom is generally inactive via the oral route due to breakdown in the gut; therefore test solutions containing venom were administered by direct subcutaneous lateroventral thoracic injections between the second and third pair of legs of each cricket (shown in Figure 2.7) at a dose of 10 µg/g bodyweight. Control crickets were injected with a solution of insect saline/0.1% BSA at 5 µl/100 mg bodyweight.

Figure 2.7: Lateroventral cricket injections of toxin solution.

The test equipment consisted of a light source, dissecting microscope and a 0.5 ml insulin syringe with a 29-gauge needle fitted inside an Arnold microapplicator (Burkard Scientific Supply, Rickmansworth, England). During the injection, crickets were gently held in place by forceps mounted between a retort stand clamp (Figure 2.8).

Figure 2.8: Apparatus used for insect toxicity testing

Following the injection, crickets were housed in groups of five in plastic Petri dishes (9 cm diameter) containing water-moistened filter paper and a portion of carrot for food. All dishes were kept at $20 \pm 2°C$ and observed at 20 and 40 min, 1, 4, 8, 24, 48 and 72 hrs after injection for signs of toxicity and changes to motor function. Toxicity was categorised based on four endpoints and are summarised in Table 2.2.

Table 2.2: Categorisation of signs of toxicity in crickets.

Endpoints	Distinguishing signs
Normal	Maintains normal posture, occasional abdominal contractions. Normal gait, feeding and moulting.
Mildly affected	Maintains normal posture, increased abdominal contractions, occasional twitches of appendages (mandible, antennae, and legs), signs of ataxia, and erratic movements.
Knockdown	Inability to maintain normal posture, immobile, intermittent or continuous twitches of appendages.

Mortality	None or extremely slight movement of appendages following stimuli such as tapping, shaking.

Subsequent determination of median lethal (LD_{50}) and median knockdown (KD_{50}) dose was performed by injecting purified toxin at doses of 0.005, 0.01, 0.02, 0.05, 0.1, 0.2, 0.5, 1, 2 and 5 µg/g body weight. The KD_{50} and LD_{50} were determined at 24, 48 and 72 hours post injection by plotting data as log dose-response curves using Prism$^{®}$ v4.0 (GraphPad Software San Diego, CA, USA) and fitting the curves with the logistic function:

$$y = 100 \times \left(1 - \frac{1}{1 + (x/\mathrm{LD}_{50})^{n}} \right) \qquad \text{(Equation 1)}$$

where *y* is the percentage response in the sample population at 24, 48 and 72 hours post-injection, *x* is the toxin dose in pmol/g and *n* is the slope factor (Hill coefficient) and LD_{50} is the dose causing 50% lethality.

2.9 Vertebrate toxicity assays

To determine whether the insecticidal peptides were active on vertebrate tissue, a vertebrate bioassay was employed using isolated chick biventer cervicis nerve-muscle preparation in an organ bath system as described by (Ginsborg and Warriner, 1960). Male Australorp chicks that were 1-7 days old (S.F. Barter and Sons, Huntingwood, Australia) were first anaesthetised with 100% CO_2 according to the protocol approved by the joint RNSH/UTS Animal Care & Ethics Committee (UTS/RNSH 0301-002A and UTS 2008-27 (formerly UTS/RNSH 0612-052A)). Once the chick was unconscious, an incision was made into the mid-thoracic region using sharp scissors to exsanguinate the animal by severing the abdominal aorta. The biventer cervicis muscle and attached nerve was removed from the posterior neck region. The nerve-muscle was then bathed in a Krebs-Henseleit solution of the following composition in Table 2.3.

Table 2.3: Composition of organ bath for vertebrate toxicity testing.

Chemical	mM
NaCl	118.4
KCl	4.7
$MgSO_4$	1.2
KH_2PO_4	1.2
$NaHCO_3$	25.0
D-glucose	11.1
$CaCl_2$	2.5
pH 7.4	

The proximal and distal ends of the muscle were tied with cotton threads and mounted in an 8 ml water-jacketed organ bath and maintained under 1 gram of resting tension (see Figure 2.9B). The nerve-muscle was then maintained at 34°C using a Thermomix M (Braun, Melsungen, Germany) water pump and heating system. The muscle was constantly carbogenated with 95% O_2 and 5% CO_2. The motor nerve of the muscle was electrically stimulated using supramaximal square wave pulses (10-20 V) of 0.05 ms duration at 0.1 Hz via silver electrodes connected to a Grass S88 Stimulator (Grass Instruments, Quincy, Massachusetts, USA). Changes in muscle tension were recorded using an isometric force transducer and the measurements were displayed on a Neotrace chart recorder (Neomedix Systems, Dee Why West, Australia). The data was simultaneously digitised using PowerLab 2/20 (ADInstruments, Castle Hill, Australia) and recorded using the software program Chart® v4.0.1. Tension traces were stored on an Apple iMac computer and analysed off-line. Figure 2.9A shows the organ bath and recording equipment used in this procedure. In the absence of electrical stimulation, responses to exogenous acetylcholine (1 mM, 30 s) and KCl (40 mM, 30 s) were obtained prior to the addition of venom and at the end of the experiment. The nerve-muscle was electrically stimulated for at least 20 minutes to allow the muscle to equilibrate before the addition of the venom fractions.
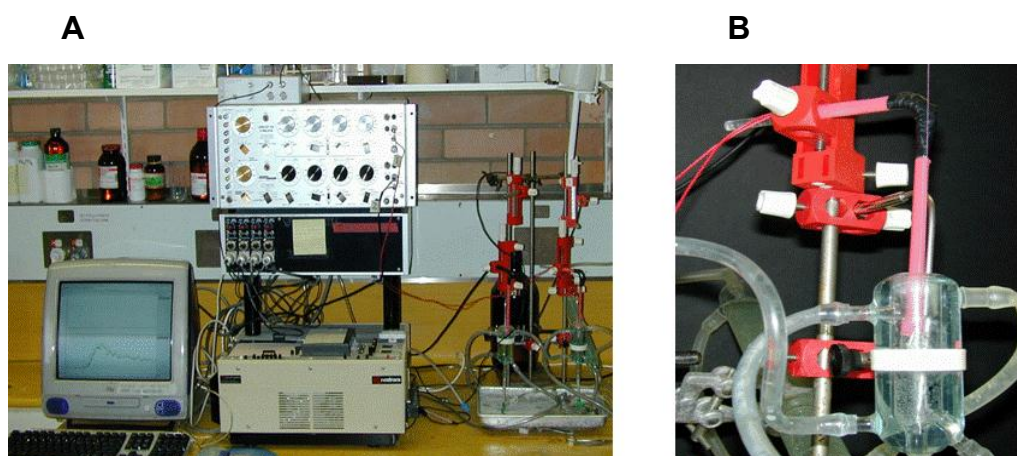
Figure 2.9: Organ bath and recording equipment. (A) Apparatus used for stimulating and recording nerve-muscle twitch activity from chick-biventer cervices muscles. (B) Organ bath demonstrating arrangement of force transducer.

2.10 **Mass spectrometry**

Toxic fractions were freeze-dried and sent to the Australian Proteome Analysis Facility (APAF, Macquarie University, NSW) where matrix-assisted laser desorption/ionisation-time of flight mass spectrometry (MALDI-TOF MS) was performed. Electrospray ionisation mass spectrometry (ESI-MS) was performed by Dr Peter Hains at the Department of Chemistry, University of Wollongong, using a Micromass Q-TOF2 (Manchester, UK) equipped with a nanospray source. Glu-fibrinopeptide (1 pmol/µL) dissolved in 50% (v/v) acetonitrile and 0.5% (v/v) formic acid were used as the calibrant and vehicle, respectively. Data was manually acquired in the positive mode using borosilicate capillaries with a source temperature of 80°C and a drying gas flow rate of 30 L/hr. A potential of 850 V was applied to the nanoflow tip combined with a back pressure of 1-2 psi. The cone voltage was set at 42 V, LM/HM Resolution 12/12 and the MCP at 2300V. Data were acquired over the m/z range 400-1600. Raw data was processed using the MaxEnt1 algorithm included in the MassLynx program.

2.11 **Pyridylethylation of purified toxin**

In preparation for amino acid sequencing, and to determine the number of cysteines, the toxin was reduced with dithiothreitol (DTT) and cysteine residues were pyridylethylated using 4-vinylpyridine (4VP) (Sigma-Aldrich, Castle, Hill, Australia) to prevent refolding. The peptide was dissolved with distilled water to a final volume of 100 µl and mixed with an equal volume of solution containing 250 mM Tris-base, 10 mM DTT and 2 mM EDTA buffered to pH 8.1 using 100% glacial acetic acid. Following incubation at 65°C for 15 minutes, 5 µl of 4VP and 20 µl of acetonitrile were added and the reaction was allowed to proceed in the dark for 20 minutes at room temperature (~23°C).

The pyridylethylated toxin was then immediately purified from the reaction mixture by rp-HPLC using an analytical C18 column and buffers as described in section 2.6. The unreacted, non-peptidic components of the mixture were eluted isocratically over 30 minutes at 5% ACN/0.1% TFA. The pyridylethylated toxin was then isolated using a linear gradient of 5-60% ACN/0.1% TFA over 55 minutes at a flow rate of 1 ml/min.

2.12 **N-terminal amino acid sequencing of toxin**

Freeze-dried peptide samples were sent to APAF where N-terminal amino acid sequencing was performed using Edman degradation.

2.13 **Insect electrophysiological experiments**

The whole-cell patch-clamp technique was used to examine the effects of neurotoxins on voltage-gated ion channel currents in neurons of insects. Patch-clamp studies are useful in probing the mechanism and function of ion channels, and have been used in insects as small as the common fruit fly, *Drosophila melanogaster* (Wu et al., 1983). Voltage-clamp recording using the patch-clamp technique was chosen because it allows high sensitivity and high resolution recording of ionic currents passing through the pore of ion channels as they open and close as a function of membrane voltage potential and time

(Hamill et al., 1981). By changing the whole cell membrane potential, and by using a feedback circuit, the currents flowing through the channels can be measured and visually displayed (Narahashi et al., 1994).

Cockroaches were chosen as the source of neurons because „insects of economic importance do not possess large neurons suitable for the application of conventional electrophysiological and neurochemical methods" (Pinnock and Sattelle, 1987), with the exception of cockroach neurons, which are ideal because of their large neuronal cell body diameter.

2.13.1 Research animals

Live adult American cockroaches (*Periplaneta americana*) were supplied by the School of Medical and Molecular Biosciences at UTS. The cockroaches were bred in large plastic containers at 37°C on a diet of commercially available dog biscuits with free access to drinking water. Around 6-8 cockroaches were dissected to obtain enough neurons for each patch-clamp experiment.

2.13.2 Selection of cockroach neuron for patch-clamp experiments

All electrophysiological experiments on insects were performed using the whole-cell patch-clamp technique on dissociated dorsal unpaired median (DUM) neurons from *P. americana* cockroaches that were maintained in short-term culture.

DUM neurons are a distinctive group of neurosecretory cells (Lapied et al., 1990) that are known to be present in the neuronal ganglion of many economically important insects (Pfluger and Watson, 1988), including cockroaches, locust (Plotnikova, 1969), and cricket (Clark, 1976) species.

DUM neurons modulate skeletal and visceral muscle activity in a role analogous to that of the sympathetic nervous system in vertebrates (Pfluger

and Watson, 1988). They regulate vital functions (e.g. cardiac muscle activity) through the release of the neurotransmitter octopamine (Sinakevitch et al., 1996) and express a variety of ion channels including voltage-activated calcium (Ca_v), sodium (Na_v) and potassium (K_v) channels (Grolleau and Lapied, 2000). In cockroaches, DUM neurons are found inside the ganglia located in the abdominal segment of the ventral nerve cord (Nassel, 1996). They are easily identified under a phase contrast microscope due to their large size (~30-60 μM diameter) and characteristic teardrop-shape (Figure 2.10) (Stevenson and Sporhase-Eichmann, 1995).

25 μM

Figure 2.10: Light micrograph of an isolated dorsal unpaired median (DUM) neuron.

2.13.3 Dissection and isolation of DUM neurons

DUM neurons were isolated from the terminal abdominal ganglia (TAG) of adult *P. americana* using methods modified from Grolleau and Lapied (1996) and Wicher and Penzlin (1997). A mixture of up to eight male/female cockroaches were selected one day before the experiment and were immobilised by placing them into a -20°C freezer for 5 minutes. Using aseptic techniques inside a laminar flow hood, cockroaches were pinned onto a petri dish that had been previously prepared with a Sylgard silicone elastomer base (Dow Corning, USA). The dorsal cuticle and underlying muscle, fat and gut tract were carefully removed using fine sterilised surgical scissors to expose the ventral nerve cord (Figure 2.11A) and TAG.

The TAG is the 6th abdominal ganglion in the cockroach and contains the somata of large nerve fibres (known as „giant fibres"). A close-up view is shown in Figure 2.11B. The TAG forms an upside down Y-shaped branch and

is identified by its large size and visible bundles of axons extending from the superior end of the ganglion and bifurcated cercal nerves radiating out of the left and right side of the ganglion to innervate the peripheral structures of the insect (Nation, 2002, Pfluger and Watson, 1988).

A   **B**

Figure 2.11: Dissection of terminal abdominal ganglia (TAG) from cockroach. (A) Top view of cockroach with dorsal cuticle removed and abdominal cavity exposed. The vertical white line is the ventral nerve cord and the TAG is located at the base of the cord. (B) The terminal abdominal ganglion (TAG) is connected to the superior ventral nerve cord and two branched inferior cercal nerves.

The TAG was removed by severing the superior and two inferior axon bundles (Figure 2.12) and subsequently placed into a sterile petri dish containing modified normal insect saline solution (Table 2.4). Whilst in the solution, the membrane sheath surrounding the TAG was carefully removed using iris scissors and forceps. This process was repeated until all of the TAGs were desheathed.

Figure 2.12: Close up view of excised TAG. The TAG is visible as an opaque white circular structure underneath the membrane sheath with projecting connective tissue.

Table 2.4: Composition of modified normal insect saline culture media for dissected terminal abdominal ganglia (TAG) of *P. americana* cockroach.

Chemical	mM	IU/ml	µg/ml
NaCl	200	-	-
KCl	3.1	-	-
HEPES	10	-	-
D-glucose	20	-	-
Sucrose	30	-	-
Pencillin**	-	2	-
Streptomycin**	-	-	2
pH 7.4 with NaOH			
Osmolality $\approx$ 440 mOsmol/L			

** Added to prevent bacterial growth (Trace Biosciences, Noble Park, Australia).

2.13.4 Enzymatic and mechanical separation of dorsal unpaired median neurons

The desheathed ganglia were placed into a 15 ml centrifuge tube containing normal insect saline (NIS) with Ca^{2+} and Mg^{2+}, collagenase (1 mg/ml) and hyaluronidase (1 mg/ml), and incubated at 37°C for 15-20 minutes to loosen the connective tissue surrounding the neurons. The enzyme-treated ganglia were then centrifuged, and the NIS/collagenase supernatant solution was removed by aspiration using a glass pipette. The ganglia were rinsed four times then suspended in 3 ml of NIS solution (Table 2.5).

A sterile pipette was used to physically separate the DUM neurons from the ganglionic membrane by mechanical trituration using a pipette. The purpose of trituration was to gently free the neurons from the surrounding support tissue by rapidly passing the ganglia in and out of the narrow tip of a heat-polished sterile Pasteur pipette. Trituration was stopped as soon as the culture medium appeared cloudy to the eye, indicating the liberation of a large number of neurons.

Table 2.5: Composition of normal insect saline culture media for dorsal median unpaired (DUM) neurons obtained from terminal abdominal ganglia (TAG) of *P. americana* cockroach.

Chemical	mM	% v/v	IU/ml	μg/ml
NaCl	200	-	-	-
KCl	3.1	-	-	-
$CaCl_2$	5	-	-	-
$MgCl_2$	4	-	-	-
HEPES	10	-	-	-
D-glucose	20	-	-	-
Sucrose	20	-	-	-
Bovine Calf Serum (BCS)	-	5	-	-
Pencillin	-	-	50	-
Streptomycin	-	-	-	50
pH 7.4 with NaOH				
Osmolality $\approx$ 440-450 mOsmol/L				

2.13.5 Culturing of DUM neurons

The separated neurons were distributed evenly into eight wells of a 24-well plate (Limbro, Ohio, USA), with each well containing a single autoclaved 12 mm diameter glass coverslip (Lomb Scientific, Taren Point, NSW). Each coverslip was previously coated with 1 mg/ml concanavalin-A (Type VI) (Sigma Chemicals, Castle Hill, NSW) to ensure adhesion of the neurons to the coverslips. The level of cell adhesion was somewhat variable and unpredictable, and in the latter parts of the project, concanavalin-A was replaced with BD Cell-Tak™ (BD Biosciences, Australia), a tissue adhesive formulated from polyphenolic proteins from the marine mussel *Mytilus edulis* (Waite and Tanzer, 1981). The plate was incubated for 12-24 hours at 37°C at 100% relative humidity, 10% CO_2 and 90% O_2. Cells were used the next day for electrophysiological experiments. This short-term culture of dissociated DUM neurons ensured that neurite outgrowth was limited and as a result cells

retained a smooth surface and spherical shape which enabled effective patch-clamp recording.

2.14 Mammalian electrophysiological experiments

Dorsal root ganglion (DRG) neurons of newborn rat pups were used for patch-clamp experiments on vertebrate ion channels.

2.14.1 Research animals

Late-term pregnant Wistar rats were supplied by the UTS Research laboratories at Gore Hill, and housed at the UTS School of Medical and Molecular Biosciences. The animals were kept at 26°C on a 12 hour light/dark cycle in stacked holding cages (30 x 45 cm). They were fed rodent pellets and water *ad libitum*. A single rat pup aged between 2 and 12 days provided enough DRG neurons for one day of electrophysiological experiments.

2.14.2 Dissection and isolation of mammalian neurons

To determine the effect of a toxin on mammalian voltage-gated ion channels, modified whole-cell voltage-clamp recording techniques developed by Hamil et al. (1981) were employed.

In preparation for the short-term culture of DRG neurons, single autoclaved round glass coverslips (12 mm diameter) (Lomb Scientific, Taren Point, NSW) were coated in 1 mg/ml poly-*D*-lysine (Sigma-Aldrich®, Castle Hill, NSW) and transferred to 4 x 6-well tissue culture plates (Linbro, Aurora Ohio, USA) using aseptic techniques.

The first step in the isolation of the DRG neurons was the physical removal of individual ganglia from a 2-5 day-old Wistar rat by dissection. A rat of either sex was selected for dissection on the afternoon prior to an electrophysiological experiment. The rat was anaesthetised by placing in a

closed glass jar, which contained cotton gauze soaked in approximately 1 ml isoflurane (Forthane) according to protocols approved by the UTS Animal Care & Ethics Committee (UTS/RNSH 0301-002A and UTS 2008-27 (formerly UTS/RNSH 0612-052A)). The rat was determined to reach a sufficient level of anaesthesia if there was a failure to evoke a withdrawal reflex upon gently squeezing the hind limb using a pair of forceps. All the procedures thereafter were performed in a laminar flow unit using aseptic techniques.

The rat was decapitated using a sharp surgical scissor and the dorsal skin surface was cut and parted with a single incision to exposure the spine. The vertebral column was removed after cutting the ribs and lumbar vertebrae to free the spinal column. The free vertebral column was transferred to a petri dish containing sterile Ca^{2+} - and Mg^{2+} -free phosphate buffered saline and 0.6% w/v glucose supplementation (CMF-PBS-glucose).

Using a dissecting microscope, the vertebral column was separated by longitudinal cuts through both ventral and dorsal walls, producing two hemisections and exposing the spinal cord. The spinal cord was removed using fine tweezers and individual DRG were carefully removed from between the vertebrae and transferred into a small petri dish containing CMF-PBS-glucose.

2.14.3   Enzyme treatment of dorsal root ganglion (DRG) neurons

Once the ganglia were physically removed from the spinal column, they were treated with the enzyme trypsin to weaken the capsule of connective tissue surrounding each ganglia. The ganglia were then transferred from the small petri dish to a centrifuge tube containing 2.5 mg/ml of trypsin in CMF-PBS-glucose solution (pre-incubated at 37°C) and incubated in a water bath at 37°C for between 18-23 minutes depending on the age of the animal (Table 2.6).

Table 2.6: Trypsin incubation times for newborn rats.

Age of animal (days)	Incubation time in 2.5 mg/ml trypsin (min)
2	18
3	19
4	21
5	23

After being taken out of the water bath, the ganglia were centrifuged at 500 rpm for 30 seconds to pellet the ganglia and the supernatant trypsin solution removed by aspiration. The ganglia were then resuspended in Dulbecco′s Modified Eagle medium (DMEM) containing newborn calf serum (10% v/v) and gentamycin (0.08 mg/ml). The resuspended ganglia were then spun at 500 rpm for 30 sec and the supernatant was removed and replaced with DMEM. This washing procedure was repeated three times. After the final wash the ganglia were re-suspended in 2 ml of the remaining DMEM culture media in preparation for mechanical trituration.

2.14.4   Trituration and tissue culture of DRG neurons

A sterile pipette was used to physically separate the neurons from the ganglionic membrane by mechanical trituration. The solution was evenly dispersed into each of 8 wells of a tissue culture plate containing 12 mm (round) glass coverslip that had been previously coated with 1 mg/ml poly-D-lysine to ensure adequate adhesion of the neurons.

The tissue culture plate was incubated overnight (37°C, 10% CO_2, 90% O_2 and 100% humidity) to allow the isolated neurons to settle and adhere to the coverslips. Cells were used for electrophysiological experiments within 24 hours.

2.15 Electrophysiological solutions

The composition of both the external and internal solutions was varied according to the cell type and the particular ion channel.

The contents, osmolarity and pH of the internal and external solutions used in patch-clamp experiments for recording voltage-gated calcium (Ca_v) and sodium (Na_v) channels in cockroach DUM neurons, and Ca_v channels in DRG neurons are detailed in Tables 2.6, 2.7 and 2.8, respectively.

Where a specific ion channel was being investigated, a combination of ion channel blockers was added to the external/internal solutions for each experiment to inhibit other undesired channel currents (Moore et al., 1967, Rudy and Iverson, 1997):

- Potassium channel blockers: Cs^+, tetraethylammonium, 4-aminopyridine (blocks fast inactivating channels)
- Calcium channel blockers: Ni^{2+}, Cd^{2+}, verapamil
- Sodium channel blockers: Tetrodotoxin

In patch-clamp experiments on Ca_v channels in cockroach DUM neurons, it was noted that time-dependent decay of current (known as rundown) was observed when Ca^{2+} was used as the charge carrier (Grolleau and Lapied, 1996). However Ba^{2+}, which is also conducted by Ca_v channels, has been reported to provide a more stable current over time when compared to Ca^{2+} (Wicher and Penzlin, 1997). Hence in all patch-clamp experiments on Ca_v channels in DUM neurons, Ba^{2+} (in the form of $BaCl_2$) replaced Ca^{2+} in the external solution in equimolar quantities for the purpose of preventing and reducing Ca_v current rundown.

Table 2.6: Composition of external and internal solutions for recording Ca_v currents from cockroach DUM neurons.

	External	*Internal*
Chemical	**mM**	**mM**
Choline chloride	160	50
TEA-Br	50	50
HEPES	10	10
$BaCl_2$	3	0.5
TTX	500	-
CsCl	-	30
ATP-Na$_2$	-	2
$BaCl_2$	-	0.5
EGTA	-	10
pH	7.4 with TEA-OH	7.25 with CsOH
Osmolarity	440 mOsmol/L	440 mOsmol/L

Table 2.7: Composition of external and internal solutions for recording Na_v currents from cockroach DUM neurons.

Chemical	External mM	Internal mM
NaCl	100	10
CsCl	5	-
CaCl$_2$	1.8	-
TEA-Cl	20	-
4-AP	1	-
HEPES	10	10
($\pm$)-verapamil.HCl	0.01	-
NiCl$_2$.2H$_2$0	0.1	-
CdCl$_2$	10	-
Cs acetate	-	135
MgCl$_2$	-	1
EGTA	-	5
pH	7.4 with NaOH	7.35 with CsOH
Osmolarity	440 mOsmol/L	440 mOsmol/L

Table 2.8: Composition of external and internal solutions for recording Ca_v currents from rat DRG neurons.

	External	Internal
Chemical	mM	mM
HEPES	10	10
$MgCl_2$	1	4
$BaCl_2$	10	-
TEA-Br	130	-
D-Glucose	10	-
TTX	500	-
CsCl	-	140
ATP-Na_2	-	2
EGTA	-	10
pH	7.3 with TEA-OH	7.25 with CsOH
Osmolarity	323 mOsmol/L	316 mOsmol/L

Abbreviations: ATP-Na_2, adenosine 5‴-triphosphate disodium salt; EGTA, ethylene glycol-bis(β-aminoethylether)-N,N,N‴,N‴-tetraacetic acid; 4-AP, 4-aminopyridine; HEPES, 4-(2-Hydroxyethyl)piperazine-1-ethanesulfonic acid ; TEA-Br, tetraethyl-ammonium bromide; TTX, tetrodotoxin

2.15 Electrophysiological whole-cell patch-clamp setup

The coverslip with its adhered neurons was placed on the floor of a glass-bottomed perfusion chamber (1 ml volume; RC Series, Warner Instruments, Connecticut, USA), which was mounted on the stage of a phase-contrast microscope (Lietz Labovert FS) (Figure 2.13).

Figure 2.13: Patch-clamp perfusion bath. The main compartment of the perfusion chamber was used to hold the coverslip in place and continuously bathe the neurons in external solution, which flowed in to the chamber via an attached tube on the left of the chamber. The fluid overflow passed into a smaller secondary chamber where it was sucked out by a metal tube to a waste reservoir by a suction pump. Cells were perfused via a perfusion needle delivering a controlled volume of solution into the main chamber. Note: The bath electrode, which would sit in the secondary chamber, is not shown in this photo.

Neurons were bathed in an iso-osmotic external solution using a pressurised 8-channel perfusion system (Automate Scientific, California, USA) that allowed for fast exchange between the external solution, and solutions containing the toxin.

The recording electrode consisted of a silver (Ag) wire coated with a composite of Ag/AgCl and provided the interface between the internal electrolyte solution and headstage input (Axon Instruments CV201). This was fitted to a recording microelectrode holder (Axon Instruments, CA, USA) (Figure 2.14). The electrode holder was connected to a long piece of tubing for physical application of suction to form a high resistance gigaohm seal on the neuron. Recording micropipettes were constructed from borosilicate glass-capillary tubing (1.5 mm outer diameter, 1.16 mm internal diameter, 7052 Glass; Harvard Apparatus Ltd., England) and individually pulled using a

Flaming/Brown flatbed electrode puller (Sutter Model P-87), and fire-polished using a microforge (model MF-83, Narashige Scientific Instruments Inc., Tokyo, Japan) to form a narrow and evenly rounded tip. The micropipettes were then filled with internal physiological solution approximating the ionic composition of the cell cytoplasm, and fitted to the recording electrode holder (Figure 2.14).

Figure 2.14: View of electrode and headstage. The recording electrode (lower left corner) connected to the headstage input mounted on a micromanipulator (top right corner). A thin polyethylene tube used for suction is attached to the microelectrode holder (bottom left).

The pH level was adjusted to 7.25 - 7.35 using CsOH. Experiments were carried out with micropipette resistances between 0.8-1.5 MΩ. The osmolarity of both internal and external solutions was adjusted to ~440 mOsmol/L by the addition of sucrose and measured with a cryoscopic osmometer (Gonotec Osmomat, Model 030, Melbourne, Victoria).

The bath electrode was made from polyethylene tubing (1.5 mm outer diameter; A-M Systems Inc., Everet, USA) and filled with 3% agar in 3 M KCl. This was fitted to the bath electrode holder (World Precision Instruments Inc., Sarasota, USA), which was composed of an Ag/AgCl pellet mounted into the base.

A micromanipulator (Sutter Instruments, CA, USA) held the electrode and headstage for correct positioning of the electrode and both the manipulator and microscope were mounted on a vibration isolation table (Newport Series 3036). The entire apparatus was isolated inside a Faraday cage and all equipment grounded to ensure that radio-frequency and 50 Hz mains interference was minimised (Figure 2.15). The recording micropipette was connected to a low-noise Axopatch 200A-integrating amplifier, and the signal filtered (internal 5 kHz low-pass Bessel filter). The amplified signal was then passed, via an ITC-16 channel A/D converter (Instrutech Corp), to an Apple Macintosh Centris 650 or Dell computer for data acquisition and analysis using the Axograph 4.0 program (Axon Instruments).

Figure 2.15: Electrophysiology apparatus. The apparatus was placed inside a metal Faraday cage on a vibration isolation table.

2.16 **Patch-clamp experimental procedure**

A single coverslip with attached neurons was transferred from the incubator to the perfusion bath on the stage of the microscope, in which the external solution was flowing at a constant rate of around 0.5 ml/min. A glass electrode was filled with internal solution and inserted into the microelectrode holder. By viewing through the microscope, a neuron was selected. The electrode was carefully lowered into the perfusion bath using the micromanipulator. The tip resistance was checked by applying a 5 mV line-frequency test pulse via the Axopatch 200A patch clamp amplifier and monitoring on the oscilloscope. The liquid junction potential (LJP) of the solutions (previously calculated using software program JPCalc (Peter H. Barry, UNSW) was taken into account by zeroing the holding current after applying the LJP .

Using the fine movement control of the micromanipulator, the tip of the electrode was positioned on the centre of the cell and lowered until the tip of the electrode made contact with the cell surface and observed on the oscilloscope as a slight increase in resistance to a 5 mV test pulse. Light suction was applied to the electrode to form a gigaohm seal between the cell membrane and electrode pipette tip („on-cell"), which was confirmed by an immediate reduction in the electrode tip resistance. The membrane holding potential was lowered to -90 mV using the patch-clamp amplifier. A quick suction was applied in order to break the through the seal of the cell membrane to allow diffusion between the intracellular and internal electrode pipette solutions („whole-cell") (Figure 2.16).
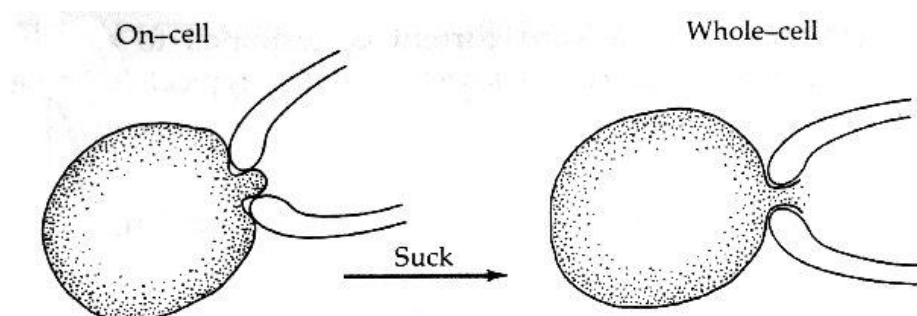
Figure 2.16: Representation of micropipette electrode forming gigaseal on cell.
Picture source: http://hebb.mit.edu/courses/8.515/lecture1/sld026.htm

Cells were rejected if ionic currents were too small (< 500 pA) to measure or the leakage current too large (> 1nA) due to a poor seal between the cell membrane and electrode. The series resistance was adjusted on the patch-clamp amplifier until capacitative currents were small and fast (>85% compensation), with care taken not to over-compensate. Leakage and capacitative currents were digitally subtracted using a *P-P/4* procedure.

The high seal resistance ensured that most of the currents originating in a small patch of membrane flowed into the pipette and current-measurement circuitry, with minimal level of background noise in the recording.

All recording traces were analysed off-line using the AxoGraph 4.0 software.

2.16.1 Voltage command protocols for calcium channel currents

At least two types of calcium channel currents have been demonstrated in Ca_v channels in cockroach DUM neurons, including high voltage-activated (HVA) Ca_v channel currents (Grolleau and Lapied, 1996, Wicher and Penzlin, 1997, Wicher et al., 2001) and mid/low voltage-activated (M-LVA) Ca_v channel currents (Grolleau and Lapied, 1996, Wicher and Penzlin, 1997). M-LVA and HVA Ca_v channel currents differ primarily in the voltage-dependence of activation and inactivation. The global M-LVA calcium channel current consists of a transient current (tLVA) that activates at a very negative membrane potential (-70 mV) and maintained current (mLVA), which is activated at a slightly more positive membrane potential (around -60 mV) (Grolleau and Lapied 1996).

In the present study, voltage command protocols were designed to evoke M-LVA and HVA subtypes of Ca_v channel currents. The currents were evoked by 100-ms pulses from a membrane holding potential (V_h) of -90 mV to depolarising potentials at 10-sec intervals to -20 mV or -30 mV for generation

of predominantly M-LVA currents (Figure 2.17A), and to +30 mV to evoke mainly HVA currents (Figure 2.17B). The voltage-dependence of calcium channel activation was recorded by applying 100-ms test pulses from the membrane holding potential of -90 mV to then +30 mV in 10-mV steps at 10-sec intervals (Figure 2.17C). Peak current amplitude was then plotted as a function of test potential, and I/V curves were fitted with Equation 5 (see section 2.16.3).
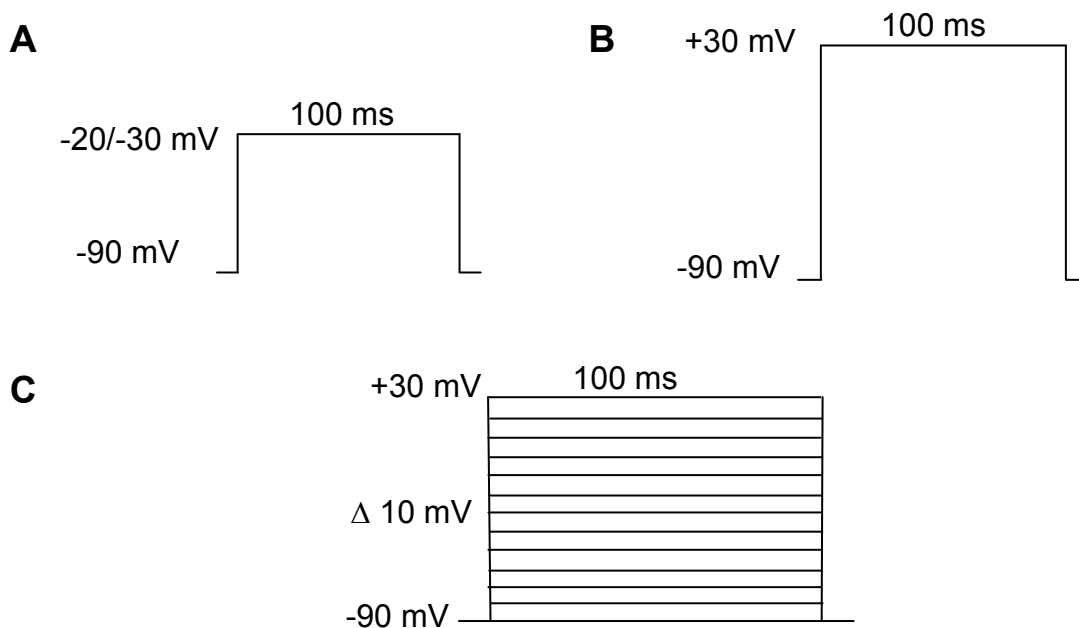
Figure 2.17: Voltage command protocols used for recording Ca_v channel currents in cockroach DUM neurons. All test pulses were 100-ms in duration, applied at 10-sec intervals. (A) Macroscopic Ca_v channel current protocol used to elicit maximal inward current. (B) HVA protocol used to selectively elicit maximal inward high-voltage activated Ca_v current. (C) Voltage-dependence of Ca_v channel (I_{Ca}/V) activation protocol.

2.16.2 Voltage command protocols for sodium channel currents

For examination of voltage-activated sodium (Na_v) channel currents in cockroach DUM neurons, a V_h of -80 mV was used. Currents were evoked by 50-ms test pulses to various depolarising potentials, at 10-sec intervals. A depolarising potential to -10 mV was used to record maximal inward sodium currents (Figure 2.18A). The voltage-dependence of Na_v channel (I/V)

activation was recorded by applying families of 50-ms command pulses from -80 mV to +70 mV in 10 mV steps (Figure 2.18B). Peak current amplitude was then plotted as a function of test potential, and *I/V* curves were fitted with Equation 5 (see section 2.16.3).

A

-10 mV
50 ms

-80 mV

B

+70 mV
50 ms

Δ 10 mV

-80 mV
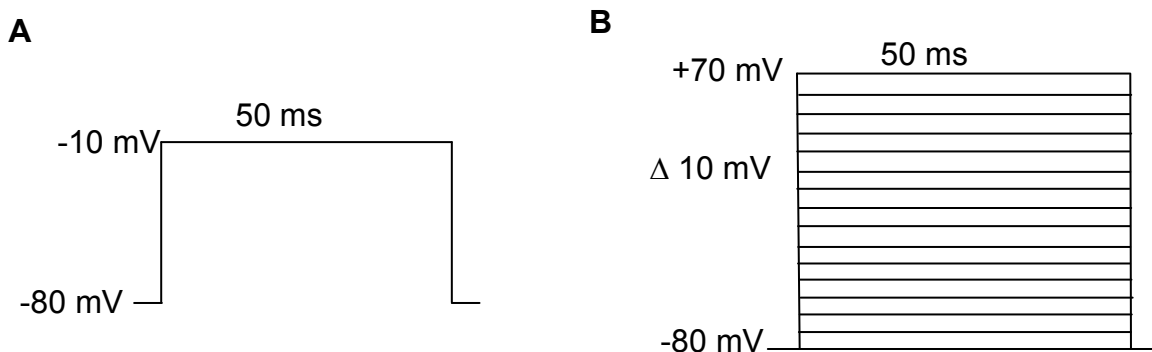
Figure 2.18: Voltage command protocols used for recording Na_v channel currents. All test pulses were 50 ms in duration, applied at 10-sec intervals. (A) Protocol, used to evoke maximal inward sodium channel currents. (B) Voltage-dependence of sodium channel activation (I_{Na}/V) protocol.

2.16.3 Data analysis

Data was analysed off-line following completion of the experiment. Mathematical curve fitting was done using Prism® v4.0 (GraphPad Software, San Diego, CA, USA) and were performed using non-linear regression analysis employing a least squares method. Concentration-response curves to determine IC_{50} values were fitted using the following equation:

$$y = \frac{1}{1 + ([x]/Conc_{50})^{n}_{H}} \qquad \text{(Equation 2)}$$

where x is the toxin concentration, n_H the Hill coefficient (slope parameter), and $Conc_{50}$ is the median inhibitory concentration causing block of membrane currents.

On-rates were determined by fitting time-course data with the following single exponential decay function:

$y = Ae^{-kx} + C$ (Equation 3)

where x is the time, A the normalised current value (usually 1.0) before application of toxin, and C is the final normalised current value following block by the toxin. The on-rate (τ_{on}) was determined from the inverse of the rate constant k.

Off-rates were determined by fitting time-course data with the following single exponential association function:

$y = C + A(1-e^{-kx})$ (Equation 4)

where x is the time, A the normalised current value after washout of the toxin (usually 1.0 if complete washout occurred), and C is the normalised current value prior to washout of the toxin. The off-rate (τ_{off}) was determined from the inverse of the rate constant k.

Current-voltage (*I/V*) curves were fitted using the following equation:

$$I = g_{max} \left(1 - \left(\frac{1}{1 + \exp[(V - V_{1/2})/s]} \right) \right) (V - V_{rev})$$ (Equation 5)

where *I* is the amplitude of the current at a given test potential *V*, g_{max} is the maximal conductance, $V_{1/2}$ is the voltage at half-maximal activation, *s* is the slope factor, and V_{rev} is the apparent reversal potential.

2.17 Synthesis of ω-hexatoxin-Hv1a and diselenide analogue

ω-hexatoxin-Hv1a (ω-HXTX-Hv1a) used in electrophysiology experiments was obtained by overproduction of a glutathione S-transferase (GST)-toxin fusion protein in *E. coli* cells using a previously described method (Tedford et al., 2001). Briefly, the recombinant fusion protein was purified from the soluble cell

fraction using affinity chromatography on glutathione sepharose, then the toxin was released by on-column thrombin cleavage and purified to >98% homogeneity using C18 rp-HPLC. The identity of the toxin was confirmed using ESI mass spectrometry.

The diselenide analogue of ω-HXTX-Hv1a was provided by Dr Aline Dantas de Araujo (Institute for Molecular Bioscience, University of Queensland) and was prepared by manual solid-phase peptide synthesis using HBTU as activation reagent and the stepwise *in situ* neutralisation protocol for Boc chemistry (Schnölzer et al., 1992). The amino acid side-chain protecting groups used were Cys(MeBzl), Thr(Bzl), Asp(OcHex), Arg(Tos), Ser(Bzl), Lys(ClZ), Glu(OcHex), Asn(Xan), and Tyr(BrZ). Boc-Sec(MeBzl)-OH was used for incorporation of selenocysteine residues (substituting cysteine positions 1 and 4). Synthesis of the toxin was carried out on a 0.3 mmol scale using MBHA resin. After assembly, 400 mg of each peptidyl resin was treated with 10 ml of HF:p-cresol:p-thiocresol (9:0.5:0.5) at 0°C for 90 min. Following evaporation of HF, crude peptides were precipitated and washed with cold diethylether, then redissolved in 50% acetonitrile/0.05% TFA, and lyophilised. The selenium analogue displayed oxidation of the two vicinal selenocysteine residues during the HF cleavage step. The unfolded peptides were purified using rp-HPLC on a Waters Delta Prep 3000 HPLC system using a preparative Vydac C8 column with detection at 220 nm. A linear gradient of 5-30% buffer B (0.043% TFA, 10% water in acetonitrile) in buffer A (0.05% TFA in water) was applied over 45 min at a flow rate of 50 ml/min.

The reduced peptide was folded/oxidised by dissolving 25 mg of pure linear peptide in 20 ml of buffer A and adding dropwise to 250 ml of oxidation buffer (0.1 M Mops pH 7.3, 0.2 M KCl, 1 mM EDTA, 2 mM GSH, 0.5 mM GSSG). The reaction mixture was stirred at room temperature for 12 h and quenched by adding a few drops of TFA. The mixture was diluted two-fold with water and the right isomer was purified by rp-HPLC using a preparative C18

column (Vydac) and a linear gradient of 5-20% buffer B over 30 min followed by an isocratic flow of 20% buffer B over 10 min at a flow rate of 8 ml/min.

3 Electrophysiological characterisation of the insect-selective toxin, ω-hexatoxin-Hv1a, from the venom of the Blue Mountains funnel-web spider (*Hadronyche versuta*)

Photo source: Australian Museum

Chapter 3 Summary

- ω-hexatoxin-Hv1a (ω-HXTX-Hv1a) is an orally-active arthropod-selective peptide neurotoxin from the venom of the Australian funnel-web, *Hadronyche versuta*, which may be a potential candidate for biopesticide development.

- ω-HXTX-Hv1a is a selective blocker of insect, but not mammalian voltage-activated calcium channels.

- Whole-cell voltage-clamping was undertaken to characterise the insect target of ω-HXTX-Hv1a using cockroach dorsal unpaired median neurons.

- ω-HXTX-Hv1a was found to reversibly inhibit both mid-low voltage-activated and high-voltage-activated insect calcium channel currents.

- Calcium current blockade is voltage-independent and occurs without alterations in the voltage-dependence of calcium channel activation suggesting that ω-HXTX-Hv1a is a channel pore blocker.

The major aim of this chapter was to further explore the potential of ω-HXTX-Hv1a as an insecticide lead by determining the voltage-activated calcium (Ca$_v$) channel subtype specificity of ω-HXTX-Hv1a and characterising the effects on insect Ca$_v$ channel currents. Firstly, it was necessary to distinguish the Ca$_v$ channel current subtypes. To this effect, electrophysiology experiments were performed under voltage-clamp conditions on cockroach (*Periplaneta americana*) dorsal unpaired median (DUM) neurons using voltage protocols and a range of different classical calcium channel blocking agents.

3.1 Voltage-gated calcium channel currents in cockroach DUM neurons
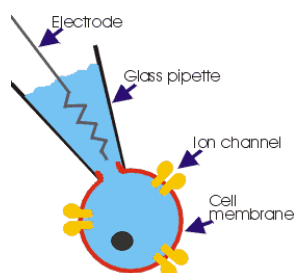
Voltage-activated (otherwise known as voltage-gated or voltage-dependent) calcium channels mediate the influx of Ca^{2+} through the plasma membrane into cells and are found in abundance in excitable tissues such as nerves and muscles (Messutat et al., 2001, Muth et al., 2001). Ca$_v$ channels are particularly promising as a new insecticide target because of their central role in synaptic transmission, neurotransmitter release, muscle contraction and hormone secretion (Mills and Pitman, 1997).

In mammals and other vertebrates, neuronal Ca$_v$ channels are divided into two major groups and several subtypes that are classified by their distinct electrophysiological and pharmacological properties. These are:

- **Low- and mid-voltage-activated (LVA, M-LVA)** Ca$_v$ channels (T-type and class E channels) (Nowycky et al., 1985, Ellinor et al., 1993, Soong et al., 1993); and

- **High voltage-activated (HVA)** Ca_v channels (L-, N-, P/Q-, and R-type channels) (Catterall, 2000, Dolphin, 2006).

In medical pharmacology, the distinction between Ca_v channel types is clinically important, for example, small organic blockers such as dihydropyridines, phenylalkylamines and benzothiazepines specifically target L-type Ca^{2+} channels and are widely prescribed for treating cardiovascular disease and migraine (Snutch et al., 2001).

Compared to vertebrates, less is known about invertebrate Ca_v channels. However they appear to play an equally important role in modulating cellular excitability and neurotransmitters. This is highlighted by the fact that the genome of the common fruit fly, *Drosophila melanogaster* contains α subunit genes for homologs of the mammalian L-type and N-type calcium channels (Adams et al., 2000), as well as a T-type calcium channel (Littleton and Ganetzky, 2000, King et al., 2008a). A mutation or severe loss of function in these genes is lethal to insect embryo (Eberl et al., 1998, Smith et al., 1998, Kawasaki et al., 2002).

Previous patch-clamp studies on cockroach DUM neurons noted at least two main Ca_v channel current components: mid/low-voltage-activated (M-LVA) and high voltage-activated (HVA) calcium currents (Grolleau and Lapied, 1996, Wicher and Penzlin, 1997), and these can be differentiated based on their sensitivity to different calcium channel blockers, but also in their voltage-dependence of activation and inactivation (Grolleau and Lapied, 2000).

Although there are some similarities in the kinetic properties to vertebrate Ca_v channels, the pharmacological profile of calcium currents in cockroaches was found to be very different from vertebrate currents (Wicher and Penzlin, 1997). It has been postulated that DUM neuron M-LVA Ca_v channel currents have no similarity with classical LVA currents characterised in vertebrates because DUM neuron M-LVA currents are not affected by the vertebrate LVA current

blockers, amiloride or flunarizine (Grolleau and Lapied, 2000). Given that classical vertebrate Ca_v channel blockers may not be effective at separating invertebrate Ca_v channel currents, the aim of these experiments were to elicit M-LVA and HVA Ca_v channel currents in DUM neurons and try to isolate each component using methods that were reported in literature to separate Ca_v channel current subtypes in vertebrates and/or invertebrates. This was done via the whole-cell patch-clamp technique using voltage-clamp protocols and application of the following pharmacological agents:

- ο ω-conotoxin-MVIIC
- ο SKF-96365
- ο Ni^{2+}

3.1.1 Use of voltage protocol to elicit **Ca_v channel** current subtypes

In all patch-clamp experiments, barium ions were used as a substitute for calcium ions to act as charge carriers through Ca_v channels due to barium"s favourable properties of reduced time-dependent current decay (rundown). Using the voltage protocol shown in section 2.16.1, a family of inward barium currents (I_{Ba}) of various amplitudes was recorded across different membrane voltages and typical current traces are shown in Figure 3.1. The macroscopic response to a depolarising voltage step consisted of an increased inward current rising to a peak, followed by a decreased inward current during sustained depolarisation. When the voltage step returned to the resting membrane potential at the end of the pulse, there was a transitory increase in inward current (tail current) due to the increased driving force on ions passing through the open channels, followed by a very rapid decrease as a result of channel deactivation. Typical current traces are shown in Figure 3.1A-D.

Current-voltage (I-V) relationships (Figure 3.1E) showed that the threshold for activation of channel opening occurred at membrane potentials around -65 mV. The maximal peak current was reached at around -35 to -10 mV and a progressive decrease in peak I_{Ba} was observed at more positive potentials.
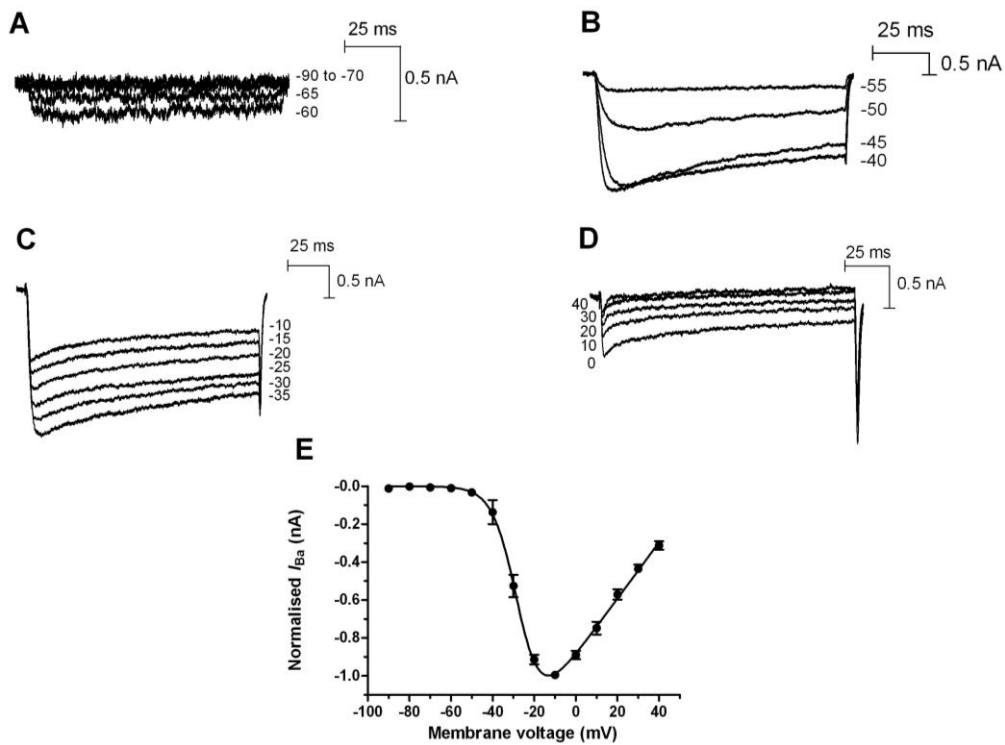
Figure 3.1: Voltage-dependent activation of Ca_v channels in DUM neurons. Typical traces showing family of barium currents recorded by depolarising command pulses for 100-ms from a holding potential of -90 to -60 mV, increasing in increments of 5 mV or 10 mV (A), -40 mV (B), -35 mV (C) and positive potentials up to +40 mV (D). (E) Current-voltage (*I-V*) relationship for Ca_v channels in DUM neurons. The I_{Ba} were normalised to the maximal inward current (*n* = 4).

Two distinct types of I_{Ba} were observed as illustrated by current traces in Figure 3.2. Depolarisations to -20 and -30 mV caused a rapid large inward current with a slow decaying component (Figure 3.2Aa), which was consistent with a previously observed reduction in Ca^{2+}-dependent fast inactivation due to the use of Ba^{2+} as the charge carrier (Wicher and Penzlin, 1997, Kostyuk, 1999). Depolarisations to +30 mV elicited a smaller current with a fast decaying component (Figure 3.2Ab).

Aa   **Ab**
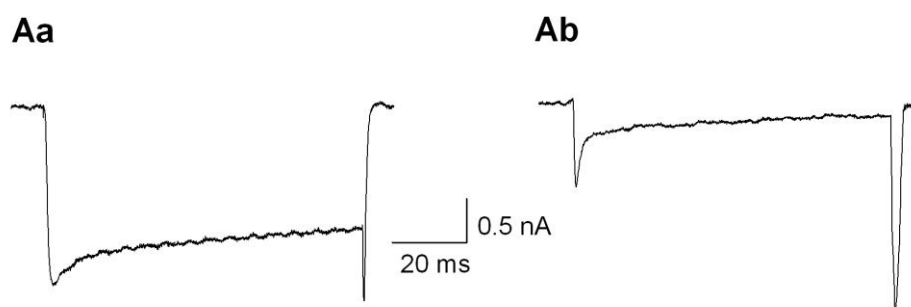
Figure 3.2: Typical Ba^{2+} currents (I_{Ba}) recorded from Ca_v channels in cockroach DUM neurons. I_{Ba} elicited by stepping from a holding potential of -90 mV to -20 mV (Aa) and +30 mV (Ab).

Cadmium has been reported to block both M-LVA ($IC_{50} \sim 10$ μM) and HVA ($IC_{50} = 5$ μM) Ca_v channel currents (Wicher and Penzlin, 1997, Wicher et al., 1994, Grolleau and Lapied, 1996) and was used to confirm that barium currents could be recorded in DUM neuron Ca_v channels. Indeed, current recordings showed that I_{Ba} evoked by depolarisation to -20 mV was almost completely inhibited within 3 mins after perfusion with 500 μM $CdCl_2$ (Figure 3.3).
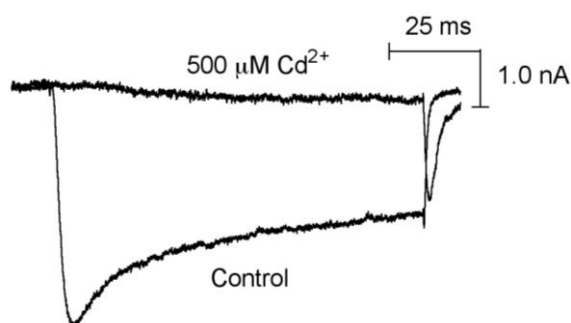
Figure 3.3: Effect of $CdCl_2$ on Ca_v channels in cockroach DUM neurons. Barium currents are carried by Ca_v channels. Typical superimposed trace of I_{Ba} elicited by test pulse to -20 mV before, and after, 5 min perfusion with 500 μM $CdCl_2$.

3.1.2 Effect of ω-conotoxin-MVIIC on M-LVA and HVA currents

There are around 500 species of the marine gastropods known as cone snails (*Conus*) that hunt fish, worms or other molluscs by injecting venom into its prey via a specialised harpoon and hypodermic needle apparatus

(Olivera, 2002). Cone snail venom contains a family of peptide toxins known as ω-conotoxins that have been used as tools for research into vertebrate Ca_v channel subtypes and as potential therapeutic leads. The ω-conotoxins bind to, and antagonise, vertebrate neuronal Ca_v channels (Olivera et al., 1984, Olivera et al., 1987, Feldman et al., 1987).

ω-conotoxin-MVIIC is a 26-amino acid peptide neurotoxin from the venom of *Conus magnus*. In rat vas deferens smooth muscle preparations, 1 μM ω-conotoxin-MVIIC completely inhibited the twitch contraction after 10 minutes (Hirata et al., 1997). The toxin binds with high affinity to vertebrate Ca_v channels in rat brain (IC_{50} ~ 1 nM) (Adams et al., 1993) and selectively inhibits high voltage-activated (HVA) Ca_v 2.1 and Ca_v 2.2 channels (Hillyard et al., 1992, Lewis et al., 2000, McDonough et al., 2002). Due to its selectivity for blocking HVA channels, ω-conotoxin-MVIIC is used as a pharmacological tool to test the effects of a chemical agent or biological toxin on LVA currents of vertebrate Ca_v channels (Randall and Tsien, 1995, Leão et al., 2000).

The blocking effect of ω-conotoxin-MVIIC on cockroach DUM neurons was previously investigated at 1 μM concentration (Wicher and Penzlin, 1997). In contrast to the effect on vertebrate Ca_v channel currents, it was noted that ω-conotoxin-MVIIC potently blocked M-LVA currents in cockroach DUM neurons and only weakly affected HVA currents. Based on these published results, ω-conotoxin-MVIIC was examined in this thesis to test whether the toxin preferentially blocks M-LVA Ca_v channel currents.
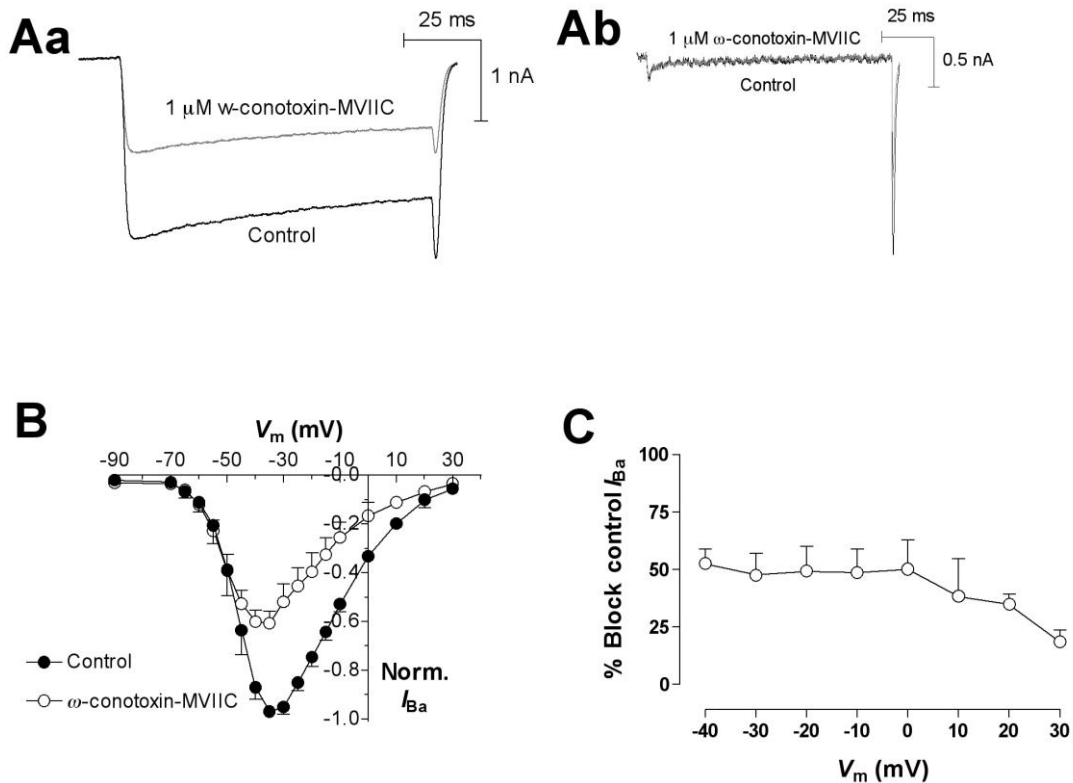
Figure 3.4: Effects of ω-conotoxin-MVIIC on Ca_v channels in cockroach DUM neurons. Typical currents elicited by depolarisation to -20 mV (Aa) or +30 mV (Ab) in the absence and presence of 1 μM ω-conotoxin-MVIIC. (B) Normalised current-voltage (I_{Ba}-V) relationships in the absence (closed circles) and presence (open circles) of 1 μM ω-conotoxin-MVIIC (n = 3). Data were fitted with Equation 5 in section 2.16.3. (C) % block of maximal control currents by 1 μM ω-conotoxin-MVIIC at various membrane potentials (n = 3).

Currents were recorded after perfusion of cockroach DUM neurons with a solution containing 1 μM ω-conotoxin-MVIIC. There was a reduction in peak I_{Ba} in DUM neurons of 48.4 ± 9.4% (n = 3) at a test pulse of -30 mV (Figure 3.4Aa) and 18.4 ± 9.6% (n = 3) at a test pulse of +30 mV (Figure 3.4Ab). Block of I_{Ba} was not reversible following washout with toxin-free external solution. *I-V* relationships (Figure 3.4B) showed that ω-conotoxin-MVIIC caused inhibition of peak I_{Ba} at test voltages above -50 mV. Increased block of peak I_{Ba} was observed at negative (M-LVA) test potentials (Figure 3.4C) but there was evidence of persisting HVA Ca_v channel currents. Based on these results, ω-conotoxin-MVIIC was not considered to be useful as a selective blocker of M-LVA Ca_v channels in cockroach DUM neurons for this project.

3.1.3 Effect of SKF-96365 on M-LVA/HVA calcium currents

1-[β-(3-(4-Methoxyphenyl)propoxy)-4-methoxyphenethyl]-1H-imidazole hydrochloride, 1-[2-(4-Methoxyphenyl)-2-[3-(4-methoxyphenyl)propoxy]ethyl]imidazole, or, SKF-96365, is a low molecular weight (MW = 402.91 Da) organic chemical that inhibits receptor-mediated calcium ion entry in various vertebrate cell and tissue types (Merritt et al., 1990). SKF-96365 also blocks voltage-gated L-type (LVA) Ca_v1 channels in vertebrate smooth muscle cells (Uchida et al., 2000) and more recently, was shown to potently inhibit voltage-gated T-type (LVA) Ca_v3 channels in vertebrates (Singh et al., 2010).

To determine if SKF-96365 blocks LVA Ca_v channels in insects, SKF-96365 was tested on cockroach DUM neurons. Voltage-clamp measurements revealed that 10 μM SKF-96365 noticeably depressed I_{Ba} at depolarisations to -20 mV (Figure 3.5A) and +30 mV (Figure 3.5B). There was reduction in I_{Ba} compared to maximal control I_{Ba} across all test potentials (Figure 3.5C). The level of I_{Ba} inhibition was relatively similar across voltage potentials (Figure 3.5D), suggesting that M-LVA and HVA Ca_v channels were both sensitive, hence SKF-96365 was ruled out as a selective pharmacological blocker of cockroach LVA Ca_v channels.
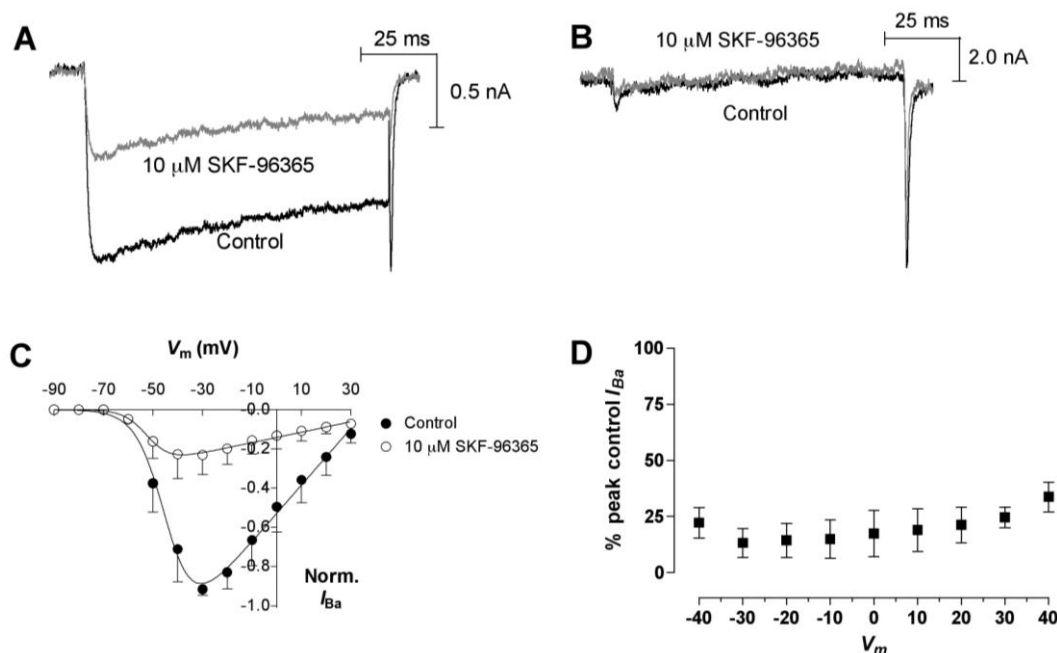
Figure 3.5: Effects of SKF-96365 on Ca_v channels in cockroach DUM neuron. (A-B) Whole-cell recording of barium currents at a test potential of -20 mV (A) and +30 mV (B) before, and after, addition of 10 μM SKF-96365. (C) Normalised current-voltage (I_{Ba}-V) relationships in the absence (closed circles) and presence (open circles) of 10 μM SKF-96365 (n = 3). Data were fitted with Equation 5 in section 2.16.3. (D) Relative amplitude of I_{Ba} as a percentage of peak control I_{Ba} in the presence of 10 μM SKF-96365 measured at various membrane test potentials (n = 3).

3.1.4 Effect of inorganic ions on calcium channels in DUM neurons

Previous studies noted that Ca_v channel currents of cockroach DUM neurons were sensitive to commonly used inorganic Ca_v channel blockers for vertebrate neurons such as Ni^{2+} and Cd^{2+}. Sensitivity to Ni^{2+} was largely voltage-dependent and M-LVA currents were effectively blocked by Ni^{2+} (IC_{50} =19-20 μM), but HVA currents were less affected by Ni^{2+} (IC_{50} = 40 μM) (Grolleau and Lapied, 1996, Wicher and Penzlin, 1997). The authors noted that these effects were similar to those observed in vertebrate neurons.

To test whether Ni^{2+} could be used to selectively block M-LVA Ca_v channel currents for this project, the effects of $NiCl_2$ on I_{Ba} amplitude was investigated before and after the addition of a high concentration of $NiCl_2$.

The *I-V* relationship was determined at each potential for peak I_{Ba} after application of 500 μM NiCl$_2$ (*n* = 3) (Figure 3.6A). There was voltage-independent block at all test potentials (*n* = 3) (Figure 3.6B).
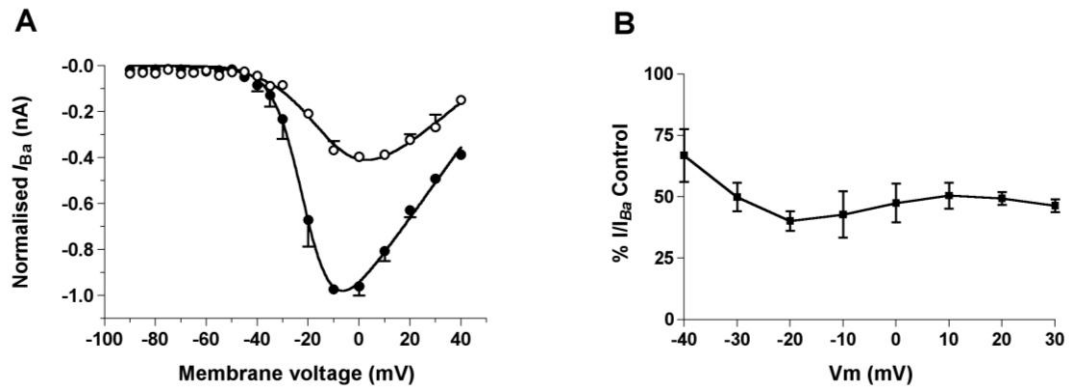
Figure 3.6: Voltage-independent block of peak I_{Ba} after addition of 500 μM NiCl$_2$. (A) *I-V* relationships of peak I_{Ba} before (closed circles) and 5 min after (open circles) addition of NiCl$_2$ (*n* = 3). Data were fitted with Equation 5 in section 2.16.3. (B) Block of peak I_{Ba} after addition of 500 μM NiCl$_2$ across different test potentials. Data represent percentage block of maximal control I_{Ba} (*n* = 3).

Figure 3.7 shows representative I_{Ba} recorded before, and after the addition of NiCl$_2$ at a membrane depolarisation from the holding potential of -90 mV to -20 and -30 mV (M-LVA currents dominating)(left panel) and +20 and +30 mV (HVA currents dominating)(right panel).

It is clear that like SKF-96365 and ω-conotoxin-MVIIC, NiCl$_2$ was unable to selectively block a specific subtype of Ca$_v$ channels in cockroach DUM neurons. This is most clearly revealed in the effects of NiCl$_2$ on the *I-V* relationship (Figure 3.6A).
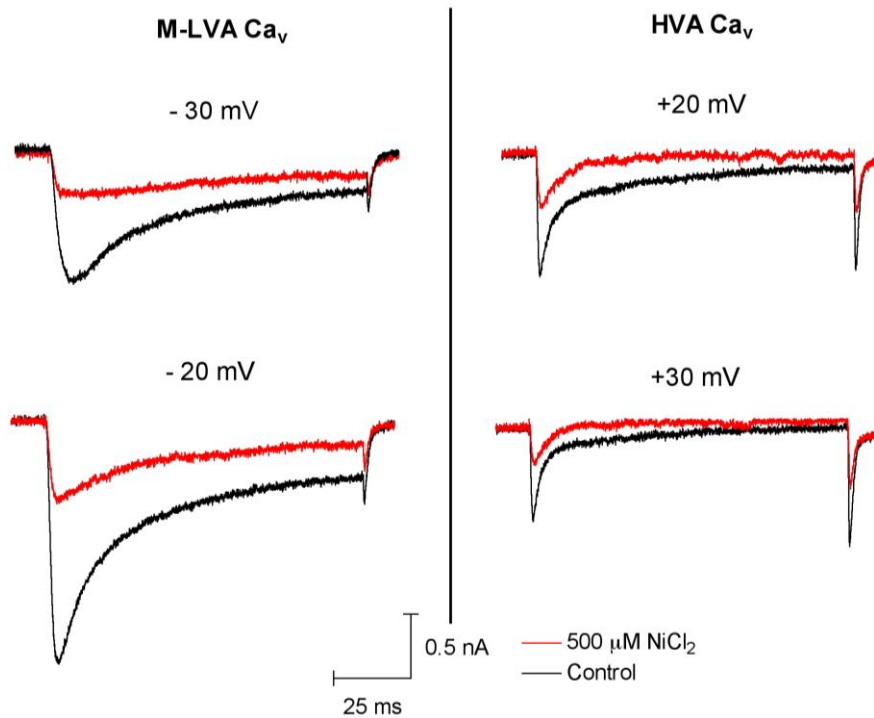
Figure 3.7: Effects of on $NiCl_2$ on Ca_v channels in cockroach DUM neurons. Typical traces showing effect of $NiCl_2$ on M-LVA I_{Ba} (left panel) and HVA I_{Ba} (right panel) before (black line), and after (red line), addition of 500 μM $NiCl_2$.

In this study, ω-conotoxin-MVIIC, $NiCl_2$ and SKF-96365 were investigated in an attempt to separate insect Ca_v channel current components. However, these classical pharmacological blockers for vertebrate neurons failed to selectively inhibit either M-LVA or HVA currents in cockroach DUM neurons. This confirms the observations of Wicher and Penzlin (1997) that the subtype profile of insect Ca_v channels is inconsistent with vertebrates and there is no single peptide, organic or inorganic blocker that can exclusively block one type of Ca_v channel. Therefore as previously reported by Wicher and Penzlin (1994, 1997), the most appropriate method for delineating Ca_v channel current subtypes for patch-clamp experiments is to program the voltage protocol to elicit M-LVA and HVA dominating currents by using two-step depolarising pulses from a holding potential of -90 mV to -20/-30 mV for M-LVA, and +20/+30 mV for HVA currents.

3.2 **Electrophysiological characterisation of ω-hexatoxin-Hv1a from Blue Mountains funnel web spiders (*Hadronyche versuta*)**

This section describes the electrophysiological characterisation of ω-HXTX-Hv1a, the prototypic insect-selective neurotoxin from Australian funnel-web spiders which is a promising insecticide lead molecule. The effect of ω-HXTX-Hv1a on insect Ca_v channels was investigated in DUM neurons of the cockroach *P. americana*.

3.2.1 Block of insect M-LVA and HVA Ca_v channels by ω-HXTX-Hv1a

ω-HXTX-Hv1a exerted a concentration-dependent block of M-LVA and HVA Ca_v channels. Figures 3.8 and 3.9 show the effects of increasing concentrations of ω-HXTX-Hv1a from 100 nM to 1600 nM on peak I_{Ba} current amplitude elicited by a 100-ms depolarising test pulse to -30 or +30 mV from a holding potential of -90 mV every 10 seconds. The addition of 300 nM ω-HXTX-Hv1a resulted in a block of peak I_{Ba} currents of 47 ± 6% (*n* = 3) within 4-5 minutes at -30 mV (Figure 3.8B) and 13 ± 11% (*n* = 3) at +30 mV (Figure 3.9B). At a concentration of 900 nM ω-HXTX-Hv1a, there was increased block to 85 ± 5% (*n* = 3) and 39 ± 13 % (*n* = 4) at -30 mV (Figure 3.8C) and +30 mV (Figure 3.9C), respectively. Complete block was achieved at concentrations greater than 1.6 μM.

The peak I_{Ba} current in the presence of ω-HXTX-Hv1a was expressed as a percentage of the control peak I_{Ba} current amplitude divided by the depressed peak amplitude after perfusion with the toxin, and this was plotted against toxin concentration. By fitting the concentration-response curve of the inhibition of peak I_{Ba} using a Logistic function (Equation 2 in section 2.16.3), the concentration at half-maximal block (IC_{50}) of M-LVA and HVA Ca_v channel currents was determined to be 279 nM (Figure 3.8F) and 1080 nM (Figure 3.9F), respectively.
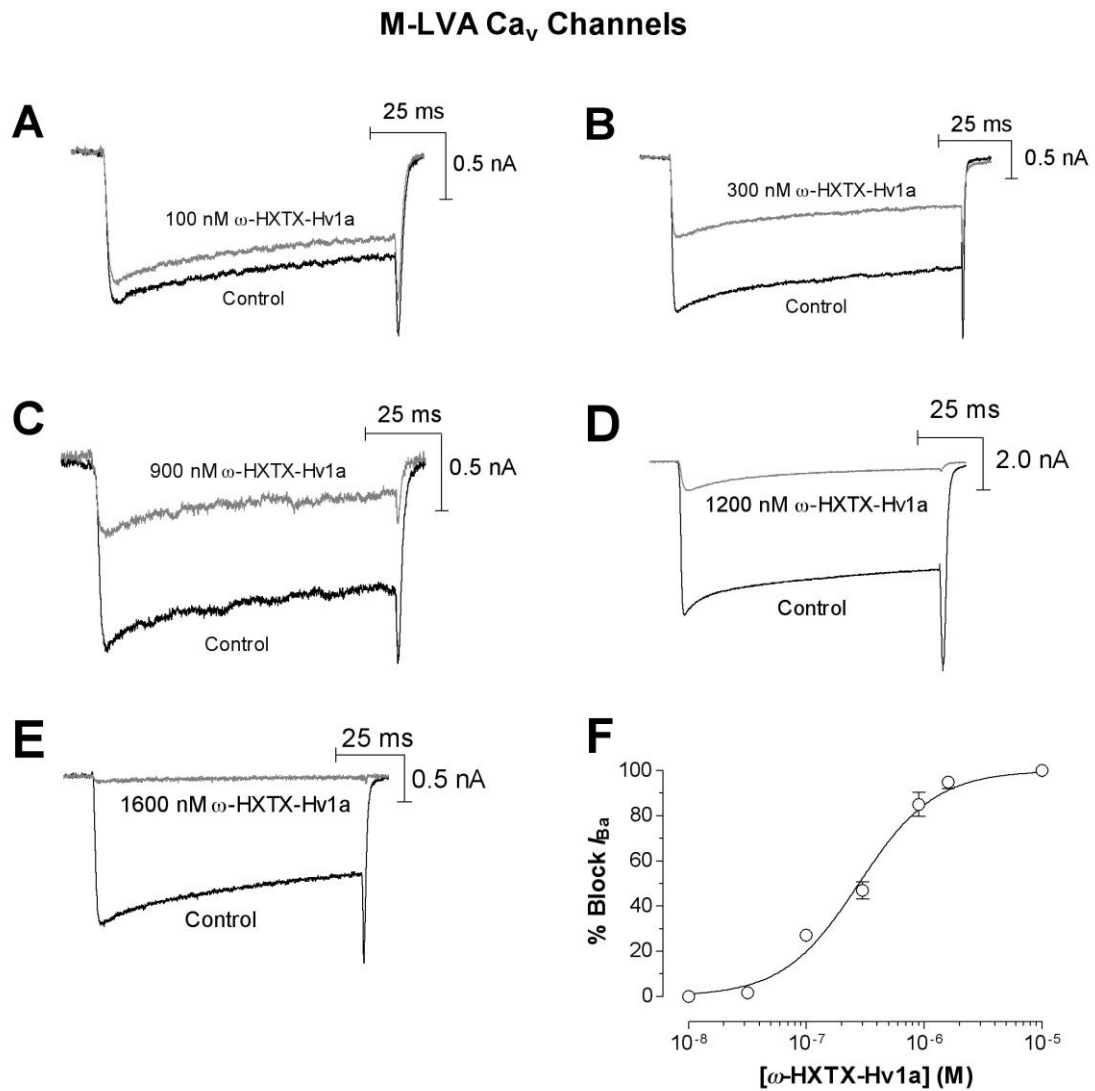
M-LVA Ca$_v$ Channels

Figure 3.8: Effects of ω-HXTX-Hv1a on low-voltage-activated (LVA) Ca$_v$ channel currents in cockroach DUM neurons. LVA currents in panels (A)-(E) were elicited by 100-ms depolarising test pulses to -30 mV from a holding potential of -90 mV. Panels show typical concentration-dependent inhibition of M-LVA I_{Ba} following perfusion with 100 nM (A), 300 nM (B), 900 nM (C), 1200 nM (D) and 1600 nM (E) ω-HXTX-Hv1a. (F) Concentration-response curve showing percentage block of M-LVA Ca$_v$ channel currents by ω-HXTX-Hv1a (n = 3-8). Data were fitted using Equation 2 in section 2.16.3.
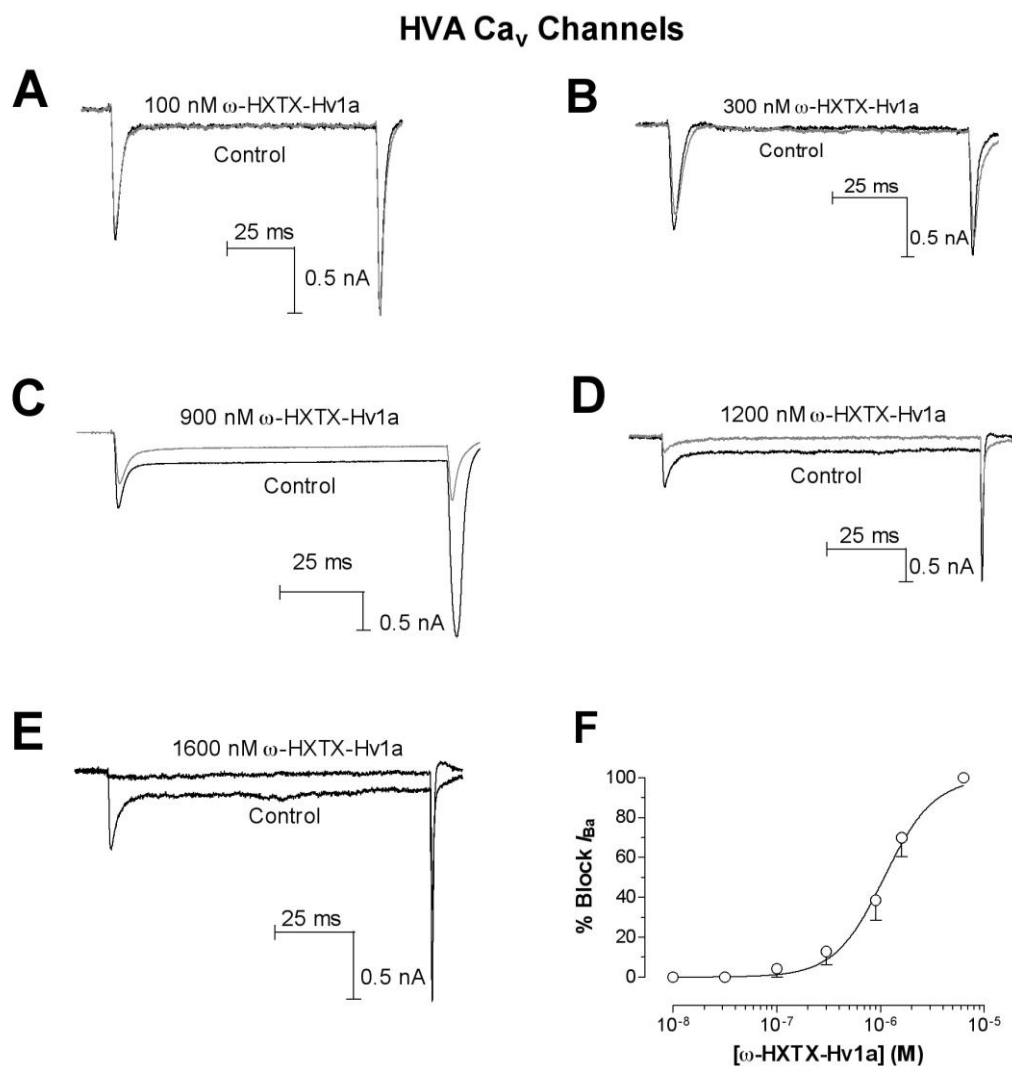
HVA Ca$_V$ Channels

Figure 3.9: Effects of ω-HXTX-Hv1a on high-voltage-activated (HVA) Ca$_V$ channels in cockroach DUM neurons. HVA Ca$_V$ channel currents in panels (A)-(E) were elicited by 100-ms depolarizing test pulses to +20 mV from a holding potential of -90 mV. Panels show typical concentration-dependent inhibition of HVA I_{Ba} following perfusion with 100 nM (A), 300 nM (B), 900 nM (C), 1200 nM (D) and 1600 nM (E) ω-HXTX-Hv1a. (F) Concentration-response curve showing percentage block of HVA Ca$_V$ channel currents by ω-HXTX-Hv1a (n = 3-8). Data were fitted using Equation 2 in section 2.16.3.

ω-HXTX-Hv1a failed to alter activation or inactivation kinetics of the Ca$_V$ channel and there was no significant effect on the time-to-peak current and time-course of current decay at all concentrations. The time-course of ω-HXTX-Hv1a association and dissociation were described by single exponential functions with a τ_{on} of 26.9 s for M-LVA Ca$_V$ channels and 29.6 s for HVA Ca$_V$ channels (Figure 3.10). The recovery after washout with toxin-

free external solution was slow but complete with an τ_{off} of 84.9 for M-LVA and 29.4 for HVA Ca_v channel currents. Similarly slow on- and off-rates have been previously noted in DUM neuron Ca_v channels with venom peptide toxins such as ω-conotoxin GVIA and ω-conotoxin MVIIC (Wicher and Penzlin, 1997) from marine *Conus* snails, and ω-ctenitoxin-Cs1a (previously CSTX-1) from *Cupiennius salei* (discussed further in Chapter 8).
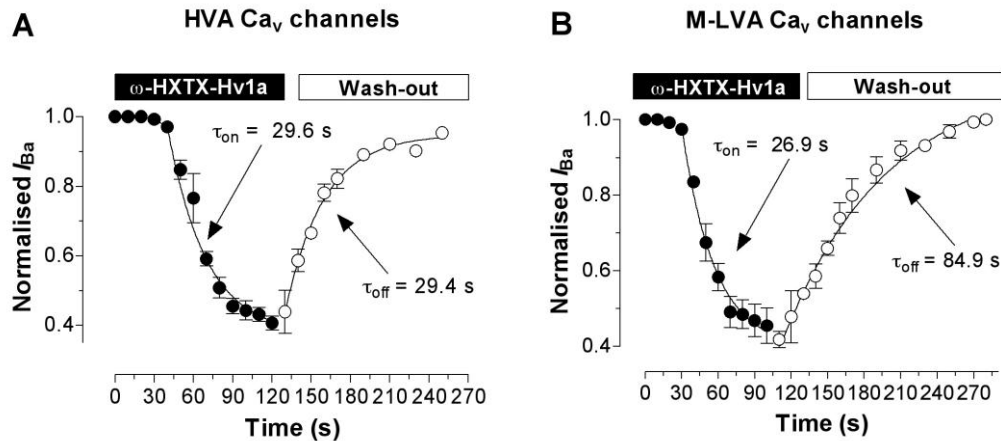
Figure 3.10: On- and off-rates for ω-HXTX-Hv1a. Rates were determined for HVA (A) and M-LVA (B) currents following application of 300 nM ω-HXTX-Hv1a and washout with toxin-free external solution (*n* = 5). Data were fitted using Equations 3 and 4 in section 2.16.3.

3.3 Effects of ω-HXTX-Hv1a on voltage-dependence of M-LVA and HVA channel activation

To determine whether ω-HXTX-Hv1a had any effect on the voltage-dependence of channel activation, families of I_{Ba} were generated by 100-ms test pulses from the membrane holding potential (-90 mV) to a maximum of +30 mV in 10-mV increments every 10 seconds. Typical effects of ω-HXTX-Hv1a on I_{Ba} were recorded before (Figure 3.11Aa), and after (Figure 3.11Ab), perfusion with 300 nM toxin. The *I-V* relationship was determined from the maximum I_{Ba} values at each membrane potential (Figure 3.11B). Data were normalised against peak maximal control I_{Ba} values and fitted with Equation 5 in section 2.16.3. A concentration of 300 nM ω-HXTX-Hv1a produced a voltage-independent block at all test potentials (Figure 3.11C).
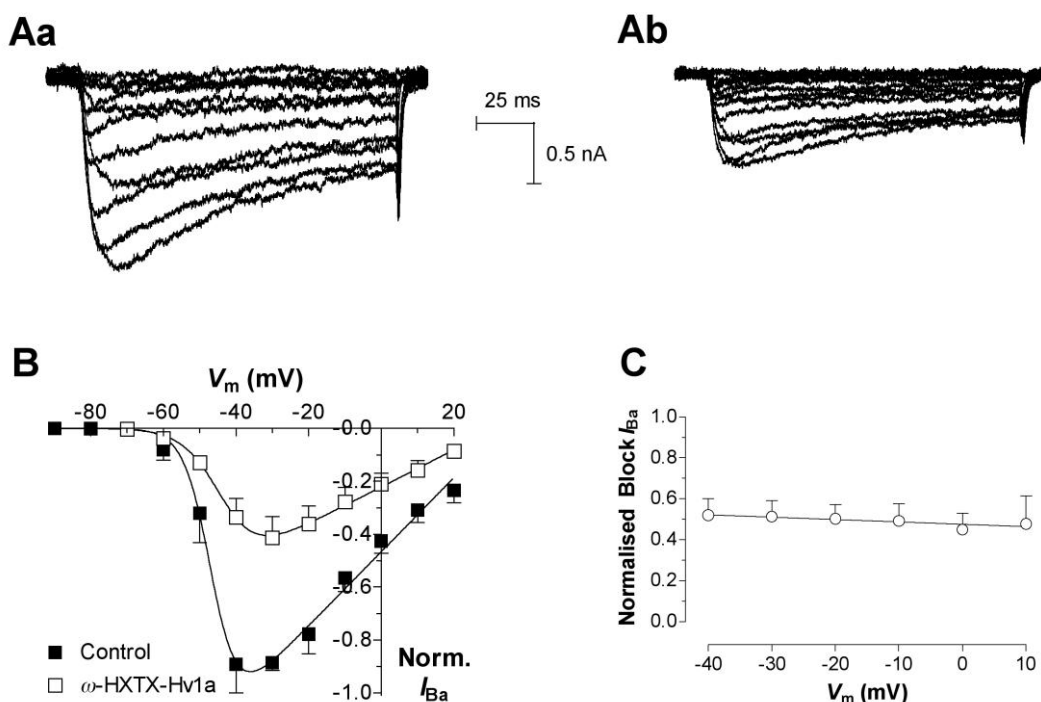
Figure 3.11: Effects of ω-HXTX-Hv1a on voltage-dependence of Ca_v channel activation. Families of Ca_v channel currents were elicited by depolarising test pulses to +30 mV from a holding potential of -90 mV in 10-mV steps. (A) Typical superimposed I_{Ba} traces recorded before (Aa), and after (Ab), perfusion with 300 nM ω-HXTX-Hv1a. (B) Peak I_{Ba}/V relationship recorded before (closed symbols), and after (open symbols), application of 300 nM ω-HXTX-Hv1a (n = 4). Data were fitted with Equation 5 in section 2.16.3. (C) Voltage-independent block of I_{Ba} by 300 nM ω-HXTX-Hv1a (n = 4). Data represent the normalised block at each test potential and were fitted by linear regression.

3.4 Diselenide ω-HXTX-Hv1a toxin

There has been significant interest in ω-HXTX-Hv1a as a potential template for insecticide development because of its insect-selectivity and target specificity toward insect Ca_v channels. Native ω-HXTX-Hv1 toxin has been proven to be orally active in some insects and ticks and has potential as a topical acaricidal agent (Khan, 2006, Mukherjee, 2006). Like many peptide toxins, ω-HXTX-Hv1a has multiple disulfide bonds that play a pivotal role in stabilising its 3D structure and biological activity. However disulfide-rich peptides pose a problem in that when attempting to synthesise the

molecule, it can be difficult to fold the peptide correctly *in vitro* due to isomerisation (Arolas et al., 2006, Bulaj and Olivera, 2008). In addition, peptide and protein frameworks with multiple disulfide bonds are generally unstable under biological reducing conditions and are susceptible to proteases, disulfide bond exchange reactions with thiols such as glutathione (Rabenstein and Weaver, 1996), a natural intracellular redox buffer present inside mammalian cells, as well as redox-active enzymes (Holmgren and Lu, 2010, Matthias et al., 2002). This reaction can have the potential for reduced potency or adverse effects in terms of drug design (Armishaw et al., 2006).

One effective method for solving these problems is to replace cysteines (Cys) with selenocysteine (Sec), a rare but naturally occurring amino acid that is identical to cysteine except for replacement of sulphur with selenium (Stadtman, 1996). Substitution of disulfide bridges with diselenide bridges in peptide conotoxins (referred to as selenoconotoxins) demonstrated excellent stability under reducing or scrambling conditions (Armishaw et al 1996) and allowed proper folding to occur without any change to the native conformation or biological activity (Armishaw et al., 2006, Gowd et al., 2010).

Furthermore, a synthesised diselenide version of κ-hexatoxin-Hv1c (previously κ-atracotoxin-Hv1c) from the venom of *Hadronyche versuta* funnel-web spider was equipotent with the native toxin in blocking calcium-activated potassium channel currents in cockroach DUM neurons, showing that the diselenide substitution does not affect the folding or function of the protein toxin (Mobli et al., 2009).

Recently, a diselenide ω-HXTX-Hv1a mutant was created by the Institute of Molecular Bioscience, University of Queensland with the replacement of one disulfide bond with a Sec[1,4] diselenide bridge. The toxin was tested on blowflies (*Lucilia cuprina*) to compare the oral activity of the diselenide analogue and native toxin in an arthopod species. Oral lethality tests in

blowflies showed that the LD_{50} at 72 hours was 38.3 ± 8 nmol/g for the native toxin and 100.1 ± 8 for the diselenide toxin (*n* = 3) (Figure 3.12; unpublished data).

Oral test in *L. cuprina*

- ■ native omega LD_{50}(3 day)= 38.3±8.1 nmol/g
- □ 1,4 Se omega LD_{50}(3 day)= 100.1±7.7 nmol/g
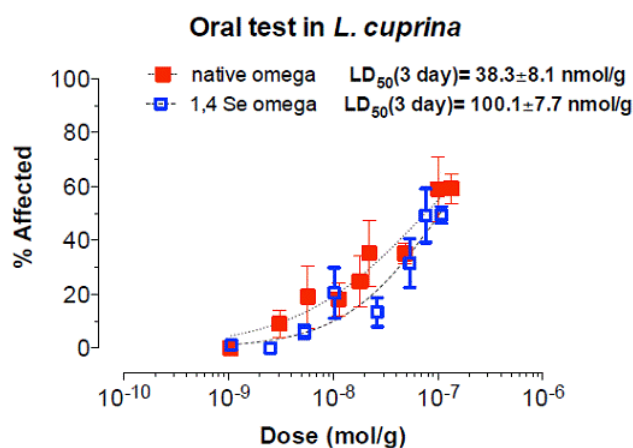
Figure 3.12: Oral toxicity test of Sec[1,4] diselenide bridged ω-HXTX-Hv1 toxin in blowfly (*L. cuprina*) (Volker Herzig and Glenn King, unpublished results).

For this thesis, a sample of 1,4 diselenide toxin analogue (see section 2.17 for method) was obtained from the Institute of Molecular Bioscience for testing on cockroach DUM neurons to compare the effect of the mutant toxin with the native toxin on M-LVA and HVA Ca_v channel currents in cockroach DUM neurons.

The Sec[1,4] diselenide toxin was tested at the M-LVA IC_{50} value of the native toxin, which was determined to be 278 nM (see section 3.2.1). Ca_v channel currents were elicited by a 100-ms depolarising pulse from the holding potential of -90 mV to -40 mV (M-LVA) and +20 mV (HVA) and recorded before, and after the addition of 278 nM diselenide ω-HXTX-Hv1a. There was 44.5 ± 8% block of peak I_{Ba} amplitude at -40 mV (Figure 3.13A) and 20 ± 10% block of peak I_{Ba} amplitude at depolarising pulses to +30 mV (Figure 3.13B). The barium *I-V* relationship was determined from the peak I_{Ba} values at each potential before, and after, perfusion with 278 nM Sec[1,4] diselenide toxin (Figure 3.13C). Similar to the native toxin, the diselenide toxin caused a block of peak I_{Ba} that was observed across a range of test potentials, and with no significant shift in the thresholds of activation. A paired t-test comparison of

maximal I_{Ba} block at a concentration of 278 nM showed there was no significant difference between the native and diselenide toxin in terms of block of peak I_{Ba} at M-LVA and HVA test potentials (Figure 3.13D).
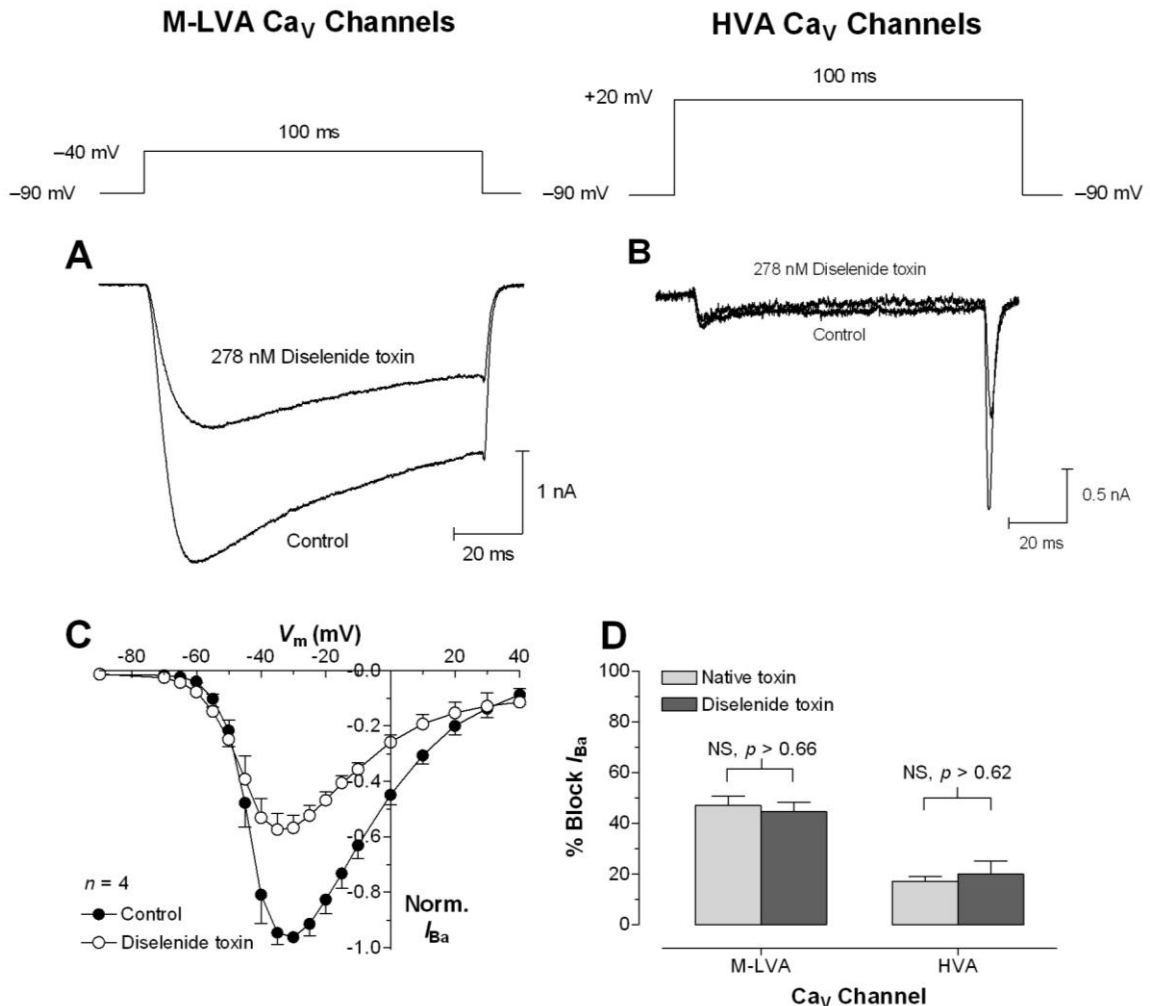
Figure 3.13: Effects of Sec[1,4] diselenide ω-HXTX-Hv1a on M-LVA and HVA Ca$_v$ channels in cockroach DUM neurons. M-LVA Ca$_v$ channel currents were elicited by a 100-ms depolarising pulse from a holding potential of -90 mV to -40 mV (A), and +20 mV (B), following perfusion with 278 nM. (C) Peak I_{Ba}/V relationship recorded before (closed symbols), and after (open symbols), application of 278 nM Sec[1,4] diselenide ω-HXTX-Hv1a (n = 4). Data represent normalised block at each test potential and were fitted with Equation 5 in section 2.16.3. (D) Block of peak I_{Ba} in M-LVA and HVA Ca$_v$ channels by native ω-HXTX-Hv1a (light grey block) and Sec[1,4] diselenide ω-HXTX-Hv1a (dark grey block) at a concentration of 278 nM. A paired t-test showed there was no statistical difference in block of maximal I_{Ba} between the two toxins.

4 Purification and characterisation of a novel insect-selective toxin, ω-hexatoxin-Ar1a from Sydney funnel web *(Atrax robustus)*

Declaration for Thesis Chapter 4

This chapter consists of the following publication:

Chong, Y., Hayes, J.L., Sollod, B., Wen, S., Wilson, D.T., Hains, P.G., Hodgson, W.C., Broady, K.W., King, G.F., Nicholson, G.M. 2007. The ω-atracotoxins: selective blockers of insect M-LVA and HVA calcium channels. *Biochemical Pharmacology*, **74, 623-38.**

I declare that my work constitutes a majority of this manuscript. The sections that were completed by the affiliate authors of the publication are:

- Peptide sequencing and mass spectrometry (sections 2.1, 3.3);
- Vas deferens vertebrate bioassay (sections 2.3, 3.2);
- DNA sequence (section 2.4, 3.4);
- Electrophysiological studies on sodium and potassium channels (sections 2.5, 3.7).

Youmie Chong: Date:

Prof. Graham Nicholson:

(Corresponding author/principal supervisor)   Date:

The ω-atracotoxins: Selective blockers of insect M-LVA and HVA calcium channels☆

Youmie Chong [a], Jessica L. Hayes [a], Brianna Sollod [b], Suping Wen [a], David T. Wilson [e], Peter G. Hains [c], Wayne C. Hodgson [d], Kevin W. Broady [a], Glenn F. King [b,1], Graham M. Nicholson [a,*]

[a] Neurotoxin Research Group, Department of Medical & Molecular Biosciences, University of Technology, Sydney, Broadway, NSW 2007, Australia
[b] Department of Molecular, Microbial & Structural Biology, University of Connecticut Health Center, Farmington, CT 06032, USA
[c] Save Sight Institute, Sydney Eye Hospital, Macquarie Street, Sydney, NSW 2001, Australia
[d] Monash Venom Group, Department of Pharmacology, Monash University, Clayton, Vic. 3800, Australia
[e] Institute for Molecular Bioscience, University of Queensland, St. Lucia, Qld 4072, Australia

ARTICLE INFO

ABSTRACT

The ω-atracotoxins (ω-ACTX) are a family of arthropod-selective peptide neurotoxins from Australian funnel-web spider venoms (Hexathelidae: Atracinae) that are candidates for development as biopesticides. We isolated a 37-residue insect-selective neurotoxin, ω-ACTX-Ar1a, from the venom of the Sydney funnel-web spider Atrax robustus, with high homology to several previously characterized members of the ω-ACTX-1 family. The peptide induced potent excitatory symptoms, followed by flaccid paralysis leading to death, in acute toxicity tests in house crickets. Using isolated smooth and skeletal nerve-muscle preparations, the toxin was shown to lack overt vertebrate toxicity at concentrations up to 1 μM. To further characterize the target of the ω-ACTXs, voltage-clamp analysis using the whole-cell patch-clamp technique was undertaken using cockroach dorsal unpaired median neurons. It is shown here for the first time that ω-ACTX-Ar1a, and its homolog ω-ACTX-Hv1a from Hadronyche versuta, reversibly block both mid–low- (M-LVA) and high-voltage-activated (HVA) insect calcium channel (Ca_v) currents. This block occurred in the absence of alterations in the voltage-dependence of Ca_v channel activation, and was voltage-independent, suggesting that ω-ACTX-1 family toxins are pore blockers rather than gating modifiers. At a concentration of 1 μM ω-ACTX-Ar1a failed to significantly affect global K_v channel currents. However, 1 μM ω-ACTX-Ar1a caused a modest 18% block of insect Na_v channel currents,

similar to the minor block of Na_v channels reported for other insect Ca_v channel blockers such as ω-agatoxin IVA. These findings validate both M-LVA and HVA Ca_v channels as potential targets for insecticides.

1. Introduction

The evolution of insect resistance to one or more classes of commonly used agrochemicals has now been reported in most major insect crop pests and disease vectors [1,2]. Over the period 1996–1998, pests were estimated to destroy around 18% of the world's food supply, with the major damage being caused by arthropods [3]. In addition, arthropods are vectors for the transmission of many new and re-emerging diseases of significant medical and veterinary importance [4]. This has necessitated the development of new strategies to combat highly resistant herbivorous and hematophagous pest species. New biological approaches include the production of transgenic crops that express insecticidal toxins from the soil bacterium *Bacillus thuringiensis* [5] and the release of insect-specific recombinant baculoviruses that express a variety of insecticidal neurotoxins from animal venoms [6]. Recent studies have investigated the potential of expressing ω-atracotoxins from the venom of Australian funnel-web spiders in plants or as orally active acaricidal agents [7,8].

The ω-atracotoxin-1 (ω-ACTX-1) toxins constitute the first family of insect-specific peptide toxins isolated from the venom of Australian funnel-web spiders (Mygalomorphae: Hexathelidae: Atracinae). These toxins are reported to inhibit insect, but not mammalian, Ca_v channels [9–12]. All family members are 36–37 residues in length, and contain six cysteine residues with a strictly conserved disulfide pattern. The three-dimensional solution structure of ω-ACTX-Hv1a comprises a structurally disordered N-terminus (residues 1–3), a core region rich in β-turns and disulfides (residues 4–21), and a β-hairpin (residues 22–37) that protrudes from the disulfide-rich core [10]. The three disulfide bonds form an inhibitory cystine-knot (ICK) motif that is present in the majority of atracotoxin structures determined to date, and which is common in peptide neurotoxins targeting ion channels [13–15]. Site-directed mutagenesis [11] and synthetic truncates [9] have been used to elucidate the toxin insectophore, the key residues involved in binding to the insect target site, of the prototypic family member ω-ACTX-Hv1a. The primary insectophore residues, Pro^{10}, Asn^{27} and Arg^{35}, form a small contiguous patch of ~200 Å^2 on one face of the toxin surface [11,12] (Fig. 1C). Residues Gln^9 and Tyr^{13} appear to be of minor functional importance in orthopterans and dictyopterans, but not dipterans, suggesting that there might be minor species-specific variations in the toxin insectophore (Fig. 1C).

These toxins are lethal over a wide range of arthropod orders including Acarina, Coleoptera, Dictyoptera, Diptera, Hemiptera, Lepidoptera, and Orthoptera [7,8,10,11,16–18]. ω-ACTX-1 toxins cause irreversible spastic paralysis, preceeding flaccid paralysis and death, yet no toxic effects have been reported following testing on vertebrate preparations. In insect preparations, ω-ACTX-Hv1a acts directly on CNS neurons rather than interganglionic axons or the peripheral neuromuscular junction [10,17]. Electrophysiological studies have shown that the phyletic specificity of this family of toxins is believed to be derived from their action on invertebrate, but not vertebrate, voltage-gated calcium (Ca_v) channels [10,12]. In preliminary experiments in unidentified cockroach metathoracic ganglia neurons, ω-ACTX-Hv1a partially blocked Ca_v channels at concentrations up to 1 μM. Competitive binding assays using radioiodinated ω-atracotoxin-Hv1a revealed that the toxin binds to orthopteran channels at nanomolar concentrations [12], whereas it had no effect on whole-cell Ca_v channel currents in a variety of vertebrate-derived neuron preparations at concentrations as high as 1 μM [10]. Moreover, the toxin does not block rat HVA $Ca_v1.2$ (L-type), $Ca_v2.1$ (P/Q-type) or $Ca_v2.2$ (N-type) channels at concentrations up to 10 μM [12]. However, the mode of channel block and the precise insect Ca_v channel subtype targeted by the ω-ACTX-1 toxins remains to be determined, and their potential action on other voltage-gated ion channels has not been investigated in detail.

Recently, ω-ACTX-Hv1a has been trialed as a novel biopesticide for protection of plants from phytophagous pest insects following expression of the toxin transgene in tobacco plants (*Nicotiana tabacum*). Transgenic expression of ω-ACTX-Hv1a effectively protected tobacco plants from the larvae of two recalcitrant agricultural pests, *Helicoverpa armigera* and *Spodoptera littoralis*, with 100% mortality at 48 h [7]. Surprisingly, a recombinant thioredoxin–ω-ACTX-Hv1a fusion protein was lethal to *H. armigera* and *S. littoralis* caterpillars when applied topically [7]. In addition, ω-ACTX-Hv1a is orally active against ticks [8] and mosquitoes (J. Huang, G. King, S. Wikel, unpublished data). These studies indicate that at least some insecticidal peptide toxins have the potential to be developed as orally active biopesticides.

Here we describe the pharmacological characterization of a novel member of the ω-ACTX-1 family that we isolated from the venom of the Sydney funnel-web spider, *Atrax robustus*. This 37-residue peptide, ω-ACTX-Ar1a, shows selective toxicity against house crickets, but it has no affect on vertebrate nerve-muscle preparations. We show that ω-ACTX-Ar1a and ω-ACTX-Hv1a block both M-LVA and HVA Ca_v channels in cockroach neurons, with minor activity against Na_v but not K_v channels. This block did not alter the voltage-dependence of Ca_v channel activation, and it was voltage-independent, suggesting that the ω-ACTX-1 toxins are pore blockers rather than gating modifiers. As far as we are aware, the ω-ACTX-1 toxins are the first peptide toxins demonstrated to selectively block both M-LVA and HVA insect Ca_v channels.

2. Materials and methods

2.1. Toxin purification and peptide sequencing

Venom was collected from female Sydney funnel-web spiders, *A. robustus*, via direct aspiration from the fangs. Venom was

then pooled and fractionated using reverse-phase high performance liquid chromatography (rpHPLC) employing a Vydac analytical column (C18, 4.6 mm × 250 mm, 5 μm) on a Shimadzu HPLC system. Peptide peaks were monitored at an absorbance of 215 nm. Elution of venom peptide components was achieved using a linear gradient of 5–25% acetonitrile/0.1% trifluoroacetic acid (TFA) over 20 min, then 25–50% acetonitrile/0.1% TFA over 20 min at flow rate of 1.0 mL/min. Selected fractions were subjected to acute toxicity bioassays using house crickets to determine insect toxicity (see Section 2.2). The major toxic fraction, ω-ACTX-Ar1a (peak 'f9' in Fig. 2A) was further purified on an analytical C18 rpHPLC column using a linear gradient of 5–14% acetonitrile/0.1% TFA over 5 min, then 14–16% acetonitrile/0.1% TFA over 20 min, at a flow rate of 1 mL/min (Fig. 2B). Purified toxin was collected, lyophilized, and stored at −20 °C until required. Toxin quantification was performed using a bicinchoninic acid protein assay kit (Pierce, Rockford, IL, USA) using bovine serum albumin as a standard. The molecular mass of the toxin was determined, via electrospray ionization quadrupole time-of-flight (ESI-Q-ToF) mass spectrometry using a Q-ToF2 system (Micromass, Manchester, England) equipped with a nanospray source. Data was manually acquired in the positive mode using borosilicate capillaries with a source temperature of 80 °C. Samples were dissolved in 5 μL 50% acetonitrile and 0.5% formic acid. A potential of 850 V was applied to the nanoflow tip. Raw data were processed using the MaxEnt algorithm included in the MassLynx program. In preparation for amino acid sequencing using Edman degradation, the toxin was reduced and cysteine residues were pyridylethylated with 4-vinylpyridine and purified using rpHPLC as described previously [10]. The entire peptide sequence was then obtained from a single sequencing run on an Applied Biosystems/Perkin-Elmer Procise 492 cLC protein sequencer.

ω-ACTX-Hv1a was obtained by overproduction of a glutathione S-transferase (GST)-toxin fusion protein in E. coli cells as described previously [11]. Briefly, the recombinant fusion protein was purified from the soluble cell fraction using affinity chromatography on glutathione-sepharose, then the toxin was released by on-column thrombin cleavage and purified to >98% homogeneity using C18 rpHPLC. The identity of the toxin was confirmed using ESI mass spectrometry [11].

2.2. Invertebrate toxicity assays

For quantitative analysis of insecticidal activity, purified toxin was dissolved in insect saline of the following composition (in mM): NaCl 200, KCl 3.1, CaCl$_2$ 5.4, MgCl$_2$ 4, NaHCO$_3$ 2, Na$_2$HPO$_4$, 0.1% (w/v) bovine serum albumin, pH 7.4. House crickets (Acheta domestica Linnaeus, 3rd–4th instar nymphs, sex not determined) of mass 50–100 mg were then injected with toxin at concentrations of 5–2000 pmol/g; injection volumes never exceeded 5 μL. An Arnold micro-applicator (Burkhard Scientific Supply, Rickmansworth, England) was used to make lateroventral thoracic injections between legs 2 and 3 using a 29-gauge needle. Ten crickets were injected at each concentration; a group of 10 control crickets each received an injection of insect saline only. Insects were monitored for 72 h following injection. Percentage knockdown and lethality were determined at 12, 24, 48

and 72 h post-injection. Knockdown was defined as the inability to maintain an upright posture, with intermittent or continuous twitches of appendages. Median knockdown (KD$_{50}$) and median lethal (LD$_{50}$) doses were then determined from log dose–response curves (see Section 2.6).

2.3. Isolated vertebrate bioassays

Vertebrate toxicity was investigated using isolated chick biventer cervicis nerve-muscle preparations as described previously [19]. Briefly, muscles were removed from male Australorp chicks (1–4 days old), mounted in 8-mL organ baths under 1 g resting tension, then bathed in Krebs–Henseleit solution containing (in mM): NaCl 118.4, KCl 4.7, CaCl$_2$ 2.5, MgSO$_4$ 1.2, KH$_2$PO$_4$ 1.2, NaHCO$_3$ 25.0, D-glucose 11.1, pH 7.4. The muscle was maintained at 34 °C and constantly carbogenated with 95% O$_2$ and 5% CO$_2$. Isometric twitch contractions were elicited by indirect stimulation of the motor nerve (supramaximal voltage, 0.05–0.2 ms, 0.1 Hz), via ring electrodes. Responses to exogenous acetylcholine (1 mM, 30 s) and KCl (40 mM, 30 s) were obtained prior to the addition of venom and at the conclusion of the experiment. For preparation of vas deferens tissue, Sprague Dawley rats (250–350 g) were killed by 80% CO$_2$ and decapitation. The vas deferens were isolated and bisected to obtain prostatic segments and mounted on electrodes in 5-mL organ baths at 32 °C under 0.75 g resting tension. Indirect twitches were evoked by electrical stimulation of the motor nerve (supramaximal voltage, 0.3 ms, 0.2 Hz). Preparations were allowed to equilibrate for at least 30 min with continuous stimulation before the addition of toxin or venom. All animal experimentation was approved by the Animal Care & Ethics Committees of the University of Technology, Sydney or Monash University. Responses were recorded for 30 min following the introduction of purified toxin to the organ bath at concentrations up to 1 μM. Contractions of muscles were recorded using a MacLab or PowerLab data acquisition system (AD Instruments, Castle Hill, NSW, Australia).

2.4. DNA sequence of the complete ω-ACTX-Ar1a transcript

2.4.1. Preparation of cDNA

Pairs of venom glands were dissected from one male and one female A. robustus spider, then poly-A+ mRNA was prepared from each pair of glands using a QuickPrep Micro mRNA Purification Kit (Amersham Pharmacia Biotech). cDNA libraries were constructed from the mRNA using a Marathon cDNA Amplification Kit (Clontech). From the adapted mRNA template, single-stranded cDNA was constructed using Superscript III reverse transcriptase (Life Technologies Inc.) and a poly-(dT) anchor primer. Second strand synthesis was carried out as per kit specifications using DNA polymerase I. The resulting double-stranded cDNA products were purified using a concert rapid PCR purification kit (GIBCO) then ligated to a Marathon cDNA amplification adaptor (Clontech) to provide a handle for rapid amplification of cDNA ends (RACE; [20]). Samples were ligated overnight at 16 °C, precipitated using glycogen–acetate–ethanol, then washed with 80% ethanol and dried for 10 min prior to resuspension in 200 μL of Tris-EDTA buffer.
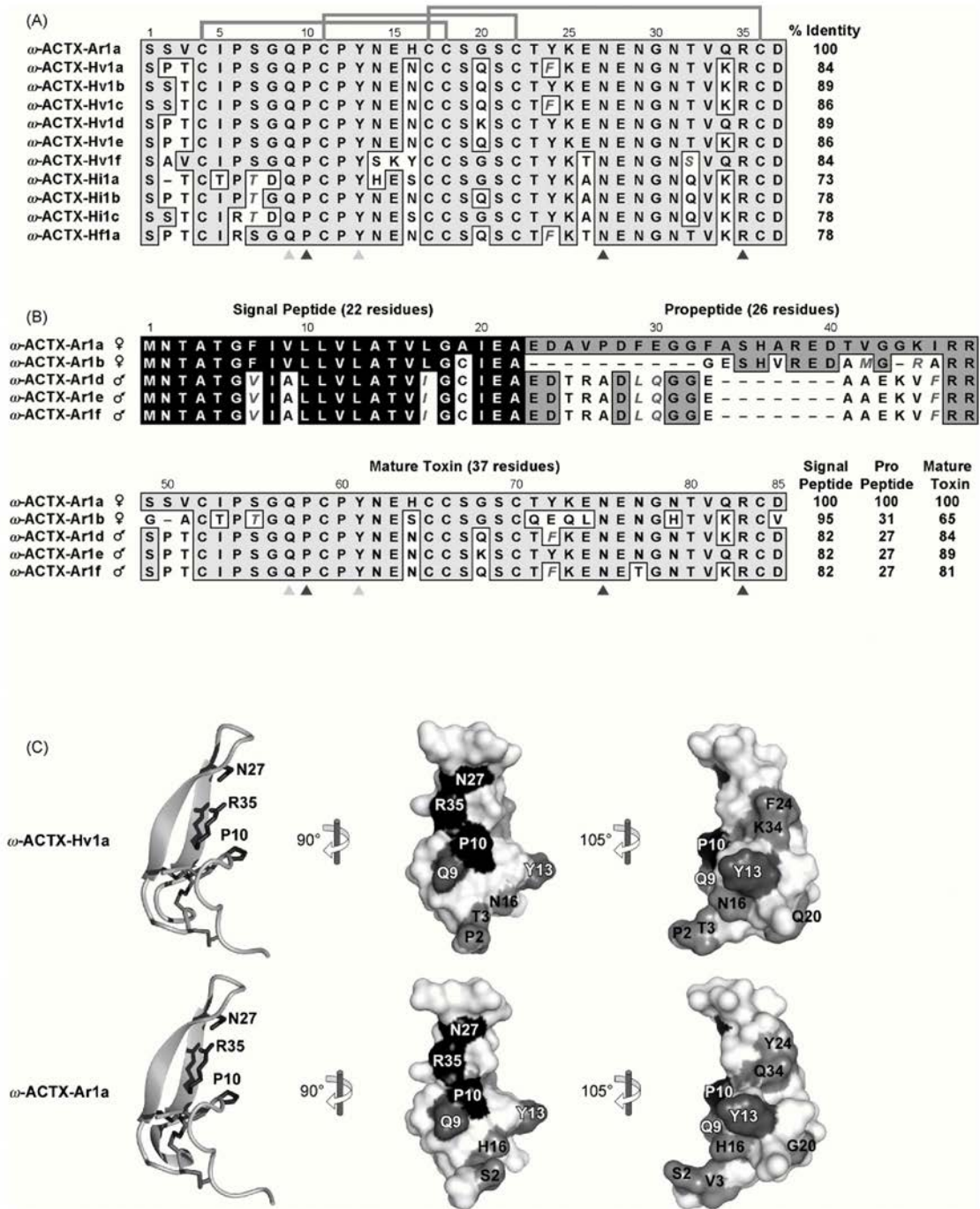
Fig. 1 – (A) Alignment of the primary structure of ω-ACTX-Ar1a with known members of the ω-ACTX-1 family, isolated from *Hadronyche versuta* (Hv), *Hadronyche infensa* (Hi) and *Hadronyche formidabilis* (Hf). Identities are boxed in gray, conservative substitutions are in grey italic text, and the disulfide bonding pattern of ω-ATCX-Hv1a is shown by the gray lines, connecting Cys residues, above the sequences. The major insectophore, identified for ω-ACTX-Hv1a [11], is shown by the black arrowheads beneath the sequences, while additional residues forming a minor insectophore in orthopterans and dictyopterans, but not dipterans, are in shown as gray arrowheads [12]. Note that these residues are conserved in the sequence of ω-ACTX-Ar1a. The column on the right indicates the % identity relative to ω-ACTX-Ar1a. (B) The primary

2.4.2. RACE analyses

The leader sequence of the mRNA transcript encoding ω-ACTX-Ar1a was obtained from 5′-RACE analysis [21], which employed a redundant 3′-primer based on the known amino acid sequence of the mature ω-ACTX-Hv1a toxin (5′-RTTNCCRTTYTCRTTYTCYTCRAA, where Y = T + C and N = A + G + T + C) and a 5′-universal adaptor primer (EchoAP1). A 3′-RACE primer based on the leader sequence obtained from 5′-RACE analysis was then used in combination with a 5′-universal adaptor oligo-d(T) primer (Clontech) to generate full-length sequences for ω-ACTX-Ar1a and paralogs. All primers not included in kits were constructed by PROLIGO Ltd.

2.4.3. PCR amplification and sequencing

PCR reactions were run on a thermal cycler using the following protocol: 95 °C for 5 min (1 cycle); 35 cycles of 95 °C for 30 s, 55 °C for 60 s, and 72 °C for 90 s; 72 °C for 10 min (1 cycle). Amplified cDNA products were electrophoresed on a 1.5% agarose gel and stained with ethidium bromide for size verification. Verified PCR products were extracted using a GIBCO gel purification kit, precipitated using Pellet Paint Co-Precipitant kit (Novagen), then phosphorylated in preparation for cloning. Samples were ligated into the pSMART vector (Lucigen) then transformed into E. cloni® competent cells using the CloneSmart Blunt Cloning kit (Lucigen). Successfully transformed clones were cultured for 1 h in Terrific Broth containing 50 μg/mL ampicillin, then plated to allow for overnight growth. Samples containing the expected insert size of ~500 bp (as verified using PCR and gel electrophoresis) were submitted for DNA sequencing.

2.5. Electrophysiological studies

Dorsal unpaired median (DUM) neurons, from the terminal abdominal ganglion (TAG) of the nerve cord of the male adult American cockroach Periplaneta americana, were isolated using methods modified from Grolleau and Lapied [22] and Wicher and Penzlin [23]. Median sections of the TAG, known to contain the highest number of DUM neurons [24], were dissected and individual DUM neurons were dissociated using a combination of mechanical and enzymatic separation techniques. The TAG was carefully dissected and placed in sterile Ca²⁺- and Mg²⁺-free insect saline of the following composition (in mM): 200 NaCl, 3.1 KCl, 10 N-2-hydroxyethyl-piperazine-N-2-ethanesulfonic acid (HEPES) and 60 sucrose. The ganglia were then desheathed and incubated at 37 °C for 15 min in Ca²⁺- and Mg²⁺-free insect saline containing collagenase (1 mg/mL) and hyaluronidase (1 mg/mL). The ganglia were then centrifuged and rinsed three times in
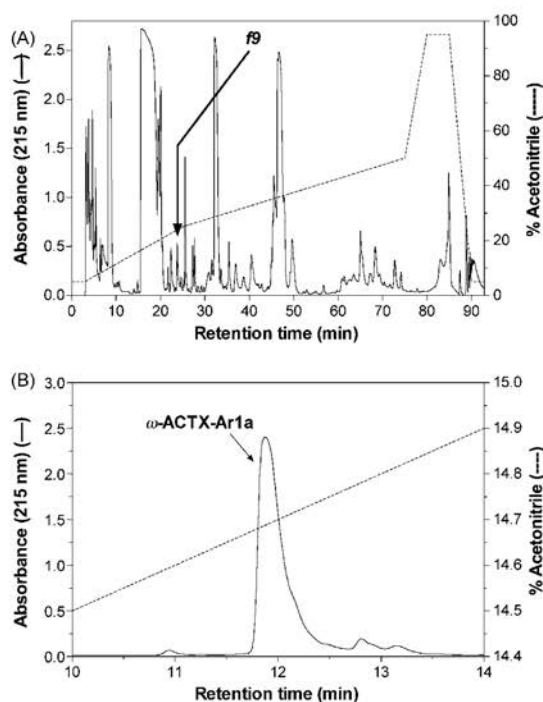
Fig. 2 – Reverse-phase HPLC chromatogram of female A. robustus venom. (A) Screening of venom fractions revealed that the peak labeled f9 induced toxicity when injected into house crickets. (B) Further rpHPLC purification of f9 using a shallow acetonitrile gradient yielded three peaks, the largest of which (ω-ACTX-Ar1a) was found to be responsible for the insect toxicity of fraction f9.

normal insect saline of the following composition (in mM): 200 NaCl, 3.1 KCl, 5 CaCl₂, 4 MgCl₂, 10 HEPES, 50 sucrose, supplemented with bovine calf serum (5%, v/v), penicillin (50 IU/mL) and streptomycin (50 μg/mL) (Trace Biosciences, Noble Park, Australia). DUM neurons were then mechanically isolated from exogenous tissue by trituration, carefully passing the ganglia in and out of a sterile Pasteur pipette. The resulting suspension was then distributed into eight wells of a 24-well cluster plate (Limbro, Ohio, USA). Each well contained a 12-mm diameter glass coverslip (Lomb Scientific, Taren Point, NSW) that had been previously coated with 1 mg/ml concanavalin-A (Type VI) (Sigma Chemicals, Castle Hill,

structures of the ω-ACTX-Ar1a prepropeptide and four paralogs thereof derived from analysis of a cDNA library prepared from female and male Atrax robustus venom glands. The propeptide cleavage site was readily discerned from the known ω-ACTX-Ar1a mature toxin sequence, shown in (A), while the consensus signal peptide cleavage site was predicted by the SignalP program [29]. (C) Structure of ω-ACTX-Hv1a and ω-ACTX-Ar1a. The upper panels show the NMR structure of ω-ACTX-Hv1a (PDB file 1AXH) while lower panels show the structure of ω-ACTX-Ar1a modeled on the known structure of ω-ACTX-Hv1a using the automated protein homology-modeling server SWISS-MODEL [44,45]. In each panel, the left-hand view shows a schematic of the 3D structure highlighting the location of β-strands (gray arrows), the side chains of residues forming the major insectophore (Pro¹⁰, Asn²⁷, Arg³⁵), and the disulfide bridges (gray tubes). The two views on the right show surface representations indicating the location of the major (black) and minor (dark gray) insectophore residues, as well as residues that differ between the two toxin sequences at positions 2, 3, 16, 20, 24, and 34 (gray).

NSW) or Cell-Tak (BD Biosciences, Australia). Isolated cells were allowed to attach to the coverslips overnight in an incubator (10% CO_2, 90% O_2, 100% relative humidity, 28 °C). DUM neurons were maintained at 28 °C for 12–24 h before electrophysiological experiments were carried out.

Standard whole cell voltage-clamp recordings of calcium (I_{Ba}), sodium (I_{Na}), and potassium (I_K) channel currents were made from DUM neurons. Due to the report of I_{Ca} rundown with calcium as a charge carrier [22], as well as reports of greater success when barium was used as the charge carrier [23], $BaCl_2$ replaced $CaCl_2$ in all experiments. Recordings of I_{Ba} were made with fire-polished borosilicate pipettes of ∼2 MΩ resistance when filled with an internal pipette solution containing (in mM): 10 sodium acetate, 110 CsCl, 50 tetraethylammonium (TEA)-Br, 2 ATP-Na_2, 0.5 $CaCl_2$, 10 EGTA and 10 HEPES, pH adjusted to 7.25–7.35 with CsOH. For recording I_{Na} the internal pipette solution contained (in mM): 135 CsF, 1 $MgCl_2$, 20 NaCl, 10 HEPES and 5 EGTA, with the pH adjusted to 7.25–7.35 with CsOH. For recording macroscopic I_K pipettes contained (in mM): 135 KCl, 25 KF, 9 NaCl, 3 ATP-Mg_2, 1 $MgCl_2$, 0.1 $CaCl_2$, 1 EGTA and 10 HEPES, pH adjusted to 7.25 with NaOH. The external solution for recording I_{Ba} contained (in mM): 160 sodium acetate, 30 TEA-Br, 3 $BaCl_2$ and 10 HEPES, with the pH adjusted to 7.4 using TEA-OH. The external solution for recording I_{Na} contained (in mM): 130 NaCl, 5 CsCl, 1.8 $CaCl_2$, 20 TEA-Cl, 1 4-aminopyridine, 10 HEPES, 0.01 (±)-verapamil, 0.1 $NiCl_2$ and 0.1 $CdCl_2$ with the pH adjusted to 7.4 using NaOH. The external solution for recording I_K contained (in mM): 130 NaCl, 20 KCl, 5 $CaCl_2$, 1.5 $MgCl_2$, 1 $CdCl_2$, 10 HEPES, pH adjusted to 7.4 using NaOH. The osmolarity of both internal and external solutions was determined with a cryoscopic osmometer (Gonotec Osmomat 030, Berlin, Germany) and adjusted to 420–430 mOsm/L with sucrose to reduce osmotic stress. The external solution was applied to the perfusion chamber, via a pressured perfusion system (Automate Scientific, San Francisco, CA, USA) at a flow rate of 0.5–1 mL/min. Data were recorded at room temperature (20–23 °C) which did not fluctuate more than 1 °C during the course of an experiment. Inverted voltage-clamp command pulses were applied to the bath through a Ag/AgCl pellet/3 M KCl-agar bridge. The liquid junction potential between internal and external solutions was determined using the program JPCalc [25], and all data were compensated for this value. The experiments used in this study were rejected if there were large leak currents or currents showed signs of poor space clamping such as an abrupt activation of currents upon relatively small depolarizing pulses. Stimulation and recording were both controlled by the pClamp v9.0 data acquisition system (Molecular Devices, CA, USA). Data were filtered at 5 kHz (four-pole lowpass Bessel filter) and the digital sampling rates were 20 kHz. Leakage and capacitive currents were digitally subtracted with P-P/4 procedures [26] and series resistance compensation was set at >80% for all cells. Neurons were voltage clamped at −90 mV, and currents were evoked by stepping the membrane potential from −90 to +40 mV (for I_{Ba}), −80 to +70 mV (for I_{Na}), and −80 to +40 mV (for I_K). Tetrodotoxin (TTX) 500 nM, a known insect Na_v channel blocker [27], or Cd^{2+} 500 μM, a known insect Ca_v channel blocker [23], were used to abolish inward I_{Na} or I_{Ba}

currents respectively, and confirmed the currents recorded were carried through these channels.

2.6. Data analysis

Data analyses were performed off-line following completion of the experiment. Mathematical curve fitting was accomplished using GraphPad Prism version 4.00 for Macintosh (GraphPad Software, San Diego, CA, USA). All curve-fitting routines were performed using non-linear regression analysis employing a least squares method. All data shown represent the mean ± S.E. Dose–response curves to determine LD_{50}, KD_{50}, and IC_{50} values were fitted using the following form of the logistic equation:

$$y = \frac{1}{1 + ([x]/Dose_{50})^{n_H}} \qquad (1)$$

where x is the toxin dose, n_H the Hill coefficient (slope parameter), and $Dose_{50}$ is the median inhibitory dose causing lethality, knockdown or block of membrane currents, respectively.

On-rates were determined by fitting timecourse data with the following single exponential decay function:

$$y = A\,e^{-kx} + C \qquad (2)$$

where x is the time, A the normalized current value (usually 1.0) before application of toxin, and C is the final normalized current value following block by the toxin. The on-rate (τ_{on}) was determined from the inverse of the rate constant k.

Off-rates were determined by fitting timecourse data with the following single exponential association function:

$$y = C + A(1 - e^{-kx}) \qquad (3)$$

where x is the time, A the normalized current value after washout of the toxin (usually 1.0 if complete washout occurred), and C is the normalized current value prior to washout of the toxin. The off-rate (τ_{off}) was determined from the inverse of the rate constant k.

Current–voltage (I/V) curves were fitted using the following equation:

$$I = g_{max}\left(1 - \left(\frac{1}{1 + \exp[(V - V_{1/2})/s]}\right)\right)(V - V_{rev}) \qquad (4)$$

where I is the amplitude of the peak current (either I_{Ba}, I_{Na} or I_K) at a given test potential V, g_{max} the maximal conductance, $V_{1/2}$ the voltage at half-maximal activation, s the slope factor, and V_{rev} is the apparent reversal potential.

3. Results

3.1. Isolation of a novel insecticidal toxin

Fig. 2 shows a typical rpHPLC fractionation of crude venom from female A. robustus. 45 fractions were individually assayed for insect and vertebrate toxicity. The fraction containing the toxin eluted at 33% acetonitrile/0.1% TFA (peak f9, Fig. 2A). This

fraction failed to alter neurotransmission on chick biventer cervicis nerve-muscle preparation at a dose of 10 μg/mL (data not shown). However, injection of 10 μg/g *f*9 into house crickets caused both excitatory and depressant toxic effects. This fraction was pooled and lyophilized, and further purification using C18 rpHPLC with a shallow acetonitrile gradient yielded three distinct components (Fig. 2B). The major peak, labeled 'ω-ACTX-Ar1a', was subsequently shown to be the active component in invertebrate toxicity assays (see Section 3.3). ESI-Q-ToF mass spectrometry revealed that the molecular mass of the peptide was 4002.8 ± 1.0 Da.

3.2. Toxicity bioassays

Acute insect toxicity testing in house crickets (*Atrax domesticus*) resulted in signs of toxicity within 15 min following injection of ω-ACTX-Ar1a at doses >100 pmol/g. These signs were initially characterized by increased abdominal contractions, occasional spasms of limbs and antennae, and decreased feeding activity. Signs steadily progressed to high frequency twitching of limbs, antennae and mandibles, with a concurrent loss of coordinated locomotion and righting reflexes. At this stage, crickets were characterized as having reached the 'knockdown' (KD) end-point. Progressive spastic paralysis was then followed by a period of flaccid paralysis, leading to death. The excitatory spastic response followed by a depressed stage prior to death has previously been shown to be the typical phenotype following injection of members of the ω-ACTX-1 family into a wide range of insects [9,10,16,17,28]. Following injection of ω-ACTX-Ar1a, no affected crickets recovered from the toxic effects over a time-course of 72 h. ω-ACTX-Ar1a was found to have an LD_{50} of 236 ± 28 pmol/g, and a KD_{50} of 147 ± 16 pmol/g (Fig. 3A), determined at a 48 h end-point ($n = 4$). However, if 72 h was taken as the endpoint, a marked decrease in the values for both the LD_{50} and the KD_{50} was noted, to 143 ± 10 pmol/g ($n = 4$) and 124 ± 12 pmol/g ($n = 4$), respectively (Fig. 3B).

Following purification of ω-ACTX-Ar1a from crude *f*9, confirmatory testing for lack of vertebrate toxicity was carried out using smooth and skeletal nerve-muscle preparations. At a concentration of 1 μM (equivalent to 4 μg/mL), no effects were seen on the twitch or resting skeletal muscle tension or on the responses to cholinergic agonists, and there was no evidence of any muscle fasciculation (Fig. 3C). The lack of effects on neuromuscular transmission were also confirmed using the electrically stimulated rat vas deferens smooth muscle preparation (Fig. 3C). The lack of any overt toxic action on the wide range of vertebrate receptors and ion channels present in these preparations provide strong evidence for the insect-selective actions of ω-ACTX-Ar1a.

3.3. Determination of amino acid sequence

The purified peptide was reduced and the cysteines pyridylethylated in preparation for automated N-terminal amino acid sequencing and to assist in determining the number of cysteine residues. The phenylthiohydantoin-Cys residues with a pyridylethylated sidechain are stable during automated N-terminal amino acid sequencing and therefore allows positive identification of Cys residues. Mass spectral analysis
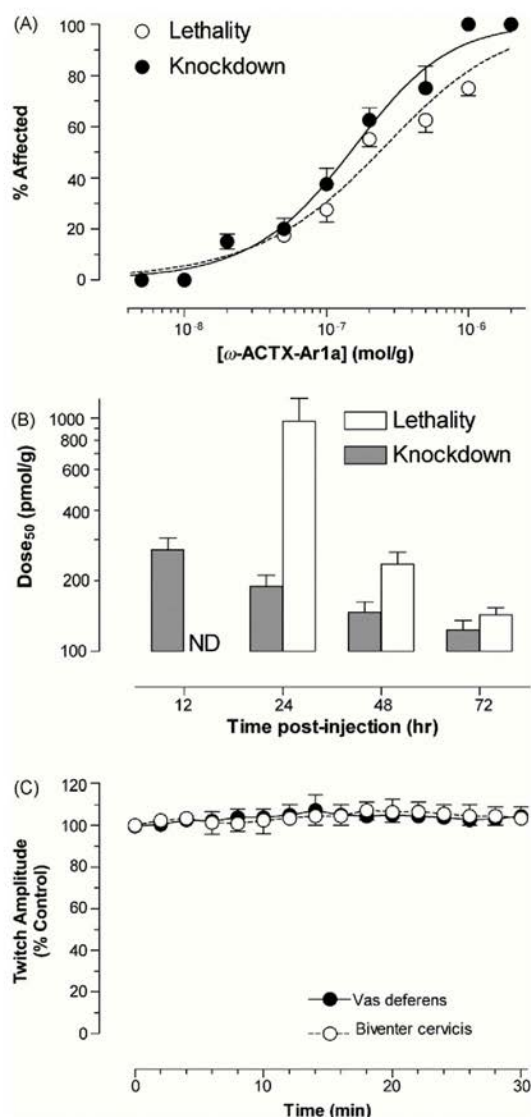
Fig. 3 – Acute toxicity of ω-ACTX-Ar1a in house crickets (*Acheta domesticus*). (A) Log-dose–response curve for death (open circles) and knockdown (closed circles) of crickets by ω-ACTX-Ar1a at 48 h post-injection. Data was fitted with Eq. (1) (see Section 2) to yield a KD_{50} value of 147 ± 16 pmol/g and LD_{50} value of 236 ± 28 pmol/g ($n = 4$). (B) KD_{50} (grey columns) and LD_{50} (open columns) of ω-ACTX-Ar1a at increasing times following intrathoracic injection ($n = 4$). ND indicates that the LD_{50} could not be determined at 12 h post-injection. (C) Timecourse of twitch amplitude in isolated rat vas deferens and chick biventer cervicis nerve-muscle preparations in the presence of 600 nM and 1 μM ω-ACTX-Ar1a, respectively ($n = 2$–3).

of the pyridylethylated toxin revealed a molecular weight of 4640.97 ± 0.41 Da, indicating the presence of six cysteine residues within the primary sequence. The amino acid sequence of the toxin (Fig. 1A), obtained in a single sequencing run without the need to resort to proteolytic digestion, revealed that it contains 37-residues, including six cysteines. The predicted monoisotopic mass of 4002.59 Da for the fully oxidized peptide, in which the six cysteine residues form three disulfide bonds, is consistent with the mass spectral analysis.

A BlastP search of the Swiss-Prot/TrEMBL database revealed that the toxin displayed significant homology with known members of the ω-ACTX-1 family (Fig. 1). The highest homology of 89% was seen with both ω-ACTX-Hv1b and -Hv1d. Members of this toxin family are insect-selective Ca_v channel blockers, and they have been isolated previously from other species of Australian funnel-web spiders belonging to the *Hadronyche* genus, namely *Hadronyche versuta*, *Hadronyche infensa*, and *Hadronyche formidabilis* [9]. Importantly, the number and spacing of cysteine residues, as well as the primary insectophore residues (Pro[10], Asn[27], Arg[35]) that are critical for binding to insect Ca_v channels [11,12], are conserved in the newly isolated toxin. The minor insectophore residues Gln[9] and Tyr[13], which are important for activity in cockroaches and crickets (but not flies) [12], are also present. However, the minor insectophore residue Asn[16] in ω-ACTX-Hv1a, which is known to be important for activity in crickets [12], was substituted by His[16] in the new toxin. Based on these sequence similarities with ω-ACTX-Hv1a, we have named the new peptide ω-ACTX-Ar1a, and deposited the sequence in the SwissProt (accession no. P83580). ω-ACTX-Ar1a is the first insecticidal toxin isolated from the venom of *A. robustus*.

3.4. Elucidation of ω-ACTX-Ar1a precursor structure

Sequencing of RACE-derived clones revealed the full-length sequences of mRNA transcripts encoding ω-ACTX-Ar1a and four paralogous toxins expressed in the venom gland of either male or female *A. robustus* spiders. The DNA sequences have been deposited in GenBank under accession numbers EF523494, EF523495, EF523497, EF523498, and EF523499. The derived amino acid sequences (Fig. 1B) reveal that the mature toxins are obtained from processing of a larger prepropeptide precursor. The propeptide cleavage site was readily discerned from the known ω-ACTX-Ar1a mature toxin sequence (see Section 3.3), while a consensus signal peptide cleavage site was predicted by the SignalP program ([29]; program available on the web at http://www.cbs.dtu.dk/services/SignalP).

The propeptide architecture is similar to that described for other atracotoxins [12,30–32] and comprises a 22-residue N-terminal signal sequence followed by a propeptide sequence of 15–26 residues that precedes a single downstream copy of the mature toxin sequence (36–37 residues). No transcripts were identified that encoded multiple mature toxin sequences. The mature toxin sequence predicted from the ω-ACTX-Hv1a transcript exactly matches the sequence obtained from Edman degradation of the purified mature toxin.

The signal peptide sequence is strongly conserved among this toxin family, with only four sites out of 22 showing any variation in the five paralogs. This is consistent with the hypothesis that the signal sequence is important for directing ω-ACTX-1 precursors to a specific secretory pathway in the venom gland. The mature toxin sequence is more variable, with substitutions observed at 16 out of 37 sites relative to ω-ACTX-Ar1a. Spiders are generalist predators, and these variations in the mature toxin sequence are presumed to provide the spider with a mini-combinatorial library of toxin isoforms for targeting variants of the target ion channel in a wide variety of arthropod prey [32].

Curiously, the propeptide sequence varies significantly between sexes. The three toxin variants isolated from the venom gland of the male *A. robustus* specimen all have identical 19-residue propeptide sequences. Surprisingly, however, the propeptide sequences in the two toxin variants isolated from the venom gland of the female *A. robustus* specimen have only limited homology with the male paralogs, although the Arg-Arg dipeptide sequence preceding the propeptide cleavage site is strictly conserved. The reason for these sex-related differences in the propeptide sequence, as well as the genetic mechanism underlying this sexual dichotomy, is unclear. Moreover, while most previously reported spider toxin propeptide sequences are highly acidic [12], the overall charge on the ω-ACTX-Ar1 propeptides ranges from −2 to +2.

3.5. Block of insect M-LVA and HVA Caᵥ channels by ω-ACTX-Ar1a and ω-ACTX-Hv1a

To test the hypothesis that ω-ACTX-1 toxins block insect Ca_v channels, we investigated the effect of ω-ACTX-Ar1a and ω-ACTX-Hv1a on insect Ca_v channels in DUM neurons of the cockroach *P. americana*. To prevent Ca^{2+}-induced rundown of Ca^{2+} currents, Ba^{2+} was used as a charge carrier instead of Ca^{2+} [23]. Since Ba^{2+} currents (I_{Ba}) are larger than Ca^{2+} currents, the normal concentration was reduced to 3 mM to decrease the risk of voltage errors due to series resistance issues. The complete block of currents following the addition of 500 μM cadmium confirmed that the inward currents recorded were carried through Ca_v channels (data not shown).

Two subtypes of Ca_v channels have been described in cockroach DUM neurons: M-LVA and HVA Ca_v channels [23,33]. Unfortunately, despite differences in the kinetic and pharmacological properties of M-LVA and HVA Ca_v channels, there remains no mechanism for recording one current in isolation from the other as no peptide or organic blockers are available that exclusively block one type of current and not the other [23]. As previously described, depolarising pulses to different levels (−30 mV and +30 mV) were used to investigate the actions of the ω-ACTX-1 toxins on M-LVA and HVA Ca_v channels, respectively [23,33]. Macroscopic I_{Ba} through Ca_v channels were elicited by 100-ms depolarising command pulses from a V_h of −90 mV. Inward I_{Ba} were evoked by depolarising pulses to −30 mV (M-LVA Ca_v channel currents dominating) and +30 mV (HVA Ca_v channel currents dominating) [23]. Depolarisations to −30 mV (Fig. 4) caused a large inward current with slow decaying component, consistent with a reduction in Ca^{2+}-dependent fast inactivation due to the use of Ba^{2+} as the charge carrier [23], whereas depolarisations to +30 mV elicited a smaller current with a fast decaying component (Fig. 5). To confirm that a −30 mV pulse preferentially elicits M-LVA Ca_v channel currents
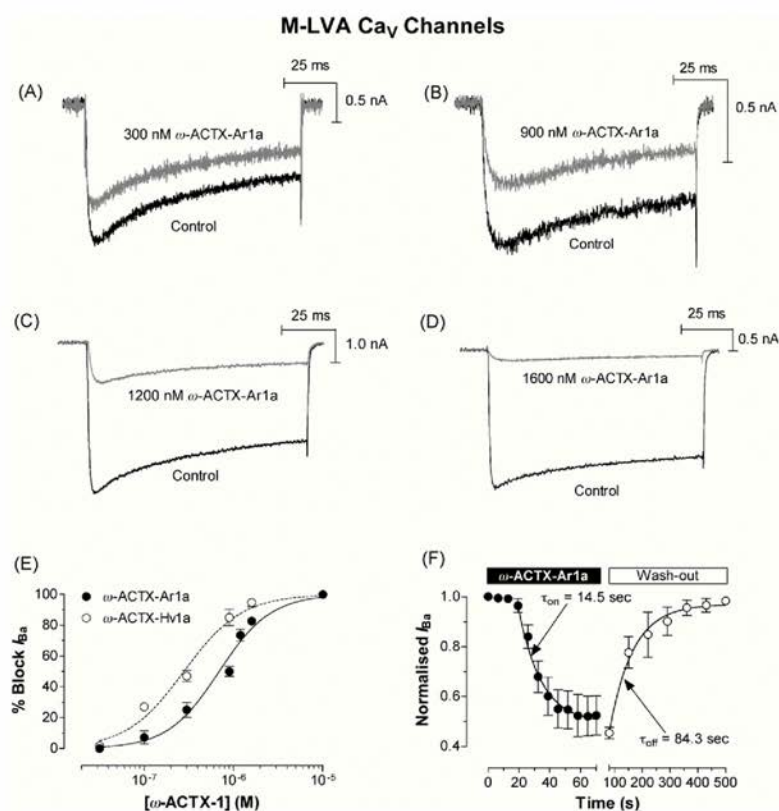
Fig. 4 – ω-ACTX-Ar1a blocks insect low-voltage-activated Ca$_v$ channels. Low-voltage activated Ca$_v$ channel currents in panels (A)–(D) were elicited by 100-ms depolarizing test pulses to −30 mV from a holding potential of −90 mV. Panels show typical concentration-dependent inhibition of M-LVA I$_{Ba}$ following perfusion with 300 nM (A), 900 nM (B), 1200 nM (C) and 1600 nM (D) ω-ACTX-Ar1a. (E) Dose–response curve showing percentage block of M-LVA Ca$_v$ channel currents by ω-ACTX-Ar1a (closed circles) and ω-ACTX-Hv1a (open circles) (n = 3–8). Data were fitted using Eq. (1). (F) On- and off-rates determined following application of 900 nM ω-ACTX-Hv1a and wash-out with toxin-free external solution (n = 5). Data were fitted using Eqs. (2) and (3).

we established that the insect M-LVA blocker ω-conotoxin MVIIC [23] produced selective inhibition of currents at −30 mV, rather than those elicited at +30 mV (HVA currents predominating). Application of 1 μM ω-conotoxin MVIIC caused a 48.4 ± 9.4% (n = 3) reduction in peak I$_{Ba}$ in DUM neurons at a test pulse of −30 mV and only 18.4 ± 9.6% (n = 3) at a test pulse of +30 mV. This is similar to previously reported values [23].

Both ω-ACTX-Ar1a and ω-ACTX-Hv1a exerted a concentration-dependent tonic block of M-LVA Ca$_v$ channels. Figs. 4 and 5 show the effects of increasing concentrations of ω-ACTX-Ar1a on peak I$_{Ba}$ amplitude elicited by a 100-ms depolarizing test pulse to −30 or +30 mV from a holding potential of −90 mV every 10 s. The addition of 300 nM ω-ACTX-Ar1a resulted in a block of peak I$_{Ba}$ of 25 ± 5% (n = 5) within 5 min at −30 mV (Fig. 4A), and 29 ± 3% (n = 3) block of depolarising pulses to +30 mV (Fig. 5A). At a concentration of 900 nM ω-ACTX-Ar1a, this block increased to 50 ± 3% (n = 5) and 54 ± 7% (n = 3) at −30 mV (Fig. 4B) and +30 mV (Fig. 5B), respectively. However, total block was only achieved at concentrations above 1.6 μM.

Washing with toxin-free solution restored peak I$_{Ba}$ within 5–7 min. The peak I$_{Ba}$ in the presence of ω-ACTX-Ar1a was expressed as a percentage of the control peak I$_{Na}$ and the depression of peak amplitude, after 10 min of perfusion, was plotted against toxin concentration. By fitting the concentration-response curve of the inhibition of peak I$_{Ba}$ using a Logistic function (Eq. (1) in Section 2) the concentration at half-maximal block (IC$_{50}$) of M-LVA Ca$_v$ channels was determined to be 692 nM for ω-ACTX-Ar1a and 279 nM for ω-ACTX-Hv1a (Fig. 4E). The IC$_{50}$ values for block of HVA Ca$_v$ channels were 644 nM for ω-ACTX-Ar1a and 1080 nM for ACTX-Hv1a (Fig. 5E). Despite a clear blocking action, both toxins failed to alter activation or inactivation kinetics, such that the time to peak current and the timecourse of current decay was not significantly affected at concentrations of ω-ACTX-Ar1a up to 1.6 μM. The time course of ω-ACTX-Ar1a association and dissociation were relatively slow and described by single exponential functions with a τ$_{on}$ of 14.5 ± 1.7 s (n = 5) for M-LVA Ca$_v$ channels (Fig. 4F) and 22.8 ± 5.8 (n = 5) for HVA
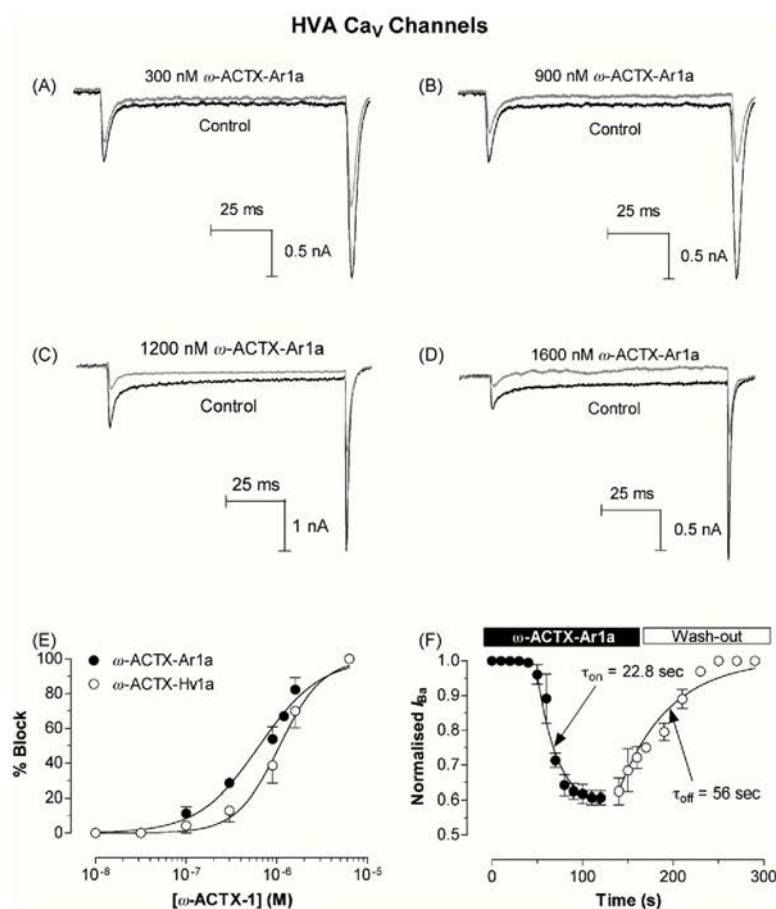
Fig. 5 – ω-ACTX-Ar1a blocks insect high-voltage activated Ca_v channels. High-voltage-activated Ca_v channel currents in panels (A)–(D) were elicited by 100 ms depolarizing test pulses to +20 mV from a holding potential of −90 mV. Panels show typical concentration-dependent inhibition of HVA I_{Ba} following perfusion with 300 nM (A), 900 nM (B) 1200 nM (C) and 1600 nM (D) ω-ACTX-Ar1a. (E) Dose–response curve showing percentage block of HVA Ca_v channel currents by ω-ACTX-Ar1a (closed circles) and ω-ACTX-Hv1a (open circles) (n = 3–5). Data were fitted using Eq. (1). (F) On- and off-rates determined following application of 900 nM ω-ACTX-Hv1a and washout with toxin-free external solution (n = 5). Data were fitted using Eqs. (2) and (3).

channels (Fig. 5F). The recovery after washout with toxin-free external solution was slow but complete with a τ_{off} of 84.3 ± 10.0 s (n = 5) for M-LVA Ca_v channels (Fig. 4F) and 56.0 ± 14.7 s (n = 5) for HVA channels (Fig. 5F). These slow on- and off-rates from DUM neuron Ca_v channels have been previously noted with peptide toxins such as ω-conotoxin GVIA and ω-conotoxin MVIIC [23] and CSTX-1 from *Cupiennius salei* venom [34].

3.6. Effects on the voltage-dependence of M-LVA and HVA Ca_v channel activation

To determine if the tonic block of Ca_v channels was due to a depolarising shift in the voltage-dependence of channel activation, we determined the action of ω-ACTX-Ar1a and ω-ACTX-Hv1a on current–voltage relationships. Families of I_{Ba}

were generated by 100-ms test pulses from V_h (−90 mV) to a maximum of +30 mV in 10-mV increments, every 10 s. Typical effects of ω-ACTX-Ar1a on I_{Ba} were recorded before (Fig. 6Aa), and after (Fig. 6Ab) perfusion with 900 nM toxin. The I_{Ba}–V relationship was determined from the maximal I_{Ba} values at each potential (Fig. 6B). Data were normalised against peak maximal control I_{Ba} and fitted with Eq. (4) (see Section 2). Similar thresholds of activation in pre- and post-toxin conditions were observed for I_{Ba} and no significant shift was observed in the voltage at half-maximal activation, $V_{1/2}$, or slope factor, s. There was also little change (<3 mV) in the apparent reversal potential, V_{rev}, in post-toxin recordings, indicating that the ionic selectivity of Ca_v channels was not altered by ω-ACTX-Ar1a or ω-ACTX-Hv1a. In addition, at a concentration of 900 nM, both toxins produced a voltage-independent block at all test potentials (Fig. 6C).
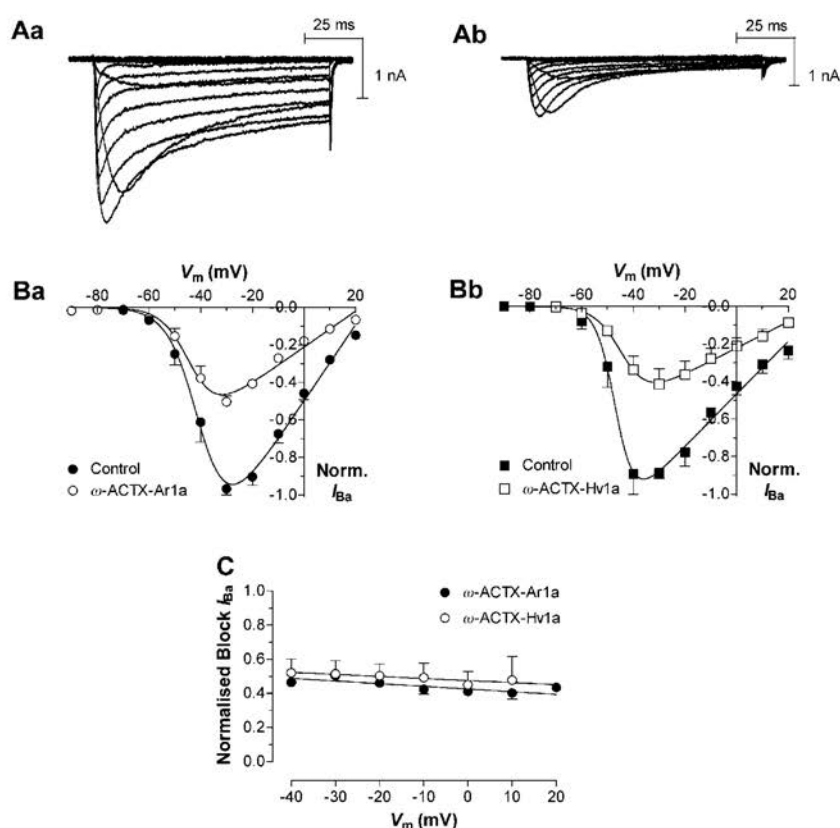
Fig. 6 – Voltage-dependence of Ca_v channel activation. Families of Ca_v channel currents were elicited by depolarizing test pulses to +30 mV from a holding potential of −90 mV in 10-mV steps. (A) Typical superimposed current traces recorded before (Aa) and after (Ab) a 10-min perfusion with 900 nM ω-ACTX-Ar1a. (B) Peak I_{Ba}/V relationship recorded before (closed symbols) and after (open symbols) application of 900 nM ω-ACTX-Ar1a (Ba, $n = 4$) and 900 nM ω-ACTX-Hv1a (Bb, $n = 4$). Data were fitted with Eq. (4). (C) Voltage-independent block of I_{Ba} by 900 nM ω-ACTX-Ar1a (closed circles, $n = 4$) and 900 nM ω-ACTX-Hv1a (open circles, $n = 4$). Data represent the normalized block at each test potential and were fitted by linear regression.

3.7. Effects on Na_v and K_v channels

To date, there are no reports in the literature investigating potential effects of any member of the ω-ACTX-1 family on insect ion channels except for the Ca_v channel. The relatively high IC_{50} values for both toxins on Ca_v channels suggested that they perhaps might target additional ion channels. It has been previously noted that peptide toxins can exert their actions both within and across voltage-gated ion channel families. This promiscuous activity has already been noted with other toxins targeting Ca_v channels such as SNX482, ω-agatoxin IVA, and protoxins I and II [35–38]. Accordingly, we examined the actions of ω-ACTX-Ar1a on both Na_v and K_v channel currents, present in cockroach DUM neurons. In contrast to the marked block of M-LVA and HVA I_{Ba}, no significant change was seen in global potassium channel current amplitude or time course, or the voltage-dependence of potassium channel activation, following perfusion of 1 μM ω-ACTX-Ar1a for up to 10 min (Fig. 7Ab–Eb). When tested on Na_v channels, 1 μM ω-ACTX-

Ar1a caused a modest 18 ± 5% ($n = 4$) block of peak I_{Na} at test pulses to −10 mV, with no effect on activation or inactivation kinetics or the voltage-dependence of Na_v channel activation (Fig. 7Aa–Ea). It is clear, therefore, that ω-ACTX-Ar1a and ω-ACTX-Hv1a selectively block Ca_v channel currents in the insect CNS although at higher concentrations they may have non-selective effects on other voltage-gated ion channels, particularly Na_v channels.

4. Discussion

The initial aim of the present project was to determine whether it was possible to isolate insect-selective neurotoxins from the venom of the Sydney funnel-web spider, A. robustus. However, the identification a 37-residue A. robustus peptide toxin with high sequence homology to members of the ω-ACTX-1 family of toxins, including complete conservation of the cysteine and insectophore residues, led us to more
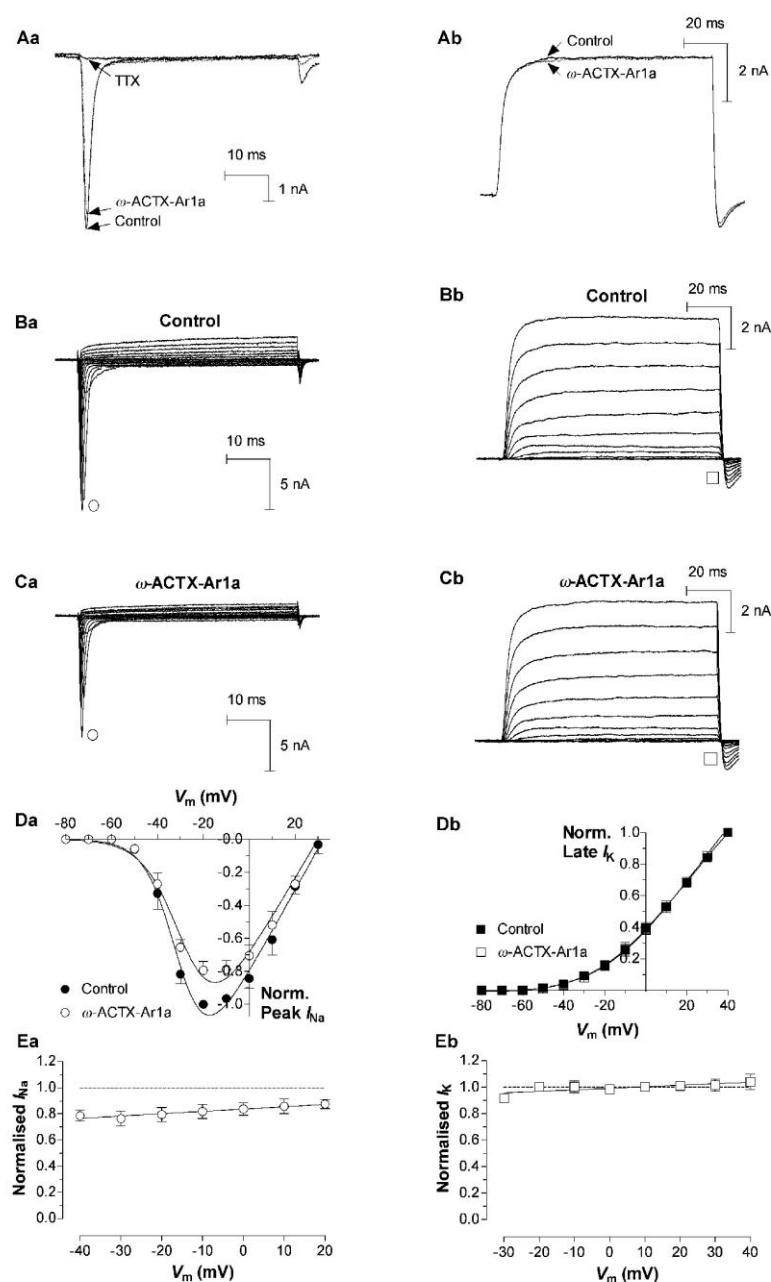
Fig. 7 – Effects of ω-ACTX-Ar1a on insect Na_v and K_v channels. Typical whole-cell macroscopic I_{Na} (left hand panels) and I_K (right hand panels) recorded from cockroach DUM neurons. Macroscopic currents in panel Aa were elicited by 100-ms depolarizing test pulses to −10 mV from a holding potential of −80 mV. (Aa) Partial inhibition of peak of I_{Na} following a 10 min perfusion with 1 μM ω-ACTX-Ar1a. The current was completely blocked by 100 nM TTX indicating that this current was mediated exclusively, via Na_v channels. (Ab) Representative traces illustrating the lack of inhibition of global K_v channel currents by 1 μM ω-ACTX-Ar1a. (B–C) Typical families of Na_v (Ba, Ca) and K_v (Bb, Cb) channel currents elicited by depolarizing test pulses to +70 and +40 mV, respectively, from a holding potential of −90 mV in 10-mV steps. Data shown represents superimposed current traces recorded before (B) and after (C) a 10-min perfusion with 1 μM ω-ACTX-Ar1a. (D) Peak I_{Na}/V (Da, n = 4) and late I_K/V (Db, n = 3) relationships recorded before (closed circles), and after (open circles), application of 1 μM ω-ACTX-Ar1a. (E) Voltage-independent block of I_{Na} (Ea, n = 4) and I_K (Eb, n = 3) by 900 nM ω-ACTX-Ar1a. Data represent the normalized block at each test potential and were fitted by linear regression. The dashed lines represent 0% block.

thoroughly characterize the effects of these toxins on insect Ca_v channels. Given that the newly isolated peptide toxin also blocks insect Ca_v channels we have named it ω-ACTX-Ar1a, in accordance with the established nomenclature system used for naming funnel-web spider toxins [10] and conotoxins [39].

Acute toxicity tests in house crickets revealed that ω-ACTX-Ar1a induces an initial excitatory response followed by a depressant phenotype prior to death. This biphasic phenotype has previously been described following injection of members of the ω-ACTX-1 family into a wide range of insects, including coleopterans, orthopterans, lepidopterans and dipterans [9,10,16,17] and has been noted in recordings of compound action potentials induced by ω-ACTX-Hv1a in a *Drosophila* CNS preparation [40]. ω-ACTX-Ar1a is a moderately potent neurotoxin when compared to other members of the ω-ACTX-Hv1 family, which have effective doses ranging from 84–1384 pmol/g in house crickets [9]. ω-ACTX-Hv1b, its closest homolog by amino acid sequence, has an LD_{50} of 224 ± 7 pmol/g [9] which is almost identical to the LD_{50} of 236 ± 28 pmol/g obtained for ω-ACTX-Ar1a. Although ω-ACTX-Ar1a is three-fold less potent than ω-ACTX-Hv1a, it should be noted the ω-ACTX-Hv1 family is one of the most potent insecticidal neurotoxin families discovered to date. Other insect-selective neurotoxins, such as those from the spider *Tegenaria agrestis*, and the primitive weaving spider *Diguetia canities*, have median effective doses ranging from 0.89 to 2.6 nmol/g and 0.38–3.2 nmol/g, respectively [41,42].

Although the insectophore of ω-ACTX-Ar1a was not determined experimentally, the major (Pro[10], Asn[27], and Arg[35]) and minor (Gln[9], Tyr[13]) insectophore residues of ω-ACTX-Hv1a [9,11] are strictly conserved. The high homology (86%) in primary structure with ω-ACTX-Hv1a, including the same number and spacing of cysteine residues, strongly suggests that ω-ACTX-Ar1a also contains three disulfide bonds that form the same ICK structural motif that is a prominent feature of this family of toxins [43], and almost certainly has a solution structure similar to ω-ACTX-Hv1a. Accordingly the structure of ω-ACTX-Ar1a was modeled on ω-ACTX-Hv1a (PDB code 1AXH) using the automated protein homology-modelling server SWISS-MODEL [44,45] (Fig. 1C). This revealed that, apart from residues 2–3, the amino acids that differ in ω-ACTX-Ar1a are located, relative to the face of the toxin containing the insectophore residues, primarily on the side and rear faces of the toxin. Thus, these sequence variations are unlikely to affect the disposition of either the major or minor insectophore.

Nevertheless, the present study identified a three-fold loss in lethality in comparison to ω-ACTX-Hv1a using the cricket bioassay (ω-ACTX-Ar1a LD_{50} 236 ± 28 pmol/g versus ω-ACTX-Hv1a LD_{50} 84 ± 10 pmol/g at 48 h [9]). Despite a structurally disordered N-terminus, the first three amino acid residues of ω-ACTX-Hv1a have been shown to be important for toxicity, as indicated by a slight reduction in insecticidal potency when these three residues are deleted [9]. Thus, the variations at position 2 and 3 in ω-ACTX-Ar1a may account for the lower toxicity in crickets compared with ω-ACTX-Hv1a. However, the decrease in potency is more likely due to substitution of Asn[16] by a His residue, since Asn[16] in ω-ACTX-Hv1a forms part of an additional minor pharmacophore in crickets, but not flies or cockroaches [12].

The IC_{50} values for the block of M-LVA and HVA Ca_v channels by ω-ACTX-Ar1a and ω-ACTX-Hv1a are not significantly different from that reported for block of macroscopic I_{Ba} by ω-ACTX-Hv1a in unidentified cockroach neurons [10]. Importantly, the three-fold lower toxicity of ω-ACTX-Ar1a following injection into house crickets, parallels the three-fold reduction in IC_{50} values for block of M-LVA Ca_v channels. This suggests that the slightly lower toxicity of ω-ACTX-Ar1a may be due to differences between ω-ACTX-1 toxins in their interaction with the Ca_v channel target in crickets rather than pharmacokinetic issues related to bioavailability of the toxins at the target site. In addition, actions on DUM neurons may suggest a CNS target for ω-ACTX-1 toxins. This is supported by the finding that ω-ACTX-Hv1a crossed the blood-brain barrier and depressed activity in *P. americana* and *Drosophila melanogaster* CNS preparations at low nanomolar doses, whereas it had no effect on peripheral neuromuscular synapses [17].

Previous studies using cockroach DUM neurons have identified the presence of both M-LVA and HVA Ca_v channel subtypes in cockroach DUM neurons [22,33]. Interestingly, these are distinct from the LVA (T-type) and HVA (P/Q-, N-, L- and R-type) Ca_v channels described in vertebrates, since the pharmacological and electrophysiological distinctions used for vertebrate Ca_v channels are not applicable to invertebrates [22,23,33,46–50]. This difference no doubt underlies the phyletic specificity of the ω-ACTX-1 family. Importantly, ω-ACTX-Hv1a has been shown to have no effect on whole-cell Ca_v channel currents in a variety of vertebrate neuron preparations at concentrations as high as 1 μM [10], and it does not block cloned rat $Ca_v2.1$ (P/Q-type), $Ca_v2.2$ (N-type), or $Ca_v1.2$ (L-type) Ca_v channels at concentrations as high as 10 μM [12].

Unfortunately, while organic compounds such as verapamil, SKF93635, ω-conotoxin GVIA and ω-conotoxin MVIIC have been useful in identifying the existence of HVA and M-LVA currents in DUM neurons [23,33], the differential sensitivity of Ca_v channel subtypes to these blockers is inadequate to completely separate these currents by pharmacological means [46]. Thus it is not possible, at present, to definitively identify the Ca_v channel subtype targeted by ω-ACTX-1 toxins in insects. Nevertheless, the voltage-independent block of currents at depolarizing test pulses to −30 mV (M-LVA Ca^{2+} currents dominating) would strongly suggest that ω-ACTX-Ar1a blocks insect M-LVA Ca_v channels. The similar degree of block at +30 mV (HVA Ca^{2+} currents dominating) indicates that ω-ACTX-1 toxins also block insect HVA currents. Thus the molecular epitope recognized by ω-ACTX-1 toxins maybe common to both M-LVA and HVA Ca_v channels, and this epitope is most likely located in the pore region of the channel given that these toxins do not modify gating.

We were unable to determine whether DUM neuron T-type-like LVA calcium channels [22] are sensitive to ω-ACTX-1 toxins since, as reported in the study of Wicher and Penzlin [23], we did not observe such currents (activating at voltages negative to −50 mV) in our preparations. It is also highly unlikely that the effects of the ω-ACTX-1 toxins seen in the present study can be explained by an inhibition of the maintained LVA non-selective calcium/sodium current [51] as this current has a threshold of −65 mV, and was not observed in any of our recordings. This is most likely because

of the presence of 2–3 mM ATP and 0.5 μM TTX which would almost abolish this current.

The selectivity of the ω-ACTX-1 toxins for insect versus vertebrate Ca_v channels no doubt arises from the significant pharmacological and kinetic differences between the two phyla. First, the electrophysiological differences between insect M-LVA and HVA Ca_v channels appear to be less prominent than in vertebrates. For example, the voltage range of activation of M-LVA and HVA Ca_v channels in insect neurons does not differ to the extent observed for these two channel superfamilies in vertebrates. In insects, the presence of both M-LVA and HVA Ca_v channel currents can only be demonstrated pharmacologically, because the currents evoked at negative potentials have a different toxicological profile than the currents that require more depolarized potentials for activation [23]. Moreover, inactivation of vertebrate L-type HVA currents can be reduced by replacing Ca^{2+} with Ba^{2+} as the charge carrier, which indicates that Ca^{2+}-dependent mechanisms play a crucial role in channel inactivation. LVA currents in vertebrate neurons are transient with Ba^{2+} as the charge carrier, suggesting that T-type channels inactivate in a Ca^{2+}-independent manner. In contrast, the transient nature of M-LVA currents in cockroach DUM neurons is similar to vertebrate L-type HVA currents, predominantly caused by Ca^{2+}-dependent inactivation, and is thus abolished if Ba^{2+} is used as the charge carrier [23]. In addition, vertebrate T-type channel antagonists such as amiloride are ineffective on insect M-LVA Ca_v channels [23]. Furthermore, both M-LVA and HVA Ca^{2+} currents in cockroach neurons can be inhibited by peptide toxins (ω-conotoxin MVIIC and ω-conotoxin GVIA, respectively) that act selectively on only HVA Ca_v channel types in vertebrate neurons [23]. Importantly, inhibition by these toxins often occurs with much slower kinetics than in vertebrate preparations ([23] and the present study). These observations indicate that Ca_v channels in cockroach neurons are functionally very different to vertebrate HVA Ca_v channels, despite ~65% identity in their amino acid sequences [46]. Finally HVA Ca_v channel currents of DUM neurons were reported to show sensitivity to both phenylalkylamines and benzylalkylamines but, unlike vertebrates, not dihydropyridines such as nifedipine [23]. Given these significant differences in insect and vertebrate Ca_v channels it is perhaps not surprising that ω-ACTX-1 toxins are able to selectively target invertebrate Ca_v channels.

Previous studies have reported a biphasic action of ω-ACTX-Hv1a in *Drosophila* CNS compound action potentials with initial neuroexcitation followed by inhibition at higher concentrations [17]. The neuroexcitation correlates with the early spastic paralysis phase observed in housefly larvae treated with ω-ACTX-Hv1a [17] and the effects of ω-ACTX-Ar1a in house crickets seen in the present study. One possible mechanism suggested by Bloomquist [17] was that multiple subtypes of CNS Ca_v channels could be involved, one responsible for excitation and the other for inhibition of neurotransmission. There could be preferential sensitivity of Ca_v channels in an inhibitory pathway participating in the patterned CNS discharge. Since there is no evidence that ω-ACTX-1 toxins cause any hyperpolarizing shift in the voltage-dependence of Ca_v channel activation, attenuation of an inhibitory influence could result in CNS disinhibition with

ensuing neuroexcitation. Alternatively, it is known that Ca_v channels subtypes in insect neurons mediate different actions on transmitter release. In spontaneously active cockroach DUM neurons, it has been demonstrated that LVA Ca_v channels contribute to the predepolarizing phase of action potentials [22,49]. Therefore block of LVA Ca_v channels leads to slower predepolarization resulting in a slower spontaneous action potential firing frequency and a consequent decrease in transmitter release. Although the functional significance of HVA Ca_v channels in cockroach DUM neurons has not been directly assessed, it has been postulated that these channels play a key role in the control of the action potential hyperpolarization, via the modulation of the large conductance calcium-activated potassium channels (BK_{Ca}) encoded by the slowpoke (Slo) gene [27]. The BK_{Ca} current contributes to membrane repolarization in *Drosophila* nerve terminals and helps to limit transmitter release by narrowing presynaptic action potentials, and reducing depolarization, to decrease Ca^{2+} entry into the nerve terminal [52]. This action is also seen at vertebrate central and peripheral nerve terminals [53–55]. Therefore block of HVA Ca_v channels leads to inhibition of BK_{Ca} channels resulting in an increase in action potential duration and a decrease in the fast afterhyperpolarization [56,57]. Block of HVA Ca_v channels by ω-ACTX-1 toxins most likely results in an increase in transmitter release. Thus the actions of ω-ACTX-1 toxins to block both M-LVA and HVA Ca_v channels could explain the biphasic effects seen in the acute toxicity tests and in electrophysiological recordings from *Drosophila* CNS preparations [17] rather than selective block of inhibitory pathways leading to disinhibition.

Notwithstanding these actions, it has been previously noted that spider peptide neurotoxins can exert their actions both within, and across, voltage-gated ion channel families. For example SNX482 is a known blocker of R-type [58] and P/Q-type [35] Ca_v channels. This toxin has also been shown to delay Na_v channel inactivation and partially block I_{Na} in bovine chromaffin cells at similar concentrations to those that block I_{Ca} [35]. This dual activity on Na_v and Ca_v channels has been reported for Protoxin-I and -II (ProTx-I and -II) that act as gating modifiers to inhibit Na_v1.2, 1.5, 1.7 and 1.8 channels by causing a depolarizing shift in the voltage-dependence of activation [37]. However ProTx-1 also potently blocks Ca_v3.1 (T-type) channels and partially inhibits K_v1.3 and K_v2.1 channels [37] while ProTX-II blocks Ca_v3.x (T-type) and Ca_v1.x (L-type) channels [38]. Most relevant to the present study on insect neurons is the P/Q-type Ca_v channel blocker ω-agatoxin IVA which also decreased TTX-sensitive I_{Na} amplitude, enhanced I_{Na} decay, and led to a slower recovery from Na_v channel inactivation in cockroach DUM neurons [36]. Therefore, the minor block of Na_v channels by ω-ACTX-Ar1a is not without precedence.

It may be argued that the IC_{50} values of the ω-ACTX-1 toxins are rather high and that the toxins may actually target other channels or receptors to produce toxicity. However, other well-characterized peptide toxins that block Ca_v channels, such as ω-conotoxin GVIA and ω-conotoxin MVIIC, also have high IC_{50} values on insect neurons in comparison to activities on vertebrate channels [23]. Moreover, it should be noted that insects have a much smaller repertoire of Ca_v channel subtypes than vertebrates [46]. *D. melanogaster*, for example,

harbours only a single ortholog of each of the vertebrate Ca_v1, Ca_v2, and Ca_v3 subtypes. Thus, unlike vertebrates, which can survive a knockout of some Ca_v channel subtypes, Ca_v channel knockouts in insects are invariably lethal [46]. Thus, it is perhaps not surprising that even moderate inhibition of insect Ca_v channels can have profound neurotoxic effects. Although the ω-ACTX-1 toxins block two types of insect Ca_v channels with only moderate potency and induce an even weaker block of insect Na_v channels, the combined actions on these three channels would be expected to markedly affect the CNS of insects. The excitatory phenotype observed after injection of ω-ACTX-Ar1a may result from a block of HVA Ca_v channels while the subsequent depressant phenotype could arise from the combined block of M-LVA Ca_v channels and modest block of Na_v channels.

The high phylogenetic specificity of these toxins recommends them as lead compounds for the development of new insecticides with novel modes of action [30]. This may include the development of small mimetics that could be used as foliar sprays, orally active acaricidal and insecticidal agents, and recombinant baculoviruses and transgenic crops containing ω-ACTX-1 transgenes [59]. Most importantly, however, these toxins validate insect Ca_v channels as a novel insecticide target, and they may prove to be useful ligands for medium- to high-throughput assays in insecticide discovery programs [46].

Acknowledgements

REFERENCES

[1] World Health Organisation. Vector resistance to insecticides. 15th Report of the WHO Expert Committee on Vector Biology and Control. World Health Org Tech Rep Ser 1992;818:1–62.

[2] Georghiou GP. Overview of insecticide resistance. ACS Symp Ser 1990;421:18–41.

[3] Oerke E-C, Dehne H-W. Safeguarding production-losses in major crops and the role of crop protection. Crop Protect 2004;23:275–85.

[4] Gubler DJ. Resurgent vector-borne diseases as a global health problem. Emerg Infect Dis 1998;4:442–50.

[5] Bravo A, Gill SS, Soberón M. *Bacillus thuringiensis* mechanisms and use. In: Gilbert LI, Iatrou K, Gill SS, editors. Comprehensive molecular insect science. Elsevier; 2005. p. 175–206.

[6] Cory JS, Hirst ML, Williams T, Hails RS, Goulson D, Green BM, et al. Field trial of a genetically improved baculovirus insecticide. Nature 1994;370:138–40.

[7] Khan SA, Zafar Y, Briddon RW, Malik KA, Mukhtar Z. Spider venom toxin protects plants from insect attack. Transgenic Res 2006;15:349–57.

[8] Mukherjee AK, Sollod BL, Wikel SK, King GF. Orally active acaricidal peptide toxins from spider venom. Toxicon 2006;47:182–7.

[9] Wang X-H, Smith R, Fletcher JI, Wilson H, Wood CJ, Howden ME, et al. Structure-function studies of ω-atracotoxin, a potent antagonist of insect voltage-gated calcium channels. Eur J Biochem 1999;264:488–94.

[10] Fletcher JI, Smith R, O'Donoghue SI, Nilges M, Connor M, Howden ME, et al. The structure of a novel insecticidal neurotoxin, ω-atracotoxin-HV1, from the venom of an Australian funnel web spider. Nat Struct Biol 1997;4:559–66.

[11] Tedford HW, Fletcher JI, King GF. Functional significance of the β hairpin in the insecticidal neurotoxin ω-atracotoxin-Hv1a. J Biol Chem 2001;276:26568–76.

[12] Tedford HW, Gilles N, Ménez A, Doering CJ, Zamponi GW, King GF. Scanning mutagenesis of ω-atracotoxin-Hv1a reveals a spatially restricted epitope that confers selective activity against insect calcium channels. J Biol Chem 2004;279:44133–40.

[13] Pallaghy PK, Neilsen KJ, Craik DJ, Norton RS. A common structural motif incorporating a cystine knot and a triple-stranded β-sheet in toxic and inhibitory polypeptides. Protein Sci 1994;3:1833–9.

[14] Pallaghy PK, Norton RS. Refined solution structure of ω-conotoxin GVIA: implications for calcium channel binding. J Pept Res 1999;53:343–51.

[15] Craik DJ, Daly NL, Waine C. The cystine knot motif in toxins and implications for drug design. Toxicon 2001;39:43–60.

[16] Atkinson RK, Tyler MI, Vonarx EJ, Howden MEH. Insecticidal toxins derived from funnel web (*Atrax* or *Hadronyche*) spiders. International Patent WO 93/15108; 1993, August 5.

[17] Bloomquist JR. Mode of action of atracotoxin at central and peripheral synapses of insects. Invert Neurosci 2003;5:45–50.

[18] Vonarx EJ, Tyler MI, Atkinson RK, Howden MEH. Characterization of insecticidal peptides from venom of Australian funnel-web spiders. J Venom Anim Toxins 2006;12:215–33.

[19] Ginsborg BL, Warriner J. The isolated chick biventer cervicis nerve-muscle preparation. Br J Pharmacol 1960;15:410–1.

[20] Frohman MA. Rapid amplification of complementary DNA ends for generation of full-length complementary DNAs: thermal RACE. Meth Enzymol 1993;218:340–56.

[21] Frohman MA, Dush MK, Martin GR. Rapid production of full-length cDNAs from rare transcripts: amplification using a single gene-specific oligonucleotide primer. Proc Natl Acad Sci USA 1988;85:8998–9002.

[22] Grolleau F, Lapied B. Two distinct low-voltage-activated Ca^{2+} currents contribute to the pacemaker mechanism in cockroach dorsal unpaired median neurons. J Neurophysiol 1996;76:963–76.

[23] Wicher D, Penzlin H. Ca^{2+} currents in central insect neurons: electrophysiological and pharmacological properties. J Neurophysiol 1997;77:186–99.

[24] Sinakevitch IG, Geffard M, Pelhate M, Lapied B. Anatomy and targets of dorsal unpaired median neurones in the terminal abdominal ganglion of the male cockroach *Periplaneta americana* L. J Comp Neurol 1996;367:147–63.

[25] Barry PH. JPCalc, a software package for calculating liquid junction potential corrections in patch-clamp, intracellular, epithelial and bilayer measurements and for correcting junction potential measurements. J Neurosci Meth 1994;51:107–16.

[26] Bezanilla F, Armstrong CM. Inactivation of sodium channels. I. Sodium current experiments. J Gen Physiol 1977;70:594–666.

[27] Lapied B, Malécot CO, Pelhate M. Ionic species involved in the electrical activity of single adult aminergic neurones isolated from the sixth abdominal ganglion of the cockroach *Periplaneta americana*. J Exp Biol 1989;144:545–9.

[28] Atkinson RK, Vonarx EJ, Howden MEH. Effects of whole venom and venom fractions from several Australian spiders, including *Atrax* (*Hadronyche*) species, when injected into insects. Comp Biochem Physiol 1996;114C:113–7.

[29] Bendtsen JD, Nielsen H, von Heijne G, Brunak S. Improved prediction of signal peptides: SignalP 3.0. J Mol Biol 2004;340:783–95.

[30] Tedford HW, Sollod BL, Maggio F, King GF. Australian funnel-web spiders: master insecticide chemists. Toxicon 2004;43:601–18.

[31] Wang X-H, Connor M, Wilson D, Wilson H, Nicholson GM, Smith R, et al. Biopesticide panning: discovery of a potent and highly specific peptide antagonist of insect calcium channels. J Biol Chem 2001;276:40306–12.

[32] Sollod BL, Wilson D, Zhaxybayeva O, Gogarten JP, Drinkwater R, King GF. Were arachnids the first to use combinatorial peptide libraries? Peptides 2005;26:131–9.

[33] Wicher D, Penzlin H. Ca^{2+} currents in cockroach neurones: properties and modulation by neurohormone D. Neuroreport 1994;5:1023–6.

[34] Kubista H, Mafra RA, Chong Y, Nicholson GM, Beirao PS, Cruz JS, et al. CSTX-1, a toxin from the venom of the hunting spider *Cupiennius salei*, is a selective blocker of L-type calcium channels in mammalian neurons. Neuropharmacology 2007;51:1650–62.

[35] Arroyo G, Aldea M, Fuentealba J, Albillos A, Garcia AG. SNX482 selectively blocks P/Q Ca^{2+} channels and delays the inactivation of Na^+ channels of chromaffin cells. Eur J Pharmacol 2003;475:11–8.

[36] Wicher D, Penzlin H. ω-Toxins affect Na^+ currents in neurosecretory insect neurons. Receptors Channels 1998;5:355–66.

[37] Middleton RE, Warren VA, Kraus RL, Hwang JC, Liu CJ, Dai G, et al. Two tarantula peptides inhibit activation of multiple sodium channels. Biochemistry 2002;41:14734–47.

[38] Kraus RL, Warren VA, Smith MM, Middleton RE, Cohen CJ. Modulation of alpha$_{1G}$ and alpha$_{1C}$ Ca channels by the spider toxin ProTx-II. Soc Neurosci Abstr 2000;623.

[39] Olivera BM, Miljanich GP, Ramachandran J, Adams ME. Calcium channel diversity and neurotransmitter release: the ω-conotoxins and ω-agatoxins. Annu Rev Biochem 1994;63:823–67.

[40] Bloomquist JR. Toxicology, mode of action and target site-mediated resistance to insecticides acting on chloride channels. Comp Biochem Physiol C 1993;106:301–14.

[41] Johnson JH, Bloomquist JR, Krapcho KJ, Kral Jr RM, Trovato R, Eppler KG, et al. Novel insecticidal peptides from *Tegenaria agrestis* spider venom may have a direct effect on the insect central nervous system. Arch Insect Biochem Physiol 1998;38:19–31.

[42] Krapcho KJ, Kral Jr RM, Vanwagenen BC, Eppler KG, Morgan TK. Characterization and cloning of insecticidal peptides from the primitive weaving spider *Diguetia canities*. Insect Biochem Mol Biol 1995;25:991–1000.

[43] King GF, Tedford HW, Maggio F. Structure and function of insecticidal neurotoxins from Australian funnel-web spiders. J Toxicol-Toxin Rev 2002;21:359–89.

[44] Schwede T, Kopp J, Guex N, Peitsch MC. SWISS-MODEL: an automated protein homology-modeling server. Nucl Acids Res 2003;31:3381–5.

[45] Guex N, Peitsch MC. SWISS-MODEL and the Swiss-PdbViewer: an environment for comparative protein modeling. Electrophoresis 1997;18:2714–23.

[46] King GF. Modulation of insect Ca_v channels by peptidic spider toxins. Toxicon 2007;49:513–30.

[47] Grolleau F, Lapied B. Separation and identification of multiple potassium currents regulating the pacemaker activity of insect neurosecretory cells (DUM neurons). J Neurophysiol 1995;73:160–71.

[48] Jeziorski MC, Greenberg RM, Anderson PA. The molecular biology of invertebrate voltage-gated Ca^{2+} channels. J Exp Biol 2000;203:841–56.

[49] Grolleau F, Lapied B. Dorsal unpaired median neurones in the insect central nervous system: towards a better understanding of the ionic mechanisms underlying spontaneous electrical activity. J Exp Biol 2000;203:1633–48.

[50] Wicher D. Peptidergic modulation of insect voltage-gated Ca^{2+} currents: role of resting Ca^{2+} current and protein kinases A and C. J Neurophysiol 2001;86:2353–62.

[51] Defaix A, Lapied B. Role of a novel maintained low-voltage-activated inward current permeable to sodium and calcium in pacemaking of insect neurosecretory neurons. Invert Neurosci 2005;5:135–46.

[52] Gho M, Ganetzky B. Analysis of repolarization of presynaptic motor terminals in *Drosophila* larvae using potassium-channel-blocking drugs and mutations. J Exp Biol 1992;170:93–111.

[53] Robitaille R, Charlton MP. Presynaptic calcium signals and transmitter release are modulated by calcium-activated potassium channels. J Neurosci 1992;12:297–305.

[54] Robitaille R, Garcia ML, Kaczorowski GJ, Charlton MP. Functional colocalization of calcium and calcium-gated potassium channels in control of transmitter release. Neuron 1993;11:645–55.

[55] Raffaelli G, Saviane C, Mohajerani MH, Pedarzani P, Cherubini E. BK potassium channels control transmitter release at CA3-CA3 synapses in the rat hippocampus. J Physiol (Lond) 2004;557:147–57.

[56] Wicher D, Berlau J, Walther C, Borst A. Peptidergic counter-regulation of Ca^{2+}- and Na^+-dependent K^+ currents modulates the shape of action potentials in neurosecretory insect neurons. J Neurophysiol 2006;95:311–22.

[57] Derst C, Messutat S, Walther C, Eckert M, Heinemann SH, Wicher D. The large conductance Ca^{2+}-activated potassium channel (pSlo) of the cockroach *Periplaneta americana*: structure, localization in neurons and electrophysiology. Eur J Neurosci 2003;17:1197–212.

[58] Newcomb R, Szoke B, Palma A, Wang G, Chen X, Hopkins W, et al. Selective peptide antagonist of the class E calcium channel from the venom of the tarantula *Hysterocrates gigas*. Biochemistry 1998;37:15353–62.

[59] Nicholson GM. Fighting the global pest problem: preface to the special Toxicon issue on insecticidal toxins and their potential for insect pest control. Toxicon 2007;49:413–22.

104

5   Purification and isolation of an insecticidal toxin from the venom of Eastern mouse spider (*Missulena bradleyi*)

Chapter 5 Summary

- Whole venom was collected from female *Missulena bradleyi* by milking spiders.

- Venom was pooled and separated into major peptide fractions using a combination of reverse-phase high-pressure and anion-exchange liquid chromatography.

- Major venom fractions were screened for insect toxicity and four insecticidal fractions (f1, f4, f5 and f6) were identified.

- Each insecticidal fraction was purified using reverse-phase high-pressure liquid chromatography and anion exchange fast-perfusion liquid chromatography in an attempt to isolate a homogenous peptide peak.

- An insecticidal peptide (f1.2.1) was successfully isolated and subjected to further biochemical and pharmacological characterisation (Chapter 6).

5.1 Venom of the eastern mouse spider: *Missulena bradleyi*

There are 11 species of mouse spiders (Araneae: Mygalomorphae Actinopodidae) belonging to the genus *Missulena*; 10 species are indigenous to Australia and 1 from Chile (*M. tusslena*) (Platnick, 2011). The Eastern mouse spider, *M. bradleyi*, inhabits the eastern seaboard of Australia from Queensland to Victoria, (Figure 5.1).

Figure 5.1: Distribution of the Australian Eastern mouse spider (*M. bradleyi*)

Bites from *M. bradleyi* are clinically important because it can result in severe systemic toxicity, with symptoms including paraesthesiae (numbness, tingling and burning), diaphoresis (excessive perspiration), headache and nausea (Isbister, 2004, Isbister and Gray, 2004). Out of 20 recorded cases of *M. bradleyi* bites, the most severe clinical case involved a 19-month girl who was bitten on the finger by a male *M. bradleyi* and experienced loss of consciousness, hypertension and muscle spasm within 30 minutes. Remarkably, she made a full recovery after being given antivenom raised against male Sydney funnel-web spider (*Atrax robustus)* some twelve hours after the bite (Underhill, 1987, Sutherland and Tibballs, 2001).

Pharmacological studies on *M. bradleyi* venom found that whole male venom produced strong effects on vertebrate neuromuscular preparations of rat vas deferens and mouse phrenic nerve-diaphragm. In the chick biventer cervicis nerve-muscle preparation, male venom induced large, sustained muscle contractions with fasciculation and decreased twitch tension height (Gunning et al., 2003). The effects were reversible by *A. robustus* antivenom (Rash et al., 2000, Gunning et al., 2003) and were attributed primarily to the peptide neurotoxin, δ-missulenatoxin-Mb1a, which modifies voltage-gated sodium channel current inactivation (Gunning et al., 2003).

In contrast to male spiders, whole venom from female *M. bradleyi* lacks overt activity on vertebrate neuromuscular preparations, indicating that vertebrate toxins are absent, or present in low concentrations (Rash et al., 2000, Herzig et al., 2008).

5.2 **Insecticidal effects of *M. bradleyi* venom**

Like other Australian mygalomorphs such as *Atrax robustus* and *Hadronyche versuta*, mouse spiders are ground-dwellers that do not use webs for catching arthropods, but instead rely on the effectiveness of neurotoxins in its venom to paralyse and disable their prey. Previous studies found that whole *M. bradleyi* venom, and certain fractionated components were neurotoxic and lethal to house crickets (*Acheta domesticus*) in acute insect toxicity assays (Khalife, 2000, Herzig et al., 2008). A comparison of acute toxicity between male and female *M. bradleyi* whole venom showed that female venom is more toxic to *A. domesticus* than male venom in terms of KD_{50} (female: 3.0 μg/g; male 7.3 μg/g) and LD_{50} values (female: 7.2 μg/g; male 8.6 μg/g) (Herzig et al., 2008). The relatively high insect toxicity of female venom and apparent non-toxicity to vertebrates makes female *M. bradleyi* venom particularly interesting as a potential source of pharmacologically unique toxins that may be candidates in bioinsecticide development.

In contrast to Australian funnel-web spiders from the *Hadronyche* genus, *M. bradleyi* venom has never been systematically examined for novel insecticidal neurotoxins. Accordingly, a project was initiated to investigate female *M. bradleyi* venom for novel insect-selective neurotoxins. The first step involved collection of whole venom by regular milking of spiders. Fractionation and purification of *M. bradleyi* whole venom components was achieved mainly by reverse-phase high-performance liquid chromatography (rp-HPLC), which was chosen as the preferred method based on the success at isolating insecticidal peptide toxins from the venom of Australian funnel-web spiders (*H. versuta* and *A. robustus)*.

Crude fractions collected from rp-HPLC were then assayed for insect toxicity. Insect-toxic fractions were further purified using rp-HPLC and anion-exchange FPLC. The process is outlined in the following flowchart:

```
┌─────────────────────────────────────────────────────────────┐
│ Milking of female Missulena bradleyi (collection of whole venom) │
└─────────────────────────────────────────────────────────────┘
                              ↓
┌─────────────────────────────────────────────────────────────┐
│ Separation of pooled venom into crude components (fractions) using rp-HPLC │
└─────────────────────────────────────────────────────────────┘
                              ↓
        ┌─────────────────────────────────────────┐
        │ Protein quantification – BCA assay        │
        └─────────────────────────────────────────┘
                              ↓
    ┌─────────────────────────────────────────────────┐
    │ Biological assay on major fractions - toxic to insects? │
    └─────────────────────────────────────────────────┘
            Yes ↙                    ↘ No
┌──────────────────────────────┐   ┌──────────────────────────────┐
│ Further purification of toxic │   │ Fraction Rejected – no further │
│ fractions with shallow        │   │ study                          │
│ gradient rp-HPLC              │   └──────────────────────────────┘
└──────────────────────────────┘
              │        ┌─────────────────────────────┐
              │        │ Anion exchange FPLC          │
              │        └─────────────────────────────┘
              ↓              ↓
        ┌─────────────────────────────────────────┐
        │ Isolation of a single peptide peak?       │
        └─────────────────────────────────────────┘
              Yes ↙              ↘ No
                            ┌──────────────────────────────┐
                            │ Fraction rejected – no further │
                            │ study                          │
                            └──────────────────────────────┘
              ↓
```

Protein analysis, characterisation of insect toxicity, vertebrate bioassay, and molecular target identification **(covered in Chapter 6).**

5.3 **Whole venom fractionation**

Venom was obtained by repetitive milking of captive female *M. bradleyi* spiders every fortnight using methods described in section 2.5. Several thousand individual milkings were performed over a period of approximately six years (part-time candidature). Each spider produced only a small amount of venom (≤ 1 μl) at each milking, therefore venom was pooled together prior to fractionation with rp-HPLC using methods described in section 2.6. Around 110 crude separation runs were performed on HPLC during this PhD project. The venom profile showed a very high degree of consistency across successive batches of pooled venom. Analysis of the chromatogram revealed

a total of up to 30 peaks of varying absorbance (Figure 5.2). Several large peaks eluted during the first 5 minutes of the run but were not collected as they represent a mixture of mostly non-peptide components such as ions, nucleic acids, glucose, polyamines, free amino acids and/or neurotransmitters (Rash and Hodgson, 2002, Escoubas et al., 2000). Due to time constraints and a limited supply of spider venom, eight major peptide fractions (f1-f8) were selected and screened for insecticidal activity on House crickets (*Acheta domesticus*) as described in section 2.8.
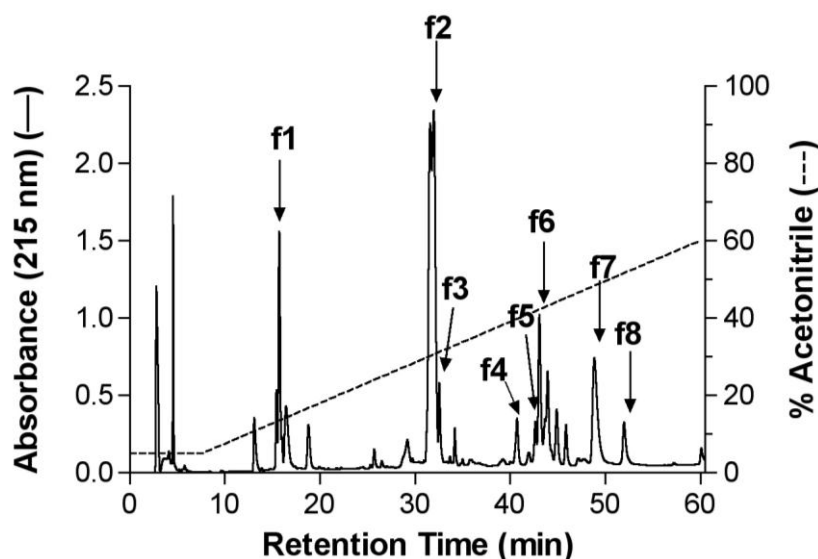
Figure 5.2: Typical C18 rp-HPLC chromatogram of pooled female *M. bradleyi* spider whole venom. Absorbance (solid line) and the percentage of acetonitrile (dashed line) are shown over a period of 60 min. Numbers indicate eight peaks that were collected for insect toxicity testing.

5.4 Insect toxicity screening of venom fractions

Fractions 1-8 were lyophilised using a freeze-drier and resuspended in a fixed volume of distilled water. Each fraction was assayed for protein concentration using BCA as described in section 2.7 and screened for insecticidal activity at a concentration of 10 μg/g bodyweight on house crickets using the methods described in section 2.8.

Crickets injected with f1 exhibited mild signs of systemic toxicity within 20 minutes of the injection with changes in motor function including ataxia and fasciculation (involuntary twitching) of the legs and antenna. At 40 minutes, crickets showed immobility or dyskinesia (staggered walking) accompanied by

rapid fasciculation of the legs. At the 1, 4 and 8-hour time-points, complete loss of locomotion with rapid intermittent or continuous fasciculation of the appendages was observed, marking the state of "knockdown". This was followed by periods of sustained skeletal muscle contractures (contractile paralysis) and 100% mortality within 24 hours. Figure 5.3 shows control and f1-injected crickets at 24 hours.

Figure 5.3: House crickets after injection with insect saline solution containing f1. Control crickets at 24 hours after injection with vehicle (insect saline/0.1% BSA) at 5 µl/100 mg body weight (left) and at 24 hours after injection with 10 µg/g bw of f1 in vehicle (right).

Crickets injected with f4 showed signs of severe systemic toxicity at the 20 minute observation with 40% of crickets lying on their back and the remainder upright but unable to walk. All crickets showed minimal response to external stimuli (tapping the petri dish). At 1 hour after injection, all crickets were lying on their back and relaxation of leg muscles was observed (flaccid paralysis) with movement only upon external stimuli. All crickets were found dead at the 4 hour observation.

At 20 minutes after injection with f5, 40% of crickets were found lying on their back with no movement except for leg twitching after tapping of the dish. The remaining crickets were upright but motionless. All crickets showed signs of flaccid paralysis and were lying on their back except for leg movements after external stimuli at 40 minutes after injection. At the 8-hour observation, one cricket had recovered from paralysis and was upright and mobile. Two crickets

had recovered and were walking at the 16-hour observation and the remaining crickets were found dead.

Four of five crickets injected with f6 were found lying on their back with flaccid paralysis at 20 minutes after injection and one cricket was upright but motionless. At 40 minutes, all crickets were on their back with signs of flaccid paralysis. This persisted until the 24-hour observation at which 100% of crickets had fully recovered and were upright, walking and appeared normal.

No toxicological signs or changes in motor function were observed in crickets tested with f2, 3, 7 & 8 as well as crickets in the control group. The full results are summarised in Table 5.1.

Based on the results of these tests, insecticidal venom fractions 1, 4, 5 and 6 were selected for further purification with the aim of isolating a homogenous peptide toxin within each fraction that was responsible for the observed insecticidal effects in the crickets.

Table 5.1: Acute effects of crude female *M. bradleyi* venom fractions tested in House crickets (*Acheta domesticus*) at 10 μg/g.

Fraction	Type of observed paralysis	Time to 100% knockdown	Time to 100% lethality	Lethality at 24 hrs (%)
1	Contractile	< 60 min	< 24 hours	100
2	None	-	-	0
3	None	-	-	0
4	Flaccid	< 20 min	< 4 hours	100
5	Flaccid, reversible	< 20 min	-	60
6	Flaccid, reversible	< 40 min	-	0
7	None	-	-	0
8	None	-	-	0

5.5   **Purification of f1**

Pooled f1 was loaded onto a C18 rp-HPLC column running a shallow concentration gradient of 10-20% acetonitrile (ACN) at a rate of 0.1%/min. One major peak eluted at 13-14 minutes/11.4% ACN with a „shoulder" on the falling phase, indicating a poor level of resolution and incomplete separation of peptides (Figure 5.4).
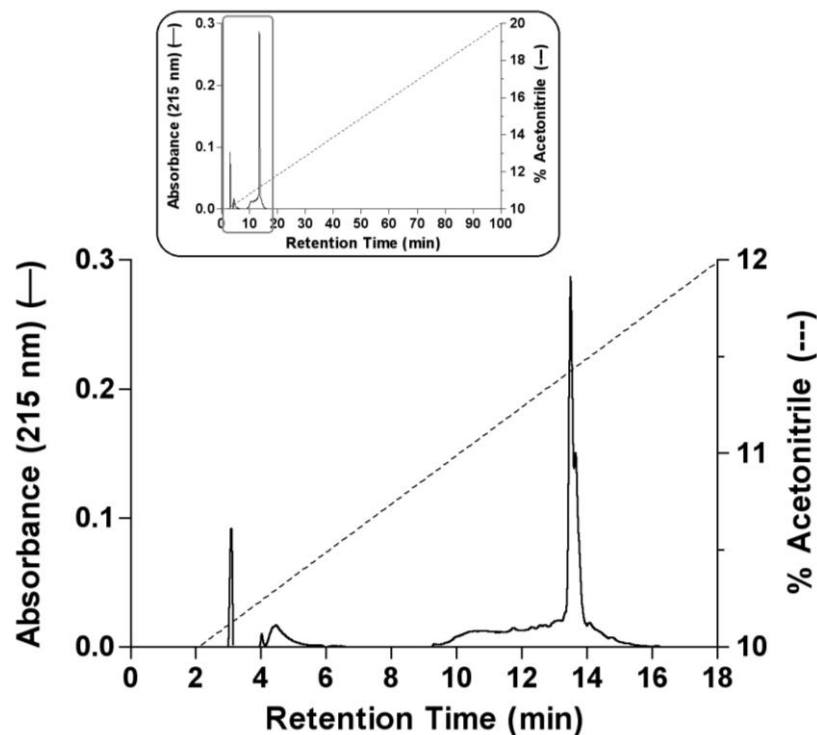
Figure 5.4: Reverse-phase HPLC chromatogram of f1. Purification of f1 using ACN/0.1% TFA buffer at 10-20% concentration (inset) resulted in one major peak containing at least two discrete peptides at 13-14 min (~11.4% ACN). Minor peaks eluted in the void within the first 5 mins.

To achieve a higher degree of separation, anion-exchange FPLC was employed in an attempt to separate the peptides based on electrostatic interactions of the negatively charged amino acid side groups with the positively charged amine groups on the resin within the anion exchange column matrix (Kopaciewicz et al, 1983).

Using an increasing NaCl concentration from 20 mM to 1 M, a group of peaks eluted within the first 3 minutes (Figure 5.5) without binding to the column and

was collected as a mixture (f1.1). A separate single peak (f1.2) was collected at a retention time of 8-9 minutes (60 mM NaCl; f1.2).
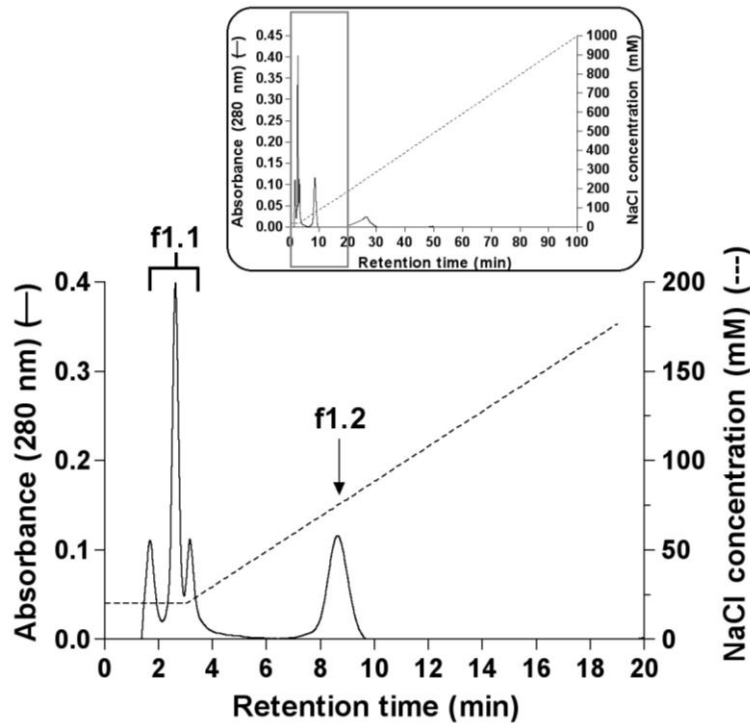
Figure 5.5: Anion exchange FPLC separation of f1. Purification of f1 using 20-1000 mM NaCl buffer, pH 7.48, on a Mono-Q column over 100 mins (inset), resulted in the elution of one peak (f1.2). At least 3 peaks (f1.1) eluted in the void and were collected separately for further purification. A final broad peak was observed at 20-30 mins (inset) but this was not collected as it represented a heterogeneous mixture of peptides at very low concentrations.

5.6   Testing of f1.1 and f1.2 for insect activity

Insect toxicity screening was carried out on the f1.1 mixture and f1.2 using the methodology described in section 2.8.

Crickets injected with f1.1 mixture exhibited rapid tremors accompanied by hyperextension of the hind legs at the 20 minute observation point. Latero-flexion of the abdomen was observed in 50% of crickets. Full knockdown was observed 15 hours after injection with all crickets unable to maintain upright posture or in a state of complete paralysis. All crickets were found dead at the 24-hour observation.

Around 20% of crickets injected with f1.2 showed signs of involuntary twitching of the legs at 20 minutes after injection. At the 40- and 60-minute observations, 60% of crickets had ceased walking and exhibited obvious twitching of the appendages. By 1 hour after the injection, all crickets showed rapid severe fasciculation of all appendages, akinesia, and were unresponsive to external stimuli. All crickets were found dead at the 48-hour observation point. The results are summarised in Table 5.2. F1.1 achieved full lethality in half the time taken for f1.2; however it was noted that insects injected with f1.2 experienced very rapid knockdown in which insects were quickly paralysed and immediately ceased moving and feeding.

Table 5.2: Acute effects of crude f1.1 and f1.2 fractions on house crickets (*Acheta domesticus*) after injection at 10 μg/g bodyweight.

Venom fraction	Type of Observed Paralysis	Time to 100% knockdown	Time to 100% lethality
f1.1	Rigid, tremorous	< 15 hrs	< 24 hours
f1.2	Contractile	< 1 hr	< 48 hours

5.7 Purification of f1.1 and f1.2

Several attempts were made to purify components within f1 on C18 rp-HPLC, which included separations runs on a 5-15% ACN/0.1% TFA buffer concentration at a shallow rising gradient of 0.1%/min (Figure 5.6A) and methanol (MeOH)/0.1% TFA buffer at 5-60% concentration at a gradient of 1%/min (Figure 5.6B). A total of four different protocols were used to separate f1.1, however in each case, there was incomplete separation and poor resolution of peaks. No fractions were collected and no further attempts were made to purify f1.1. Table 5.3 summarises the rp-HPLC procedures that were used in an attempt to separate the components in f1.1.

A
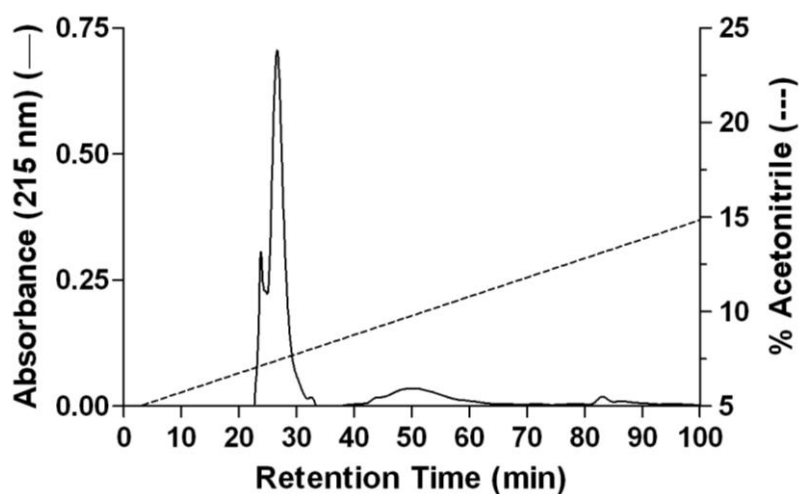
B
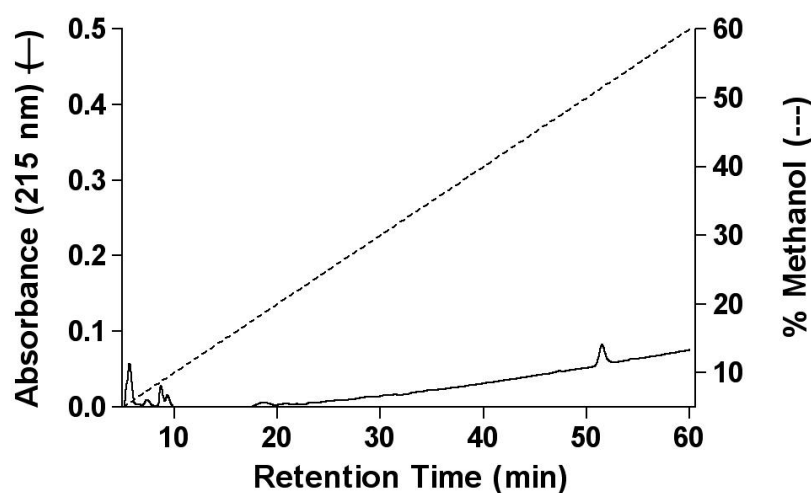
Figure 5.6: Typical analytical C18 rp-HPLC chromatograms of f1.1 purification. (A) 5-15% ACN/0.1% TFA concentration increasing at 0.1%/min. (B) 5-60% MeOH/0.1% TFA at 1%/min resulted in poor or incomplete separation of f1.1

Table 5.3:Summary of rp-HPLC protocols used in attempts to purify f1.1.

Fraction	*Rp-HPLC* ACN conc (%)	*Rp-HPLC* MeOH conc *(%)*	Result
f1.1	5-15 at 0.1%/min	-	Incomplete separation. No purified fractions collected.
f1.1	15-16 at 0.1%/min	-	Incomplete separation. No purified fractions collected.
f1.1	-	5-60% at	Several peaks of very low

		1%/min	absorbance (< 0.05 nm) detected. No purified fractions collected.
f1.1	-	30-32% at 0.1%/min	Several peaks of very low absorbance (< 0.05 nm) detected. No purified fractions collected.

5.8 Purification of f1.2

During anion-exchange FPLC (Figure 5.5), the f1.2 peak eluted in a solution that contained a high concentration of salts, which required removal in preparation for further analyses. This process (referred to as „desalting) was achieved via rp-HPLC on a C18 column running 5-15% ACN/0.1% TFA buffer concentration rising at a shallow gradient rate of 0.1% ACN/min. The desalting procedure resulted in the elution of a single homogeneous peptide peak (f1.2.1) at 8.5 min (15.2% ACN) (Figure 5.7), which was subsequently freeze-dried.

This peak represents a novel insecticidal peptide neurotoxin from *M. bradleyi* venom that became the subject of further investigation as a potential candidate for a lead bioinsecticide molecule. The molecular mass, structure, insect toxicity profile and electrophysiological effects of f1.2.1 is characterised and described in Chapter 6.
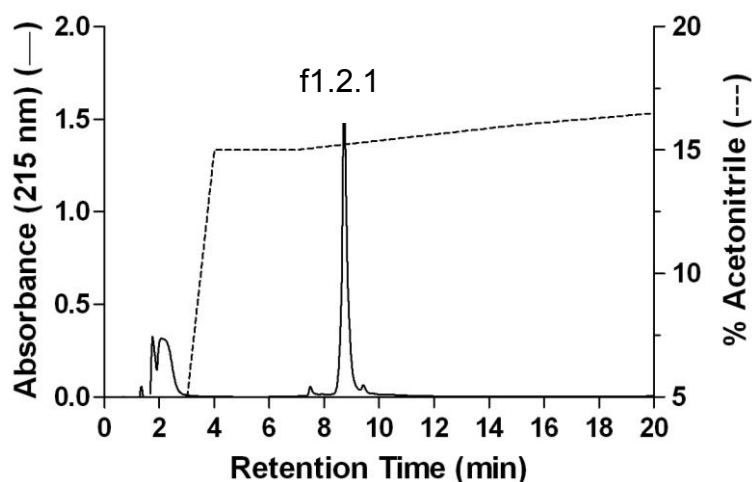
Figure 5.7: Typical rp-HPLC chromatogram of f1.2. The f1.2.1 peak obtained from anion-exchange FPLC was purified at 15-16% ACN/0.1% TFA at 0.1%/min.

5.9 **Purification of f4, f5 and f6**

Based on the successful purification of f1.2.1, rp-HPLC and anion exchange FPLC techniques were once again utilised in an attempt to purify a homogeneous peak from f4, f5 and f6.

5.9.1 Attempted separation of f4

In the acute insect toxicity assay described in section 5.4, f4 achieved 100% lethality in all insects in less than 4 hours from time of injection, which is the shortest time period taken for lethality of all the fractions tested. Given this result, f4 was viewed as a promising biopesticide candidate; hence particular attention was paid to the separation of f4 components. The dried material (pooled and lyphophilised f4) was dissolved in a solution of 5% Buffer B (0.1% TFA in ACN) and loaded onto an analytical C18 column. The flow rate was set at 1 ml/min, starting at 5% ACN for 3 minutes to allow the dissolved solution to run through the C18 column. A shallow concentration gradient (0.1%/min) was employed to try and improve peak separation. Based on the crude whole venom separation chromatogram (Figure 5.2) which showed that f4 eluted at ~38% ACN/0.1% TFA concentration, two rp-HPLC protocols were designed with ACN buffer concentrations ranging from 5% to 40%. Examples of typical chromatograms are shown in Figure 5.8. Results showed that these methods failed to adequately separate f4 into its constituents, or produced peaks with very low absorbance that were insufficient for further analyses. Based on these chromatograms, no purified peaks were collected.
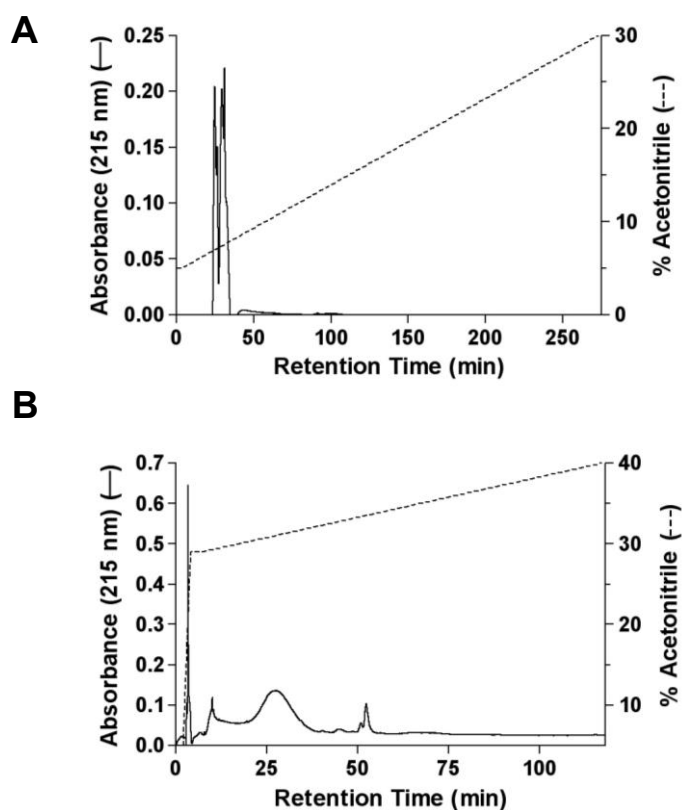
Figure 5.8: Typical analytical C18 rp-HPLC chromatograms of f4. Purification of f4 using -30% ACN/0.1% TFA at a shallow gradient of 0.1%/min resulted in a mixture of peaks eluting at 8% ACN (A). 29-40% ACN/0.1% TFA produced one major peak in the void and several minor peaks of very low absorbance (B).

Anion exchange FPLC was investigated as an alternative separation method. Lyophilised and pooled f4 was dissolved in 20mM NaCl and injected into a Mono-Q or Phenosphere column running NaCl buffer at concentrations ranging from 20 mM to 500 mM. The pH values of the buffer solutions were varied for the purpose of achieving high resolution separation. Figure 5.9 shows typical examples of anion exchange FPLC chromatograms of 20 - 400 mM NaCl, pH 7.48 (Figure 5.9A) and 20-500 mM NaCl, pH 7.55 (Figure 5.9B). A total of nine different protocols were used in the attempt to separate f4, but none of these methods were able to isolate a homogenous peak. The full list of protocols is detailed in Table 5.4.

A

B
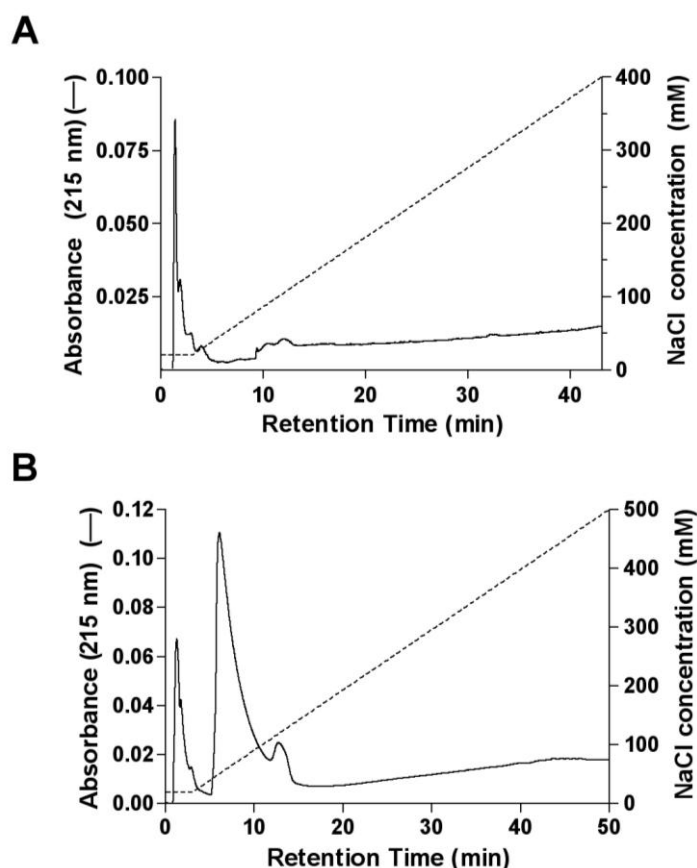
Figure 5.9: Typical anion exchange FPLC chromatograms of f4. (A) 0-400 mM NaCl buffer at pH 7.48, and (B) 0-500 mM NaCl at pH 7.55 on a Mono-Q column. A heterogeneous mixture of peptides were eluted, therefore no fractions were collected.

Table 5.4: Summary of rp-HPLC and anion exchange methods used in the attempt to purify f4. Anion exchange FPLC was performed using a Mono-Q column (Pharmacia Biotech, Sweden), unless otherwise specified.

Sample	*Reverse-phase* ACN conc (%)	*Anion exchange* NaCl conc (mM)	Result
f4	5-30% at 0.1%/min	-	Mixture of peaks eluted, separation unsuccessful. No fractions collected.
f4	29-40 at 0.1%/min	-	Mixture of peaks eluted, separation unsuccessful. No fractions collected.
f4	35-40% at 0.1%/min	-	Mixture of peaks eluted, separation unsuccessful. No fractions collected.
f4	-	0-400, pH 7.48 at 1%/min	Mixture of peaks eluted, separation unsuccessful. No fractions collected.

f4	-	0-500, pH 7.48 at 1%/min	Broad peak containing mixture of peptides eluted. Separation unsuccessful. No fractions collected.
f4	-	0-500, pH 7.55 at 1%/min	Broad peak containing mixture of peptides eluted. Separation unsuccessful. No fractions collected.
f4	-	0-500, Phenosphere*, pH 7.48 at 1%/min	Mixture of peaks eluted, separation unsuccessful. No fractions collected.
f4	-	0-480, pH 3.11 at 1%/min	Mixture of peaks eluted, separation unsuccessful. No fractions collected.
f4	-	0-200, pH 4.45 at 1%/min	Mixture of peaks eluted, separation unsuccessful. No fractions collected.

* Phenosphere 5 μ SAX column (Phenomenex, USA)

5.9.2 Attempted separation of f5 and f6

The whole venom profile (Figure 5.2) showed that fractions 5 and 6 roughly co-eluted on analytical C18 rp-HPLC at ~40% ACN/0.1% TFA. In an attempt to separate the peptides, f5 and f6 were pooled together into a single fraction (named f5/6) and lyophilised using a freeze-drier. The dried material was then resuspended in a solution of 5% Buffer B (0.1% TFA in ACN) and loaded onto a C18 analytical rp-HPLC column. The flow rate was set at 1 ml/min, starting at 5% ACN for 3 minutes to allow the sample to bind to the column. The ACN/0.1% TFA was then ramped up to 40% ACN to expedite the run-time and elute early peaks. The buffer concentration was sustained at 40% for 3 minutes to equilibrate the column at this concentration before beginning a gradient of 0.1%/min up to 50%. The resulting profile showed that this method was not successful as most of the material eluted in the void and a mixture of small peaks were detected at around 7-25 minutes (Figure 5.10). These peaks were deemed too small and insufficient in quantity to collect.
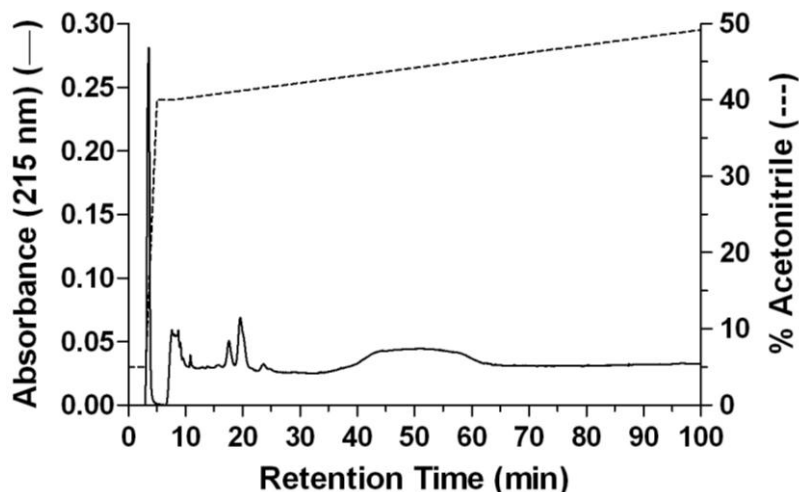
Figure 5.10: Typical analytical C18 rp-HPLC chromatogram of pooled f5/6. A linear gradient of 40-55% ACN/0.1% TFA at 0.1%/min resulted in large peaks eluting early in the void, followed by multiple peaks of very low absorbance.

Given that rp-HPLC was unsuccessful at separating f5/6, anion exchange FPLC was employed using a Phenosphere 5 μ SAX column and mobile phase running 0-500 mM NaCl, pH 7.48, at 1%/min. Figure 5.11A is a typical chromatogram showing some material eluting in the void within the first 3 minutes of the run without column binding and one broad absorbance peak at around 5-9min (50 mM NaCl). This peak was collected and labelled f5/6.1.

Subsequently, f5/6.1 was desalted and fractionated on C18 rp-HPLC running a shallow concentration gradient (0.1%/min) from 40-55% ACN. The chromatogram showed the elution of a sharp peak in the void, followed by multiple small peaks, including one very broad peak between 25-50 minutes retention time (Figure 5.12B), suggesting that f5/6.1 consisted of minor heterogeneous peptides, rather than one major peptide. Given the number of peaks and very small absorbance, f5/6.1 was not investigated further. The purification steps are summarised in Table 5.5.
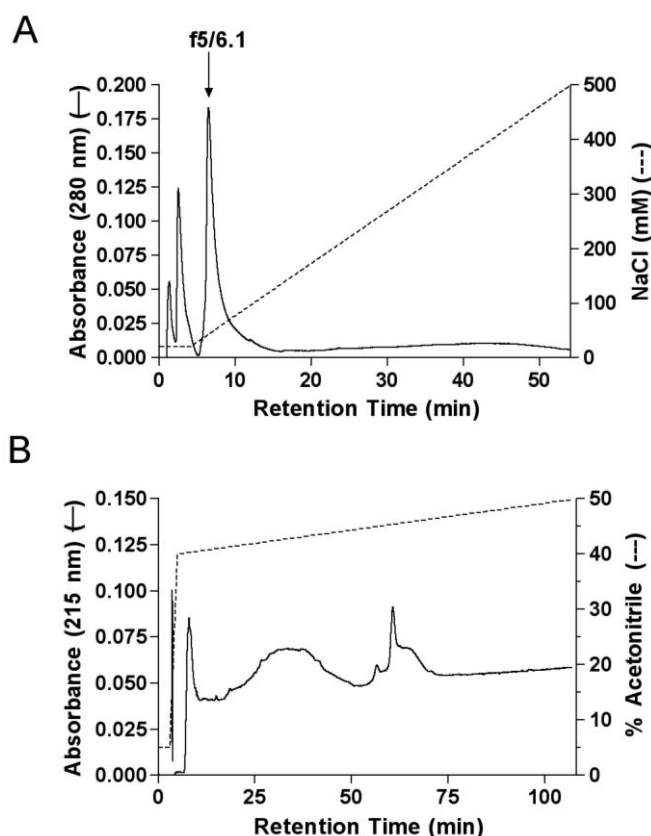
Figure 5.11: Typical anion exchange FPLC and analytical C18 rp-HPLC chromatograms of f5/6. (A) f5/6 was separated on a Phenosphere 5 μ SAX column with a 0 – 500 mM NaCl buffer at pH 7.48. One major peak eluted at 5-9 mins (f5/6.1), with the remainder eluting in the void. (B) rp-HPLC purification of f5/6.1 on a shallow gradient (0.1%/min) of 40-55% ACN/0.1% TFA resulted in elution of a heterogeneous mixture of small absorbance peptides, which were not collected for further study.

Table 5.5: Summary of f5/6 and f5/6.1 purification steps.

Sample	*Reverse-phase* ACN conc (%)	*Anion exchange* NaCl conc (mM)	Result
f5/6	40-55 at 0.1%/min	-	Non-binding to column, separation unsuccessful. No fractions collected.
f5/6	-	0-500, pH 7.48 at 1%/min	Peak f5/6.1 collected.
f5/6.1	40-55% at 0.1%/min	-	Multiple small mixed peaks. No fractions collected.

5.10 **Summary and conclusion**

M. bradleyi whole venom was crudely fractionated on rp-HPLC using an analytical C18 column, and four crude insecticidal fractions (f1, 4, 5 and 6) were identified. These crude fractions were assumed to be mixtures of peptides present in small quantities and hence could not be adequately separated on a C18 rp-HPLC column, nor could they be separated using an anion exchange FPLC column on a NaCl mobile phase. The exception was f1, which was successfully separated into its components (f1.1 and f1.2) using a combination of rp-HPLC and anion exchange FPLC techniques. Further purification of f1.2 on rp-HPLC yielded a single peptide peak (f1.2.1). The f1.2.1 peak was then subjected to biochemical and pharmacological characterisation in Chapter 6.

6 Characterisation of the insecticidal ω-actinopoditoxin-Mb1a from Eastern mouse (*Missulena bradleyi*) spider venom

Chapter 6 Summary

- F1.2.1, an insecticidal peptide identified in the venom of female *M. bradleyi*, has a molecular mass of 4167 Da and displays no overt toxic activity in the chick biventer cervicis nerve-muscle preparation, but is lethal to house crickets in insect toxicity bioassays.

- N-terminal sequencing revealed that f1.2.1 is a 39 amino acid residue peptide with 6 cysteines, and has up to 59% sequence homology to ω-hexatoxin-1 family of insect-selective peptide neurotoxins from the venom of Australian funnel-web spiders.

- The f1.2.1 peptide toxin was assigned the name ω- actinopoditoxin-Mb1a in accordance with nomenclature for peptide toxins derived from spider venoms.

- Whole-cell voltage- clamping on cockroach neurons revealed that ω-actinopoditoxin-Mb1a irreversibly blocks voltage-gated calcium (Ca_v) channels and inhibits both high- (HVA) and mid/low-voltage-activated (M-LVA) Ca_v channel currents in insect neurons in a concentration-dependent manner.

- ω- actinopoditoxin-Mb1a causes voltage-independent inhibition of HVA and M-LVA Ca_v channel currents with no alteration to activation and inactivation kinetics, suggesting it is a channel pore blocker.

6.1 **Background and Overview**

The f1.2.1 peptide obtained from rp-HPLC and anion exchange FPLC separation of female *M. bradleyi* venom was characterised to assess the potential of this peptide as a novel insecticide lead. An overview of the processes that were undertaken is shown below:

Milking of female *Missulena bradleyi*

Purification of whole venom with rp-HPLC

Collect crude fraction „f1"

Anion exchange FPLC of f1

Collect anion exchange fraction „f1.2"

Shallow gradient rp-HPLC of insect-toxic fraction

f1.2.1

Mass spectrometry

Insect toxicity assays to determine of KD_{50} and LD_{50}

Bioassays to confirm non-toxicity in vertebrates

Pyridylethylation and amino acid sequencing (Edman degradation)

Molecular target identification and characterisation (patch–clamp technique)

6.2 **Whole venom fractionation and purification of f1.2.1**

Female *M. bradleyi* spiders were continuously milked on a fortnightly basis throughout the duration of this project to ensure that sufficient quantities of f1.2.1 peptide were available for each experiment. After each milking session, the venom was pooled then fractionated in the following sequence:

A. Steep gradient rp-HPLC (1%/min) of 5-60% ACN/0.1% TFA mobile phase to separate whole venom and collect crude fraction, f1 (Figure 6.1A);

B. Further purification of f1 by anion exchange FPLC on 0-200 mM NaCl buffer (Figure 6.1B) to collect f1.2;

C. Desalting and final purification of f1.2 on shallow gradient (0.1%/min) rp-HPLC using 15-16% ACN/0.1% TFA (Figure 6.1C) to obtain peptide peak, f1.2.1.
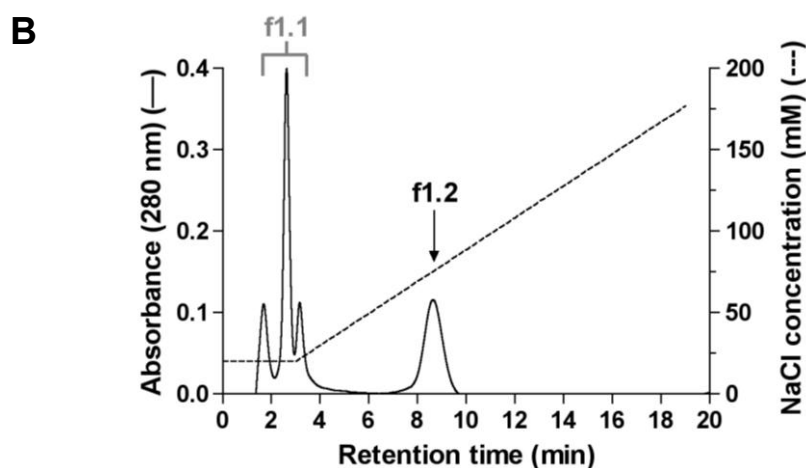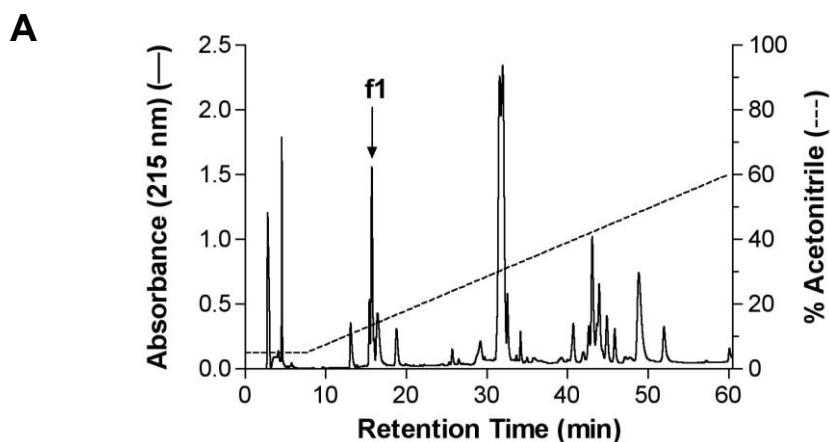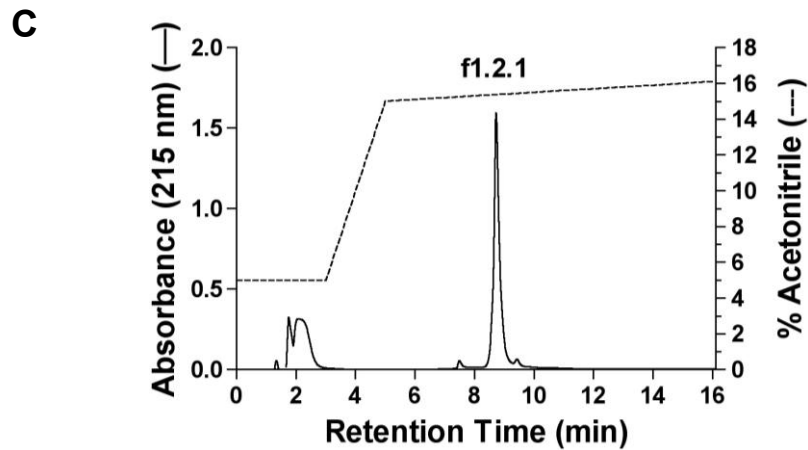
Figure 6.1: Typical rp-HPLC and anion exchange chromatograms of f1.2.1 purification. (A) Analytical C18 rp-HPLC chromatogram of pooled female *M. bradleyi* whole venom showing „f1‟ peak. Venom was fractionated using 5-60% ACN/0.1% TFA. (B) Purification of f1 by anion exchange FPLC using 0-200 mM NaCl buffer concentration. A group of peaks eluted in the void („f1.1‟), and one major peak („f1.2‟) eluted at 8-9 mins. (C) Desalting and final purification of f1.2 by shallow gradient (0.1%/min) analytical C18 rp-HPLC using 15-16% ACN/0.1% TFA. One major peak (f1.2.1) eluted from the column. Solid lines represent absorbance and dashed lines represent percentage of liquid phase.

6.3 Mass spectrometry of f1.2.1

Matrix-assisted laser desorption/ionisation time-of-flight (MALDI-TOF) mass spectrometry was performed to confirm purity of purified f1.2.1 and determine the molecular mass. The mass spectrum (Figure 6.2) shows that the major mass was 4166.7 Da.
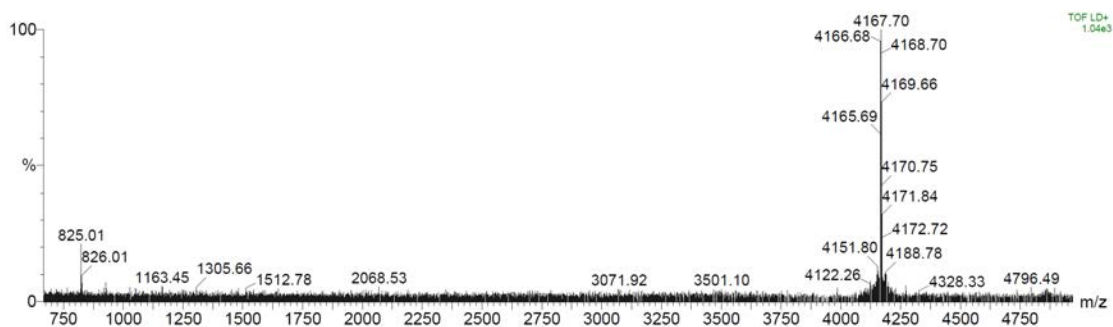
Figure 6.2: Determination of molecular mass of peptide f1.2.1. Matrix-assisted laser desorption/ionisation time-of-flight mass spectrum (reflector mode) shows the monoisotopic mass/charge (*m/z*) signals. The major mass at 4167.7 indicates a monoisotopic mass of 4166.7 Da.

6.4   **Biological activities of f1.2.1**

Purified f1.2.1 was pooled and lyophilised so that the protein content could be quantitated using a BCA assay. To confirm the biological activity of f1.2.1 on insects, five house crickets (*A. domesticus*) were firstly injected with f1.2.1 at 5 μg/g body weight. Following this, acute toxicity testing was performed on house crickets to determine the „knockdown" (KD) and lethal dose endpoints by injection of f1.2.1 at 5 μg/g body weight. The crickets showed symptoms of toxicity within 20 min, which included body tremors, continuous high frequency twitching of limbs and antennae and the inability to maintain upright posture. At this point, crickets were characterised as having reached the KD endpoint. Progressive spastic paralysis was followed by death in all crickets over a time-course of 72 hours. The KD_{50} and LD_{50} values for f1.2.1 at the 48-hour endpoint were determined to be 34.89 ± 1.81 pmol/g and 49.80 ± 4.10 pmol/g, respectively ($n = 5$) (Figure 6.3A). A summary table of KD and LD endpoints is show in Figure 6.3B.

A
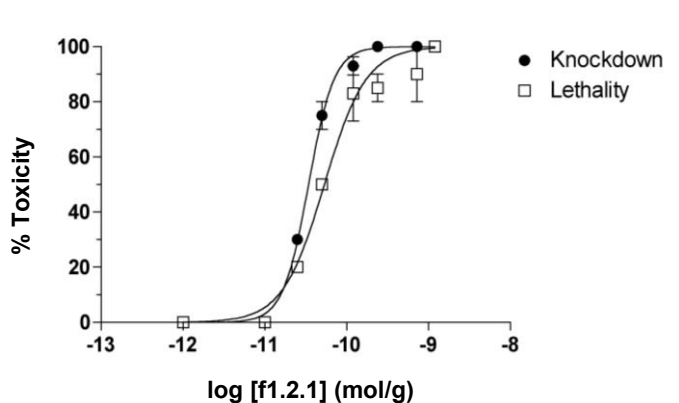
B

Time post-injection (hrs)	KD_{50} (pmol/g)	LD_{50} (pmol/g)
24	43.51 ± 1.62	261.18 ± 30.0
48	34.89 ± 1.81	49.80 ± 4.10
72	31.31 ± 2.14	36.94 ± 0.60

Figure 6.3: Acute toxicity of f1.2.1 in house crickets. (A) Log-dose response curves for lethality (open symbols) and knockdown (closed symbols) of crickets at 48 hours after injection of f.1.2.1 at 5 μg/g body weight (n = 5). Doses are shown as log-transformed data. Data was fitted with Equation 1 in section 2.8.2. (B) KD_{50} and LD_{50} values of f1.2.1 in house crickets at 24, 48 and 72 hours post-injection expressed in pmol/g body weight (n = 5).

To confirm that the purified f1.2.1 peptide toxin was not biologically active on vertebrate tissue, an *in vitro* bioassay was performed on the isolated chick biventer cervicis nerve-muscle preparation. The preparation was firstly challenged with the cholinergic agonists, ACh (1 mM), CCh (20μM) and KCl (40 mM) in the absence of electrical stimulation and repeatedly washed out until a stable baseline was observed for 1 hour. The f1.2.1 toxin was added to the bath solution at a concentration of 1 μM, and indirectly stimulated twitch contractions were recorded for a period of 2 hours. There was no effect on the resting or twitch tension of the nerve-muscle and no other observable sign of overt toxicity (Figure 6.4).

1 μM f1.2.1
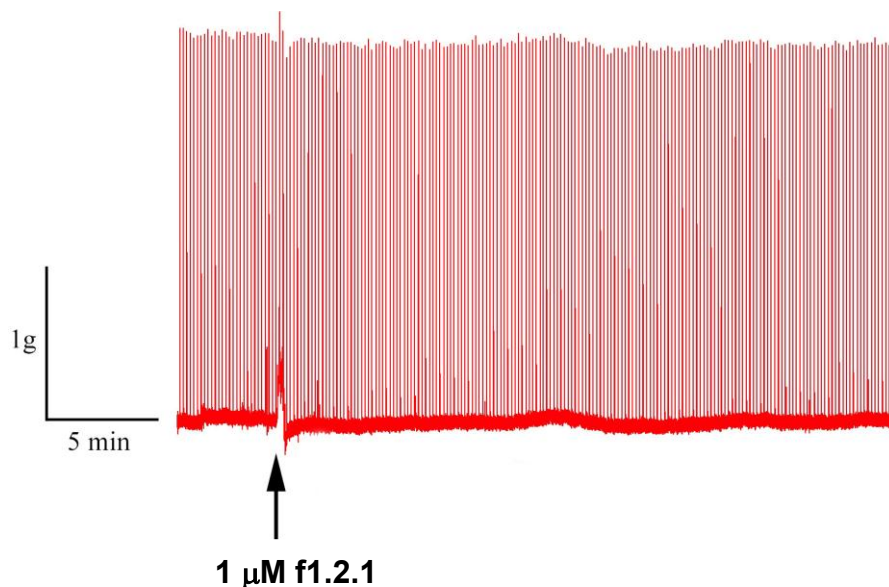
Figure 6.4: The effect of f1.2.1 toxin on the isolated chick biventer cervicis nerve-muscle preparation. Calibration scale shows 1g of tension and 5 mins. The muscle was indirectly stimulated at 0.1 Hz for 0.05 ms using a 20 V square wave pulse. A 1 μM concentration of f1.2.1 was added after 1 hour of equilibration time and recording continued for at least 2 hours afterward.

6.5 **Pyridylethylation of f1.2.1**

In preparation for amino acid sequencing, f1.2.1 was reduced using DTT and alkylated using 4VP. Prior to separation of pyridylethylated toxin, a blank C18 rp-HPLC run, using only the alkylation reaction mixture, was performed to serve as reference. Following the reaction, the f1.2.1 toxin was purified on analytical C18 rp-HPLC. Both blank (Figure 6.5A) and f1.2.1 toxin (Figure 6.5B) runs used a liquid phase of 5-60% ACN/0.1% TFA. The chromatograms showed that a large amount of material eluted within the first 20 min and was followed by a single peak at approximately 53 min (28% ACN). An additional peak at 48 min (25% ACN) (Figure 6.5B) represented the pyridylethylated f1.2.1 toxin. This peak was collected and analysed on electrospray ionisation mass spectrometry (ESI-MS) to determine the molecular mass of the pyridylethylated f1.2.1 peptide.

A
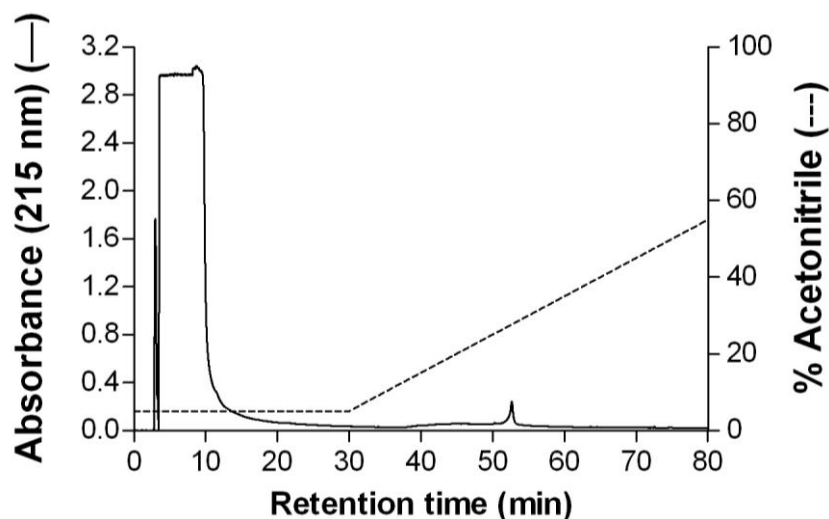
B
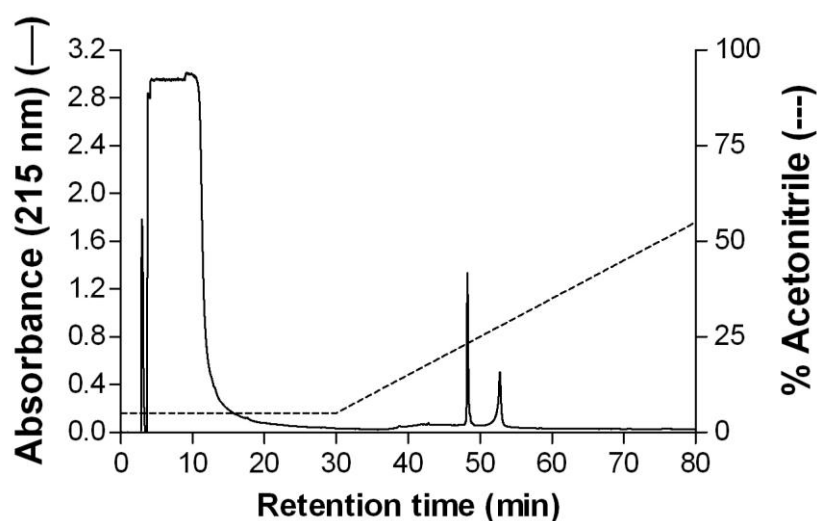
Figure 6.5: Reverse-phase analytical C18 HPLC separation of pyridylethylated f1.2.1 toxin. (A) Blank run with reaction mixture in the absence of toxin. (B) Separation of pyridylethylated toxin with single peak eluting at 48 mins (25% ACN). The liquid phase was 5-60% ACN/0.1% TFA. The mobile phase for the first 30 min was maintained at 5% ACN to allow the reaction mixture to elute from the column.

The pyridylethylated f1.2.1 toxin was found to have a mass of 4802 Da (see Figure 6.6). As 4-vinylpyridine has a molecular weight of 105.1 Da, the mass increase from the native toxin corresponded to six cysteine residues in the amino acid sequence when compared to the molecular weight of the native (unalkylated) f1.2.1 toxin. However the ESI-MS data showed the presence of an additional mass (4908.5 Da), which is equivalent to an extra pyridylethyl group. This suggested the possibility that either the peptide was not fully reduced, or there was overalkylation of residues by 4-vinylpyridine (Dr Peter Hains, personal communication). In order to clarify the number of cysteine residues, as well as to determine the amino acid composition of the f1.2.1 peptide toxin, N-terminal sequencing was performed.

A
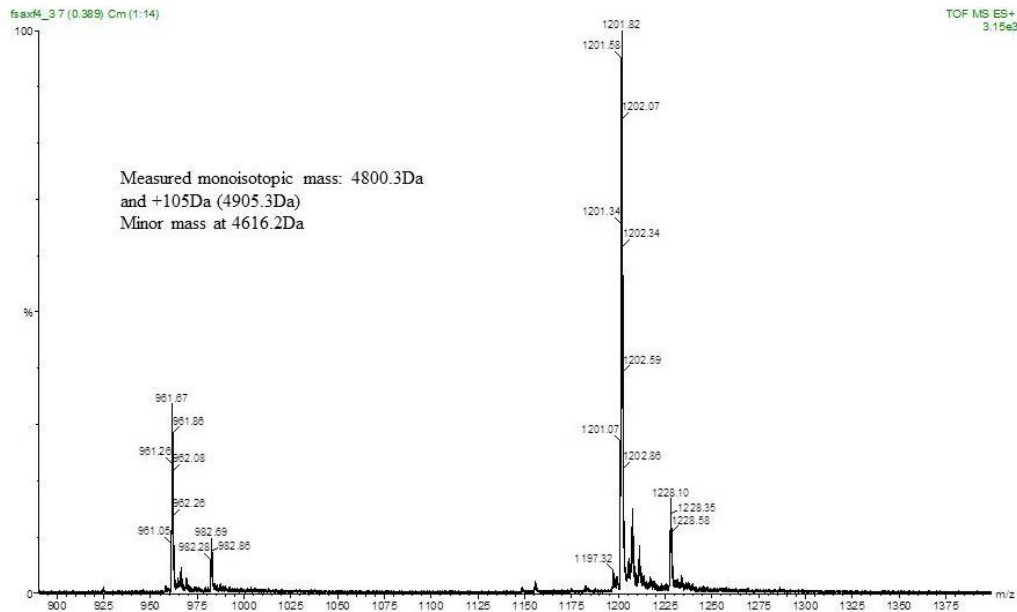
B
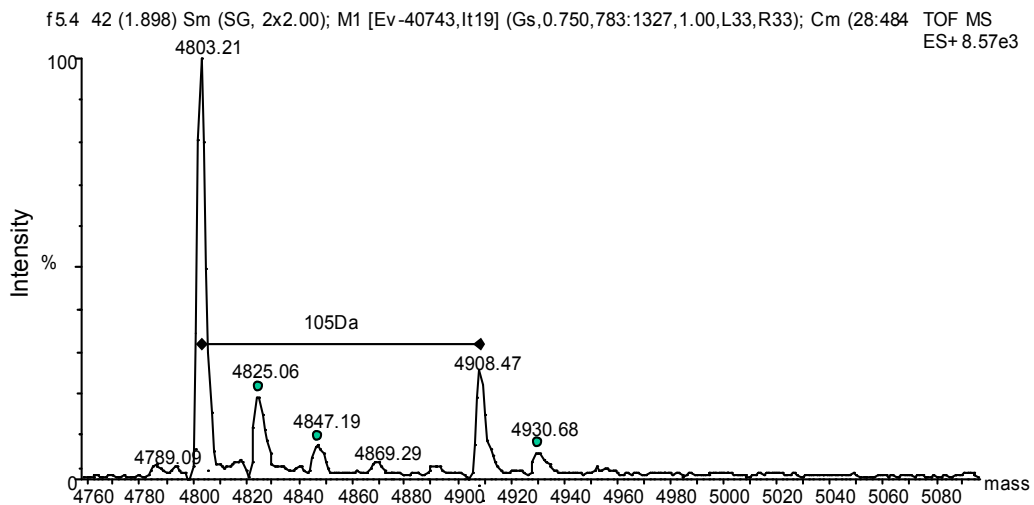
Figure 6.6: ESI-MS of pyridylethylated f1.2.1 toxin. (A) Raw data file showing mass/charge (m/z) peaks, and a measured major monoisotopic mass of 4800.3 Da and 4905.3 Da. (B) Deconvoluted ESI mass spectra showing main molecular mass of 4802.2 Da. The mass increase corresponds to pyridylethylation of 6 cysteine residues by 4-vinylpyridine (molecular mass of 105 Da). Round spots represent sodium adducts of +22 Da or +44 Da. An additional mass of 4908.5 Da, which is equivalent to an additional pyridylethyl group (105 Da), was noted.

6.6 Amino acid sequencing of f1.2.1 toxin

N-terminal amino acid sequencing of the f1.2.1 peptide toxin was performed using Edman degradation. The complete sequence of 39 amino acids was determined from a single run and identified as:

SPVCTPSGQPCQPNTQPCCNNAEEEQTINCNGNTVYRCA

Based on the amino acid sequence, f1.2.1 had six cysteines, the average reduced mass was 4172.5 Da, and the monoisotopic reduced mass was 4169.7 Da. A Blastp search of the protein database UniProt KB revealed that the sequence showed homology with many members of the ω-HXTX-1 family (formerly ω-ACTX-1) from hexathelid Australian funnel-web spiders belonging to the *Hadronyche* genus, as well as *Atrax robustus* (Figure 6.7). There was up to 59% homology (identical residues plus conserved substitutions) and up to 54% overall identity (identical residues) to ω-HXTX-1, with a significant number occurring between residue position 6-11. Importantly, there was complete conservation of key residues of the primary insectophore (Pro^{10}, Asn^{27}, Arg^{35}) that are critical for insecticidal activity in ω-HXTX-Hv1a toxin (Tedford et al., 2001, Tedford et al., 2004a). There is also a conservation of one of the two minor insectophore (Gln^9) that is important for insecticidal activity in cockroaches and crickets, but excluding flies (Tedford et al., 2004a). The other minor insectophore (Tyr^{13} in ω-HXTX-Hv1a) is not conserved; as is the case for some other ω-HXTX-1 toxins (see Figure 6.7).

Based on the sequence homology and functional similarities with the ω-HXTX-Hv1 family, f1.2.1 peptide was assigned the name ω-actinopoditoxin-Mb1a (ω-AOTX-Mb1a) in line with the rational nomenclature for spider peptide toxins (King et al., 2008b), where:

- The Greek letter omega (ω) indicates that this toxin is presumed to block insect voltage-gated calcium channels, due to sequence similarity to ω-HXTX-1 toxins;

- „Actinopoditoxin" (AOTX) refers to a toxin from the family Actinopodidae*;*

- „Mb" refers to the acronyms of the genus and species, *Missulena bradleyi*;

- „1" refers to the first identified toxin from this species with this activity;

- „a" allows for any subsequent discovery of homologues of ω-AOTX-Mb1a.

The positions of six cysteines (C) were unequivocally identified and are equivalent to ω-HXTX-1 except at position 23/24 where the cysteine residue is absent from ω-AOTX-Mb1a and is located at position 30. Significant variation in the sequence was noted between residues 20-28, such as the presence of three sequential glutamates in ω-AOTX-Mb1a (Figure 6.7).
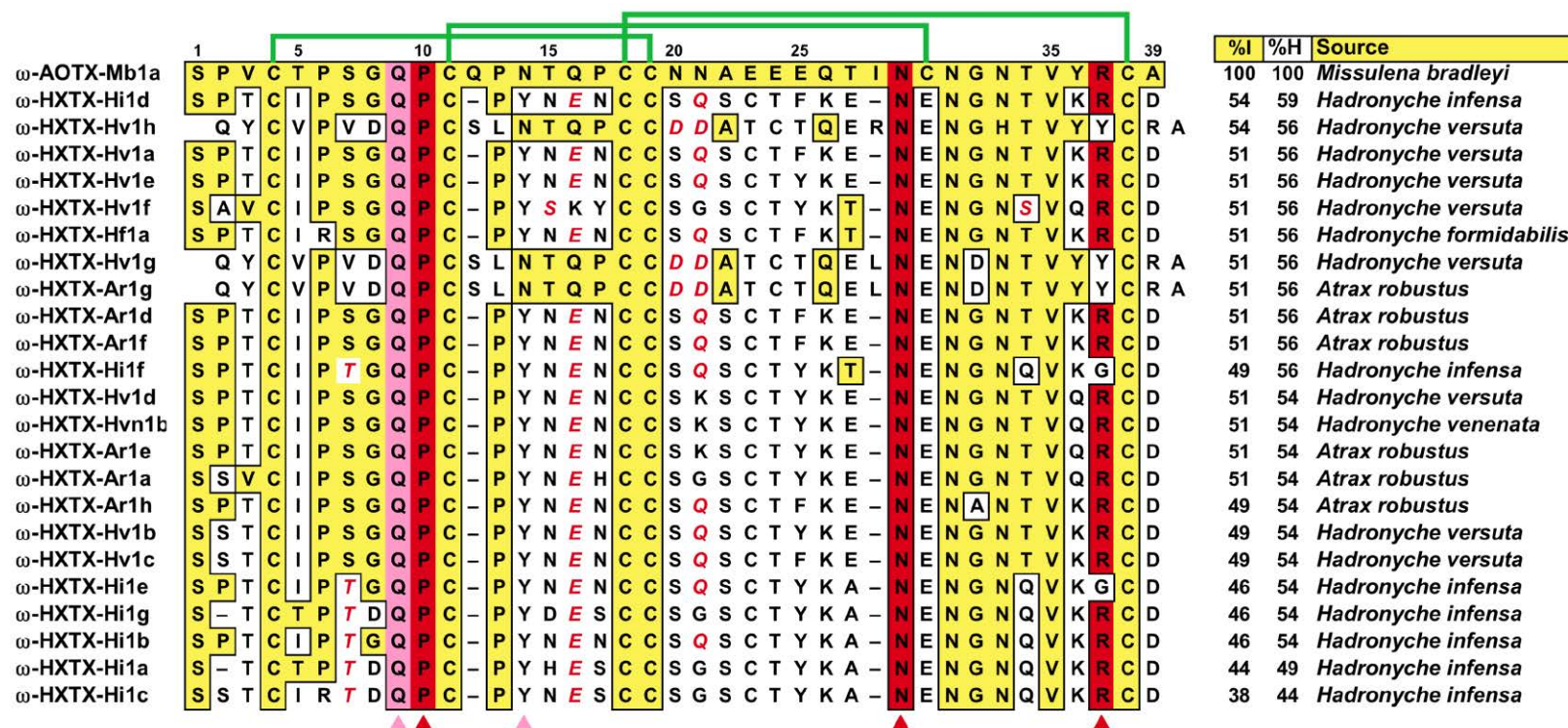
Figure 6.7: Comparison of the primary structure of ω-AOTX-Mb1a with known members of the ω-HXTX-1 family of toxins. Identical residues are shown in yellow boxes and red letters show conservative substitution. There is conservation of three key functional residues (indicated by red arrows) previously identified in ω-HXTX-Hv1a that are critical for insecticidal activity. There is also conservation of a minor functional residue (Gln[9]) (pink box). Minor insectophore Tyr[13] (indicated by pink triangle) is not conserved. The disulfide bonds linking the cysteines (green lines) are based on characteristic disulfide bond pairing (C_I-C_{IV}, C_{II}-C_V, C_{III}-C_{VI}) seen inhibitory knot cystine (ICK) peptide toxins of mass 3500-4500 Da (Norton and Pallaghy, 1998, Craik et al., 2001, Escoubas and Rash, 2004).

The sequence of ω-AOTX-Mb1a was then deposited in the UniProt KB databank under accession number P83588. ω-AOTX-Mb1a represents the first insecticidal toxin isolated from the venom of *M. bradleyi*.

6.7 Molecular target identification of ω-AOTX-Mb1a

To confirm insect Ca_v channels as the molecular target of ω-AOTX-Mb1a, whole-cell patch-clamp analysis using dorsal unpaired median (DUM) neurons from the *Periplaneta americana* cockroach was undertaken.

6.7.1 Block of insect M-LVA and HVA Ca_v channels by ω-AOTX-Mb1a

As described in previous chapters, depolarising pulses to different levels were used to investigate the actions of ω-AOTX-Mb1a on M-LVA and HVA calcium channels. Macroscopic barium currents (I_{Ba}) through Ca_v channels were evoked by depolarising command pulses from a membrane holding potential of -90 mV. Inward I_{Ba} were evoked by depolarising pulses to -20 mV (M-LVA Ca_v channel currents dominating) and +30 mV (HVA Ca_v channel currents dominating) (Wicher and Penzlin, 1997).

There was a concentration-dependent inhibition of both M-LVA and HVA Ca_v channel currents in the presence of ω-AOTX-Mb1a as compared with the control currents under the same conditions (referred to as „tonic block"). Figure 6.8 and 6.9 show the effects of increasing concentrations of ω-AOTX-Mb1a (30 nM to 900 nM) on peak I_{Ba} amplitude elicited by a depolarising test pulse to -20 mV and +30 mV from a holding potential of -90 mV every 10 s. The addition of 300 nM ω-AOTX-Mb1a resulted in a block of peak I_{Ba} of 40.0 ± 14% (n = 10) at -20 mV (Figure 6.8C) and 37.6 ± 11% (n = 4) block at depolarising pulses to +30 mV (Figure 6.9C) within 5 minutes. At a concentration of 900 nM ω-AOTX-Mb1a, this block increased to 74.9 ± 4 % (n = 7) and 73.3 ± 8% (n = 3) at -20 mV (Figure 6.8D) and +30 mV (Figure 6.9D), respectively. Washing with toxin-free external solution for 10 min did not

restore peak I_{Ba} amplitudes to control current levels, indicating that the toxin binds irreversibly to the Ca_v channels.
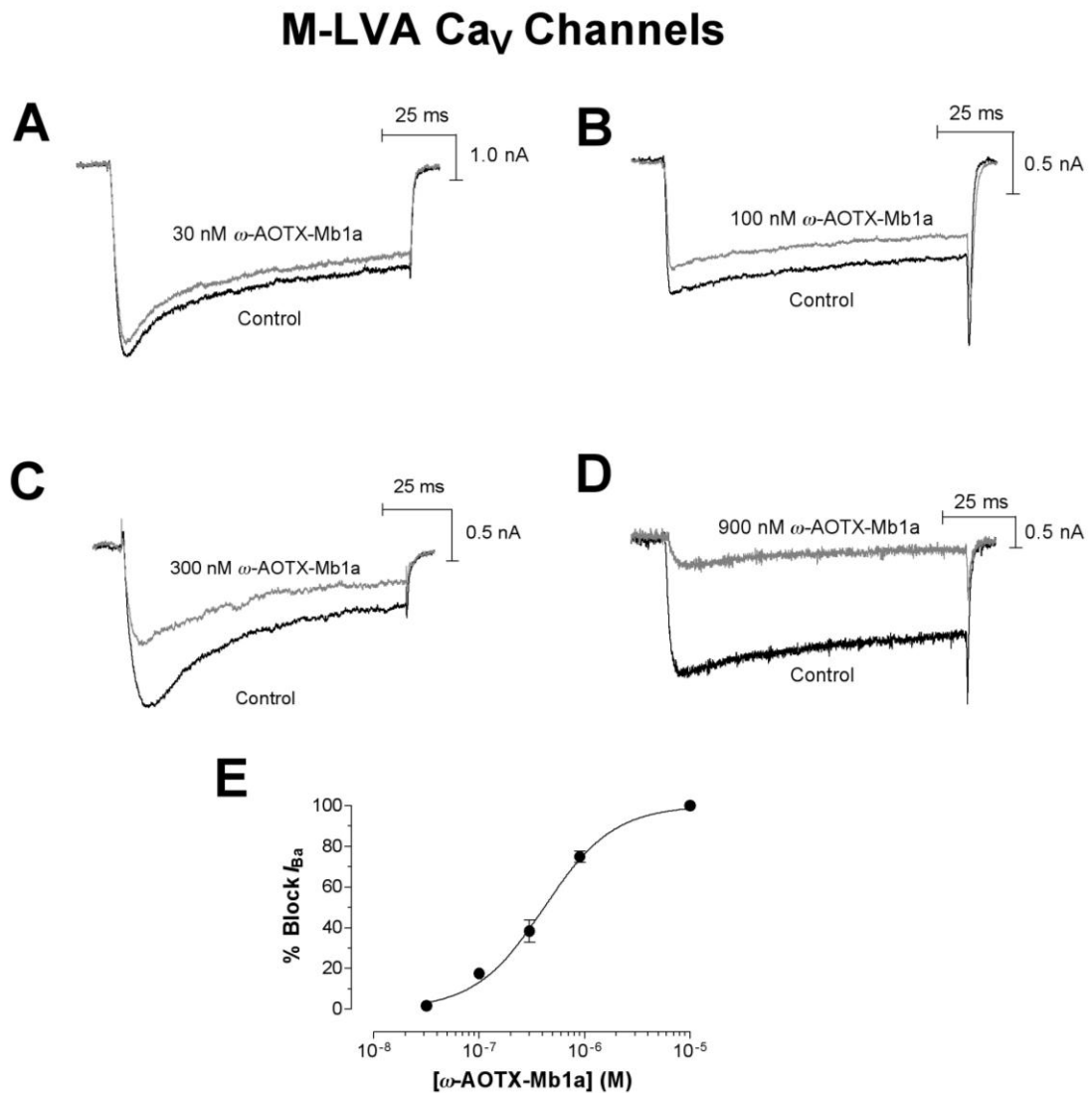
M-LVA Ca$_V$ Channels

Figure 6.8: Effects of ω-AOTX-Mb1a on M-LVA Ca$_v$ channels in cockroach DUM neurons. M-LVA currents in panels (A)-(D) were elicited by a 100-ms depolarising test pulses to -20 mV from a holding potential of -90 mV. Panels show typical tonic block of currents following perfusion with 30 nM (A), 100 nM (B), 300 nM (C) and 900 nM (D) ω-AOTX-Mb1a. (E) Concentration-response curve showing percentage block of M-LVA Ca$_v$ channel currents by ω-AOTX-Mb1a (*n* = 3 -11). Data were fitted using Logistic Equation 2 (section 2.16.3).

HVA Ca$_V$ Channels
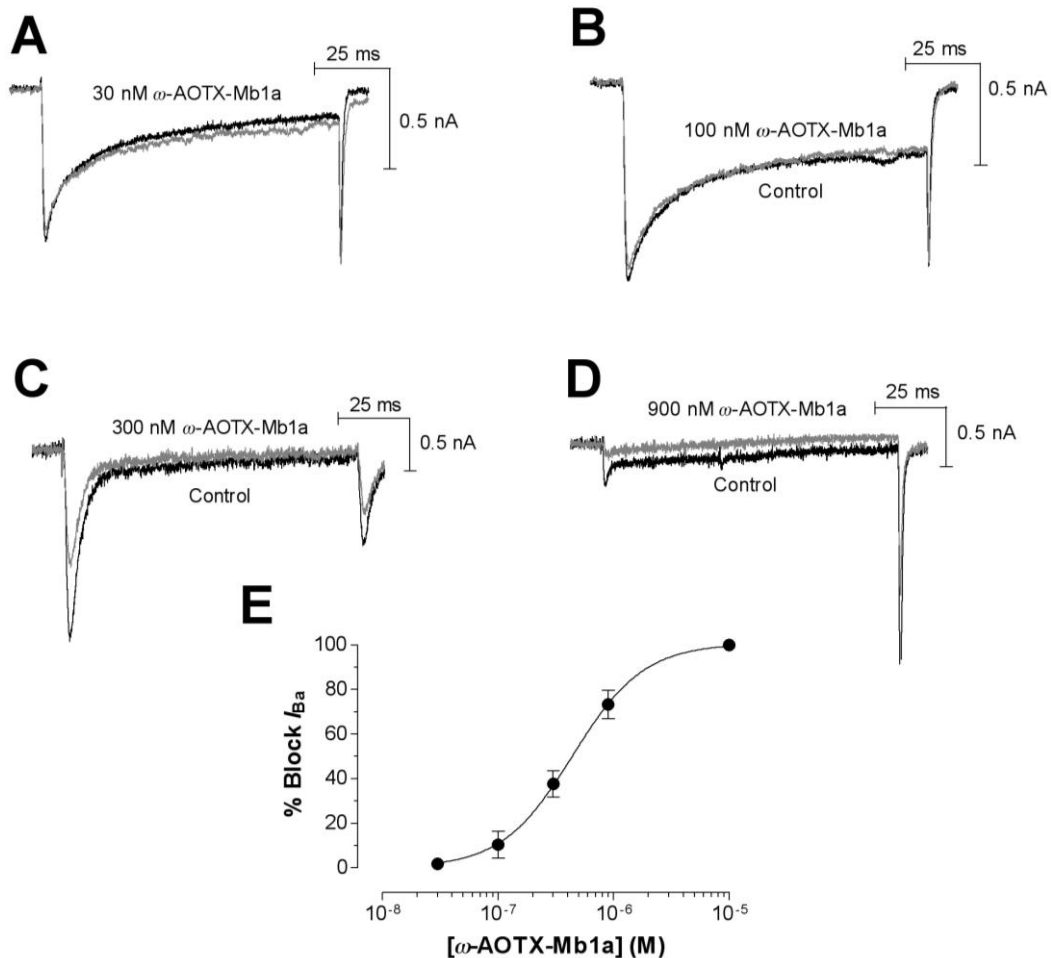
Figure 6.9: Effects of ω-AOTX-Mb1a on HVA Ca$_v$ channels in cockroach DUM neurons. HVA currents in panels (A)-(D) were elicited by 100-ms depolarising test pulses to +30 mV from a holding potential of -90 mV. Panels show typical tonic block of HVA currents following perfusion with 30 nM (A), 100 nM (B), 300 nM (C) and 900 nM (D) ω-AOTX-Mb1a. (E) Concentration-response curve showing percentage block of HVA currents by ω-AOTX-Mb1a (*n* = 3 - 4). Data were fitted with Equation 2 (section 2.16.3).

The peak barium current in the presence of ω-AOTX-Mb1a was expressed as a percentage of the control peak current and the reduction of peak amplitude, after 5-10 mins of perfusion with toxin-containing solution. This was plotted against toxin concentration. By fitting the concentration-response curve of the inhibition of peak barium currents using a Logistic function (Equation 2 in section 2.16.3), the concentration at half-maximal block (IC$_{50}$) of Ca$_v$ channel currents was determined to be 397 nM for M-LVA (Figure 6.8E) and 439 nM for HVA (Figure 6.9E) Ca$_v$ channel currents, respectively.

Although there was a clear blocking action, the toxin failed to alter activation inactivation kinetics of the channels.

6.7.2 Effects of ω-AOTX-Mb1a on the voltage dependence of M-LVA and HVA Ca$_v$ channel activation

To determine whether a depolarising shift in the voltage-dependence of channel activation was responsible for the concentration-dependent block of Ca$_v$ channels, the action of ω-AOTX-Mb1a on current-voltage (*I-V*) relationships was determined. Families of I_{Ba} were generated by 100-ms test pulses from a holding potential of -90 mV to a maximum of +20 mV in 10-mV increments, every 10 s. Effects of ω-AOTX-Mb1a on I_{Ba} were recorded before, and after, perfusion with 300 nM ω-AOTX-Mb1a. The I_{Ba}-V relationship was determined by plotting the maximal I_{Ba} values against maximal control I_{Ba} values at each potential (*n* = 3) (Figure 6.10A). Data were normalised against peak maximal control I_{Ba} and fitted with Equation 5 (section 2.16.3). The threshold of activation for I_{Ba} was similar in both pre- and post-toxin environments. The voltage at half-maximal activation ($V_{1/2}$) was determined to be -39 mV and -40 mV for pre- and post-toxin I_{Ba}, respectively, indicating that there was no significant shift in $V_{1/2}$. There was also no significant shift in the slope factor (*s*) (5.1 and 5.9 for pre- and post-toxin I_{Ba}, respectively). There was little change (<3 mV) in the apparent reversal potential, V_{rev}, in post-toxin recordings, indicating that the ionic selectivity of Ca$_v$ channels was not altered by ω-AOTX-Mb1a. In addition, a voltage-independent block was observed at all test potentials at a concentration of 300 nM (Figure 6.10B).
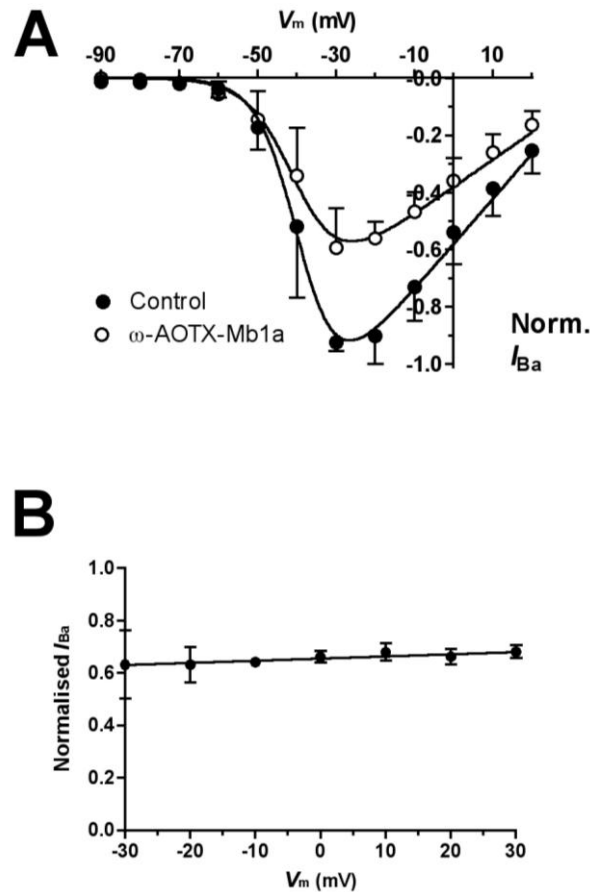
Figure 6.10: Voltage-dependence of Ca_v channel activation. Families of Ca_v channel currents were elicited by depolarising test pulses to +30 mV from a holding potential of -90 mV in 10-mV steps. (A) Peak I_{Ba}-V relationship recorded before (closed symbols), and after (open symbols) application of 300 nM ω-AOTX-Mb1a ($n = 3$). Data were normalised and fitted with Equation 5 (section 2.16.3). (B) Voltage-independent block of I_{Ba} by 300 nM ω-AOTX-Mb1a ($n = 3$). Data represent the normalised block at each test potential and were fitted by linear regression.

6.8 Effects of ω-AOTX-Mb1a on other voltage-activated ion channels

The IC_{50} values are somewhat high for ω-AOTX-Mb1a in comparison to its relative insecticidal activity when compared to ω-HXTX-Hv1a. This suggests that it may be possible for ω-AOTX-Mb1a to target additional types of voltage-activated ion channels. It has been previously noted that peptide toxins can exert activity across multiple voltage-activated ion channel families, presumably due to common structural elements shared between ion channels that belong to members of the same ion channel superfamily (King et al.,

2008a). Magi 3 from *Macrothele gigas*, ω-agatoxin-IVA from *Agelenopsis aperta*, as well as ω-HXTX-Hv1a and ω-HXTX-Ar1a are examples of spider venom peptide toxins that have „promiscuous" activity across both voltage-gated sodium and calcium channels (King et al., 2008a).

Therefore, the action of ω-AOTX-Mb1a on Na_v channel currents was examined in a whole-cell patch-clamp experiment on cockroach DUM neurons. There was no observable change in the global Na_v channel current amplitude following perfusion of 100 nM ω-AOTX-Mb1a for up to 10 min at a depolarising test pulse of -10 mV from a holding potential of -90 mV ($n = 2$) (Figure 6.11). Due to constraints on the available quantity of ω-AOTX-Mb1a toxin, it was not possible to perform repeat tests on Na_v channels at higher concentrations.
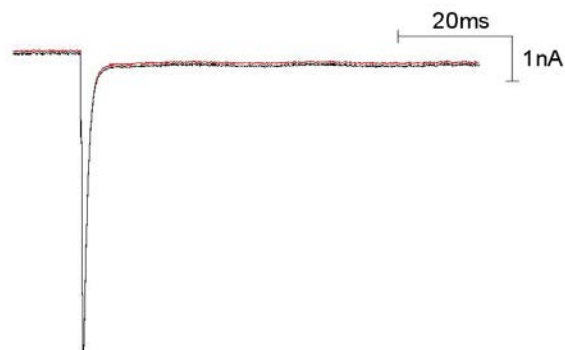
Figure 6.11: Effects of ω-AOTX-Mb1a on Na_v channels in cockroach DUM neurons. Typical whole-cell macroscopic Na_v channel currents (I_{Na}) recorded from cockroach DUM neurons ($n = 2$) after 10 min perfusion with 100 nM ω-AOTX-Mb1a. Macroscopic currents were elicited by 100-ms depolarising test pulses to -10 mV from a holding potential of -90 mV.

CONCLUSION

This study describes the first complete purification and characterisation of a peptide neurotoxin from female *M. bradleyi* spider venom. The neurotoxin, ω-actinopoditoxin-Mb1a (ω-AOTX-Mb1a), was isolated from venom by reverse-phase high performance liquid chromatography and anion exchange fast-perfusion liquid chromatography. This toxin is insect-selective and represents

one of the principle components in *M. bradleyi* venom responsible for irreversible paralysis and death of an insect upon envenomation. Interestingly, there is conservation of all major and one minor insectophore, as well as similarity in toxin action and target to the ω-HXTX-1 family of toxins from hexathelid funnel web spiders despite variation in primary structure. The number of cysteine residues is the same, but there is variation in the spacing of cysteine residues. This may indicate a difference in the disulfide bonding pattern of ω-AOTX-Mb1a compared with ω-HXTX-1 toxins, although this has not been confirmed through structural analysis.

Acute toxicity tests in house crickets revealed that like ω-HXTX-Hv1a and ω-HXTX-Ar1a, the toxicity phenotype of ω-AOTX-Mb1a is an initial excitatory response followed by depressant activity and death. ω-AOTX-Mb1a is a relatively potent neurotoxin when compared to members of the ω-HXTX-1 family, which have LD_{50} doses ranging from 84-1384 pmol/g (Wang et al., 1999). ω-HXTX-Hv1a, the second closest homolog by amino acid sequence (56% homology), has an LD_{50} of 89 ± 10 pmol/g, which is almost two-fold less potent than ω-AOTX-Mb1a.

The IC_{50} value for the block of M-LVA Ca_v channels by ω-AOTX-Mb1a (397 nM) is intermediate between ω-HXTX-Hv1a (279 nM) and ω-HXTX-Ar1a (692 nM), and the IC_{50} for the block of HVA Ca_v channels by ω-AOTX-Mb1a (439 nM) is lower than either ω-HXTX-Hv1a (1080 nM) and ω-HXTX-Ar1a (644 nM). Although the IC_{50} values of ω-AOTX-Mb1a is high, even a moderate block of Ca_v channels in insects is usually lethal, given the limited repertoire of Ca_v channel subtypes (King, 2007). Therefore ω-AOTX-Mb1a is a potential lead compound for the development of new insecticides and validates insect Ca_v channels as a novel insecticide target.

7   Purification and toxicity characterisation of δ-actinopoditoxin-Mb1a from male Eastern mouse (*Missulena bradleyi*) spider venom

Declaration for Thesis Chapter 7

This chapter consists of the following publication:

Gunning, S.J., Chong, Y., Khalife, A.A., Hains, P.G., Broady, K.W., Nicholson, G.M. 2003. Isolation of δ-missulenatoxin-Mb1a, the major vertebrate-active spider δ-toxin from the venom of *Missulena bradleyi* (Actinopodidae), *FEBS Letters*, 554, 211-18.

I declare that my work constitutes a proportion of this manuscript. The specific sections are:

- Crude venom collection from Eastern mouse (*M. bradleyi*) spiders (section 2.1);
- Toxin purification (sections 2.2, 3.2);
- Effects of δ-MSTX-Mb1a on the isolated chick isolated biventer cervicis nerve-muscle preparation (sections 2.3, 3.4);
- Insecticidal activity of δ-MSTX-Mb1a (sections 2.5, 3.6);
- Contribution to writing of discussion (section 4).

Youmie Chong: Date:

Prof. Graham Nicholson

(Corresponding author/principal supervisor):   Date:

Isolation of δ-missulenatoxin-Mb1a, the major vertebrate-active spider δ-toxin from the venom of *Missulena bradleyi* (Actinopodidae)[1]

Simon J. Gunning[a], Youmie Chong[a], Ali A. Khalife[a], Peter G. Hains[b], Kevin W. Broady[c], Graham M. Nicholson[a,*]

[a]*Department of Health Sciences, University of Technology, Sydney, NSW 2007, Australia*
[b]*Department of Chemistry, University of Wollongong, Wollongong, NSW 2522, Australia*
[c]*Department of Cell and Molecular Biology, University of Technology, Sydney, NSW 2007, Australia*

Abstract The present study describes the isolation and pharmacological characterisation of the neurotoxin δ-missulenatoxin-Mb1a (δ-MSTX-Mb1a) from the venom of the male Australian eastern mouse spider, *Missulena bradleyi*. This toxin was isolated using reverse-phase high-performance liquid chromatography and was subsequently shown to cause an increase in resting tension, muscle fasciculation and a decrease in indirect twitch tension in a chick biventer cervicis nerve-muscle bioassay. Interestingly, these effects were neutralised by antivenom raised against the venom of the Sydney funnel-web spider *Atrax robustus*. Subsequent whole-cell patch-clamp electrophysiology on rat dorsal root ganglion neurones revealed that δ-MSTX-Mb1a caused a reduction in peak tetrodotoxin (TTX)-sensitive sodium current, a slowing of sodium current inactivation and a hyperpolarising shift in the voltage at half-maximal activation. In addition, δ-MSTX-Mb1a failed to affect TTX-resistant sodium currents. Subsequent Edman degradation revealed a 42-residue peptide with unusual N- and C-terminal cysteines and a cysteine triplet (Cys^{14-16}). This toxin was highly homologous to a family of δ-atracotoxins (δ-ACTX) from Australian funnel-web spiders including conservation of all eight cysteine residues. In addition to actions on sodium channel gating and kinetics to δ-ACTX, δ-MSTX-Mb1a caused significant insect toxicity at doses up to 2000 pmol/g. δ-MSTX-Mb1a therefore provides evidence of a highly conserved spider δ-toxin from a phylogenetically distinct spider family that has not undergone significant modification.
© 2003 Published by Elsevier B.V. on behalf of the Federation of European Biochemical Societies.

Key words: Spider; Peptide; δ-Missulenatoxin; Sodium channel; Scorpion toxin; δ-Atracotoxin

*Corresponding author. Fax: (61)-2-9514 2228.
E-mail address: graham.nicholson@uts.edu.au (G.M. Nicholson).

Abbreviations: δ-MSTX-Mb1a, δ-missulenatoxin-Mb1a from the eastern mouse spider *Missulena bradleyi*; TTX, tetrodotoxin; δ-ACTX, δ-atracotoxins from Australian funnel-web spiders; δ-ACTX-Ar1a, δ-atracotoxin-Ar1a (formerly robustoxin) from the Sydney funnel-web spider *Atrax robustus*; δ-ACTX-Hv1a, δ-atracotoxin-Hv1a (formerly versutoxin) from the Blue Mountains funnel-web spider *Hadronyche versuta*; δ-ACTX-Hv1b, δ-atracotoxin-Hv1b from *Hadronyche versuta*; δ-ACTX-Hs20.1a, δ-atracotoxin-Hs20.1a from *Hadronyche* sp. 20; Lqh II, anti-mammal α-toxin from the scorpion *Leiurus quinquestriatus hebraeus*; Aah-II, anti-mammal α-toxin from the scorpion *Androctonus australis hector*; LqhαIT, α-insect toxin from the scorpion *Leiurus quinquestriatus hebraeus*; SDS–PAGE, sodium dodecyl sulphate–polyacrylamide gel electrophoresis; PVDF, polyvinylidene fluoride; TBS, Tris-buffered saline; FWS-AV, Sydney funnel-web spider antivenom; RP-HPLC, reverse-phase high-performance liquid chromatography; TFA, trifluoroacetic acid; DRG, dorsal root ganglion; HEPES, *N*-2-hydroxyethylpiperazine-*N*-2-ethanesulfonic acid; TEA, tetraethylammonium; (+)-TC, (+)-tubocurarine; LD_{50}, median lethal dose; PD_{50}, median paralytic dose; ApB, anthopleurin-B from the sea anemone *Anthopleura xanthogrammica*; Magi 4, sodium channel toxin from the spider *Macrothele gigas*

1. Introduction

Australian mouse spiders (Araneae, Mygalomorphae, Actinopodidae) are one of the oldest groups of spiders in the Australo-Papuan region. Importantly, the male eastern mouse spider (*Missulena bradleyi*), restricted to the east coast of mainland Australia, can cause systemic envenomation in humans. The symptoms of envenomation, including muscle fasciculation, tachycardia, dyspnoea, and profuse sweating, are remarkably similar to those reported for Australian funnel-web spiders (Araneae, Mygalomorphae, Hexathelidae, Atracinae). The only reported case of severe envenomation involved a 19-month-old girl who lost consciousness within 30 min of being bitten on the finger by a male *M. bradleyi*. The administration of Sydney funnel-web spider antivenom, raised against *Atrax robustus* venom, surprisingly produced a dramatic improvement in her condition and a full recovery was made following a second dose of antivenom [1]. This prompted a recent study to characterise the pharmacological actions of mouse spider venom. Whole male *M. bradleyi* venom caused rapid muscle fasciculation, a large contracture and a rapid decrease in indirectly evoked twitches in the chick biventer cervicis muscle, with activity blocked by *A. robustus* antivenom [2]. These actions were found to be due to a reduction in the rate of tetrodotoxin (TTX)-sensitive sodium current inactivation and a hyperpolarising shift in the threshold of activation of TTX-sensitive sodium currents [2]. The modulation of sodium channel gating and kinetics, and reversal by *A. robustus* antivenom, indicate that the venom from male *M. bradleyi* may contain vertebrate-active neurotoxins that have a similar action to those found in Australian funnel-web spider venoms, despite the fact that mouse spiders are taxonomically distinct from funnel-web spiders.

Previous studies on the venom of Australian funnel-web spiders have revealed a number of toxins, called atracotoxins

(ACTX), that are responsible for the neurotoxic action seen with whole venom (for a review see [3]). However, the lethal toxins responsible for the major primate-specific symptoms of envenomation are the δ-ACTX shown to target the voltage-gated sodium channel (for a review see [4]). To date, four δ-ACTX have been identified, these include δ-ACTX-Ar1a from the Sydney funnel-web spider (*A. robustus*) [5], δ-ACTX-Hv1a [6] and -Hv1b [7] from the Blue Mountains funnel-web spider (*Hadronyche versuta*) and δ-ACTX-Hs20.1a from *Hadronyche* sp. 20 [4]. All δ-ACTX are highly homologous 42-residue peptides with a high proportion of basic residues and are cross-linked by four conserved intramolecular disulfide bonds. These peptide, like many spider neurotoxins, also contain an 'inhibitor cystine-knot' motif [8–10]. δ-ACTX produce a slowing of TTX-sensitive sodium current inactivation, a modest hyperpolarising shift in the voltage dependence of activation and a reduction in peak sodium current [4,7,11,12]. This results in spontaneous repetitive firing accompanied by plateau potentials [13,14]. Of great interest has been the finding that δ-ACTX, in addition to being mammalian toxic, are also insecticidal. Both δ-ACTX-Ar1a and -Hv1a are toxic by lateroventral injection into crickets [15] and target the insect voltage-gated sodium channel to cause similar actions on neuronal excitability as seen in vertebrate preparations [13]. Notably, these actions on insect and mammalian voltage-gated sodium channels are similar, but not identical, to the mechanism of action of scorpion α-toxins and sea anemone toxins [16,17].

Neurochemical studies have shown that at nanomolar concentrations δ-ACTX compete with both anti-mammalian (e.g. Lqh-II and Aah-II) and anti-insect (e.g. LqhαIT) scorpion α-toxins for neurotoxin receptor site-3 on voltage-gated sodium channels [15,18,19] (for a review of sodium channel neurotoxin receptor sites, see Gordon [20]). Therefore, it is clear that the δ-ACTX are extremely potent and define a new class of toxins affecting both insect and mammalian voltage-gated sodium channels.

Interestingly, the three-dimensional fold of δ-ACTX is different from the previously determined structures of all other site-3 neurotoxins despite similar actions on sodium current inactivation [8]. At present, the toxin pharmacophore of δ-ACTX is unknown but is believed to involve a number of basic residues distributed in a topologically similar manner to basic residues in scorpion α-toxins and sea anemone toxins despite distinctly different protein scaffolds [8]. This is supported by the finding that δ-ACTX-Hv1b, a neurotoxin that is devoid of insecticidal activity and has reduced mammalian activity, lacks several N-terminal basic residues [7].

The present investigation describes the biochemical and pharmacological characterisation of a novel neurotoxin, δ-missulenatoxin-Mb1a (δ-MSTX-Mb1a), from the phylogenetically distinct spider family Actinopodidae. This spider neurotoxin has a similar mode of action and primary structure to the δ-ACTX and provides further evidence for the key role of N-terminal basic residues in the action of δ-ACTX.

2. Materials and methods

2.1. Venom electrophoresis and Western blotting

Crude venom from male and female eastern mouse spiders (*M. bradleyi*) was collected as previously described [2]. Sodium dodecyl sulphate–polyacrylamide gel electrophoresis (SDS–PAGE) of *M. bradleyi* venom was performed under reducing conditions according to the method of Laemmli [21] using 10–20% Tris–tricine gradient gels (Novex, San Diego, CA, USA). The molecular weight marker lane consisted of markers of 3.4–26.6 kDa (Life Science Research Products, Regents Park, NSW, Australia). Following electrophoresis, protein bands were stained using silver nitrate.

Western blotting was performed following initial SDS–PAGE electrophoresis as described above. Proteins were transblotted onto polyvinylidene fluoride (PVDF) membrane (Bio-Rad Laboratories, Hercules, CA, USA) in Tris–tricine–methanol transfer buffer using 200 mA constant current for 1 h. The PVDF membrane was incubated with 3% w/v bovine serum albumin (BSA) in phosphate-buffered saline for 1 h at room temperature. It was then washed in Tris-buffered saline (pH 8.0)–Tween 0.05% v/v (TBS-Tween), followed by incubation with funnel-web spider antivenom raised against male Sydney funnel-web spider (*A. robustus*) venom (FWS-AV) (Commonwealth Serum Laboratories, Melbourne) at a dilution of 1:500 for 1 h. The washing step was repeated and the blot was then incubated with a 1:5000 dilution of the secondary antibody, alkaline phosphatase conjugated goat-anti-rabbit IgG (Sigma Laboratories, St Louis, MO, USA), for 1 h. It was then washed again with TBS–Tween and developed with 5-bromo-4-chloro-indoyl phosphate *p*-toluidine plus nitroblue tetrazolium.

2.2. Toxin purification and sequencing

Pooled venom was initially fractionated using reverse-phase high-performance liquid chromatography (RP-HPLC) employing a Vydac analytical column (C_{18}, 4.6×250 mm, 5 μm) on a Shimadzu HPLC system. Peptide peaks were monitored at an absorbance of 215 nm. Elution of venom peptide components was achieved using a linear gradient of 5–60% v/v acetonitrile/0.1% v/v trifluoroacetic acid (TFA) over 55 min at a flow rate of 1 ml/min. Selected fractions were subjected to vertebrate toxicity bioassays using a chick biventer cervicis nerve-muscle preparation to determine vertebrate toxicity (see Section 2.3). The major toxic fraction, δ-MSTX-Mb1a (peak *a* in Fig. 1C), eluted around 33% acetonitrile concentration and was further purified on an analytical C_{18} RP-HPLC column using a linear gradient of 5–32% acetonitrile/0.1% TFA over 5 min, then 32–34% acetonitrile/0.1% TFA over 20 min, at a flow rate of 1 ml/min. Purified toxin was collected, lyophilised and stored at −20°C until required. Toxin quantification was performed using a BCA (bicinchoninic acid) Protein Assay Kit (Pierce, Rockford, IL, USA) using BSA as a standard. Absorbances were read at 560 nm on a Titertek Multiscan microplate reader (Eflab, Finland). The molecular mass was determined by electrospray ionisation mass spectrometry. In preparation for amino acid sequencing, the toxin was reduced and cysteine residues were pyridylethylated as described previously [8]. The reduced, pyridylethylated toxin was purified using RP-HPLC as described previously [8], then the entire peptide sequence was obtained from a single sequencing run on an Applied Biosystems/Perkin Elmer Procise 492 cLC protein sequencer.

2.3. Chick isolated biventer cervicis nerve-muscle bioassay

Vertebrate toxicity was confirmed by the use of an isolated chick biventer cervicis nerve-muscle preparation as described previously [22,23]. Briefly, biventer cervicis muscles with attached nerve were removed from male Australorp chicks (1–4-day-old), mounted in 8-ml organ baths and bathed in Krebs–Henseleit solution containing (in mM): NaCl 118.4, KCl 4.7, $CaCl_2$ 2.5, $MgSO_4$ 1.2, KH_2PO_4 1.2, $NaHCO_3$ 25.0, D-glucose 11.1, pH 7.4. The muscle was maintained at 34°C and constantly carbogenated with 95% O_2 and 5% CO_2. Twitch contractions were elicited by indirect supramaximal stimulation of the motor nerve (supramaximal voltage, 0.05 ms, 0.1 Hz) via ring electrodes connected to a Grass S88 stimulator. Isometric contractions of the muscle were recorded using a Neomedix isometric force transducer, connected to a T-218 amplifier and a MacLab/4s data acquisition system (AD Instruments, Castle Hill, NSW, Australia) connected to a Centris 650 Macintosh computer. In the absence of electrical stimulation, responses to exogenous acetylcholine (1 mM, 30 s) and KCl (40 mM, 30 s) were obtained prior to the addition of venom and at the conclusion of the experiment. Preparations were allowed to equilibrate for at least 30 min with continuous stimulation before the addition of venom or antivenom. All animal experimentation was approved by the joint Animal Care and Ethics Committee of the University of Technology, Sydney, and the Royal North Shore Hospital, Sydney, Australia.

2.4. Electrophysiological studies

Acutely dissociated dorsal root ganglion (DRG) neurones were prepared from 4–12-day-old Wistar rats and maintained in short-term primary culture using the method described by Nicholson et al. [11]. Voltage-clamp recordings were made with the whole-cell patch-clamp technique [24] using an AxoPatch 200A patch-clamp amplifier (Axon Instruments, Foster City, CA, USA). Micropipettes were pulled from borosilicate glass capillary tubing (Corning 7052 Glass, Warner Instruments) and had d.c. resistances of 0.8–2.0 MΩ.

To record macroscopic sodium currents, micropipettes were filled with a solution of the following composition (in mM): CsF 135; NaCl 10; N-2-hydroxyethylpiperazine-N-2-ethanesulfonic acid (HEPES) 5; with the pH adjusted to 7.0 with 1 M CsOH. The external bathing solution contained (in mM): NaCl 30; $MgCl_2$ 1; $CaCl_2$ 1.8; CsCl 5; KCl 5; D-glucose 25; HEPES 5; tetraethylammonium (TEA)–Cl 20; tetramethylammonium chloride 70; with the pH adjusted to 7.4 with 1 M TEA–OH.

The osmolarity of both solutions was adjusted to 290–300 mOsm/l with sucrose to reduce osmotic stress. The external solution was applied to the perfusion chamber via a gravity-fed perfusion system and the flow rate maintained at 0.5 ml/min using a Gilmont flowmeter (Barrington, IL, USA). Data were recorded at room temperature (20–23°C) which did not fluctuate more than 1°C during the course of an experiment. In all voltage-clamp experiments the holding potential was −80 mV and the sodium concentration of the external solution was reduced to 30 mM to improve series resistance compensation and to avoid saturation in the recording system [25]. Inverted voltage-clamp command pulses were applied to the bath through a Ag/AgCl pellet/3 M KCl–agar bridge. The liquid junction potential between internal and external solutions was approximately −6 mV, and all data were compensated for this value.

Large round DRG cells with diameters of 30–50 μm were selected for experiments. Larger cells from older animals tended to express fast TTX-sensitive sodium currents (I_{Na}) whilst smaller cells tended to express predominantly TTX-resistant I_{Na} [26]. In those experiments that assessed the actions of the toxin on TTX-resistant I_{Na}, 200 nM TTX was applied to the external solution to eliminate any residual TTX-sensitive I_{Na}. Only those cells that exhibited less than 10% TTX-resistant I_{Na}, as determined from differences in the steady-state sodium channel inactivation profile, were used to determine the actions of toxin on TTX-sensitive I_{Na}. After breaking through the membrane, experiments did not commence for a period of 15–20 min to allow for the complete block of calcium and potassium currents and any fast time-dependent shifts in steady-state inactivation. The experiments used in this study were rejected if there were large leak currents or currents showed signs of poor space clamping such as an abrupt activation of currents upon relatively small depolarising pulses.

Stimulation and recording were both controlled by an AxoData® data acquisition system (Axon Instruments) running on an Apple Macintosh Quadra 700. Data was filtered at 5 kHz (four-pole low-pass Bessel filter) and digital sampling rates were between 15 and 25 kHz depending on voltage protocol length. Leakage and capacitive currents were digitally subtracted with P-P/4 procedures [27] and series resistance compensation was set at >80% for all cells. Data analysis was performed off-line following completion of the experiment. Mathematical curve fitting employed algorithms available in KaleidaGraph® for Macintosh using a non-linear least-squares method. The curve fits for the I/V data were obtained using the following equation:

$$I_{Na} = g_{max}\left(1 - \left(\frac{1}{1 + \exp[(V - V_{1/2})/s]}\right)\right)(V - V_{rev}) \qquad (1)$$

where I_{Na} is the amplitude of the peak sodium current at a given potential, V, g_{max} is the maximal sodium conductance, $V_{1/2}$ is the voltage at half-maximal activation, s is the slope factor and V_{rev} is the reversal potential.

2.5. Invertebrate toxicity assays

Insect toxicity was determined by lateroventral thoracic injection of the purified toxin into 3rd–4th instar house crickets nymphs (*Acheta domesticus*, sex undetermined) as described previously [28] at doses up to 2000 pmol/g. Crickets received injections of toxin dissolved in insect saline of the following composition (in mM): NaCl 200, KCl 3.1, $CaCl_2$ 5, $MgCl_2$ 4, HEPES 10, sucrose 50, pH 7.4. Insects were monitored for 72 h postinjection for signs of paralysis or lethality.

2.6. Statistics

Comparisons of two sample means were made using a Wilcoxon signed-rank test or paired Student's *t*-test (as specified). A test was considered to be significant when $P < 0.05$. Data, when quantified, were expressed as means ± S.E.M.

3. Results

3.1. Venom electrophoresis and Western blotting

SDS–PAGE revealed considerable variability in the number of protein bands between pooled male and female *M. bradleyi* venom. In particular, constant bands were only present around 7 kDa and 90 Da. In addition, separation patterns of both male and female venom was less complex than funnel-web spider venoms [29]. Notably, male venom appears to have a band around 4900 Da that is absent from female venom (see band marked with * in Fig. 1A). It has been previously reported that female *M. bradleyi* venom does not produce neurotoxicity in vertebrate nerve-muscle preparations [2] and that male venom appears to contain a vertebrate-active neurotoxin with similar actions as δ-ACTX that have a molecular weight of ~4900 Da.

Given that FWS-AV reverses the effects of male *M. bradleyi* envenomation, we assessed if FWS-AV would bind to protein fractions in either male or female venom. Western blotting revealed that FWS-AV bound to protein fractions above a molecular weight of 14 kDa. There was little antivenom binding to protein fractions between 5 and 14 kDa. Importantly, only male venom showed bands less than 5 kDa consistent with the presence of a possible δ-ACTX-like neurotoxin (see band marked with * in Fig. 1B).

3.2. Toxin purification

A vertebrate-active neurotoxin in male *M. bradleyi* venom was purified by RP-HPLC. Fig. 1C shows a RP-HPLC chromatogram of pooled venom. The fraction containing the toxin eluted at 33% acetonitrile/0.1% TFA (peak *a*, Fig. 1C). This peak was found to cause strong muscle contracture, fasciculation and to decrease nerve-evoked twitch contractions of chick isolated biventer cervicis muscle (data not shown) similar to those elicited by δ-ACTX-Hv1a and other Australian funnel-web spider venoms [29]. This fraction was pooled and lyophilised, and further purification, using C_{18} RP-HPLC with a shallow acetonitrile gradient, yielded three distinct components (Fig. 1D). The major peak, labelled peak *b* in Fig. 1D, was subsequently shown to be the most active component in the chick biventer cervicis nerve-muscle assay. MALDI-TOF (matrix-assisted laser desorption/ionisation time-of-flight) mass spectrometry revealed that the molecular mass of the peptide peak *b* was 4933 ± 1 Da.

3.3. Determination of amino acid sequence

Peak *b* was reduced and the cysteines pyridylethylated in preparation for N-terminal amino acid sequencing to assist in determining the number of cysteine residues. In addition, phenylthiohydantoin-Cys with a pyridylethylated sidechain is stable during automated N-terminal amino acid sequencing and therefore allows positive identification of Cys residues.

Mass spectral analysis of the pyridylethylated toxin indicated that it contained eight cysteine residues. The amino acid sequence of the toxin (see Fig. 2), obtained in a single sequencing run without the need to resort to proteolytic di-
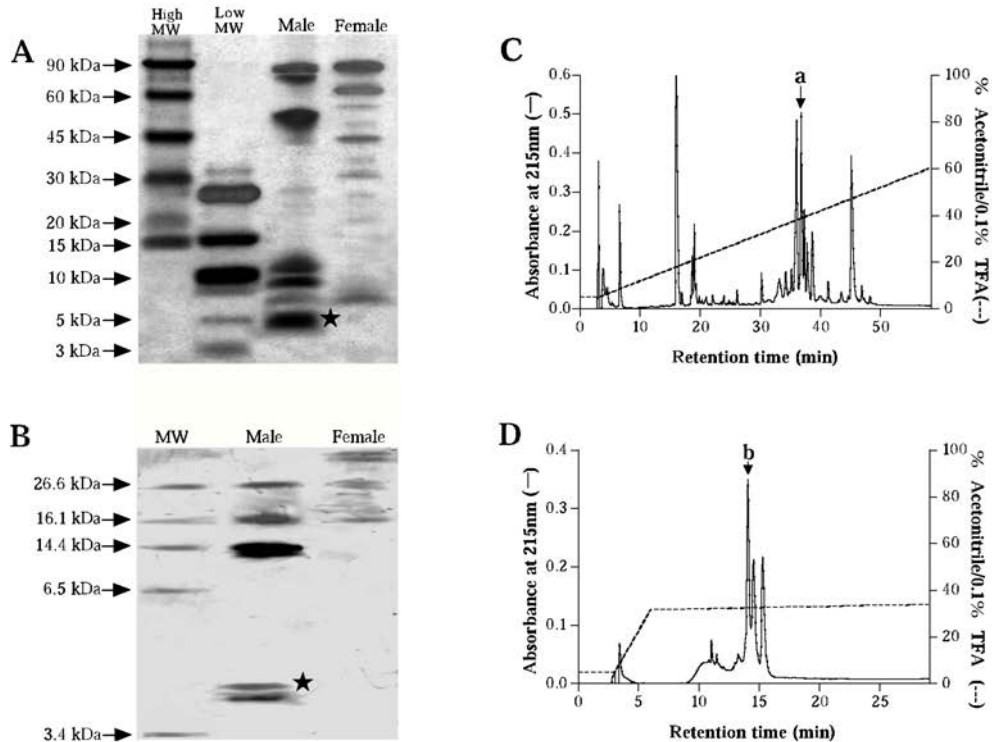
Fig. 1. A,B: SDS–PAGE gel and Western blot of *M. bradleyi* venom. A: Silver-stained SDS–PAGE gel showing protein components of male and female *M. bradleyi* venom. Left-hand lanes shows high (High MW) and low (Low MW) molecular weight markers. Note a band consistent with δ-MSTX-Mb1a at 4933 Da in whole male venom that is absent in whole female venom. B: Western blot analysis of male and female *M. bradleyi* venom using Sydney funnel-web spider antivenom. The left-hand lane (MW) contains molecular weight markers. Note a positive reaction consistent with δ-MSTX-Mb1a in whole male venom that is absent in whole female venom. C,D: RP-HPLC chromatogram of pooled male *M. bradleyi* venom. C: Screening of venom fractions revealed that peak *a* caused spontaneous contractions of chick isolated biventer cervicis nerve-muscle preparations. D: Further RP-HPLC purification of this fraction yielded three major peaks, the largest of which (peak *b*) was found to be the most active component in the chick isolated biventer cervicis nerve-muscle preparation.

gestion, revealed that it contains 42 residues, including eight cysteines. Importantly, it possesses both N- and C-terminal cysteines and an unusual cysteine triplet (Cys$^{14-16}$). The predicted mass of 4934 Da for the fully oxidised peptide, in which the eight cysteine residues form four disulphide bonds, is consistent with the mass spectral analysis.

The toxin displayed significant homology with three other Australian funnel-web spider toxins, δ-ACTX-Hv1a [2] and δ-ACTX-Hv1b [7] isolated from the venom of the female Blue Mountains funnel-web spider, *H. versuta*, and δ-ACTX-Ar1a [21] isolated from the venom of the male Sydney funnel-web spider, *A. robustus*. The sequence shows conservation in the number and spacing of cysteine residues. When conservative substitutions are taken into consideration, the homology
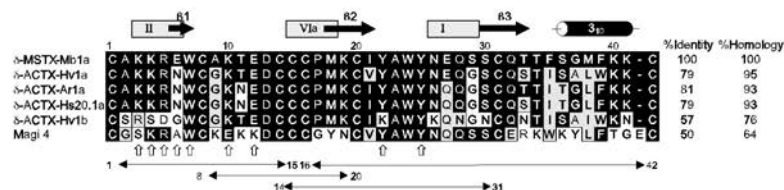
Fig. 2. Comparison of the amino acid sequences of δ-MSTX-Mb1a with currently known members of the δ-ACTX family and Magi 4. Identical residues are shaded black and conservatively substituted residues, relative to δ-MSTX-Mb1a, are shaded grey. Toxins are ordered by homology to δ-MSTX-Mb1a. Gaps (dashes) have been inserted to maximise alignment. The disulphide bonding pattern for the strictly conserved cysteine residues determined for δ-ACTX-Ar1a [9] and δ-ACTx-Hv1a [8] is indicated below the sequences; it is assumed that δ-MSTX-Mb1a, δ-ACTX-Hs20.1a [4], δ-ACTX-Hv1b [7] and Magi 4 [30] have the same disulphide bonding pattern. Suspected key residues critical for function [4] are indicated by the arrows. Secondary structure for δ-ACTX-Hv1a is shown at the top of the figure where shaded rectangles represent β-turns (the type of turn is indicated in the rectangle), black arrows represent β-strands, and the black cylinder represents a 3$_{10}$ α-helix [8]. The percentage identity and homology with δ-MSTX-Mb1a is also shown to the right of the sequences.
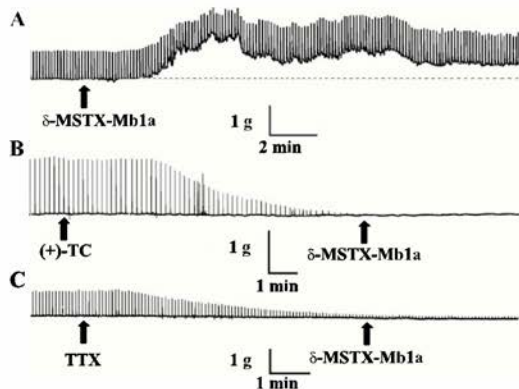
Fig. 3. Typical effects of antagonists on responses to δ-MSTX-Mb1a in the isolated chick biventer cervicis nerve-muscle preparation. A: Development of muscle fasciculation and contracture following addition of 85 nM δ-MSTX-Mb1a. The dotted line indicates the resting tension of the muscle. B,C: Following exposure to 10 μM (+)-TC (B) or 200 nM TTX (C) 85 nM δ-MSTX-Mb1a fails to alter twitch or resting muscle tension.

with other δ-ACTX ranges from 76 to 95%. The toxin has nine amino acid substitutions relative to δ-ACTX-Hv1a, its closest ortholog (see Fig. 2). In addition, the toxin shows 64% sequence homology to the recently identified sodium channel toxin Magi 4 from the hexathelid spider *Macrothele gigas* [30].

Based on the sequence homology and functional similarities (see below) with δ-ACTX, we have named the toxin δ-MSTX-Mb1a in accordance with the nomenclature previously described for toxins isolated from Australian funnel-web spiders [5]. The sequence of δ-MSTX-Mb1a has been deposited in the SwissProt Databank under the accession number P83608.

Although the pairing of cysteines was not determined experimentally, the high homology in primary structure with previously described spider δ-toxins strongly suggests that δ-MSTX-Mb1a conforms to an inhibitor cystine-knot motif (Cys1-Cys4, Cys2-Cys6, Cys3-Cys7, Cys5-Cys8)[10,31] as has been observed for most spider neurotoxins.

3.4. Effects of δ-MSTX-Mb1a on the isolated chick biventer cervicis nerve-muscle preparation

In the indirectly stimulated chick biventer cervicis muscle, δ-MSTX-Mb1a (85 nM) caused a rapid muscle contracture (increase in resting tension), associated with muscle fasciculation and a decrease in twitch tension (Fig. 3A). However, δ-MSTX-Mb1a had no significant effect on responses to acetylcholine (1 mM: 2.4 ± 1.4 g before toxin, 2.38 ± 1.4 g after toxin), carbachol (20 μM: 1.52 ± 0.8 g before toxin, 1.45 ± 0.8 g after toxin) or KCl (40 mM: 2.78 ± 1.6 g before toxin, 2.23 ± 1.3 g after toxin) ($n = 3$, $P > 0.05$, Wilcoxon signed-rank test) (data not shown). The contracture induced by δ-MSTX-Mb1a (85 nM) was completely abolished by the skeletal muscle nicotinic receptor antagonist (+)-tubocurarine [(+)-TC; 10 μM] and by the sodium channel blocker TTX (200 nM) (Fig. 3B,C).

A 10-min pretreatment of the indirectly stimulated chick biventer cervicis muscle with 0.6 U/ml Sydney funnel-web spider antivenom completely prevented the contracture, fasciculations and the attenuation of twitches caused by δ-MSTX-

Mb1a (85 nM) ($n = 3$, Fig. 4A). It was also found that the effects of δ-MSTX-Mb1a on the nerve-muscle preparation could be reversed by subsequent addition of Sydney funnel-web spider antivenom (0.6 U/ml) ($n = 3$, Fig. 4B).

3.5. Effects of δ-MSTX-Mb1a on voltage-gated sodium currents

Under voltage-clamp conditions, δ-ACTX have been previously shown to cause a concentration-dependent reduction in peak TTX-sensitive I_{Na} amplitude and slowing of I_{Na} inactivation [4,7,11,12]. Fig. 5A shows the effect of δ-MSTX-Mb1a on TTX-sensitive I_{Na}. At 30 nM, δ-MSTX-Mb1a reduced peak TTX-sensitive I_{Na} amplitude by 24 ± 8% ($n = 3$, $P < 0.05$, paired Student's t-test) and slowed the rate of TTX-sensitive I_{Na} inactivation. Analysis of the toxin effect on inactivation was estimated by measuring the I_{Na} remaining after 50 ms following a step depolarisation to indicate the proportion of channels with permanently modified inactivation. At −10 mV the remaining current was 19.2 ± 4.2% ($n = 3$) of control peak I_{Na}. Since the reduction in peak I_{Na} at 30 nM was found to be similar for δ-MSTX-Mb1a and both δ-ACTX-Hv1a and -Ar1a [11], we conclude that δ-MSTX-Mb1a is approximately equipotent with δ-ACTX-Hv1a and -Ar1a on TTX-sensitive sodium channels. Similar to δ-ACTX, the reduction in sodium current amplitude and slowing of current inactivation produced by δ-MSTX-Mb1a was only partially reversible after prolonged washing with toxin-free solution. In marked contrast to its action on TTX-sensitive sodium channels, δ-MSTX-Mb1a (300 nM), like other δ-ACTX [11,12], failed to significantly alter either the amplitude or time course of TTX-resistant I_{Na} (Fig. 5E).

Previous studies have shown that δ-ACTX shift the threshold of activation of TTX-sensitive I_{Na} in the hyperpolarising direction [4,7,11,12]. Analysis of the I/V relationship of TTX-sensitive I_{Na} in the presence of 30 nM δ-MSTX-Mb1a (Fig. 5B–D) revealed a similar 10-mV hyperpolarising shift in the threshold of sodium channel activation. Data were normalised
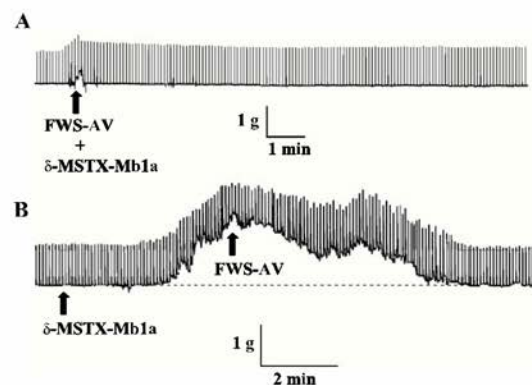
Fig. 4. Typical traces showing neutralisation of the effects of δ-MSTX-Mb1a by Sydney funnel-web spider antivenom on the indirectly stimulated chick biventer cervicis nerve-muscle preparation. A: Funnel-web spider antivenom (FWS-AV, 0.6 U/ml) was applied to the preparation 10 min *prior* to the application of δ-MSTX-Mb1a (85 nM). Note lack of toxin response. B: FWS-AV (0.6 U/ml) was applied *following* the application of δ-MSTX-Mb1a (85 nM). Note the rapid return of muscle tension to control levels and reversal of muscle fasciculation.
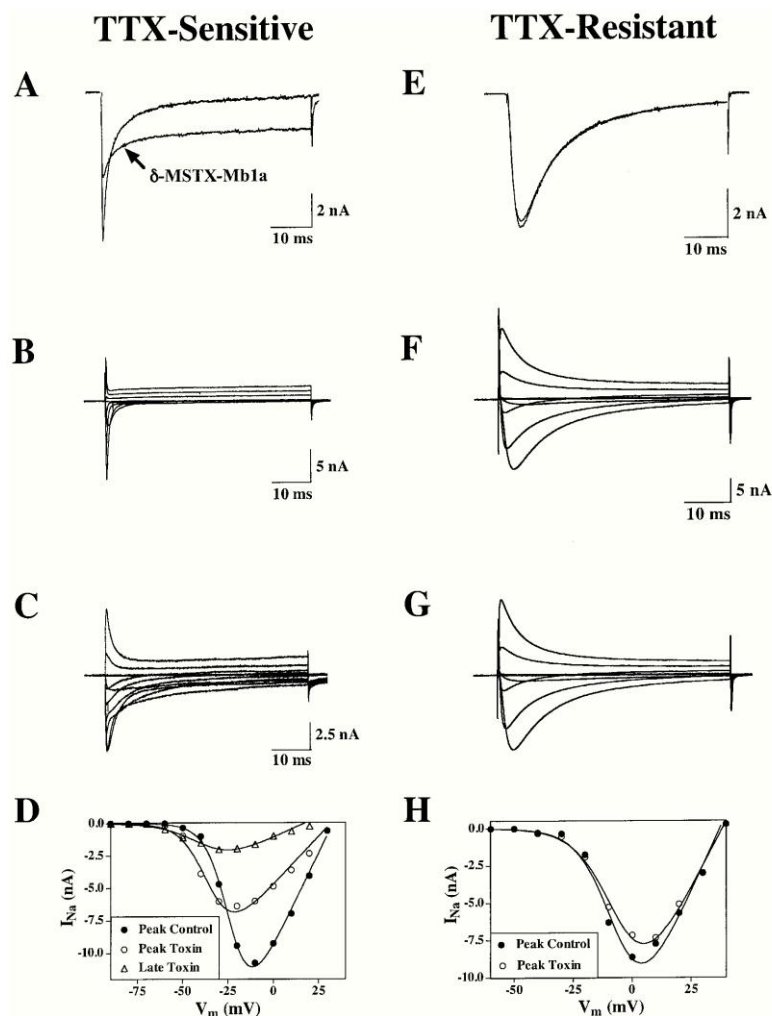
Fig. 5. Typical effects of δ-MSTX-Mb1a on TTX-sensitive and TTX-resistant I_{Na} in rat DRG neurones. Panels show the effect of δ-MSTX-Mb1a on TTX-sensitive (left hand) and TTX-resistant (right hand) I_{Na}. A,E: Superimposed current traces recorded following a 50-ms depolarisation to −10 mV from a holding potential of −90 mV, before, and 10 min after, toxin application. A: Note the reduction in peak current amplitude of TTX-sensitive I_{Na} and slowed inactivation kinetics. E: Lack of effect of 300 nM δ-MSTX-Mb1a on TTX-resistant I_{Na} elicited by the same stimulus protocol. Both current responses were recorded in the presence of 200 nM TTX to eliminate residual TTX-sensitive I_{Na}. Remaining panels show typical effects of δ-MSTX-Mb1a on the current–voltage (I/V) relationship of TTX-sensitive (B–D) and TTX-resistant (F–H) I_{Na}. Families of I_{Na} were evoked by a series of 50-ms depolarisations from −90 to +70 mV in 10-mV steps applied every 10 s from a holding potential of −90 mV. Families of I_{Na} before (B,F) and after (C,G) application of 30 nM δ-MSTX-Mb1a. For clarity, I_{Na} recorded in 20-mV steps are presented. Note that the inactivation kinetics of both inward and outward currents are slowed and incomplete in panel C only. D,H: Peak (circles) and late (triangles) I/V relationships are shown before (empty symbols) and following (filled symbols) a 10-min perfusion with 30 nM δ-MSTX-Mb1a. Late currents were measured at the end of each 50-ms depolarising test pulse. Peak and late currents were fitted according to Eq. 1 described in Section 2. Note that no shift in the threshold of activation is seen in panel H.

149

and fitted using a single Boltzmann distribution. δ-MSTX-Mb1a caused a hyperpolarising shift in the voltage at half-maximal activation ($V_{1/2}$) from -22.6 ± 1.4 mV ($n = 3$, $P < 0.05$, paired Student's *t*-test) in controls to -33.2 ± 0.4 mV with no change in the slope factor *s*. Fig. 5 also shows that these changes occurred in the absence of significant changes in the reversal potential which were only slightly decreased from 29.8 mV (calculated from the Nernst equation) by 1.2 ± 0.5 mV ($P > 0.05$, paired Student's *t*-test). These changes could not be explained by spontaneous time-dependent shifts in the voltage dependence of activation, which in general are < 5 mV in DRG neurones (G. Nicholson, unpublished results).

Consistent with δ-ACTX, and in marked contrast to its action on TTX-sensitive I_{Na}, δ-MSTX-Mb1a (300 nM) failed to significantly alter the voltage dependence of activation of TTX-resistant I_{Na} (see Fig. 5F–H).

3.6. Insecticidal activity of δ-MSTX-Mb1a

δ-ACTX-Hv1a was previously shown to be a moderately potent insecticidal toxin, with a median lethal dose (LD_{50}) of 770 pmol/g in house crickets (*A. domesticus*) [15] Furthermore, δ-ACTX-Hv1a caused contractile paralysis at significantly lower doses [median paralytic dose (PD_{50}) = 200 pmol/g], with the higher LD_{50} reflecting the fact that most crickets recover from the contractile paralysis at doses near or below the PD_{50} [15]. However δ-ACTX-Hv1b showed a complete absence of insect toxicity at doses up to 2000 pmol/g. Crickets were injected with δ-MSTX-Mb1a at doses up to 2000 pmol/g and within 20 min of injection showed signs of neurotoxicity including continuous and involuntary spasms of the appendages, abdomen and head. There was a moderate loss of co-ordination when walking, and some crickets showed marked lateroflexion of their abdomen. Interestingly, there was some reversal of these signs of toxicity, with the exception of abdominal lateroflexion, within 24 h post-injection and at doses below 1000 pmol/g insects recovered completely. Nevertheless, lethality was observed in 60% of crickets at a dose of 2000 pmol/g after 48 h, indicating that δ-MSTX-Mb1a is approximately two-fold less toxic to crickets than δ-ACTX-Hv1a.

4. Discussion

This paper describes the isolation and characterisation of a peptide neurotoxin that modulates vertebrate sodium channel inactivation from a spider species unrelated to Australian funnel-web spiders (Hexathelidae). N-terminal sequencing showed that the actinopodid toxin δ-MSTX-Mb1a corresponds to a 42-residue peptide of molecular weight 4933 Da that is clearly a close ortholog of δ-ACTX-Hv1a and related hexathelid spider δ-toxins. The cysteine spacing with characteristic N- and C-terminal cysteines and cysteine triplet, characteristic of spider δ-toxins, strongly suggests that this novel toxin belongs to the inhibitor cystine-knot motif group of peptides. δ-MSTX-Mb1a mimics the neurotoxicity of δ-ACTX-Hv1a [29], causing a sustained contracture and muscle fasciculation of vertebrate skeletal muscle, consistent with similar signs of envenomation in vivo. This appears to be the result of spontaneous neurotransmitter release from motor nerve terminals and not an alteration in postjunctional excitation–contraction coupling. This was evident from the fact

that responses of slow muscle fibres to KCl and acetylcholine in the chick nerve-muscle preparation were unaffected and the contracture was blocked by prior application of TTX or (+)-TC. These presynaptic actions to induce neurotransmitter release, particularly in cholinergic nerve fibres, are consistent with those reported in clinical cases of severe envenomation or in vitro studies with whole venom [1,2]. In addition, the actions of the toxin could be neutralised or reversed by Sydney funnel-web spider antivenom consistent with previous in vitro and in vivo studies [2]. The present findings provide additional evidence for the cross-reactivity of Sydney funnel-web spider antivenom and supports the potential effectiveness of this antivenom in cases of systemic envenomation by male *M. bradleyi*.

Given that previously characterised spider δ-toxins are, by definition, potent modulators of sodium channel inactivation [14,15], we investigated whether δ-MSTX-Mb1a modulated sodium channel gating or kinetics. The findings of this study demonstrate that δ-MSTX-Mb1a has selective effects on TTX-sensitive I_{Na} including: (a) a slowing of channel inactivation, (b) a reduction in peak current amplitude, and (c) shifts in the voltage dependence of activation. In contrast, and consistent with spider δ-toxins, TTX-resistant sodium channel gating and kinetics remained unaffected.

These actions, especially the slowing of I_{Na} inactivation in the absence of large shifts in the voltage dependence of activation or profound slowing of deactivation, indicates that δ-MSTX-Mb1a acts in a manner similar to scorpion α-toxins, sea anemone toxins, and previously characterised δ-ACTX that bind to neurotoxin receptor site-3. The above actions of δ-MSTX-Mb1a indicate that it inhibits conversion of the voltage-gated sodium channel from the open to the inactivated state, resulting in sodium currents remaining at membrane potentials where inactivation is normally complete. This is qualitatively similar to all other δ-ACTX, apart from the vertebrate-selective δ-ACTX-Hv1b that appears to be approximately 15- to 30-fold less potent in its modulation of vertebrate sodium channel gating and kinetics. In addition, δ-MSTX-Mb1a like other spider δ-toxins, except δ-ACTX-Hv1b, possesses both insect and vertebrate toxicity, albeit with slightly reduced insecticidal potency. This is presumably due to binding to insect voltage-gated sodium channels at site-3 to slow inactivation as has been previously observed with δ-ACTX-Hv1a [13,15,32].

Given the high similarity in the primary sequence, cysteine spacing and bioactivity, as well as a common antibody epitope, it seems plausible that δ-MSTX-Mb1a shares a similar inhibitor cystine-knot motif, 3D structure and importantly a similar pharmacophore to that of δ-ACTX. Unfortunately, work to identify the bioactive surface of δ-ACTX has been hampered by the four disulfide bonds preventing the refolding of synthetic or recombinant toxin in sufficient yields to attempt mutagenesis studies. Nevertheless, critical residues involved in δ-ACTX binding have been delineated by matching topologically related residues on the bioactive surface of LqhαIT, a scorpion α-toxin. Previous mutagenesis studies have shown that several basic, non-polar and aromatic residues that constitute the bioactive surface of LqhαIT [33] cluster in a similar fashion on the counterpart surface of the site-3 toxins Aah-II and ApB and, interestingly, also appear on the surface of both δ-ACTX-Hv1a and -Ar1a, despite distinctly different protein scaffolds [32]. In the spider δ-toxins, that are

toxic to both insects and vertebrates, these are the positively charged residues Lys^3, Lys^4, Arg^5 and Lys^{10}, the non-polar Asn^6 and the aromatic residues Trp^7 and Tyr^{22}/Tyr^{25} [32] (for a review see [4]). Importantly all residues apart from Asn^6 are conserved in the ortholog δ-MSTX-Mb1a lending further support to the hypothesis that they form the bioactive surface of spider δ-toxins targeting site-3 of the sodium channel.

Importantly, close inspection of the primary structure of the spider δ-toxins reveals that a number of amino acids are not conserved between δ-ACTX-Hv1b and other hexathelid spider δ-like toxins including Magi 4 from *M. gigas* [30] and the actinopodid spider δ-toxin, δ-MSTX-Mb1a (see Fig. 2). It is assumed that Magi 4 is a spider δ-toxin since it shows sequence homology to δ-ACTX, is lethal to mammals and insects, and competes with LqhαIT for site-3 on insect sodium channels. Interestingly though, it fails to compete with Lqh-II for binding to rat brain synaptosomes and therefore shows unusual binding characteristics despite being toxic when injected intracerebroventricularly in mice [30]. Significantly, δ-ACTX-Hv1b lacks insect toxicity and has a 15- to 30-fold reduction in vertebrate toxicity, however, it has non-conservative K4S, R5D, and Y22K substitutions in comparison to spider δ-toxins and Magi 4 that are all known to be toxic to insects and vertebrates. This lends support to the hypothesis that these basic and aromatic residues are important for full vertebrate and insect activity.

The similar disposition of these residues on the distinctly dissimilar 3D surface of site-3 peptide toxins from scorpions, sea anemones and spiders, demonstrates the putative route of convergent evolution of receptor site-3 ligands. In addition, the highly conserved sequence homology between two phylogenetically distinct and primitive spider families (Actinopodidae vs. Hexathelidae) provides evidence to suggest that there is strong selection pressure to maintain such highly toxic peptides despite potential evolutionary mutation. This provides strong evidence of the highly optimised nature of peptide neurotoxins especially those from spider venoms.

References

[1] Underhill, D. (1987) in: Australia's Dangerous Creatures (Sutherland, S.K., Ed.), 175 pp., Readers Digest Services, Sydney.
[2] Rash, L.D., Birinyi-Strachan, L.C., Nicholson, G.M. and Hodgson, W.C. (2000) Br. J. Pharmacol. 130, 1817–1824.
[3] King, G.F., Tedford, H.W. and Maggio, F. (2002) J. Toxicol. Toxin Rev. 21, 359–389.
[4] Nicholson, G.M., Little, M. and Birinyi-Strachan, L.C. (2003) Toxicon, in press.
[5] Sheumack, D.D., Claassens, R., Whiteley, N.M. and Howden, M.E.H. (1985) FEBS Lett. 181, 154–156.
[6] Brown, M.R., Sheumack, D.D., Tyler, M.I. and Howden, M.E.H. (1988) Biochem. J. 250, 401–405.
[7] Szeto, T.H., Birinyi-Strachan, L.C., Wang, X.-H., Smith, R., Connor, M., Christie, M.J., King, G.F. and Nicholson, G.M. (2000) FEBS Lett. 470, 293–299.
[8] Fletcher, J.I., Chapman, B.E., Mackay, J.P., Howden, M.E.H. and King, G.F. (1997) Structure 5, 1525–1535.
[9] Pallaghy, P.K., Alewood, D., Alewood, P.F. and Norton, R.S. (1997) FEBS Lett. 419, 191–196.
[10] Pallaghy, P.K., Neilsen, K.J., Craik, D.J. and Norton, R.S. (1994) Protein Sci. 3, 1833–1839.
[11] Nicholson, G.M., Willow, M., Howden, M.E.H. and Narahashi, T. (1994) Pflügers Arch. (Eur. J. Physiol.) 428, 400–409.
[12] Nicholson, G.M., Walsh, R., Little, M.J. and Tyler, M.I. (1998) Pflügers Arch. (Eur. J. Physiol.) 436, 117–126.
[13] Grolleau, F., Stankiewicz, M., Birinyi-Strachan, L.C., Wang, X.-H., Nicholson, G.M., Pelhate, M. and Lapied, B. (2001) J. Exp. Biol. 204, 711–721.
[14] Alewood, D., Birinyi-Strachan, L.C., Pallaghy, P., Norton, R., Nicholson, G.M. and Alewood, P.F. (2003) Biochemistry, in press.
[15] Little, M.J., Wilson, H., Zappia, C., Cestèle, S., Tyler, M.I., Martin-Eauclaire, M.-F., Gordon, D. and Nicholson, G.M. (1998) FEBS Lett. 439, 246–252.
[16] Hanck, D.A. and Sheets, M.F. (1995) J. Gen. Physiol. 106, 601–616.
[17] Strichartz, G.R. and Wang, G.K. (1986) J. Gen. Physiol. 88, 413–435.
[18] Little, M.J., Zappia, C., Gilles, N., Connor, M., Tyler, M.I., Martin-Eauclaire, M.-F., Gordon, D. and Nicholson, G.M. (1998) J. Biol. Chem. 273, 27076–27083.
[19] Gilles, N., Leipold, E., Chen, H., Heinemann, S.H. and Gordon, D. (2001) Biochemistry 40, 14576–14584.
[20] Gordon, D. (1997) in: Toxins and Signal Transduction: Cellular And Molecular Mechanisms of Toxin Action Series (Lazarowici, P. and Gutman, Y., Eds.), pp. 119–149, Harwood Press, Amsterdam.
[21] Laemmli, U.K. (1970) Nature 227, 680–685.
[22] Ginsborg, B.L. and Warriner, J. (1960) Br. J. Pharmacol. 15, 410–411.
[23] Tzeng, M.C. and Tian, S.S. (1983) Toxicon 21, 879–881.
[24] Hamill, O.P., Marty, A., Neher, E., Sakmann, B. and Sigworth, F.J. (1981) Pflügers Arch. (Eur. J. Physiol.) 391, 85–100.
[25] Ogata, N., Nishimura, M. and Narahashi, T. (1989) J. Pharmacol. Exp. Ther. 248, 605–613.
[26] Roy, M.L. and Narahashi, T. (1992) J. Neurosci. 12, 2104–2111.
[27] Bezanilla, F. and Armstrong, C.M. (1977) J. Gen. Physiol. 70, 549–566.
[28] Eitan, M., Fowler, E., Herrmann, R., Duval, A., Pelhate, M. and Zlotkin, E. (1990) Biochemistry 29, 5941–5947.
[29] Graudins, A., Wilson, D., Alewood, P.F., Broady, K.W. and Nicholson, G.M. (2002) Toxicon 40, 259–266.
[30] Corzo, G., Gilles, N., Satake, H., Villegas, E., Dai, L., Nakajima, T. and Haupt, J. (2003) FEBS Lett. 547, 43–50.
[31] Norton, R.S. and Pallaghy, P.K. (1998) Toxicon 36, 1573–1583.
[32] Gilles, N., Harrison, G., Karbat, I., Gurevitz, M., Nicholson, G.M. and Gordon, D. (2002) Eur. J. Biochem. 269, 1500–1510.
[33] Tugarinov, V., Kustanovich, I., Zilberberg, N., Gurevitz, M. and Anglister, J. (1997) Biochemistry 36, 2414–2424.

ADDITIONAL EXPERIMENTAL DATA NOT INCLUDED IN ORIGINAL PUBLICATION

As shown in Figure 1D of the above publication, rp-HPLC separation of peak *a* (Figure 1C) yielded three major peaks, of which peak *b* was the largest and „the most active component in the chick isolated biventer cervis nerve-muscle preparation". This section shows raw data of vertebrate toxicity tests conducted on the two remaining unlabelled peaks in Figure 1D that were not included in this publication.

Figure 1D of the paper is reproduced below with the two remaining peaks labelled as peak *c* and *d*.
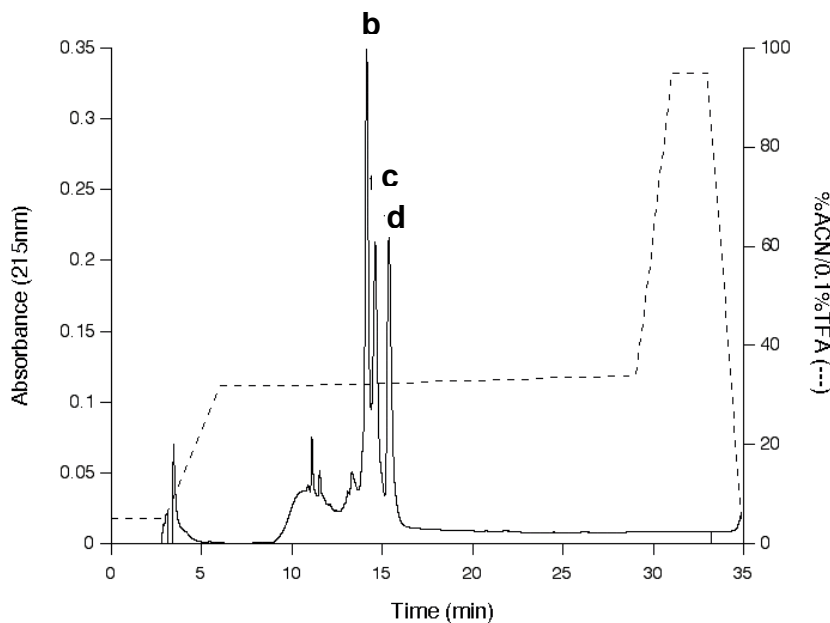
7.1 **Vertebrate toxicity assays of peaks *c* and *d***

In the indirectly stimulated chick biventer cervicis nerve-muscle, a concentration of 30 nM and 60 nM peak *c* had no significant effect on the twitch amplitude and baseline resting tension (Figure 7.1A). Similarly, peak *d* had no observable on the twitch and baseline resting tension at a concentration of 65 nM (Figure 7.1B).

A

B
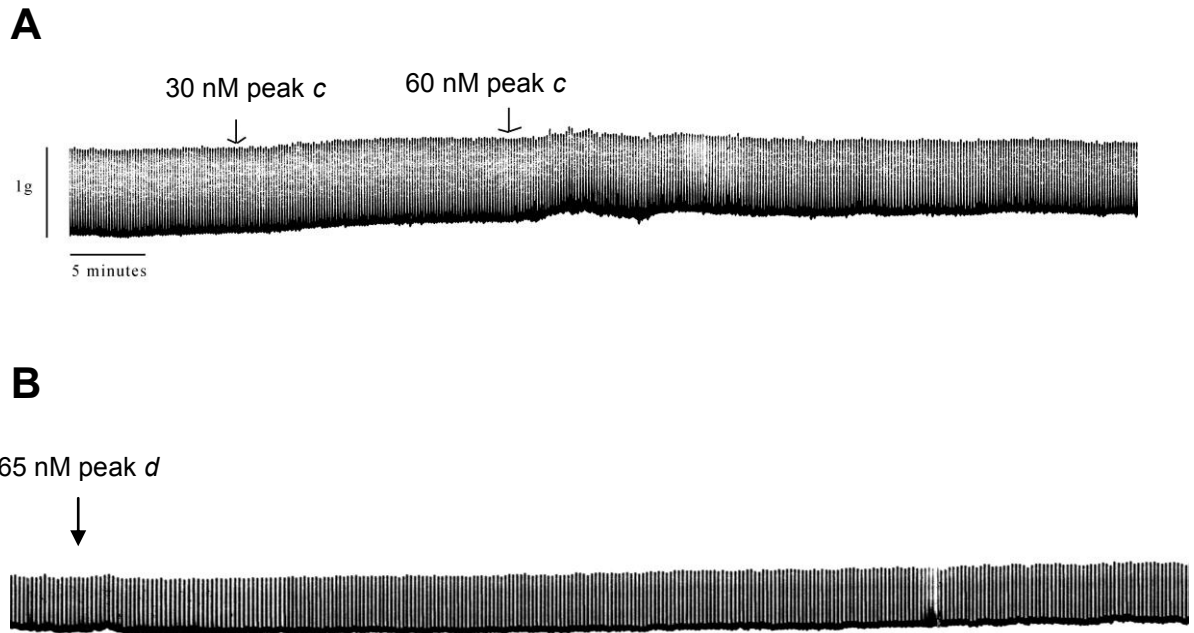
Figure 7.1: Effects of male *M.bradleyi* venom peak *c* and *d* on isolated chick biventer cervicis nerve-muscle preparation. Peak *c* was added at a concentration of 30 nM and subsequently at a dose of 60 nM (A), and peak *d* was tested at 65 nM concentration (B).

8   Electrophysiological characterisation of ω-ctenitoxin-Cs1a from *Cupiennius salei* on cockroach DUM neurons

Declaration for Thesis Chapter 8

This chapter consists of the following publication:

Kubista, H., Mafra, R.A., Chong, Y., Nicholson, G.M., Beirao, P.S., Cruz, J.S., Boehm, S., Nentwig, W., & Kuhn-Nentwig, L. 2007. CSTX-1, a toxin from the venom of the hunting spider *Cupiennius salei*, is a selective blocker of L-type calcium channels in mammalian neurons. *Neuropharmacology*, 51, 1650–62.

I declare that my work constitutes a proportion of this manuscript. The specific sections are:

- Isolation and culturing of DUM neurons from cockroach (section 2.2);
- Electrophysiology: whole-cell voltage clamp recordings from DUM neurons (section 2.5);
- Effects of CSTX-1 on insect neurons (section 3.1);
- Discussion relating to action of CSTX-1 on insect neurons (section 4).

Youmie Chong: Date:

Prof. Graham Nicholson   Date:

(Corresponding author/principal supervisor):

CSTX-1, a toxin from the venom of the hunting spider *Cupiennius salei*, is a selective blocker of L-type calcium channels in mammalian neurons

Helmut Kubista [a,*], Roberta A. Mafra [b], Youmie Chong [c], Graham M. Nicholson [c], Paulo S.L. Beirão [b], Jader S. Cruz [b], Stefan Boehm [d], Wolfgang Nentwig [e], Lucia Kuhn-Nentwig [e]

[a] *Center for Biomolecular Medicine and Pharmacology, Institute of Pharmacology, Medical University of Vienna, Waehringerstrasse 13a, A-1090 Vienna, Austria*
[b] *Department of Biochemistry and Immunology, Instituto de Ciências Biológicas, Universidade Federal de Minas Gerais, Av. Antonio Carlos 6627, 31270-901 Belo Horizonte, MG, Brazil*
[c] *Neurotoxin Research Group, Department of Medical and Molecular Biosciences, University of Technology, Sydney, City Campus, Broadway, Sydney, NSW 2007, Australia*
[d] *Institute of Experimental and Clinical Pharmacology, Medical University of Graz, Universitätsplatz 4, A-8010 Graz, Austria*
[e] *Zoological Institute, University of Bern, Baltzerstrasse 6, CH-3012 Bern, Switzerland*

Abstract

The inhibitor cystine-knot motif identified in the structure of CSTX-1 from *Cupiennius salei* venom suggests that this toxin may act as a blocker of ion channels. Whole-cell patch-clamp experiments performed on cockroach neurons revealed that CSTX-1 produced a slow voltage-independent block of both mid/low- (M-LVA) and high-voltage-activated (HVA) insect Ca_v channels. Since *C. salei* venom affects both insect as well as rodent species, we investigated whether Ca_v channel currents of rat neurons are also inhibited by CSTX-1. CSTX-1 blocked rat neuronal L-type, but no other types of HVA Ca_v channels, and failed to modulate LVA Ca_v channel currents. Using neuroendocrine GH3 and GH4 cells, CSTX-1 produced a rapid voltage-independent block of L-type Ca_v channel currents. The concentration–response curve was biphasic in GH4 neurons and the subnanomolar IC_{50} values were at least 1000-fold lower than in GH3 cells. L-type Ca_v channel currents of skeletal muscle myoballs and other voltage-gated ion currents of rat neurons, such as $I_{Na(v)}$ or $I_{K(v)}$ were not affected by CSTX-1. The high potency and selectivity of CSTX-1 for a subset of L-type channels in mammalian neurons may enable the toxin to be used as a molecular tool for the investigation of this family of Ca_v channels.
© 2007 Elsevier Ltd. All rights reserved.

Keywords: Cupiennius salei venom; CSTX-1; Voltage-gated calcium channels; DUM neurons; Rat neurons

1. Introduction

A multitude of applications make venom toxins important molecular tools. Cell biologists are employing a variety of animal, plant and microbial toxins to investigate the contribution of their molecular targets to various cell functions and as lead compounds for the development of pesticides and therapeutics (Bailey and Wilce, 2001). For example, phyla-specific spider neurotoxins that interact selectively with insect membrane proteins are being examined for their potential as biopesticides (Tedford et al., 2004a,b). More recently, the pharmaceutical industry has discovered the pre-optimised combinatorial peptide library that animal venoms represent, and are searching for toxins as templates for drug design or directly as therapeutics (Harvey, 2002; Bogin, 2005).

In neurobiology, specific antagonists are required to study the structure and role of voltage- and transmitter-gated ion channels. Venoms of different animals provide a rich but, as yet, largely unexplored source of ion channel modulators. Many of the toxins studied to date are selective blockers and discriminate between closely related ion channel subtypes. Families of Ca_v channels have been identified pharmacologically using specific peptide toxins from marine cone snail and spider venoms (Doering and Zamponi, 2003). However, at present, many of the Ca_v channel subtypes identified using molecular biology techniques cannot be isolated pharmacologically. This holds true for the L-type ($Ca_v1.x$) family of Ca_v channels, which, for mammalian neurons, are characterized by their sensitivity to dihydropyridines. The differences in the affinity of dihydropyridines for the four L-type Ca_v channel subtypes ($Ca_v1.1$–1.4), identified to date, were found to be too small to permit the study of the functional role of these channels in various cell types (Bourinet et al., 2004). It is therefore valuable to further isolate and characterize venom components in a search for novel toxins that may be used as pharmacological tools to further dissect the structure and function of Ca_v channels.

Cupiennius salei (Araneae: Ctenidae) is a nocturnal hunting spider inhabiting tropical rain forests from Central Mexico to northern South America (Kuhn-Nentwig et al., 2004). The venom of this spider is a complex mixture containing ions (Na^+ 8.9 mM, K^+ 215 mM, and Ca^{2+} 0.94 mM), low molecular mass substances as amino acids (mainly glycine 43.3 pmol/μl and taurine 70.0 pmol/μl), amines (histamine 5.7 nmol/μl) and polyamines in low quantities (Kuhn-Nentwig et al., 1994, 2004). Besides proteins (M_r 25–27 kDa) such as the enzyme hyaluronidase, peptides in the molecular range between 3 and 4 kDa were identified and therein two peptide families were named cupiennin 1 and cupiennin 2 (Kuhn-Nentwig et al., 2004). These cationic cupiennins exhibit a toxic activity towards insects, a strong cytolytic activity to erythrocytes and are bactericidal in the submicromolar range towards Gram positive as well as Gram negative bacteria (Kuhn-Nentwig et al., 2002). Additionally, cupiennin 1a inhibits the formation of NO from neuronal nitric oxide synthase by involving complexation with the regulatory protein calcium calmodulin (Pukala et al., 2007). Synergistic toxic effects were

demonstrated in a *Drosophila* bioassay between cupiennin 1a and members of a family of peptides (CSTX-1 to -13) with molecular masses between 6 and 8 kDa, which are mainly responsible for the lethality of the venom (Wullschleger et al., 2005). Interestingly, bioassays revealed that mice, despite not being usual prey species, are the most sensitive species to *C. salei* venom when compared to a wide range of arthropods (Kuhn-Nentwig et al., 1998). Among the 13 peptide toxins identified in *C. salei* venom, the 74-residue peptide CSTX-1 is the most abundant and displays the highest toxicity in mammalian and insect bioassays (Kuhn-Nentwig et al., 1994). Despite the comprehensive knowledge of venom composition and peptide structure acquired within the last decade (Kuhn-Nentwig et al., 2004), evidence for the molecular targets of *C. salei* toxins remains obscure. CSTX-1, CSTX-9 and CSTX-13 are characterized by four disulfide bridges. Three of the four disulfide bridges form linkages between C1–C4, C2–C5 and C3–C8 and conform to an 'inhibitor cystine-knot' (ICK) motif (Norton and Pallaghy, 1998). This motif is characteristic for many ion channel blocking peptide toxins (Mouhat et al., 2004), especially from spider venoms (Nicholson, 2006). In this study we therefore tested the hypothesis that CSTX-1 may act as an antagonist of neuronal ion channels. We show that CSTX-1 blocks voltage-gated calcium (Ca_v) channel currents in neurons of the cockroach *Periplaneta americana*, but does not appear to discriminate between mid/low- (M-LVA) and high-voltage-activated (HVA) Ca_v channels. In rat neurons, CSTX-1 leaves LVA Ca_v channel currents unaffected but acts as a selective blocker of dihydropyridine-sensitive L-type HVA Ca_v channels. The potency of block appears to depend on the subtype of L-type Ca_v channels expressed in these neurons. Our data suggest that CSTX-1 has evolved as a blocker of insect Ca_v channels, and has a structure that permits a high affinity interaction with a subtype of L-type Ca_v channels expressed in mammalian neurons. CSTX-1 may thus have a potential as a research tool to investigate the physiological role of L-type Ca_v channel subtypes. Some of these results have recently been presented in abstract form (Kubista et al., 2006).

2. Materials and methods

2.1. Toxin isolation

Spider maintenance, venom collection and purification of CSTX-1 were carried out as previously described (Kuhn-Nentwig et al., 1994) with the following modifications. Cation exchange liquid chromatography was performed on an Mono S HR 10/10 (10 cm × 1 cm, Pharmacia, Sweden) at a flow rate of 0.5 ml/min using a 200 mM ammonium acetate buffer, pH 5.5 and a gradient (B) of 200 mM ammonium acetate and 2 M NaCl, pH 5.5. The separation profile was 0% B for 20 min followed by a linear gradient from 0 to 100% from 20 to 74 min. The fraction containing CSTX-1, which eluted at 1 M NaCl (50% B), was desalted and separated by RP-HPLC using a Nucleosil 300-5 C_4 column (4.6 mm × 250 mm, Macherey & Nagel, Germany) with 0.1% v/v trifluoroacetic acid (TFA) in water for 0–15 min followed by a linear gradient of 0.1% TFA in acetonitrile from 0 to 10% from 15 to 30 min and from 10 to 50% from 30 to 125 min. Rechromatography of the peptide was performed on the same column using isocratic conditions with 32% acetonitrile in TFA for 30 min. Starting with 1.8 ml of crude venom we obtained 15 mg of highly purified CSTX-1, by a combination of gel filtration, cationic exchange chromatography and successive RP-HPLC. The purity of CSTX-1

156

was confirmed by RP-HPLC (Fig. 1), N-terminal amino acid sequencing, amino acid composition and electrospray ionisation-mass spectrometry (ESI-MS).

2.2. DUM neurons

Dorsal unpaired median (DUM) neurons from the terminal abdominal ganglion (TAG) of the nerve cord of the adult American cockroach, *P. americana* were isolated using methods modified from Grolleau and Lapied (1996) and Sinakevitch et al. (1996). Briefly, the sixth abdominal ganglia were excised, desheathed and incubated for 15 min at 37 °C in insect saline of the following composition (in mM): 200 NaCl, 3.1 KCl, 5 CaCl$_2$, 4 MgCl$_2$, 10 *N*-2-hydroxyethylpiperazine-*N'*-2-ethanesulfonic acid (HEPES), 40 D-glucose supplemented with 5% v/v foetal calf serum and 50 000 IU/l penicillin and streptomycin at pH 7.4, containing 1 mg/ml of collagenase and hyaluronidase. After washing in enzyme-free insect saline, DUM neurons were mechanically isolated from exogenous tissue by trituration, carefully passing the ganglia in and out of a sterile Pasteur pipette. The resulting suspension was then distributed into eight wells of a 24-well cluster plate (Limbro, Ohio, USA). Each well contained a 12-mm diameter glass coverslip (Lomb Scientific, Taren Point, NSW, Australia), which had been previously coated with BD Cell-Tak™ (BD Biosciences, North Ryde, Sydney, Australia). Isolated cells were allowed to attach to the coverslips overnight in an incubator (5% CO$_2$, 95% O$_2$, 100% relative humidity, 28 °C) in normal insect saline supplemented with 5% v/v foetal calf serum, prior to experimentation.

2.3. Rat SCG and DRG neurons

Primary cultures of dissociated superior cervical ganglia (SCG) and dorsal root ganglia (DRG) neurons from neonatal rats were prepared as described previously (Lechner et al., 2003). Briefly, ganglia were dissected from 2 to 6-day-old Sprague–Dawley rat pups that had been killed by decapitation in accordance with the rules of the Animal Welfare Committee of the Medical University of Vienna. Ganglia were cut into 3–4 pieces and incubated in 1.5 mg/ml collagenase and 3.0 mg/ml dispase (Sigma, Vienna, Austria) for 20 min at 36 °C. Subsequently, they were trypsinised (2.5 mg/ml trypsin; Worthington, Lakewood, NJ, USA) for 15 min at 36 °C, dissociated by trituration, and resuspended in Dulbecco's-modified Eagle's Medium (DMEM; Invitrogen, Lofer, Austria) containing 2.2 g/l D-glucose, 10 mg/l insulin, 50 000 IU/l penicillin and 50 mg/l streptomycin (Invitrogen, Lofer, Austria), 50 μg/l nerve growth factor (Invitrogen, Lofer, Austria), and 5% v/v foetal calf serum (Invitrogen, Lofer, Austria). Thereafter, the cells were plated onto 35 mm diameter culture dishes, previously coated with rat tail collagen, for electrophysiological

experiments. DRG neurons were used on the day of plating, whereas SCG neurons were used for recordings within 1 week following plating. During that period SCG neurons were maintained in a humidified 5% CO$_2$ atmosphere at 37 °C. Media were exchanged on day one after plating and after another 4–5 days.

2.4. Cell lines

GH3 cells (American Type Culture Collection, Manassas, USA) were cultured in DMEM–HEPES modification (Sigma, USA) supplemented with 10% v/v foetal calf serum (Cultilab, Brazil). The cells were routinely grown as stocks in 75 cm^2 flasks (Costar, USA) at 37 °C in a humidified 5% CO$_2$ atmosphere. The medium was changed three times a week. For electrophysiological recordings the cells were detached by trypsinisation, subcultured on glass coverslips (Corning #1, USA) without any pretreatment and plated in 47 mm diameter dishes. Trypsinisation was carried out with 0.1% w/v trypsin in the culture medium without serum and with 1 mM EDTA. Cells were used for electrophysiological recordings 1–2 days after plating.

GH4 cells (provided by T. Weiger, University of Salzburg, Austria) were grown in Nutrient Mixture F-10 Ham media supplemented with 15% v/v horse serum, 2.5% v/v foetal calf serum, 50 000 IU/l penicillin, 50 mg/l streptomycin and 2 mM L-glutamine. The cells were routinely grown as stocks in 10 cm diameter dishes (Iwaki, Japan) at 37 °C in a humidified 5% CO$_2$ atmosphere. Cells were split once a week and growth media were replaced once between passages. For patch-clamp experiments, GH4 cells were detached by trypsinisation and seeded at low density on poly-D-lysine-coated 35 mm diameter dishes.

Cell culture and differentiation of the C3H murine skeletal C2C12 cell line was carried out as described elsewhere (Zebedin et al., 2004). Briefly, cultures were maintained in serum containing 20% v/v foetal calf serum and differentiation of myoblasts was induced by serum reduction (2% v/v horse serum instead of 20% v/v foetal calf serum) on cells plated onto Matrigel. Electrophysiological experiments were performed 14 days after induction of differentiation on C2C12 myoballs as described previously (Zebedin et al., 2004).

2.5. Electrophysiology

Whole cell voltage-clamp recordings were performed at room temperature (20–24 °C) using borosilicate glass patch pipettes of 2–3.5 MΩ tip resistance when filled with internal solution (see below) and patch-clamp amplifiers from Axon Instruments (Axon Instruments, Foster City, CA, USA) or HEKA (HEKA Elektronik, Germany). Currents were elicited by voltage steps from a holding potential (V_h) of −80 mV in GH3 and GH4 cells, C2C12 myoballs
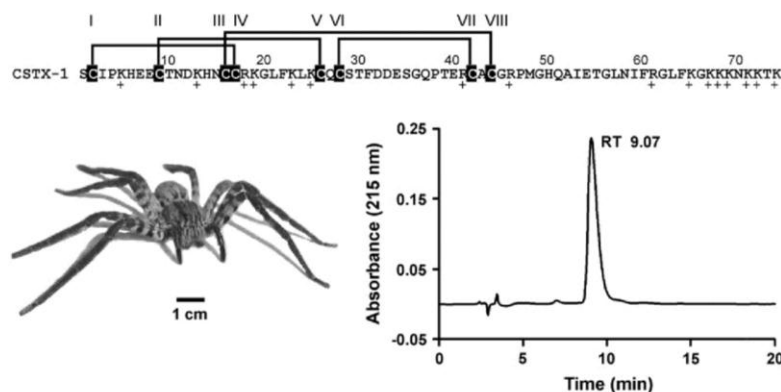
Fig. 1. Purification and primary structure of CSTX-1. Purity control of CSTX-1 (10 μg) isolated from the venom of *Cupiennius salei* by RP-HPLC on an Atlantis dC$_{18}$ 3 μm column (3.9 × 150 mm, Waters) under isocratic conditions (0.1% v/v TFA in 32% acetonitrile, retention time RT 9.07 min). For complete details of isolation see Section 2. The disulfide-bridge pattern for the cysteine residues (boxed in black) are indicated above the sequences as well as the positive charge, especially of the C-terminus of the peptide.

and SCG neurons, from −100 mV in DRG neurons, and from −90 mV in DUM neurons, to the indicated depolarised potentials. Voltage steps were in most cases applied every 15 s, but pulse frequency was increased up to every 5 s in some experiments for a better resolution of the kinetics of current inhibition. Leakage and capacitive currents were digitally subtracted online with *P-P/4* procedures. Data were low-pass filtered at 2−5 kHz, digitised at 10−50 kHz and stored on computer for subsequent off-line analysis.

In whole-cell voltage-clamp recordings from DUM neurons, I_{Ba} were recorded using an Axopatch 200A patch-clamp amplifier and AxoData v3.0 software (Axon Instruments). Patch pipettes were filled with an internal solution of the following composition (in mM): 50 choline-Cl, 30 CsCl, 50 TEA-Br, 2 Na$_2$-ATP, 0.5 CaCl$_2$, 10 ethylene glycol-bis (β-aminoethylether)-*N,N,N′,N′*-tetraacetic acid (EGTA), 10 HEPES and adjusted to pH 7.25 using CsOH. The external solution for recording I_{Ba} in DUM neurons contained (in mM): 160 choline-Cl, 50 TEA-Br, 3 BaCl$_2$, 10 HEPES, 500 nM tetrodotoxin (TTX), and the pH was adjusted to 7.4 using TEA-OH. 500 μM Cd^{2+}, a known insect Ca$_v$ channel blocker, was used to abolish peak inward I_{Ba}, and confirmed the currents recorded were carried through this channel. Toxins and drugs were applied via a pressurised fast perfusion system (AutoMate Scientific, San Francisco CA, USA).

In whole-cell voltage-clamp recordings from GH3 cells, I_{Ba} were recorded using a HEKA EPC-9 patch-clamp amplifier. The internal pipette solution was of the following composition (in mM): 130 CsCl, 10 TEA-Cl, 2 Mg-ATP, 0.1 Li-GTP, 5 EGTA, 5 HEPES, and adjusted to pH 7.2 using CsOH. The cells were perfused continuously with an external solution containing (in mM): 140 NaCl, 25 BaCl$_2$, 0.5 MgCl$_2$, 5 CsCl, 5 HEPES, 0.1 μM TTX, and adjusted to pH 7.4 using NaOH.

Whole-cell ionic currents from SCG neurons, DRG neurons, GH4 cells and C2C12 myoballs were recorded as described previously (Vartian and Boehm, 2001), using an Axopatch 200B amplifier and pCLAMP v8.0 software. The internal pipette solution consisted of (in mM): (A) 140 KCl, 1.59 CaCl$_2$, 10 HEPES, 10 EGTA, 2 Mg-ATP, 2 Li-GTP, adjusted to pH 7.2 with KOH for measurement of outward $I_{K(v)}$, or (B) 130 CsCl, 20 tetraethylammonium (TEA)-Cl, 0.24 CaCl$_2$, 10 D-glucose, 10 HEPES, 5 EGTA, 2 Mg-ATP, and 2 Li-GTP, adjusted to pH 7.2 with CsOH, for measurement of I_{Ba} and $I_{Na(v)}$ currents, respectively. The external bathing solution contained (in mM): (A) 120 NaCl, 3 KCl, 2 MgCl$_2$, 2 CaCl$_2$, 20 D-glucose, 10 HEPES, adjusted to pH 7.4 with NaOH for the measurement of outward $I_{K(v)}$, or (B) 120 NaCl, 3 KCl, 2 MgCl$_2$, 5 CaCl$_2$ ($I_{Na(v)}$) or 5 BaCl$_2$ (I_{Ba}), 20 TEA-Cl, 20 D-glucose, 10 HEPES, adjusted to pH 7.4 with NaOH for the measurement of high-voltage activated I_{Ba} and $I_{Na(v)}$. In addition, TTX (0.5 μM) or CdCl$_2$ (0.5 mM) were added to the external solution to isolate either high-voltage activated I_{Ba} or $I_{Na(v)}$ currents, respectively. For the measurement of LVA Ca$_v$ channel currents in DRG neurons, TTX-sensitive and -insensitive $I_{Na(v)}$ were eliminated by replacement of NaCl with choline-Cl using the following bathing solution (in mM): 120 choline-Cl, 3 KCl, 2 MgCl$_2$, 5 BaCl$_2$, 20 TEA-Cl, 20 D-glucose, 10 HEPES, adjusted to pH 7.4 with CsOH. Drugs and toxins were applied via a DAD-12 drug application device (Adams & List, Westbury, NY, USA).

2.6. Data analysis

Traces were analysed off-line using Clampfit or AxoGraph v4.0 (Axon Instruments) or Pulse-Fit (HEKA). Unless otherwise stated, current measurements were taken at the end of the voltage pulse. Mathematical curve fitting employed algorithms available in ORIGIN v5.0 software (Microcal Software, Northampton, MA), Sigma Plot v5.0 (SPSS Inc., Richmond, CA) or GraphPad Prism v4.0 for Macintosh (GraphPad Software, San Diego CA, USA) using non-linear least-squares methods. Concentration−response curves in GH3 and DUM neurons were fitted using the following form of the Langmuir equation:

$$y = B_{max} \frac{[C]}{IC_{50} + [C]} \qquad (1)$$

where *y* is the percentage current inhibition, B_{max} is the maximum response (typically 100), [*C*] is the toxin concentration, and IC$_{50}$ is the concentration at half-maximal block.

Concentration−response curves in GH4 cells were fitted using a two-site binding model using the following equation:

$$y = B_{max1} \frac{[C]}{IC_{50(1)} + [C]} + B_{max2} \frac{[C]}{IC_{50(2)} + [C]} \qquad (2)$$

Current−voltage (*I−V*) curves were fitted using the following equation:

$$I = g_{max} \left(1 - \left(\frac{1}{1 + \exp\left[(V - V_{1/2})/s \right]} \right) \right) (V - V_{rev}) \qquad (3)$$

where *I* is the amplitude of the current at a given test potential *V*, g_{max} is the maximal conductance, $V_{1/2}$ is the voltage at half-maximal activation, *s* is the slope factor, and V_{rev} is the apparent reversal potential.

2.7. Chemicals

ATP-Mg, GTP-Li, TEA-Cl, Nutrient Mixture F-10 Ham, poly-D-lysine, nitrendipine, nicardipine hydrochloride and bulk chemicals were from Sigma (Vienna, Austria or St. Louis, USA). Unless otherwise stated all sera and antibiotics were from Life Technologies (Vienna, Austria). Matrigel was obtained from Becton Dickinson (Schwechat, Austria), rat tail collagen was from Biomedical Technologies (Stoughton, MA), TTX was purchased from Latoxan (Valence, France), and ω-conotoxin GVIA was obtained from Alomone Labs (Jerusalem, Israel).

3. Results

3.1. Effects of CSTX-1 on insect neurons

To test the hypothesis that ion channel antagonism may underlie the toxicity of CSTX-1 in typical prey animals of *C. salei* we investigated the blocking effect of CSTX-1 on insect Ca$_v$ channels in DUM neurons of the cockroach *P. americana*. We focused our attention on two subtypes of Ca$_v$ channels that are activated by suprathreshold voltages: a mid- to low- (M-LVA) and a high-voltage-activated (HVA) Ca$_v$ channel (Wicher and Penzlin, 1994, 1997). To prevent Ca^{2+}-induced rundown of Ca^{2+} currents, Ba^{2+} was used as a charge carrier instead of Ca^{2+} (Wicher and Penzlin, 1997). Macroscopic I_{Ba} through Ca$_v$ channels were elicited by 100-ms depolarising command pulses from a V_h of −90 mV. Inward I_{Ba} were evoked by depolarising pulses to −30 mV (M-LVA Ca$_v$ channel currents dominating) and +30 mV (HVA Ca$_v$ channel currents dominating). Depolarisations to −30 mV (Fig. 2A, C, E) caused a large inward current with slow decaying component, whereas depolarisations to +30 mV elicited a smaller current with a fast decaying component (Fig. 2B, D, F). As illustrated in Fig. 2 CSTX-1 inhibited the currents at both voltages in a concentration-dependent manner. The addition of 300 nM CSTX-1 resulted in a block of peak I_{Ba} of 34.2 ± 4% (*n* = 5) within 5 min at −30 mV (Fig. 2A), and 44.2 ± 2% block of peak I_{Ba} at depolarising pulses to +30 mV (*n* = 5) (Fig. 2B). At a concentration of 900 nM CSTX-1, this block increased to 72.9 ± 5% and 90.0 ± 2% at −30 mV (Fig. 2C) and +30 mV (Fig. 2D), respectively (*n* = 4), with total block only being achieved at concentrations above 1 μM CSTX-1. The time course of toxin-induced I_{Ba} inhibition was relatively slow and described by a single exponential function with τ_{on} of 33.1 s. In addition, the recovery after prolonged washout with toxin-free external solution was incomplete. By fitting
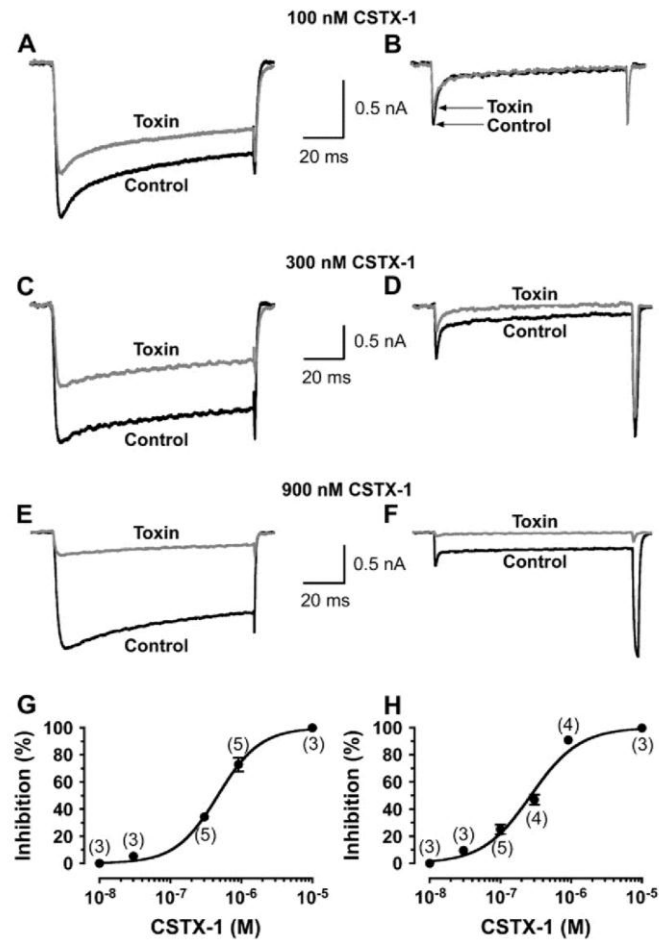
Fig. 2. Concentration-dependent block of Ca_v channels in cockroach DUM neurons by CSTX-1. Whole-cell I_{Ba} were evoked by 100-ms depolarising test pulses from a holding potential of −90 mV to −30 mV (left-hand panels) and +30 mV (right-hand panels), respectively, in the absence, and presence, of CSTX-1. Panels show effects following a 10-min perfusion with 100 nM (A, B), 300 nM (C, D) and 900 nM CSTX-1 (E, F). Washout with toxin-free solution did not significantly reverse these effects. (G, H) Concentration−response curves for the inhibition of peak I_{Ba} by CSTX-1 at −30 mV (G) and +30 mV (H). Data were fitted with Eq. (1) in Section 2. Numbers in brackets above each data point represent the number of experiments performed at that concentration.

the concentration−response curve of the inhibition of peak I_{Ba} using a Langmuir equation (Eq. (1); see Section 2), the concentration of CSTX-1 at half-maximal block (IC_{50}) at a −30 mV depolarising pulse was determined to be 467 nM, and 274 nM at +30 mV (Fig. 2G, H).

To determine if the block of Ca_v channels by CSTX-1 was due to a depolarising shift in the voltage-dependence of channel activation, families of I_{Ba} were generated by 100-ms test pulses from V_h (−90 mV) to a maximum of +40 mV in 10-mV increments, every 10 s. Barium currents were recorded before (Fig. 3A), and after (Fig. 3B) perfusion with 300 nM CSTX-1 ($n = 3$). The I_{Ba}−V relationship was determined from the maximal I_{Ba} values at each potential (Fig. 3C). Data were normalised against peak maximal control I_{Ba} and fitted with Eq. (3) (see Section 2). No significant shift was observed in the voltage at half-maximal activation, $V_{1/2}$, or slope

factor, s. In addition, CSTX-1 at concentrations of 100 and 300 nM produced a voltage-independent block at all test potentials between −20 and +20 mV (Fig. 3D).

3.2. Effects of CSTX-1 on barium currents in SCG neurons

The experiments on cockroach DUM neurons indicated that CSTX-1 acts as a blocker of Ca_v channels. Since mice were found to be the most sensitive species to *C. salei* venom (Kuhn-Nentwig et al., 1998), we tested CSTX-1 on various Ca_v channel currents of rodent neurons. Initially we investigated the effects of CSTX-1 on currents flowing through Ca_v channels in primary cultures of rat SCG neurons, because these neurons express Ca_v channels of the L-, N- and R-type families (Lin et al., 1996). To avoid Ca^{2+}-dependent inactivation of Ca_v

159
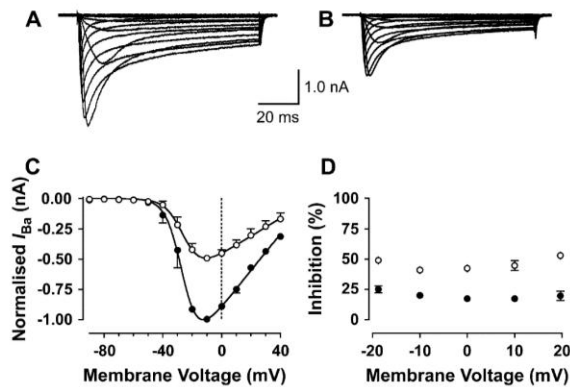
Fig. 3. Effects of CSTX-1 on the voltage-dependence of Ca_v channel activation in cockroach DUM neurons. Families of I_{Ba} were elicited by depolarising test pulses to +40 mV from a holding potential of −90 mV in 10-mV steps. Data shown represent superimposed current traces recorded before (A), and after (B), a 10-min perfusion with 300 nM CSTX-1. (C) Peak $I_{Ba}− V$ relationship showing I_{Ba} recorded before (closed circles), and after (open circles), application of 300 nM CSTX-1 ($n = 3$). Data were fitted with Eq. (3) in Section 2. (D) Voltage-independent block by CSTX-1. Percentage inhibition of peak I_{Ba} by 100 nM (closed circles) and 300 nM (open circles) CSTX-1 at different depolarising test pulses ($n = 3$).

channels and to prevent Ca^{2+}-induced rundown of Ca^{2+} currents (Kepplinger et al., 2000; Soldatov, 2003), Ba^{2+} was substituted for Ca^{2+} as the charge carrier. Ba^{2+} currents were evoked by 30-ms voltage steps from a holding potential of

−80 mV−0 mV. At a concentration of 1 μM CSTX-1 inhibited, on average, $28.5 \pm 6.4\%$ ($n = 11$) of I_{Ba}. An example of this effect is shown in Fig. 4A. To identify which subtype(s) of Ca_v channels is affected by CSTX-1 we tested the additivity of CSTX-1 and blockers of L- and N-type Ca_v channels. When the L-type component of I_{Ba} was blocked by 1 μM nitrendipine, CSTX-1 at 1 μM did not further reduce the current ($n = 4$, Fig. 4B). CSTX-1 did, however, block I_{Ba} when the N-type component was removed by 1 μM ω-conotoxin GVIA ($n = 3$, Fig. 4C, D). Our data indicate that CSTX-1 selectively blocks L-type Ca_v channels in SCG neurons, whilst sparing other Ca_v channel subtypes, for example N-type channels.

3.3. Effects of CSTX-1 on barium currents in GH3 and GH4 cells

To corroborate the finding that CSTX-1 may act as an inhibitor of L-type Ca_v channels, we tested CSTX-1 on GH3 cells, because $I_{Ca(v)}$ in these cells flows primarily via L-type Ca_v channels (Lievano et al., 1994; Leão et al., 2000; Glassmeier et al., 2001; Safa et al., 2001). Barium currents were elicited in GH3 cells by 50-ms voltage pulses to 0 mV from a holding potential of −80 mV. The dihydropyridine nicardipine (4 μM) inhibited I_{Ba} by more than 90% (typically 95%, $n = 4$, data not shown). CSTX-1 at a concentration of 1 μM markedly and reversibly inhibited these currents ($n = 5$), as depicted in Fig. 5A and B. The time course of inhibition could be described by a single exponential function with a time constant (τ_{on}) of 3.1 s, indicating that the rate of inhibition is
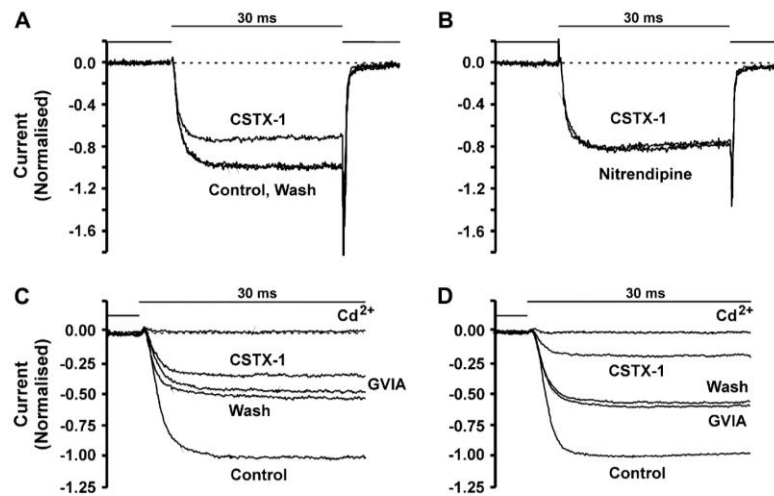
Fig. 4. CSTX-1 blocks L-type Ba^{2+} currents in SCG neurons. I_{Ba} were elicited by 30-ms voltage steps from a holding potential of −80 mV to 0 mV. Currents are shown normalised to their respective control currents. (A) Current traces recorded before (control), during and after (wash) application of 1 μM CSTX-1. (B) Current traces recorded from the same neuron as in A in the presence of 1 μM nitrendipine and after the subsequent addition of 1 μM CSTX-1. In this neuron CSTX-1 blocked I_{Ba} by 33% (A) but did not further reduce the current in the presence of nitrendipine (B). (C, D) Currents recorded under control conditions, after addition of 1 μM ω-conotoxin GVIA (GVIA), after subsequent addition of 1 μM CSTX-1 and after washout of toxins (wash). Note that block by ω-conotoxin GVIA is irreversible. The current recorded in the presence of 0.5 mM Cd^{2+} is also shown (Cd^{2+}). In the experiment shown in (C), the conotoxin blocked I_{Ba} by 50%. CSTX-1 blocked 28% of the remaining non-N-type current, which equals 14% of total I_{Ba}. Thirty-six percentage of total I_{Ba} in this neurone were insensitive to conotoxin and CSTX-1. In the experiment shown in (D), 41% of I_{Ba} was blocked by the conotoxin, CSTX-1 inhibited the remaining current by 68%, which equals 40% of total I_{Ba} recorded in the absence of toxins. In (C) and (D) the current traces are shown truncated at the time where the voltage returned to the holding potential.
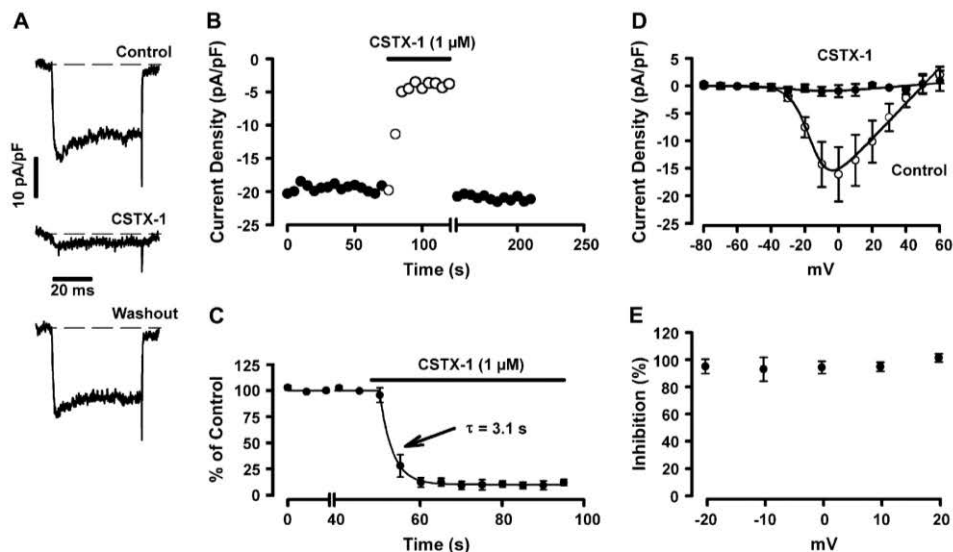
Fig. 5. CSTX-1 inhibits Ba^{2+} currents in GH3 cells in a voltage-independent manner. Currents were induced in GH3 cells, voltage-clamped to −80 mV, by 50-ms voltage steps to 0 mV at a stimulation frequency of 0.2 Hz. (A) Sample traces of I_{Ba} recorded before, during and after application of 1 μM CSTX-1. (B) Plot of current density (pA/pF) from the experiment shown in (A). (C) Time course of inhibition: I_{Ba} recorded before (50 s) and after addition of 1 μM CSTX-1. I_{Ba} recorded in the presence of the toxin were normalised to control I_{Ba}. The rate of inhibition is described by a single exponential function with a time constant (τ_{on}) of 3.1 s. Data represent the mean of five independent experiments. (D) Current–voltage curves for I_{Ba} elicited by 50-ms voltage steps from a holding potential of −80 mV to a series of depolarised potentials under control conditions (open circles) and in the presence of 1 μM CSTX-1 (closed circles). Data represent the mean of three independent experiments. (E) Evaluation of current inhibition at various depolarised potentials from the current–voltage relation shown in (D).

very rapid ($n = 5$, Fig. 5C). CSTX-1 caused an inhibition of I_{Ba} that, at the holding potential ($V_h = -80$ mV), was independent of the test potential ($n = 3$, Fig. 5D, E). To investigate the potency of CSTX-1 we tested the blocking effect at concentrations between 30 and 1000 nM. Inhibition was allowed to fully develop and amplitudes of inhibited currents were determined 30–60 s after toxin application. Fig. 6A shows representative superimposed current traces obtained in the absence (control) and presence of 30 nM and 300 nM CSTX-1. The concentration–response graph determined from these experiments shows that CSTX-1 inhibits I_{Ba} in GH3 cells in a concentration-dependent manner ($n = 5$ for each concentration) (Fig. 6B). At the highest toxin concentration tested, the inhibition of I_{Ba} amounted to 91.5 ± 3.3% ($n = 5$). The concentration–response data were fitted to a Langmuir isotherm, assuming a single-site inhibition model, and the parameters B_{max} and IC$_{50}$ were estimated using Eq. (1) (see Section 2). B_{max} was constrained to a maximum of 100% inhibition, and the best fit was obtained with an IC$_{50}$ value of 263 nM (continuous line on Fig. 6B, $r^2 = 0.915$). Little alteration occurred when B_{max} was constrained to 95%, the typical percentage of nicardipine-sensitive I_{Ba} (IC$_{50} = 233$ nM, $r^2 = 0.900$) or when the Hill coefficient (n) was treated as a variable (IC$_{50} = 265$ nM, $n = 1.09$, $r^2 = 0.918$). The data suggest that CSTX-1 can completely inhibit L-type Ca$_v$ channels. We performed similar experiments on GH4 cells, a clonal isolate of GH3, because these cells lack Na$_v$ channels and, in the presence of K$_v$ channel blockers, depolarising voltage steps evoke only inward currents via Ca$_v$ channels. In this cell line, I_{Ba}

were also inhibited by CSTX-1 in a fully reversible (control current levels were restored within at least 30 s after toxin removal, data not shown) and concentration-dependent manner (Fig. 7A). Here, the apparent affinity of the toxin was considerably higher than in GH3 cells. Maximum current inhibition was observed at concentrations below 100 nM, because 30 and 100 nM CSTX-1 blocked the same percentage of total I_{Ba} (namely 80.0 ± 5.1%, and 76.7 ± 9.0%, respectively). This is illustrated in the concentration–response curve shown in Fig. 7B ($n = 3–5$ for each concentration) and in the sample traces in Fig. 7C and D. The concentration–response data in Fig. 7B could be best fitted ($r^2 = 0.989$) by employing a two-site binding model using Eq. (2) (see Section 2). With this fit, two plateaus with $B_{max1} = 34.2\%$ and $B_{max2} = 45.2\%$ with corresponding IC$_{50}$ values of IC$_{50(1)} = 0.03$ pM and IC$_{50(2)} = 393$ pM were determined. To confirm that I_{Ba} was carried by L-type Ca$_v$ channels in the GH4 cells we performed experiments using the dihydropyridine Ca$_v$ channel antagonist nitrendipine. A concentration–response curve for the current block by nitrendipine was established to determine the contribution of the L-type Ca^{2+} current to I_{Ba} at a saturating concentration of the dihydropyridine. These experiments revealed an IC$_{50}$ for nitrendipine of 267 nM and showed that on average 73.9 ± 6.1% ($n = 5–9$) of I_{Ba} in GH4 cells are carried via L-type Ca$_v$ channels (Fig. 8). These data also indicate clonal variation between GH3 and GH4 cells, since in the former cell line we observed up to a 95% contribution of the dihydropyridine-sensitive channel subtype to whole cell Ca^{2+} currents (see above).
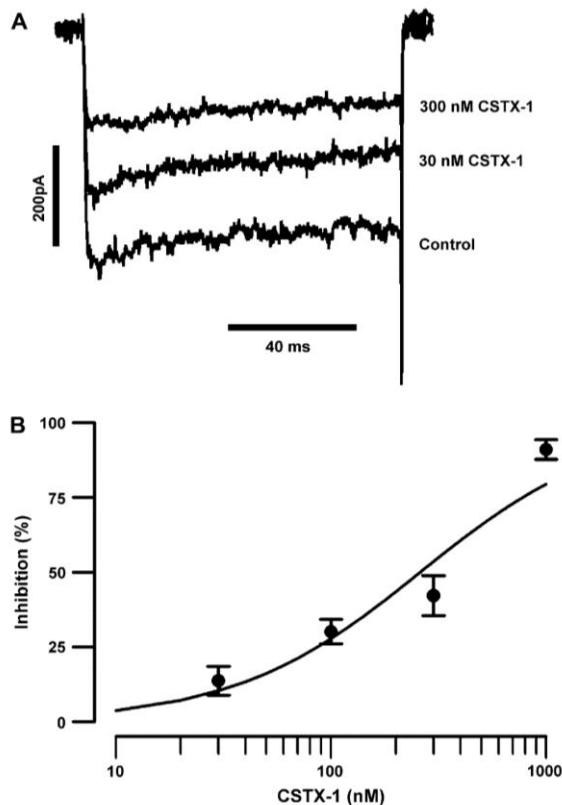
Fig. 6. CSTX-1 inhibits Ba^{2+} currents in GH3 cells in a concentration-dependent manner. (A) Representative superimposed I_{Ba} traces obtained in the absence (control) and presence of 30 nM and 300 nM CSTX-1. (B) Concentration−response relationship for the inhibition of I_{Ba} by CSTX-1.

3.4. CSTX-1 does not affect T-type and muscle L-type Ca_v channels

Having identified L-type Ca_v channels as a high affinity target of CSTX-1, we aimed to further address the subtype selectivity of this toxin. Because 100 nM CSTX-1 induced a saturating effect on I_{Ba} in GH4 cells and caused considerable inhibition in GH3 cells, we used this concentration to test for a specific effect of the spider toxin on other types of Ca_v channels. Since the effect of CSTX-1 on L-type Ca_v channels in GH3/GH4 cells was rapid, we evaluated current amplitudes after a 60 s toxin application period, a duration during which maximum inhibition had always been reached in the experiments on GH3 and GH4 cells.

Dihydropyridine-insensitive I_{Ba} in SCG neurons were not affected by CSTX-1. While this current was suggested to flow via N-, R- and P/Q-type Ca_v channels (Lin et al., 1996), other types of Ca_v channels are not present in this neuronal cell type and thus need to be investigated separately in other preparations. We used dorsal root ganglion (DRG) neurons to test CSTX-1 on T-type Ca_v channels. Currents carried via these channels are characterized by their transient nature,

low-voltage-activation (LVA channels) and by pronounced steady-state inactivation at depolarised potentials. When TTX-resistant $I_{Na(v)}$ were eliminated by replacement of sodium chloride with choline chloride in the bathing solution, a population of Ca_v channel currents that fitted these criteria were evoked in DRG neurons by voltage steps from a holding potential of -100 mV to a range of potentials between -55 mV and -25 mV. Voltage steps to more depolarised potentials also evoked long-lasting HVA Ca_v channel currents (Fig. 9A, B and data not shown). We chose -40 mV as a suitable test potential to study the effect of CSTX-1 on isolated T-type Ca_v channel currents, because at this potential LVA currents appear to be maximally activated and minimally contaminated by HVA Ca_v channel currents. Following application of 100 nM CSTX-1, T-type Ca_v channel current amplitudes remained at $100.6 \pm 10.0\%$ ($n = 14$, Fig. 9C). Because CSTX-1 inhibited M-LVA Ca_v channel currents in DUM neurons with comparably low affinity (IC_{50} 282 nM, see Section 3.1) we also tested 1 μM CSTX-1 on the rat LVA Ca_v channel currents: however, T-type Ca_v channel current amplitudes still remained unaffected and current amplitudes amounted to $96.1 \pm 13.6\%$ of control ($n = 7$, data not shown).

The data therefore demonstrate that CSTX-1 blocks vertebrate ion channels belonging to the L-type family of Ca_v channels, whereas channels of the N-, R- and T-type families appear to be insensitive to CSTX-1. To test for subtype-selectivity within the L-type family of Ca_v channels, we also addressed the question of whether Ca_v channels in skeletal muscle cells, which belong to the $Ca_v 1.1$ subtype of the L-type Ca_v channel family (Catterall et al., 2003), could be inhibited by CSTX-1. We evoked I_{Ba} in C2C12 myoballs, using voltage steps to $+20$ mV from a holding potential of -80 mV. In these muscle cells, I_{Ba} remained largely unaltered by 100 nM CSTX-1 with current amplitudes only decreased to $94.2 \pm 0.6\%$ of control ($n = 3$). The overlay of current traces obtained before and after toxin application revealed that neither current kinetics nor the amplitude is significantly affected by 100 nM CSTX-1 (Fig. 9D).

3.5. CSTX-1 does not affect potassium and sodium currents

To determine whether CSTX-1 affects ionic currents other than those flowing via Ca_v channels, $I_{K(v)}$ were evoked in GH4 cells by 150-ms voltage steps from a V_h of -80 mV to $+120$ mV. Application of 20 mM TEA significantly reduced these outward currents. CSTX-1 did not alter the TEA-sensitive outward $I_{K(v)}$. With 100 nM CSTX-1 outward currents remained at $99.1 \pm 2.5\%$ (peak) and $99.4 \pm 3.4\%$ (at the end of the 150-ms voltage step, Fig. 10A, $n = 5$). For the investigation of $I_{Na(v)}$ we used primary cultures of SCG neurons. Sodium currents were evoked by 30-ms voltage steps from a holding potential of -80 mV to -10 mV. In the presence of 100 nM CSTX-1 $I_{Na(v)}$ remained largely unaltered with peak currents measuring $105.5 \pm 8.6\%$ of control ($n = 5$). These currents were, however, sensitive to TTX, which produced a complete block at a concentration of 0.5 μM

162
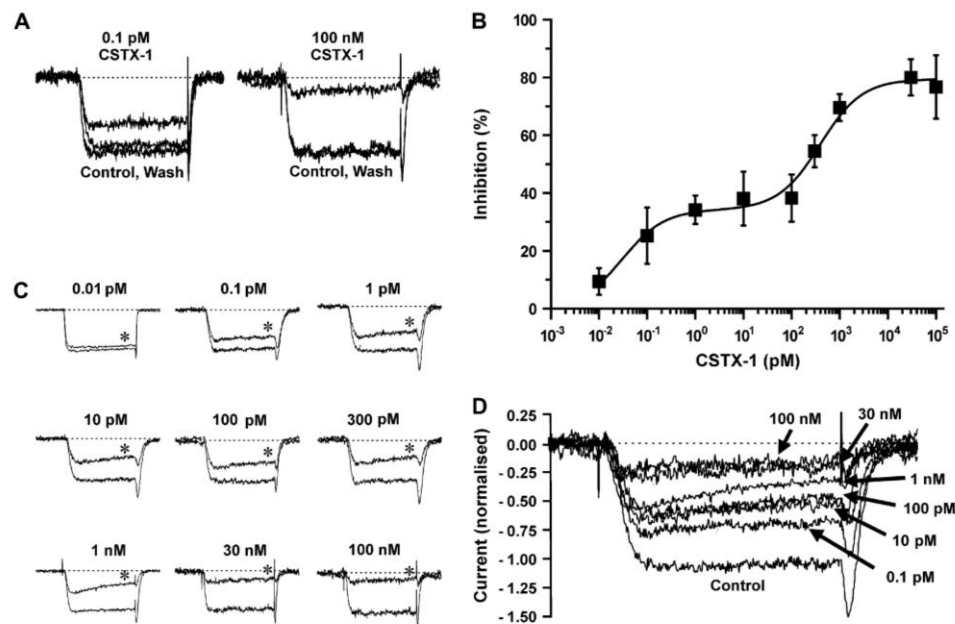
Fig. 7. CSTX-1 blocks Ba^{2+} currents in GH4 cells in a concentration-dependent and reversible manner. (A) Ba^{2+} currents activated by 30-ms voltage steps from a holding potential of −80 mV to 0 mV in the absence (control), presence of the indicated concentration of CSTX-1 and after washout of the toxin (wash). (B) Concentration−response curve for the inhibition of I_{Ba} by CSTX-1. The curve was fitted to the data using a two-site binding model (see Eq. (2) in Section 2). (C) Ba^{2+} currents evoked by 30-ms voltage steps as in (A) in the absence, and presence (*), of the indicated concentration of CSTX-1. (D) Superimposed traces of I_{Ba} evoked as in (A) in the absence (control) or the presence of the indicated concentrations of CSTX-1. All currents are shown normalised to the current obtained under control conditions.

(Fig. 10B). Additionally, we tested $I_{Na(v)}$ in GH3 cells for CSTX-1 sensitivity, but again observed no alterations of the currents upon toxin application (data not shown).

4. Discussion

CSTX-1 is the most important component of *C. salei* venom in terms of relative abundance and toxicity and therefore is likely to contribute significantly to the overall toxicity of the whole venom (Kuhn-Nentwig et al., 2004). The inhibitor cystine-knot structural motif identified for CSTX-1 indicated that this toxin may act as a modulator of voltage-gated ion channels. Moreover, the partial sequence homology with ω-toxins from *Phoneutria nigriventer* venom (another South American species also belonging to the Ctenidae family), namely ω-phonetoxin IIA and ω-PnTx3-6 (Cassola et al., 1998; Vieira et al., 2005) suggested that CSTX-1 may interact with Ca_v channels. This prompted us to investigate whether CSTX-1 toxicity may be caused by its putative action as an ion channel modulator. Using the whole-cell configuration of the patch-clamp technique in cockroach and a variety of rat neurons, we studied the effect of CSTX-1 on currents flowing through various voltage-gated ion channels.

In cockroach neurons, CSTX-1 inhibited Ba^{2+} currents evoked at −30 mV as well as +30 mV with similar potency. This indicates that both M-LVA and HVA Ca_v channels are blocked by this toxin in insects. Many spider toxins have

evolved as effective blockers of Ca_v channels expressed in prey animals. Considering the differences between insect and mammalian Ca_v channels (Wicher and Penzlin, 1997, and see below), it is not surprising that several of these spider toxins, namely the ω-atracotoxin-1 and 2 families, potently block Ca^{2+} currents in insects, but are ineffective on their mammalian counterpart (Wang et al., 1999, 2001; Tedford et al., 2004b). This phyla selectivity identifies several spider toxins as suitable lead compounds for the development of insecticides (Tedford et al., 2004a). On the other hand some spiders, for example *Agelenopsis aperta* (Adams, 2004), produce channel blockers that show potent actions in mammals, although animals from this phylum rarely contribute to the spider's prey. In particular, this has been observed in binding and electrophysiological experiments using mammalian vs. insect neurons with the δ-atracotoxin-1 family of Na_v channel modulators from Australian funnel-web spiders (Nicholson et al., 2004). Such toxins cannot be used as biopesticides but may become useful as molecular research tools in cell biology or as leads for drug development, with their therapeutic potential being dependent on ion channel subtype selectivity.

CSTX-1 appears to fall into the latter group of spider toxins, because it not only inhibits Ca_v channel currents of cockroach neurons but also exerted the same effect on rat neurons. However, while in the insect preparation both M-LVA and HVA Ca_v channels were affected, CSTX-1 only inhibited L-type HVA Ca_v channel currents in neurons of the rat, leaving

163
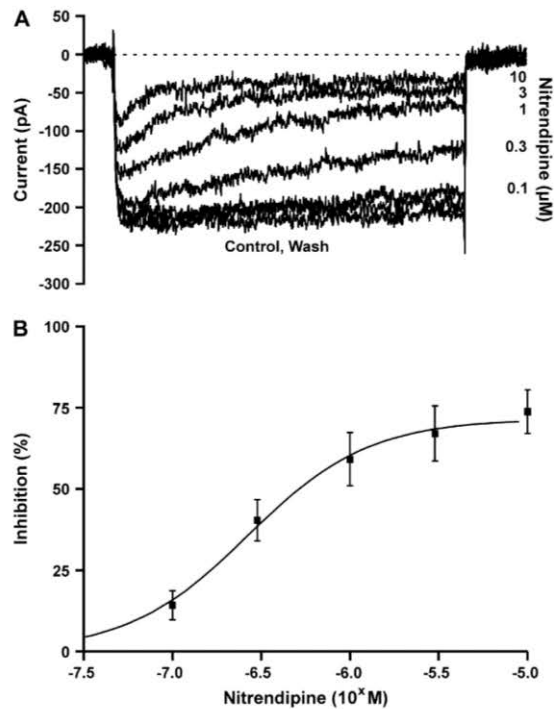
Fig. 8. Ba^{2+} currents in GH4 cells are via L-type Ca$_v$ channels. (A) Ba^{2+} currents induced in GH4 cells by 100-ms voltage steps from a holding potential of −80 mV to 0 mV in the absence (control) and presence of 0.1−10 μM nitrendipine, as well as after washout of the dihydropyridine (wash). (B) Concentration−response curve for the inhibition of I_{Ba} by nitrendipine derived from experiments ($n = 5$−9 for each concentration) carried out under the same conditions as shown in panel (A).

all other voltage-gated sodium, potassium and non-L-type Ca$_v$ channel currents tested unaffected. Therefore we attempted to identify the molecular target of this toxin enabling it to block Ca$_v$ channels in both invertebrates and vertebrates. To examine this issue we need to reconsider the currents that were blocked by CSTX-1. In SCG neurons, various Ca$_v$ channel subtypes (L-, N-, and R-type) contribute to total Ca^{2+} currents (Lin et al., 1996). Several studies have shown that while N-type Ca^{2+} currents predominate, L-type Ca^{2+} currents contribute by up to 30% of the total current (Barrett and Rittenhouse, 2000; Liu et al., 2001; Martinez-Pinna et al., 2002). We found similar contributions of these Ca$_v$ channel subtypes to I_{Ba} using the N-type blocker ω-conotoxin GVIA and the L-type antagonist nitrendipine. CSTX-1 inhibited I_{Ba} in SCG neurons in a fully reversible manner. The lack of additivity of CSTX-1 and nitrendipine indicates that inhibition of I_{Ba} is due to a blocking effect of CSTX-1 on L-type Ca$_v$ channels. Nevertheless, the contribution of L-type I_{Ba} to total macroscopic I_{Ba} was variable (15−40%) among different SCG neurons. Therefore, we employed GH3/GH4 cells to further characterize the actions of CSTX-1 on Ca$_v$ channels because these pituitary cell lines have been previously reported to exhibit a high proportion of L-type Ca$_v$ channels (Leão et al., 2000). Experiments performed in this study revealed that, on average, 95% of HVA Ca$_v$ channel currents flow via the dihydropyridine-sensitive L-type Ca$_v$ channels in GH3 cells. Barium currents in GH3 cells were inhibited by CSTX-1 in a concentration-dependent and entirely reversible manner, with an IC$_{50}$ of 260 nM and an inhibition of 92% ± 3% at the highest toxin concentration tested (1 μM). In GH4 cells (a clonal isolate of GH3 cells) a saturating effect of CSTX-1 on I_{Ba} was obtained with concentrations between 30 and 100 nM, which blocked 80% and 77% of total I_{Ba},
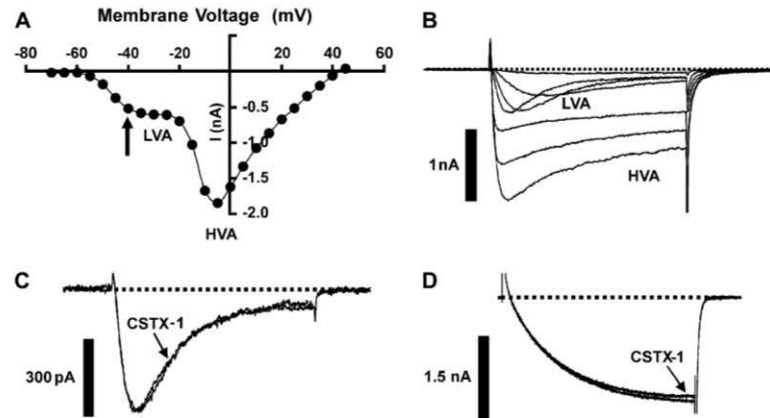
Fig. 9. CSTX-1 neither inhibits T-type nor skeletal muscle L-type Ca$_v$ channels. (A) Current−voltage relation from a DRG neuron of peak Ca$_v$ channel currents evoked by 100-ms voltage steps from a holding potential of −100 mV to a range of potentials between −70 mV and +45 mV. (B) Superimposed currents from the current−voltage relation shown in (A) recorded at −55 mV, −45 mV, −35 mV, −25 mV and at −5 mV, +5 mV as well as +15 mV. (LVA) and (HVA) in (A) and (B) denote transient LVA and sustained HVA I_{Ba}, respectively. The arrow in (A) indicates the test potential at which CSTX-1 was studied on LVA (T-type) Ca$_v$ channel currents. (C) Superimposition of T-type I_{Ba} elicited in DRG neurons from a holding potential of −100 mV by 100-ms voltage steps to −40 mV before, and 60 s after, application of 100 nM CSTX-1, as indicated. (D) Superimposed I_{Ba} elicited in C2C12 myoballs from a holding potential of −80 mV by 100-ms voltage steps to +20 mV before and 60 s after application of 100 nM CSTX-1. Note that the fast current transients that occur at the beginning and at the end of the voltage pulse are shown truncated.

164
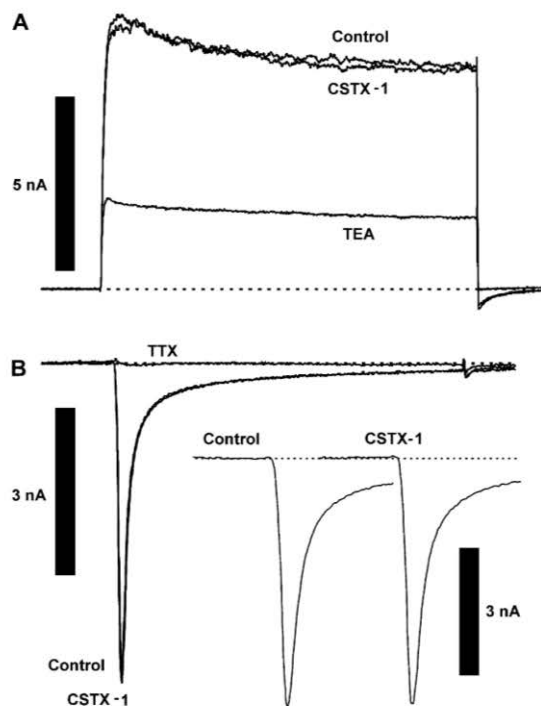
Fig. 10. CSTX-1 does not modulate outward potassium or inward sodium currents. (A) Outward $I_{K(V)}$ were evoked in GH4 cells by 150-ms voltage steps from a holding potential of −80 mV to +120 mV. The traces show currents recorded before (control) and after addition of 100 nM CSTX-1, as well as in the presence of 20 mM TEA. (B) Inward $I_{Na(V)}$ were evoked in SCG neurons by 30-ms voltage steps to −10 mV from a holding potential of −80 mV. The superimposed traces show currents recorded before (control), and after addition, of 100 nM CSTX-1, as well as after the addition of 0.5 μM TTX. The total overlap of the current trace recorded in the presence of CSTX-1 with the control current trace illustrates that neither amplitude nor inactivation kinetics are affected by the toxin. For clarity, parts of the control current and the current recorded during CSTX-1 application are also shown separately (shifted by 5 ms) and on an expanded time-scale (including the first 5 ms of the evoked current).

respectively. Using the dihydropyridine nitrendipine, we determined that a similar percentage of total I_{Ba} flows via L-type Ca_v channels in this cell line. Therefore, CSTX-1 appears capable of blocking up to 100% of this Ca_v channel subtype in GH3 and GH4 cells and can be considered as an effective antagonist of L-type Ca_v channels. The concentration–response curve established with GH4 cells appeared to be biphasic. The data could be best fitted using a two-site binding model yielding two IC_{50} values differing by ∼10,000-fold. This indicates that two high affinity targets for CSTX-1 are present in GH4 L-type Ca_v channels. The concentration–response data indicate that L-type Ca_v channels in GH3 cells have considerably lower affinity than corresponding channels in GH4 cells. The variation in affinities suggests that several different subtypes of L-type Ca_v channels may be affected by CSTX-1.

Native Ca_v channels are heteromultimers of a pore-forming $α_1$-subunit and the auxiliary $α_2δ$, $β$ and, in some tissues, $γ$

subunits. These are encoded by four genes for β-subunits ($β_1$ through $β_4$), four genes for the $α_2δ$ complex ($α_2δ$-1 through $α_2δ$-4), and eight genes for the γ-subunits (Doering and Zamponi, 2003). Available RT-PCR and electrophysiology data on GH3 cells suggest that L-type $I_{Ca(v)}$ in this cell line are mediated via the $α_1$-subunit of $Ca_v1.2$ ($α_{1C}$) and $Ca_v1.3$ ($α_{1D}$), with a predominance of the $Ca_v1.3$ subtype that is expressed as several splice variants (Safa et al., 2001). Considering this, the different L-type Ca_v channel targets suggested by the variation of CSTX-1 affinity in GH4 and GH3 cells may correspond to (i) different $α_1$-subunits, e.g. $Ca_v1.2$ and $Ca_v1.3$, (ii) splice variants of $Ca_v1.3$, or (iii) the presence of different isoforms of the various auxiliary subunits in the Ca_v channel heteromultimer, because the subunit composition has been found to significantly affect the interaction with ligands (Martin et al., 2002; Gurnett et al., 1997; Felix et al., 1997; Mould et al., 2004; Helton et al., 2002). The biphasic nature of the concentration–response curve obtained in GH4 cells may be caused by similar variations in channel subunits forming the Ca_v channel heteromer.

Considering the published channel expression data for GH3 cells, CSTX-1 appears to target vertebrate $Ca_v1.2$ and $Ca_v1.3$ channels. Our experiments on Ca_v channels in skeletal muscle cells suggest that this toxin, at least at submicromolar concentrations, does not inhibit $Ca_v1.1$ channels, which argues for subtype-selectivity within the L-type family of Ca_v channels.

In contrast to the apparent target-selectivity of CSTX-1 in rat neurons, the similar degree of current block at −30 mV (M-LVA currents dominating) and +30 mV (HVA currents dominating) in DUM neurons indicates that the molecular target of CSTX-1 may be common to both M-LVA and HVA Ca_v channels in insects. The conclusion that M-LVA and HVA calcium currents were carried by different calcium channel populations was drawn based on pharmacological differences, such as sensitivity to cone snail and spider toxins (Wicher and Penzlin, 1997). Importantly, inhibition by these toxins often occurs with much slower kinetics than in vertebrate preparations (Wicher and Penzlin, 1997). It should be noted that relatively slow association and dissociation kinetics of CSTX-1 on insect neurons as compared to rat neurons were also observed in this study as evidenced by a $τ_{on}$ of 33.1 s for insect DUM neurons vs. a $τ_{on}$ value of 3.1 s for GH3 cells. These observations indicate that Ca_v channels in cockroach neurons are only distantly related to vertebrate HVA Ca_v channels. In support of this view, antibodies directed against N- and P/Q-type Ca_v channels failed to immunostain membranes of cockroach neurons, although specific peptide toxin blockers of N- and P/Q-type channels were found capable of inhibiting $I_{Ca(v)}$ recorded from neurons of this arthropod (Wicher et al., 2001). With regard to L-type channels, Ca_v channel currents of DUM neurons were reported to show sensitivity to both phenylalkylamines and benzylalkylamines but, unlike vertebrates, not dihydropyridines such as nifedipine (Wicher and Penzlin, 1997). On the other hand, in *Drosophila* four genes have been reported to encode for the $α_1$-subunits of Ca_v channels based on homology to their mammalian counterparts. *Dmca1A* encodes for N-type Ca_v channels, *Dmca1D* for

L-type, *Dmα₁G* for T-type while *Dmα₁U* is homologous to two Ca$_v$ channel genes of *C. elegans* (Littleton and Ganetzky, 2000). *Dmca*1D is expressed in *Drosophila* muscle and throughout the nervous system, where alternative splicing causes substantial channel heterogeneity (Zheng et al., 1995; Ren et al., 1998). This gene is considered a candidate for encoding the phenylalkylamine-sensitive, dihydropyridine-insensitive Ca$_v$ channel in *Drosophila* brain membranes (Zheng et al., 1995). Moreover, the Dmca1D Ca$_v$ channel is thought to carry the dihydropyridine- and phenylalkylamine-sensitive Ca^{2+} current underlying action potentials in *Drosophila* muscle cells (Littleton and Ganetzky, 2000). In support of this suggestion, mutations in *Dmca*1D cause defects in muscle Ca^{2+} currents (Eberl et al., 1998). Thus, *Dmca*1D provides a perfect target for a spider toxin, since its blockade would cause muscular paralysis. The 78% sequence similarity between Dmca1D and rat brain Ca$_v$1.3 (α$_{1D}$) and the observation that *Drosophila* muscle HVA Ca^{2+} currents are sensitive to both phenylalkylamines and dihydropyridines (Gielow et al., 1995; Zheng et al., 1995; Morales et al., 1999) indicate that *Drosophila* skeletal muscle Ca$_v$ channels strongly resemble vertebrate L-type Ca$_v$ channels. A similar situation may hold true for other insect species, because binding sites for both phenylalkylamines and dihydropyridines were identified in *Periplaneta* muscle cells but not in the nervous system, where only phenylalkylamines binding sites were found (Skeer and Sattelle, 1993). We therefore suggest that CSTX-1 has evolved as a blocker of muscle 'L-type-like' Ca$_v$ channels in insects to assist the spider in capturing insect prey. Similarities between this channel and certain mammalian L-type channels of the Ca$_v$1.3 subfamily may explain the toxicity of CSTX-1 in rodent species. In support of this hypothesis, GH3 and GH4 cells preferentially express Ca$_v$1.3 α$_1$-subunits, and dihydropyridine-sensitive $I_{Ca(v)}$ in SCG neurons are mediated by Ca$_v$1.3, rather than Ca$_v$1.2, α$_1$-subunits (Lin et al., 1996). However, the degree of homology between L-type-like insect Ca$_v$ channels and mammalian Ca$_v$ channels of the Ca$_v$1.3 family varies among insect species. Using the ClustalW alignment program (European Informatics Institute) we found sequence identities of 47−66% between rodent Ca$_v$1.3 α$_1$-subunits and α$_1$-subunits of dipteran insects. This diversity may explain the differences in the susceptibility of various insect species to *C. salei* venom described previously (Kuhn-Nentwig et al., 1998). Flies, such as *Drosophila* and *Protophormia* spp. are the most sensitive arthropod species to *C. salei* venom (LD$_{50}$ of <0.02 nl/mg), whereas the LD$_{50}$ of *C. salei* venom in *P. americana* was 10 nl/mg (Wullschleger and Nentwig, 2002) some 1000-fold less than in mice. This is borne out by the ~1000-fold reduction in IC$_{50}$ values for CSTX-1 on rat GH4 cells compared to *P. americana* DUM neurons.

In conclusion, we postulate that a Ca$_v$ channel heteromultimer containing an L-type pore-forming α$_1$-subunit is the most probable candidate for the molecular target of CSTX-1, especially given the potency in GH4 cells. Further experiments using heterologous expression of different combinations of L-type α$_1$- and auxiliary Ca$_v$ channel subunits will be needed to unambiguously identify the high affinity molecular target of CSTX-1. Moreover, CSTX-1 appears to discriminate between channel subtypes within the L-type family of Ca$_v$ channels in terms of potency of channel block. Other voltage-gated ion channels appear to be insensitive to CSTX-1, including K$_v$ and Na$_v$ channels as well as N-type and P/Q type Ca$_v$ channels, which are likely to be responsible for the non-L-type I_{Ba} in GH3/GH4 cells (Safa et al., 2001). Therefore, our findings provide evidence that CSTX-1 may become a useful molecular tool that allows dissection of the functional role of various L-type Ca$_v$ channel subtypes in cell biology.

References

Adams, M.E., 2004. Agatoxins: ion channel specific toxins from the American funnel web spider, *Agelenopsis aperta*. Toxicon 43, 509−525.

Bailey, P., Wilce, J.A., 2001. Venom as a source of useful biologically active molecules. Emerg. Med. Australas. 13, 28−36.

Barrett, C.F., Rittenhouse, A.R., 2000. Modulation of N-type calcium channel activity by G-proteins and protein kinase C. J. Gen. Physiol. 115, 277−286.

Bogin, O., 2005. Venom peptides and their mimetics as potential drugs. Modulator 19, 14−20.

Bourinet, E., Mangoni, M.E., Nargeot, J., 2004. Dissecting the functional role of different isoforms of the L-type Ca^{2+} channel. J. Clin. Invest. 113, 1382−1384.

Cassola, A.C., Jaffe, H., Fales, H.M., Castro Afeche, S., Magnoli, F., Cipolla-Neto, J., 1998. ω-Phonetoxin-IIA: a calcium channel blocker from the spider *Phoneutria nigriventer*. Pflügers Archiv (Eur. J. Physiol.) 436, 545−552.

Catterall, W.A., Striessnig, J., Snutch, T.P., Perez-Reyes, E., 2003. International Union of Pharmacology. XL. Compendium of voltage-gated ion channels: calcium channels. Pharmacol. Rev. 55, 579−581.

Doering, C.J., Zamponi, G.W., 2003. Molecular pharmacology of high voltage-activated calcium channels. J. Bioenerg. Biomembr. 35, 491−505.

Eberl, D.F., Ren, D., Feng, G., Lorenz, L.J., Van Vactor, D., Hall, L.M., 1998. Genetic and developmental characterization of Dmca1D, a calcium channel alpha1 subunit gene in *Drosophila melanogaster*. Genetics 148, 1159−1169.

Felix, R., Gurnett, C.A., De Waard, M., Campbell, K.P., 1997. Dissection of functional domains of the voltage-dependent Ca^{2+} channel α$_2$δ subunit. J. Neurosci. 17, 6884−6891.

Gielow, M.L., Gu, G.G., Singh, S., 1995. Resolution and pharmacological analysis of the voltage-dependent calcium channels of *Drosophila* larval muscles. J. Neurosci. 15, 6085−6093.

Glassmeier, G., Hauber, M., Wulfsen, I., Weinsberg, F., Bauer, C.K., Schwarz, J.R., 2001. Ca^{2+} channels in clonal rat anterior pituitary cells (GH3/B6). Pflügers Archiv (Eur. J. Physiol.) 442, 577−587.

Grolleau, F., Lapied, B., 1996. Two distinct low-voltage-activated Ca^{2+} currents contribute to the pacemaker mechanism in cockroach dorsal unpaired median neurons. J. Neurophysiol. 76, 963−976.

Gurnett, C.A., Felix, R., Campbell, K.P., 1997. Extracellular interaction of the voltage-dependent Ca^{2+} channel $\alpha_2\delta$ and α_1 subunits. J. Biol. Chem. 272, 18508–18512.

Harvey, A.L., 2002. Toxins 'R' Us: more pharmacological tools from nature's superstore. Trends Pharmacol. Sci. 23, 201–203.

Helton, T.D., Kojetin, D.J., Cavanagh, J., Horne, W.A., 2002. Alternative splicing of a β_4 subunit proline-rich motif regulates voltage-dependent gating and toxin block of Ca$_v$2.1 Ca^{2+} channels. J. Neurosci. 22, 9331–9339.

Kepplinger, K.J., Forstner, G., Kahr, H., Leitner, K., Pammer, P., Groschner, K., Soldatov, N.M., Romanin, C., 2000. Molecular determinant for run-down of L-type Ca^{2+} channels localized in the carboxyl terminus of the α_{1C} subunit. J. Physiol. 529, 119–130.

Kubista, H., Mafra, R.A., Chong, Y., Nicholson, G.M., Beirão, P.S., Cruz, J.S., Boehm, S., Nentwig, W., Kuhn-Nentwig, L., 2006. CSTX-1, a neurotoxin from the venom of the hunting spider *Cupiennius salei*, is a selective blocker of L-type calcium channels in rat neurons. FENS Abstr. 3, A084.16.

Kuhn-Nentwig, L., Schaller, J., Nentwig, W., 1994. Purification of toxic peptides and the amino acid sequence of CSTX-1 from the multicomponent venom of *Cupiennius salei* (Araneae: Ctenidae). Toxicon 32, 287–302.

Kuhn-Nentwig, L., Bücheler, A., Studer, A., Nentwig, W., 1998. Taurine and histamine: low molecular compounds in prey hemolymph increase the killing power of spider venom. Naturwissenschaften 85, 136–138.

Kuhn-Nentwig, L., Müller, J., Schaller, J., Walz, A., Dathe, M., Nentwig, W., 2002. Cupiennin 1, a new family of highly basic antimicrobial peptides in the venom of the spider *Cupiennius salei* (Ctenidae). J. Biol. Chem. 277, 11208–11216.

Kuhn-Nentwig, L., Schaller, J., Nentwig, W., 2004. Biochemistry, toxicology and ecology of the venom of the spider *Cupiennius salei* (Ctenidae). Toxicon 43, 543–553.

Leão, R.M., Cruz, J.S., Diniz, C.R., Cordeiro, M.N., Beirão, P.S.L., 2000. Inhibition of neuronal high-voltage activated calcium channels by the ω-*Phoneutria nigriventer* Tx3-3 peptide toxin. Neuropharmacology 39, 1756–1767.

Lechner, S.G., Mayer, M., Boehm, S., 2003. Activation of M1 muscarinic receptors triggers transmitter release from rat sympathetic neurons through an inhibition of M-type K$^+$ channels. J. Physiol. 553, 789–802.

Lievano, A., Bolden, A., Horn, R., 1994. Calcium channels in excitable cells: divergent genotypic and phenotypic expression of α_1-subunits. Am. J. Physiol. 267, C411–C424.

Lin, Z., Harris, C., Lipscombe, D., 1996. The molecular identity of Ca channel alpha 1-subunits expressed in rat sympathetic neurons. J. Mol. Neurosci. 7, 257–267.

Littleton, J.T., Ganetzky, B., 2000. Ion channels and synaptic organization: analysis of the *Drosophila* genome. Neuron 26, 35–43.

Liu, L., Barrett, C.F., Rittenhouse, A.R., 2001. Arachidonic acid both inhibits and enhances whole cell calcium currents in rat sympathetic neurons. Am. J. Physiol. Cell Physiol. 280, C1293–C1305.

Martin, D.J., McClelland, D., Herd, M.B., Sutton, K.G., Hall, M.D., Lee, K., Pinnock, R.D., Scott, R.H., 2002. Gabapentin-mediated inhibition of voltage-activated Ca^{2+} channel currents in cultured sensory neurones is dependent on culture conditions and channel subunit expression. Neuropharmacology 42, 353–366.

Martinez-Pinna, J., Lamas, J.A., Gallego, R., 2002. Calcium current components in intact and dissociated adult mouse sympathetic neurons. Brain Res. 951, 227–236.

Morales, M., Ferrus, A., Martinez-Padron, M., 1999. Presynaptic calcium-channel currents in normal and csp mutant *Drosophila* peptidergic terminals. Eur. J. Neurosci. 11, 1818–1826.

Mouhat, S., Jouirou, B., Mosbah, A., De Waard, M., Sabatier, J.-M., 2004. Diversity of folds in animal toxins acting on ion channels. Biochem. J. 378, 717–726.

Mould, J., Yasuda, T., Schroeder, C.I., Beedle, A.M., Doering, C.J., Zamponi, G.W., Adams, D.J., Lewis, R.J., 2004. The $\alpha_2\delta$ auxiliary subunit reduces affinity of ω-conotoxins for recombinant N-type (Ca$_v$2.2) calcium channels. J. Biol. Chem. 279, 34705–34714.

Nicholson, G.M., 2006. Spider venom peptides. In: Kastin, A. (Ed.), The Handbook of Biologically Active Peptides. Elsevier, San Diego, CA, pp. 369–381.

Nicholson, G.M., Little, M.J., Birinyi-Strachan, L.C., 2004. Structure and function of δ-atracotoxins: lethal neurotoxins targeting the voltage-gated sodium channel. Toxicon 43, 587–599.

Norton, R.S., Pallaghy, P.K., 1998. The cystine knot structure of ion channel toxins and related polypeptides. Toxicon 36, 1573–1583.

Pukala, T.L., Doyle, J.R., Llewellyn, L.E., Kuhn-Nentwig, L., Separovic, F., Bowie, J.H., 2007. Cupiennin 1a, an antimicrobial peptide from the venom of the neotropical wandering spider Cupiennius salei, also inhibits the formation of nitric oxide by neuronal nitric oxide synthase. FEBS J 274, 1778–1784.

Ren, D., Xu, H., Eberl, D.F., Chopra, M., Hall, L.M., 1998. A mutation affecting dihydropyridine-sensitive current levels and activation kinetics in *Drosophila* muscle and mammalian heart calcium channels. J. Neurosci. 18, 2335–2341.

Safa, P., Boulter, J., Hales, T.G., 2001. Functional properties of Ca$_v$1.3 (alpha1D) L-type Ca^{2+} channel splice variants expressed by rat brain and neuroendocrine GH3 cells. J. Biol. Chem. 276, 38727–38737.

Sinakevitch, I.G., Geffard, M., Pelhate, M., Lapied, B., 1996. Anatomy and targets of dorsal unpaired median neurones in the terminal abdominal ganglion of the male cockroach *Periplaneta americana* L. J. Comp. Neurol. 367, 147–163.

Skeer, J.M., Sattelle, D.B., 1993. Characterization of phenylalkylamine binding sites in insect (*Periplaneta americana*) nervous system and skeletal muscle membranes. Arch. Insect Biochem. Physiol. 23, 111–124.

Soldatov, N.M., 2003. Ca^{2+} channel moving tail: link between Ca^{2+}-induced inactivation and Ca^{2+} signal transduction. Trends Pharmacol. Sci. 24, 167–171.

Tedford, H.W., Sollod, B.L., Maggio, F., King, G.F., 2004a. Australian funnel-web spiders: master insecticide chemists. Toxicon 43, 601–618.

Tedford, H.W., Gilles, N., Menez, A., Doering, C.J., Zamponi, G.W., King, G.F., 2004b. Scanning mutagenesis of omega-atracotoxin-Hv1a reveals a spatially restricted epitope that confers selective activity against insect calcium channels. J. Biol. Chem. 279, 44133–44140.

Vartian, N., Boehm, S., 2001. P2Y receptor-mediated inhibition of voltage-activated Ca^{2+} currents in PC12 cells. Eur. J. Neurosci. 13, 899–908.

Vieira, L.B., Kushmerick, C., Hildebrand, M.E., Garcia, E., Stea, A., Cordeiro, M.N., Richardson, M., Gomez, M.V., Snutch, T.P., 2005. Inhibition of high voltage-activated calcium channels by spider toxin PnTx3-6. J. Pharmacol. Exp. Ther. 314, 1370–1377.

Wang, X., Smith, R., Fletcher, J.I., Wilson, H., Wood, C.J., Howden, M.E., King, G.F., 1999. Structure-function studies of omega-atracotoxin, a potent antagonist of insect voltage-gated calcium channels. Eur. J. Biochem. 264, 488–494.

Wang, X.H., Connor, M., Wilson, D., Wilson, H.I., Nicholson, G.M., Smith, R., Shaw, D., Mackay, J.P., Alewood, P.F., Christie, M.J., King, G.F., 2001. Discovery and structure of a potent and highly specific blocker of insect calcium channels. J. Biol. Chem. 276, 40306–40312.

Wicher, D., Penzlin, H., 1994. Ca^{2+} currents in cockroach neurones: properties and modulation by neurohormone D. Neuroreport 5, 1023–1026.

Wicher, D., Penzlin, H., 1997. Ca^{2+} currents in central insect neurons: electrophysiological and pharmacological properties. J. Neurophysiol. 77, 186–199.

Wicher, D., Walther, C., Wicher, C., 2001. Non-synaptic ion channels in insects-basic properties of currents and their modulation in neurons and skeletal muscles. Prog. Neurobiol. 64, 431–525.

Wullschleger, B., Nentwig, W., 2002. Influence of venom availability on a spider's prey-choice behaviour. Funct. Ecol. 16, 802–807.

Wullschleger, B., Nentwig, W., Kuhn-Nentwig, L., 2005. Spider venom: enhancement of venom efficacy mediated by different synergistic strategies in *Cupiennius salei*. J. Exp. Biol. 208, 2115–2121.

Zebedin, E., Sandtner, W., Galler, S., Szendroedi, J., Just, H., Todt, H., Hilber, K., 2004. Fiber type conversion alters inactivation of voltage-dependent sodium currents in murine C2C12 skeletal muscle cells. Am. J. Physiol. Cell Physiol. 287, C270–C280.

Zheng, W., Feng, G., Ren, D., Eberl, D.F., Hannan, F., Dubald, M., Hall, L.M., 1995. Cloning and characterization of a calcium channel alpha 1 subunit from *Drosophila melanogaster* with similarity to the rat brain type D isoform. J. Neurosci. 15, 1132–1143.

9   Conclusion

Spider venom is a pharmacopoeia of preoptimised toxins that have evolved over millions of years of natural combinatorial chemistry (Escoubas and King, 2009, Ueberheide et al., 2009, Vetter et al., 2011). Selective pressure has meant that these peptide neurotoxins are highly efficient at killing or paralyzing prey and/or repelling aggressors (Vassilevski et al., 2009). The venom is by and large optimised for arthropod prey, however toxins in spider venom can also be active on vertebrates, with potentially lethal effects.

Australia is home to a number of clinically important Araneae species, most notably the funnel-web (Hexathelidae) spiders, as well as the lesser known mouse spiders (*Missulena* spp.), which are often mistaken for a Sydney funnel-web spider (*Atrax robustus*). According to Isbister (2004), severe envenoming from mouse spider bites is assumed to be rare (2.5%); hence these spiders are unlikely to be a major public concern. However, male *M. bradleyi* venom has been shown to cause similar toxicological effects to funnel-web spider venom *in vitro* (Rash et al., 2000), and has been linked to a medical case of serious envenomation in Australia (Underhill, 1987). For that reason, male *M. bradleyi* venom was further investigated in this project, with the main aim to identify the major neurotoxin responsible for the envenomation syndrome and determine its molecular target. This led to the isolation of the peptide neurotoxin δ-AOTX-Mb1a which exerts its effects by modulating vertebrate Na_v channels. This was not surprising, given that δ-AOTX-Mb1a mimicked the neurotoxicity of δ-HXTX-Hv1a and δ-HXTX-Ar1a in primates (reviewed in Nicholson et al, 2006). The observed effects appears to be the result of presynaptic action on motor nerve terminals to induce neurotransmitter release, which is consistent with reported clinical cases of severe envenomation or *in vitro* studies with whole venom (Underhill, 1987, Rash et al., 2000). Importantly, the neutralisation of toxic effects by *A. robustus* antivenom provides evidence for the cross-reactivity of *A. robustus* antivenom, and its potential effectiveness in clinical cases of systemic envenomation by male *M. bradleyi*.

Peptide toxins in venoms are also being exploited as molecular tools for structure-function studies of ion channels, including delineation of subtypes and their role in disease (Dutertre and Lewis, 2010). This is particularly important for the drug discovery pipeline because voltage-activated ion channels are attractive drug targets for the treatment of neurological or cardiovascular diseases and there is always a need to find new selective antagonists and agonists (Escoubas and Bosmans, 2007, Bulaj, 2008). From this perspective, ω-CNTX-Cs1a from *Cupiennius salei* venom was interesting because it appeared to be a highly selective blocker of L-type (Ca_V1) channels in mammalian neurons, and therefore has the potential to become a useful neurobiological tool, in a similar way to ω-agatoxin-Aa4a (previously ω-aga-IVA), which is the defining pharmacology for vertebrate P/Q-type ($Ca_V2.1$) channels (Bindokas and Adams, 1989, Adams et al., 1990, Adams, 2004). ω-CNTX-Cs1a is also insecticidal, and cross-phylum activity has been observed in the δ-hexatoxin-1 family of Na_V channel peptide toxins from Australian funnel-web spiders (Nicholson et al, 2004), presumably due to similarities in the receptors between invertebrate and vertebrate ion channels. Also of note is that ω-CNTX-Cs1a toxin did not selectively block a particular Ca_V channel component in invertebrates, rather it displayed activity on both M-LVA and HVA type Ca_V channels in cockroach DUM neurons.

Insect voltage-activated calcium channels

One of the main drivers for this thesis was the growing problem of insect resistance which is resulting in an urgent need to develop new insecticides with novel modes of action. Spider venom is an effective and high evolved insecticide cocktail containing disulfide-rich peptide neurotoxins that can be used as lead compounds for new insecticidal agents, and can help identify novel target ion channels for future insecticide design (King et al., 2008a). Therefore the focus of this project was on the isolation and characterisation of insect-selective spider toxins. Firstly, we isolated and characterised novel insecticidal peptide toxins from female *M. bradleyi* (ω-AOTX-Mb1a) and *A. robustus* venom (ω-HXTX-Ar1a). In addition, we also determined the target of ω-HXTX-Hv1a from *Hadronyche versuta* on insect Ca_V channels given that it

had been previously identified as a Ca_V channel blocker (Fletcher et al., 1997) and is considered a prime candidate for development as an innovative „green" pesticide because it is potently insecticidal but non-toxic to humans, and appeared to have a novel mode of action.

ω-HXTX-Hv1a, ω-HXTX-Ar1a and ω-AOTX-Mb1a are promising biopesticide candidates. In vertebrate bioassays, there was a lack of overt toxicity. Acute insect toxicity assays in house crickets showed that ω-AOTX-Mb1a was a very potent insecticidal agent (see table below), and in relation to the ω-HXTX-Hv1 family, which have lethal doses ranging from 84-1384 pmol/g in house crickets (Wang et al., 1999). ω-HXTX-Ar1a was moderately toxic, and fell within the LD_{50} value of other ω-HXTX-Hv1 toxins. A comparison of the IC_{50} values showed a similar order of potency, with the exception of ω-HXTX-Hv1a, which had the lowest M-LVA IC_{50} despite having the highest concentration for HVA Ca_V channels. There were variations in the level of toxicity in house cricket bioassays versus block of Ca_V channels in cockroach neurons for all three toxins. Compared to ω-HXTX-Ar1a, ω-AOTX-Mb1a had a five-fold higher toxicity following injection into crickets and the IC_{50} values for both Ca_V channel types was ca. 1.5-2 times greater. The toxicity of ω-AOTX-Mb1a was more comparable to ω-HXTX-Hv1a, with a two-fold higher toxicity in crickets and block of M-LVA (not HVA) Ca_V channels. Comparing the two ω-HXTX-1 toxins, a three-fold lower toxicity of ω-HXTX-Ar1a in crickets parallels the three-fold reduction in IC_{50} values for block of M-LVA Ca_V channels. Nevertheless, it may also be that the combined block of both M-LVA and HVA Ca_V channels is critical for lethality. In support, M-LVA and HVA currents in cockroach DUM neurons are believed to be mediated by different isoforms of the same cockroach Ca_V2 channel (King et al., 2008). Possible additional reasons for the variations in between the toxins may be related to the bioavailability of the toxins at the target sites.

Toxin	LD_{50} (pmol/g)	IC_{50} (nM)	
		M-LVA Ca_v	HVA Ca_v
ω-HXTX-Hv1a	84 ± 10	279	1080
ω-HXTX-Ar1a	236 ± 28	692	644
ω-AOTX-Mb1a	50 ± 4	397	439

Whole-cell patch clamp analysis showed these toxins blocked M-LVA and HVA Ca_v channels in cockroaches in a voltage-independent and concentration-dependent manner without any alteration in the voltage-dependence of Ca_v channel activation, suggesting that the action of these toxins was to block the channel pore rather than by altering gating or the inactivation/activation kinetics of the channel.

Whole-cell patch clamp analysis showed these toxins blocked M-LVA and HVA Ca_v channels in cockroaches in a voltage-independent and concentration-dependent manner. This occurs without any alteration in the voltage-dependence of Ca_v channel activation, which suggests that the action of these toxins is to block the channel pore rather than by altering gating or the inactivation/activation kinetics of the channel. The observed effects are consistent with those of known pore-blockers such as ω-agatoxin-IIIA (McDonough et al., 2002). By comparison, the gating modifier toxin ω-agatoxin-IVA inhibits Ca_v channels by dramatically shifting the voltage-dependence of Ca_v channel activation to more depolarised potentials (Mintz et al., 1992, McDonough et al., 1997).

This mode of action differs from known insecticidal agents such as DDT, pyrethroids and indoxacarb, a newer type of oxadiazine pesticide developed by DuPont, which primarily target Na_v channels (Dong 2007). Pyrethroids cause prolonged opening of Na_v channels by inhibiting channel deactivation (Narahashi, 1996, Raymond-Delpech et al., 2005), and indoxabarb blocks Na_v channel currents in a state-dependent manner by preferentially binding to the inactivated state of the Na_v channel (see review in Dong 2007).

It was previously speculated that the pharmacological distinctions used to describe vertebrate Ca_V subtypes are not directly applicable to invertebrates (Wicher and Penzlin, 1997, Jeziorski et al., 2000, Grolleau and Lapied, 2000). Using classical pharmacological blockers, we confirmed that classical blockers of vertebrate Ca_V channels including Ni^{2+}, ω-conotoxin-MVIIC and SKF-96365 were unable to pharmacologically separate M-LVA and HVA Ca_V channel components in cockroach DUM neurons. These results provide an explanation as to why there was no activity of these toxins in vertebrate bioassays, and pave the way for insect-selective insecticidal agents.

One of the obstacles to overcome when designing insecticides based on natural peptide toxins is the presence of endogenous proteases in the invertebrate system that has the potential to reduce the bioavailability of the toxin. A possible solution is to form peptide toxins that are more stable under reducing conditions by replacing cysteines with selenocysteines to form diselenide bonds. The results of patch-clamp analysis on a diselenide ω-HXTX-Hv1a mutant indicated that the molecular function was not affected. Although there was a three-fold decrease in oral activity of the diselenide version of the toxin, the modification did not significantly affect the toxicity of the toxin in terms of block of peak barium currents through Ca_V channels. This suggests that the oral bioavailability of the diselenide toxin has decreased compared to the native toxin, but the interaction at the Ca_V channel target site has remained unaffected.

Another approach for overcoming the protease problem is to increase oral bioavailability by creating fusion proteins with GNA (Fitches et al., 2010). Snowdrop lectin (*Galanthus nivalis* agglutinin; GNA) has already been shown to be an effective transport carrier for venom peptide toxins across the insect gut and holds great promise for topical spray treatments and endogenous application in transgenic plants (Pham Trung et al., 2006)(see section 1.5.3.2).

Future directions

The utility of spider venom peptide toxins in the biotechnological and therapeutic sectors are still in its early stages and there are greater than 99% of venom peptides that have yet to be pharmacologically characterised (Saez et al., 2010). Nevertheless it is envisaged that the toxins described in this project may aid the development of environmentally-benign biopesticides. Several approaches have been mentioned previously, including the creation of viral vectors containing toxin genes that target particular insect species (i.e. recombinant baculoviruses) or the design of peptidomimetic molecules based on key insectophore residues of these toxins for delivery as foliar sprays. Given that ω-HXTXs are innately orally active, these toxins may be delivered via transgenic modification of plants. These concepts are being applied by Vestaron Corporation, a US-based biotechnology company that was founded in 2005 to develop a new generation of potent and environmentally-benign insecticides derived from spider venom peptides. Vestaron is currently pursuing toxins that target Ca_V and calcium-activated potassium channel receptors for the rational design of new synthetic insecticidal compounds based on the 3D structure and pharmacophore of these toxins, and therefore the ω-toxins we described could potentially be useful for this venture (http://www.vestaron.com/exploiting-discoveries.html).

10 Bibliography

ADAMS, M. D., CELNIKER, S. E., HOLT, R. A., EVANS, C. A., GOCAYNE, J. D., AMANATIDES, P. G., SCHERER, S. E., LI, P. W., HOSKINS, R. A., GALLE, R. F., GEORGE, R. A., LEWIS, S. E., RICHARDS, S., ASHBURNER, M., HENDERSON, S. N., SUTTON, G. G., WORTMAN, J. R., YANDELL, M. D., ZHANG, Q., CHEN, L. X., BRANDON, R. C., ROGERS, Y. H., BLAZEJ, R. G., CHAMPE, M., PFEIFFER, B. D., WAN, K. H., DOYLE, C., BAXTER, E. G., HELT, G., NELSON, C. R., GABOR, G. L., ABRIL, J. F., AGBAYANI, A., AN, H. J., ANDREWS-PFANNKOCH, C., BALDWIN, D., BALLEW, R. M., BASU, A., BAXENDALE, J., BAYRAKTAROGLU, L., BEASLEY, E. M., BEESON, K. Y., BENOS, P. V., BERMAN, B. P., BHANDARI, D., BOLSHAKOV, S., BORKOVA, D., BOTCHAN, M. R., BOUCK, J., BROKSTEIN, P., BROTTIER, P., BURTIS, K. C., BUSAM, D. A., BUTLER, H., CADIEU, E., CENTER, A., CHANDRA, I., CHERRY, J. M., CAWLEY, S., DAHLKE, C., DAVENPORT, L. B., DAVIES, P., DE PABLOS, B., DELCHER, A., DENG, Z., MAYS, A. D., DEW, I., DIETZ, S. M., DODSON, K., DOUP, L. E., DOWNES, M., DUGAN-ROCHA, S., DUNKOV, B. C., DUNN, P., DURBIN, K. J., EVANGELISTA, C. C., FERRAZ, C., FERRIERA, S., FLEISCHMANN, W., FOSLER, C., GABRIELIAN, A. E., GARG, N. S., GELBART, W. M., GLASSER, K., GLODEK, A., GONG, F., GORRELL, J. H., GU, Z., GUAN, P., HARRIS, M., HARRIS, N. L., HARVEY, D., HEIMAN, T. J., HERNANDEZ, J. R., HOUCK, J., HOSTIN, D., HOUSTON, K. A., HOWLAND, T. J., WEI, M. H., IBEGWAM, C., et al. 2000. The genome sequence of *Drosophila melanogaster*. *Science*, 287**,** 2185-95.

ADAMS, M. E. 2004. Agatoxins: ion channel specific toxins from the American funnel web spider, *Agelenopsis aperta*. *Toxicon*, 43**,** 509-25.

ADAMS, M. E., BINDOKAS, V. P., HASEGAWA, L. & VENEMA, V. J. 1990. ω-Agatoxins: novel calcium channel antagonists of two subtypes from funnel web spider (*Agelenopsis aperta*) venom. *J Biol Chem*, 265**,** 861-7.

ADAMS, M. E., MYERS, R. A., IMPERIAL, J. S. & OLIVERA, B. M. 1993. Toxityping rat brain calcium channels with ω-toxins from spider and cone snail venoms. *Biochemistry*, 32**,** 12566-70.

ADAMS, M. E. & OLIVERA, B. M. 1994. Neurotoxins: overview of an emerging research technology. *Trends Neurosci*, 17**,** 151-5.

ALEWOOD, D., BIRINYI-STRACHAN, L. C., PALLAGHY, P. K., NORTON, R. S., NICHOLSON, G. M. & ALEWOOD, P. F. 2003. Synthesis and characterisation of δ-atracotoxin-Ar1a, the lethal neurotoxin from venom of the Sydney funnel-web spider (*Atrax robustus*). *Biochemistry*, 42**,** 12933-40.

ARMISHAW, C. J., DALY, N. L., NEVIN, S. T., ADAMS, D. J., CRAIK, D. J. & ALEWOOD, P. F. 2006. α-Selenoconotoxins, a new class of potent α7 neuronal nicotinic receptor antagonists. *J Biol Chem*, 281**,** 14136-43.

AROLAS, J. L., AVILES, F. X., CHANG, J. Y. & VENTURA, S. 2006. Folding of small disulfide-rich proteins: clarifying the puzzle. *Trends Biochem Sci,* 31**,** 292-301.

ATKINSON, R. K., HOWDEN, M. E. H., TYLER, M. I. & VONARX, E. J. 1998. *Insecticidal toxins derived from funnel web (Atrax or Hadronyche) spiders*. USA patent application.

ATKINSON, R. K., VONARX, E. J. & HOWDEN, M. E. H. 1996. Effects of whole venom and venom fractions from several Australian spiders, including *Atrax* (*Hadronyche*) species, when injected into insects. *Comp Biochem Phys Part C*, 114**,** 113-7.

BAGLA, P. 2010. India. Hardy cotton-munching pests are latest blow to GM crops. *Science,* 327**,** 1439.

BARRETT, C. B. 2010. Measuring food insecurity. *Science,* 327**,** 825-8.

BATES, S. L., ZHAO, J. Z., ROUSH, R. T. & SHELTON, A. M. 2005. Insect resistance management in GM crops: past, present and future. *Nat Biotechnol,* 23**,** 57-62.

BERGVINSON, D. & GARCIA-LARA, S. 2004. Genetic approaches to reducing losses of stored grain to insects and diseases. *Curr Opin Plant Biol,* 7**,** 480-5.

BINDOKAS, V. P. & ADAMS, M. E. 1989. ω-Aga-I: a presynaptic calcium channel antagonist from venom of the funnel web spider, *Agelenopsis aperta*. *J Neurobiol,* 20**,** 171-88.

BLACK, B. C., BRENNAN, L. A., DIERKS, P. M. & GARD, I. E. 1997. Commercialization of baculoviral insecticides. *In:* MILLER, L. K. (ed.) *The Baculoviruses.* New York: Plenum Press.

BLOOMQUIST, J. R. 1996. Ion channels as targets for insecticides. *Annu Rev Entomol,* 41**,** 163-90.

BLOOMQUIST, J. R. 2003. Mode of action of atracotoxin at central and peripheral synapses of insects. *Invert Neurosci,* 5**,** 45-50.

BONNING , B. C. & HAMMOCK, B. D. 1996. Development of recombinant baculoviruses for insect control. *Annu Rev Entomol,* 41**,** 191-210.

BORDAS, B., KOMIVES, T. & LOPATA, A. 2003. Ligand-based computer-aided pesticide design. A review of applications of the CoMFA and CoMSIA methodologies. *Pest Manag Sci,* 59**,** 393-400.

BRAVO, A., GILL, S. S. & SOBERON, M. 2007. Mode of action of *Bacillus thuringiensis* Cry and Cyt toxins and their potential for insect control. *Toxicon,* 49**,** 423-35.

BROGDON, W. G. & MCALLISTER, J. C. 1998. Insecticide resistance and vector control. *Emerg Infect Dis,* 4**,** 605-13.

BULAJ, G. 2008. Integrating the discovery pipeline for novel compounds targeting ion channels. *Curr Opin Chem Biol,* 12**,** 441-7.

BULAJ, G. & OLIVERA, B. M. 2008. Folding of conotoxins: formation of the native disulfide bridges during chemical synthesis and biosynthesis of *Conus* peptides. *Antioxid Redox Signal,* 10**,** 141-55.

BURDEN, J. P., HAILS, R. S., WINDASS, J. D., SUNER, M. M. & CORY, J. S. 2000. Infectivity, speed of kill, and productivity of a baculovirus expressing the itch mite toxin txp-1 in second and fourth instar larvae of *Trichoplusia ni*. *J Invertebr Pathol,* 75**,** 226-36.

CAPINERA, J. L. 2008. *Encyclopedia of entomology,* Gainesville, Springer.

CARPENTER, S., WILSON, A. & MELLOR, P. S. 2009. Culicoides and the emergence of bluetongue virus in northern Europe. *Trends Microbiol,* 17**,** 172-8.

CARRIERE, Y., ELLERS-KIRK, C., SISTERSON, M., ANTILLA, L., WHITLOW, M., DENNEHY, T. J. & TABASHNIK, B. E. 2003. Long-term regional suppression of pink bollworm by *Bacillus thuringiensis* cotton. *Proc Natl Acad Sci U S A,* 100, 1519-23.

CASIDA, J. E. 2009. Pest toxicology: the primary mechanisms of pesticide action. *Chem Res Toxicol,* 22**,** 609-19.

CASIDA, J. E. & QUISTAD, G. B. 1998. Golden age of insecticide research: past, present, or future? *Annu Rev Entomol,* 43**,** 1-16.

CASSMAN, K. G. 1999. Ecological intensification of cereal production systems: yield potential, soil quality, and precision agriculture. *Proc Natl Acad Sci USA,* 96**,** 5952-9.

CATTERALL, W. A. 2000. Structure and regulation of voltage-gated Ca^{2+} channels. *Annu Rev Cell Dev Biol,* 16**,** 521-55.

CHEJANOVSKY, N., ZILBERBERG, N., RIVKIN, H., ZLOTKIN, E. & GUREVITZ, M. 1995. Functional expression of an α anti-insect scorpion neurotoxin in insect cells and lepidopterous larvae. *FEBS Letters,* 376**,** 181-4.

CHEN, X., SUN, X., ZHIHONG, H., LI, M., O'REILLY, D. R., ZUIDEMA, D. & VLAK, J. M. 2000. Genetic engineering of *Helicoverpa armigera* single-nucleocapsid nucleopolyhedrovirus as an improved pesticide. *J Invertebr Pathol,* 76**,** 140-6.

CHRISTOU, P., CAPELL, T., KOHLI, A., GATEHOUSE, J. A. & GATEHOUSE, A. M. 2006. Recent developments and future prospects in insect pest control in transgenic crops. *Trends Plant Sci,* 11**,** 302-8.

CLARK, R. D. 1976. Structural and functional changes in an identified cricket neuron after separation from the soma. I. Structural changes. *J Comp Neurol,* 170**,** 253-65.

CLYNE, D. 1969. *A guide to Australian spiders.,* Sydney, Thomas Nelson (Aust) Ltd.

CODDINGTON, J. A. & LEVI, H. W. 1991. Systematics and evolutions of spiders (Araneae). *Annu Rev Ecol Syst,* 22**,** 565-92.

COPPING, L. G. & MENN, J. J. 2000. Biopesticides: a review of their action, applications and efficacy. *Pest Manag Sci,* 56**,** 651-76.

CORY, J. S., HIRST, M. L., WILLIAMS, T., HALLS, R. S., GOUSON, D., GREEN, B. M., CURTY, T. M., POSSEE, R. D., CAYLEY, P. J. & BISHOP, D. H. L. 1994. Field trial of a genetically improved baculovirus insecticide. *Nature,* 370**,** 138-40.

CRAIK, D. J., DALY, N. L. & WAINE, C. 2001. The cystine knot motif in toxins and implications for drug design. *Toxicon,* 39**,** 43-60.

DENT, D. 2000. *Insect Pest Management,* Wallingford, CABI.

DOLPHIN, A. C. 2006. A short history of voltage-gated calcium channels. *Br J Pharmacol,* 147 Suppl 1**,** S56-62.

DONG, K. 2007. Insect sodium channels and insecticide resistance. *Invert Neurosci,* 7**,** 17-30.

DOWN, R. E., FITCHES, E. C., WILES, D. P., CORTI, P., BELL, H. A., GATEHOUSE, J. A. & EDWARDS, J. P. 2006. Insecticidal spider venom toxin fused to snowdrop lectin is toxic to the peach-potato aphid, *Myzus persicae* (Hemiptera: Aphididae) and the rice brown

planthopper, *Nilaparvata lugens* (Hemiptera: Delphacidae). *Pest Manag Sci,* 62**,** 77-85.

DOWNES, S., MAHON, R. & OLSEN, K. 2007. Monitoring and adaptive resistance management in Australia for *Bt*-cotton: current status and future challenges. *J Invertebr Pathol,* 95**,** 208-13.

DUKE, S. O., CANTRELL, C. L., MEEPAGALA, K. M., WEDGE, D. E., TABANCA, N. & SCHRADER, K. K. 2010. Natural toxins for use in pest management. *Toxins,* 2**,** 1943-62.

DUNCAN, A. W., TIBBALLS, J. & SUTHERLAND, S. K. 1980. Effects of Sydney funnel-web spider envenomation in monkeys, and their clinical implications. *Med J Aust,* 2**,** 429-35.

DUTERTRE, S. & LEWIS, R. J. 2010. Use of venom peptides to probe ion channel structure and function. *J Biol Chem,* 285**,** 13315-20.

EBERL, D. F., REN, D., FENG, G., LORENZ, L. J., VAN VACTOR, D. & HALL, L. M. 1998. Genetic and developmental characterisation of Dmca1D, a calcium channel α1 subunit gene in *Drosophila melanogaster*. *Genetics,* 148**,** 1159-69.

ELAZAR, M., LEVI, R. & ZLOTKIN, E. 2001. Targeting of an expressed neurotoxin by its recombinant baculovirus. *J Exp Biol,* 204**,** 2637-45.

ELLINOR, P. T., ZHANG, J. F., RANDALL, A. D., ZHOU, M., SCHWARZ, T. L., TSIEN, R. W. & HORNE, W. A. 1993. Functional expression of a rapidly inactivating neuronal calcium channel. *Nature,* 363**,** 455-8.

ELLIOTT, M. 1976. Properties and applications of pyrethroids. *Environ Health Perspect,* 14**,** 1-13.

ENSERINK, M. 2006. Emerging infectious diseases. During a hot summer, bluetongue virus invades northern Europe. *Science,* 313**,** 1218-9.

EPSTEIN, P. R. 2005. Climate change and human health. *N Engl J Med,* 353**,** 1433-6.

ESCOUBAS, P. & BOSMANS, F. 2007. Spider peptide toxins as leads for drug development. *Expert Opin Drug Discov,* 2**,** 823-35.

ESCOUBAS, P., DIOCHOT, S. & CORZO, G. 2000. Structure and pharmacology of spider venom neurotoxins. *Biochimie,* 82**,** 893-907.

ESCOUBAS, P. & KING, G. F. 2009. Venomics as a drug discovery platform. *Expert Rev Proteomics,* 6**,** 221-4.

ESCOUBAS, P., QUINTON, L. & NICHOLSON, G. M. 2008. Venomics: unravelling the complexity of animal venoms with mass spectrometry. *J Mass Spectrom,* 43**,** 279-95.

ESCOUBAS, P. & RASH, L. 2004. Tarantulas: eight-legged pharmacists and combinatorial chemists. *Toxicon,* 43**,** 555-74.

ESCOUBAS, P., SOLLOD, B. & KING, G. F. 2006. Venom landscapes: mining the complexity of spider venoms via a combined cDNA and mass spectrometric approach. *Toxicon,* 47**,** 650-63.

ESTRADA, G., VILLEGAS, E. & CORZO, G. 2007. Spider venoms: a rich source of acylpolyamines and peptides as new leads for CNS drugs. *Nat Prod Rep,* 24**,** 145-61.

FAJLOUN, Z., KHARRAT, R., CHEN, L., LECOMTE, C., DI LUCCIO, E., BICHET, D., EL AYEB, M., ROCHAT, H., ALLEN, P. D., PESSAH, I. N., DE WAARD, M. & SABATIER, J. M. 2000. Chemical synthesis and characterisation of maurocalcine, a scorpion toxin that activates Ca^{2+} release channel/ryanodine receptors. *FEBS Letters,* 469**,** 179-85.

FAULDER, R. J. 1995. *Systematics and biogeography of the spider genus Missulena Walkenaer.* MScAgr Thesis, University of Sydney.

FAUQUET, C. M., MAYO, M. A., MANILOFF, J., DESSELBERGER, U. & BALL, L. A. (eds.) 2005. *Virus taxonomy. Eighth Report of the International Committee on Taxonomy of Viruses,* Amsterdam: Elsevier.

FEDERICI, B. A. 2005. Insecticidal bacteria: an overwhelming success for invertebrate pathology. *J Invertebr Pathol,* 89**,** 30-8.

FELDMAN, D. H., OLIVERA, B. M. & YOSHIKAMI, D. 1987. ω *Conus geographus* toxin: a peptide that blocks calcium channels. *FEBS Lett,* 214**,** 295-300.

FENG, Q., ARIF, B. M., PALLI, S. R., SOHI, S. S. & RETNAKARAN, A. 2001. Molecular modifications of baculoviruses for the control of forest insect pests. *Adv Virus Res,* 57**,** 263-90.

FENTON, J. 2002. *Toxicology: a case-oriented approach,* Boca Raton, CRC Press.

FERRÉ, J. & VAN RIE, J. 2002. Biochemistry and genetics of insect resistance to *Bacillus thuringiensis*. *Annu Rev Entomol,* 47**,** 501-33.

FEYEREISEN, R. 1995. Molecular biology of insect resistance. *Toxicology Letters,* 82/83**,** 83-90.

FFRENCH-CONSTANT, R. H., DABORN, P. J. & LE GOFF, G. 2004. The genetics and genomics of insecticide resistance. *Trends Genet,* 20**,** 163-70.

FISHER, M. M., CARR, G. A., MCGUINNESS, R. & WARDEN, J. C. 1980. *Atrax robustus* envenomation. *Anaesth Intensive Care,* 8**,** 410-20.

FITCHES, E., EDWARDS, M. G., MEE, C., GRISHIN, E., GATEHOUSE, A. M., EDWARDS, J. P. & GATEHOUSE, J. A. 2004. Fusion proteins containing insect-specific toxins as pest control agents: snowdrop lectin delivers fused insecticidal spider venom toxin to insect haemolymph following oral ingestion. *J Insect Physiol,* 50**,** 61-71.

FITCHES, E., WOODHOUSE, S. D., EDWARDS, J. P. & GATEHOUSE, J. A. 2001. In vitro and in vivo binding of snowdrop (*Galanthus nivalis* agglutinin; GNA) and jackbean (*Canavalia ensiformis*; Con A) lectins within tomato moth (*Lacanobia oleracea*) larvae; mechanisms of insecticidal action. *J Insect Physiol,* 47**,** 777-87.

FITCHES, E. C., BELL, H. A., POWELL, M. E., BACK, E., SARGIOTTI, C., WEAVER, R. J. & GATEHOUSE, J. A. 2010. Insecticidal activity of scorpion toxin (ButaIT) and snowdrop lectin (GNA) containing fusion proteins towards pest species of different orders. *Pest Manag Sci,* 66**,** 74-83.

FLETCHER, J. I., SMITH, R., O'DONOGHUE, S. I., NILGES, M., CONNOR, M., HOWDEN, M. E., CHRISTIE, M. J. & KING, G. F. 1997. The structure of a novel insecticidal neurotoxin, ω-atracotoxin-Hv1, from the venom of an Australian funnel web spider. *Nat Struct Biol,* 4**,** 559-66.

GADEK, T. R. & NICHOLAS, J. B. 2003. Small molecule antagonists of proteins. *Biochem Pharmacol,* 65**,** 1-8.

GAHAN, L. J., GOULD, F. & HECKEL, D. G. 2001. Identification of a gene associated with *Bt* resistance in *Heliothis virescens*. *Science,* 293**,** 857-60.

GAN-MOR, S. & MATTHEWS, G. A. 2003. Recent developments in sprayers for application of biopesticides-an overview. *Biosyst Eng,* 84**,** 119-25.

GATEHOUSE, J. A., A, M. R. G. & FITCHES, E. 1997. Effects of snowdrop lectin (GNA) delivered via artificial diet and transgenic plants on the development of tomato moth (*Lacanobia oleracea*) larvae in laboratory and glasshouse trials. *J Insect Physiol,* 43**,** 727-39.

GATTON, M. L., KAY, B. H. & RYAN, P. A. 2005. Environmental predictors of Ross River virus disease outbreaks in Queensland, Australia. *Am J Trop Med Hyg,* 72**,** 792-9.

GERSHBURG, E., STOCKHOLM, D., FROY, O., RASHI, S., GUREVITZ, M. & CHEJANOVSKY, N. 1998. Baculovirus-mediated expression of a scorpion depressant toxin improves the insecticidal efficacy achieved with excitatory toxins. *FEBS Letters,* 422**,** 132-6.

GINSBORG, B. L. & WARRINER, J. 1960. The isolated chick-biventer cervicis nerve-muscle preparation. *Br J Pharmacol,* 15**,** 410-1.

GODFRAY, H. C., BEDDINGTON, J. R., CRUTE, I. R., HADDAD, L., LAWRENCE, D., MUIR, J. F., PRETTY, J., ROBINSON, S., THOMAS, S. M. & TOULMIN, C. 2010. Food security: the challenge of feeding 9 billion people. *Science,* 327**,** 812-8.

GOULD, F. 1998. Sustainability of transgenic insecticidal cultivars: integrating pest genetics and ecology. *Annu Rev Entomol,* 43**,** 701-26.

GOWD, K. H., YAROTSKYY, V., ELMSLIE, K. S., SKALICKY, J. J., OLIVERA, B. M. & BULAJ, G. 2010. Site-specific effects of diselenide bridges on the oxidative folding of a cystine knot peptide, ω-selenoconotoxin GVIA. *Biochemistry,* 49**,** 2741-52.

GRATZ, N. G. 1999. Emerging and resurging vector-borne diseases. *Annu Rev Entomol,* 44**,** 51-75.

GRAUDINS, A., WILSON, D., ALEWOOD, P. F., BROADY, K. W. & NICHOLSON, G. M. 2002. Cross-reactivity of Sydney funnel-web spider antivenom: neutralisation of the *in vitro* toxicity of other Australian funnel-web (*Atrax* and *Hadronyche*) spider venoms. *Toxicon,* 40**,** 259-66.

GRAY, M. R. 2010. A revision of the Australian funnel-web spiders (Hexathelidae: Atracinae). *Rec Aust Mus,* 62**,** 285-392.

GRIFFIN, T. J. & AEBERSOLD, R. 2001. Advances in proteome analysis by mass spectrometry. *J Biol Chem,* 276**,** 45497-500.

GRIFFITTS, J. S. & AROIAN, R. V. 2005. Many roads to resistance: how invertebrates adapt to *Bt* toxins. *Bioessays,* 27**,** 614-24.

GROLLEAU, F. & LAPIED, B. 1996. Two distinct low-voltage-activated Ca^{2+} currents contribute to the pacemaker mechanism in cockroach dorsal unpaired median neurons. *J Neurophysiol,* 76**,** 963-76.

GROLLEAU, F. & LAPIED, B. 2000. Dorsal unpaired median neurones in the insect central nervous system: towards a better understanding of the ionic mechanisms underlying spontaneous electrical activity. *J Exp Biol,* 203**,** 1633-48.

GROLLEAU, F., STANKIEWICZ, M., BIRINYI-STRACHAN, L., WANG, X.-H., NICHOLSON, G. M., PELHATE, M. & LAPIED, B. 2001. Electrophysiological analysis of the neurotoxic action of a funnel-web spider toxin, δ-atracotoxin-Hv1a, on insect voltage-gated Na^+ channels. *J Exp Biol,* 204**,** 711-21.

GUBLER, D. J. 2002. The global emergence/resurgence of arboviral diseases as public health problems. *Arch Med Res,* 33**,** 330-42.

GUNNING, S. J., CHONG, Y., KHALIFE, A. A., HAINS, P. G., BROADY, K. W. & NICHOLSON, G. M. 2003. Isolation of δ-missulenatoxin-Mb1a, the major vertebrate-active spider δ-toxin from the venom of *Missulena bradleyi* (Actinopodidae). *FEBS Lett,* 554**,** 211-8.

HAINES, A., KOVATS, R. S., CAMPBELL-LENDRUM, D. & CORVALAN, C. 2006. Climate change and human health: impacts, vulnerability, and mitigation. *Lancet,* 367**,** 2101-9.

HAJEK, A. E., MCMANUS, M. L. & DELALIBERA, I. 2007. A review of introductions of pathogens and nematodes for classical biological control of insects and mites. *Biol Contr,* 41**,** 1-13.

HAMILL, O. P., MARTY, A., NEHER, E., SAKMANN, B. & SIGWORTH, F. J. 1981. Improved patch-clamp techniques for high-resolution current recording from cells and cell-free membrane patches. *Pflügers Arch,* 391**,** 85-100.

HARTMAN, L. J. & SUTHERLAND, S. K. 1984. Funnel-web spider (*Atrax robustus*) antivenom in the treatment of human envenomation. *Med J Aust,* 141**,** 796-9.

HELM, R., COCKRELL, G., STANLEY, J. S., BRENNER, R. J., BURKS, W. & BANNON, G. A. 1996. Isolation and characterization of a clone encoding a major allergen (*Bla g* Bd90K) involved in IgE-mediated cockroach hypersensitivity. *J Allergy Clin Immunol,* 98**,** 172-80.

HEMINGWAY, J. 2009. Vector biology diagnostics and public health pesticide development through the product development partnership route. *In:* CLARK, J., BLOOMQUIST, J. R. & KAWADA, H. (eds.) *Advances in human vector control.* Washington DC: American Chemical Society.

HEMINGWAY, J. & RANSON, H. 2000. Insecticide resistance in insect vectors of human disease. *Annu Rev Entomol,* 45**,** 371-91.

HERNANDEZ-CAMPUZANO, B., SUAREZ, R., LINA, L., HERNANDEZ, V., VILLEGAS, E., CORZO, G. & ITURRIAGA, G. 2009. Expression of a spider venom peptide in transgenic tobacco confers insect resistance. *Toxicon,* 53**,** 122-8.

HERNIOU, E. A., OLSZEWSKI, J. A., CORY, J. S. & O'REILLY, D. R. 2003. The genome sequence and evolution of baculoviruses. *Annu Rev Entomol,* 48**,** 211-34.

HERZIG, V., KHALIFE, A. A., CHONG, Y., ISBISTER, G. K., CURRIE, B. J., CHURCHILL, T. B., HORNER, S., ESCOUBAS, P., NICHOLSON, G. M. & HODGSON, W. C. 2008. Intersexual variations in Northern (*Missulena pruinosa*) and Eastern (*M. bradleyi*) mouse spider venom. *Toxicon,* 51**,** 1167-77.

HILLYARD, D. R., MONJE, V. D., MINTZ, I. M., BEAN, B. P., NADASDI, L., RAMACHANDRAN, J., MILJANICH, G., AZIMI-ZOONOOZ, A., MCINTOSH, J. M. & CRUZ, L. J. 1992. A new *Conus* peptide ligand for mammalian presynaptic Ca^{2+} channels. *Neuron,* 9**,** 69-77.

HIRATA, H., ALBILLOS, A., FERNANDEZ, F., MEDRANO, J., JURKIEWICZ, A. & GARCIA, A. G. 1997. ω-Conotoxins block neurotransmission in the rat vas deferens by binding to different presynaptic sites on the N-type Ca^{2+} channel. *Eur J Pharmacol,* 321**,** 217-23.

HODGSON, E. & KUHR, R. J. (eds.) 1990. *Safer insecticides: development and use,* New York: Marcel Dekker.

HOLMGREN, A. & LU, J. 2010. Thioredoxin and thioredoxin reductase: current research with special reference to human disease. *Biochem Biophys Res Commun,* 396**,** 120-4.

HOLT, R. A., SUBRAMANIAN, G. M., HALPERN, A., SUTTON, G. G., CHARLAB, R., NUSSKERN, D. R., WINCKER, P., CLARK, A. G., RIBEIRO, J. M., WIDES, R., SALZBERG, S. L., LOFTUS, B., YANDELL, M., MAJOROS, W. H., RUSCH, D. B., LAI, Z., KRAFT, C. L., ABRIL, J. F., ANTHOUARD, V., ARENSBURGER, P., ATKINSON, P. W., BADEN, H., DE BERARDINIS, V., BALDWIN, D., BENES, V., BIEDLER, J., BLASS, C., BOLANOS, R., BOSCUS, D., BARNSTEAD, M., CAI, S., CENTER, A., CHATURVERDI, K., CHRISTOPHIDES, G. K., CHRYSTAL, M. A., CLAMP, M., CRAVCHIK, A., CURWEN, V., DANA, A., DELCHER, A., DEW, I., EVANS, C. A., FLANIGAN, M., GRUNDSCHOBER-FREIMOSER, A., FRIEDLI, L., GU, Z., GUAN, P., GUIGO, R., HILLENMEYER, M. E., HLADUN, S. L., HOGAN, J. R., HONG, Y. S., HOOVER, J., JAILLON, O., KE, Z., KODIRA, C., KOKOZA, E., KOUTSOS, A., LETUNIC, I., LEVITSKY, A., LIANG, Y., LIN, J. J., LOBO, N. F., LOPEZ, J. R., MALEK, J. A., MCINTOSH, T. C., MEISTER, S., MILLER, J., MOBARRY, C., MONGIN, E., MURPHY, S. D., O'BROCHTA, D. A., PFANNKOCH, C., QI, R., REGIER, M. A., REMINGTON, K., SHAO, H., SHARAKHOVA, M. V., SITTER, C. D., SHETTY, J., SMITH, T. J., STRONG, R., SUN, J., THOMASOVA, D., TON, L. Q., TOPALIS, P., TU, Z., UNGER, M. F., WALENZ, B., WANG, A., WANG, J., WANG, M., WANG, X., WOODFORD, K. J., WORTMAN, J. R., WU, M., YAO, A., ZDOBNOV, E. M., ZHANG, H., ZHAO, Q., et al. 2002. The genome sequence of the malaria mosquito *Anopheles gambiae. Science,* 298**,** 129-49.

HUANG, J. K., HU, R. F., PRAY, C., QIAO, F. B. & ROZELLE, S. 2003. Biotechnology as an alternative to chemical pesticides: a case study of *Bt* cotton in China. *Agri Econ,* 29**,** 55-67.

HUGHES, P. R., WOOD, H. A., BREEN, J. P., SIMPSON, S. F., DUGGAN, A. J. & DYBAS, J. A. 1997. Enhanced bioactivity of recombinant baculoviruses expressing insect-specific spider toxins in Lepidopteran crop pests. *J Invertebr Pathol,* 69**,** 112-8.

IMOTO, T. & YAMADA, H. 1983. Peptide separation by reversed-phase high-performance liquid chromatography. *Mol Cell Biochem,* 51**,** 111-21.

INCEOGLU, A. B., KAMITA, S. G., HINTON, A. C., HUANG, Q., SEVERSON, T. F., KANG, K. & HAMMOCK, B. D. 2001. Recombinant baculoviruses for insect control. *Pest Manag Sci,* 57**,** 981-7.

ISAACS, N. W. 1995. Cystine knots. *Curr Opin Struct Biol,* 5**,** 391-5.

ISBISTER, G. K. 2004. Mouse spider bites (*Missulena* spp.) and their medical importance. A systematic review. *Med J Aust,* 180**,** 225-7.

ISBISTER, G. K. & GRAY, M. R. 2004. Bites by Australian mygalomorph spiders (Araneae, Mygalomorphae), including funnel-web spiders (Atracinae) and mouse spiders (Actinopodidae: *Missulena* spp). *Toxicon,* 43**,** 133-40.

ISBISTER, G. K., GRAY, M. R., BALIT, C. R., RAVEN, R. J., STOKES, B. J., PORGES, K., TANKEL, A. S., TURNER, E., WHITE, J. & FISHER, M. M. 2005. Funnel-web spider bite: a systematic review of recorded clinical cases. *Med J Aust,* 182**,** 407-11.

JACKSON, H. & PARKS, T. N. 1989. Spider toxins: recent applications in neurobiology. *Annu Rev Neurosci,* 12**,** 405-14.

JEZIORSKI, M. C., GREENBERG, R. M. & ANDERSON, P. A. 2000. The molecular biology of invertebrate voltage-gated Ca^{2+} channels. *J Exp Biol,* 203**,** 841-56.

JONGEJAN, F. & UILENBERG, G. 2004. The global importance of ticks. *Parasitology,* 129 Suppl**,** S3-14.

KAISER, J. & ENSERINK, M. 2000. Environmental toxicology. Treaty takes a POP at the dirty dozen. *Science,* 290**,** 2053.

KARLAGANIS, G., MARIONI, R., SIEBER, I. & WEBER, A. 2001. The elaboration of the 'Stockholm convention' on persistent organic pollutants (POPs): a negotiation process fraught with obstacles and opportunities. *Environ Sci Pollut Res Int,* 8**,** 216-21.

KAWASAKI, F., COLLINS, S. C. & ORDWAY, R. W. 2002. Synaptic calcium-channel function in *Drosophila*: analysis and transformation rescue of temperature-sensitive paralytic and lethal mutations of cacophony. *J Neurosci,* 22**,** 5856-64.

KEDZIERSKI, L., ZHU, Y. & HANDMAN, E. 2006. Leishmania vaccines: progress and problems. *Parasitology,* 133 Suppl**,** S87-112.

KHALIFE, A. A. 2000. *Isolation of a lethal neurotoxin from the Eastern mouse spider.* BMedSc(Hons), UTS.

KHAMBAY, B. P. S. 2002. Pyrethroid Insecticides. *Pesticide Outlook,* 13**,** 49-54.

KHAN, S. A., ZAFAR, Y., BRIDDON, R. W., MALIK, K. A. & MUKHTAR, Z. 2006. Spider venom toxin protects plants from insect attack. *Transgenic Res,* 15**,** 349-57.

KING, G. F. 2007. Modulation of insect Ca_v channels by peptidic spider toxins. *Toxicon,* 49**,** 513-30.

KING, G. F., ESCOUBAS, P. & NICHOLSON, G. M. 2008a. Peptide toxins that selectively target insect Na_v and Ca_v channels. *Channels (Austin),* 2**,** 100-16.

KING, G. F., GENTZ, M. C., ESCOUBAS, P. & NICHOLSON, G. M. 2008b. A rational nomenclature for naming peptide toxins from spiders and other venomous animals. *Toxicon,* 52**,** 264-76.

KING, G. F., TEDFORD, H. W. & MAGGIO, F. 2002. Structure and function of insecticidal neurotoxins from Australian funnel-web spiders. *Toxin Rev,* 21**,** 361-89.

KOPACIEWICZ, W., ROUNDS, M.A., FAUSNAUGH, J. AND REGNIER, F.E. 1983. Retention model for high-performance ion-exchange chromatography. *J Chromatogr A,* 266**,** 3-21.

KOSTYUK, P. G. 1999. Low-voltage activated calcium channels: achievements and problems. *Neuroscience,* 92**,** 1157-63.

KREBS, J. R., WILSON, J. D., BRADBURY, R. B. & SIRIWARDENA, G. M. 1999. The second silent spring? *Nature,* 400**,** 611-2.

KRUGER, M., VAN RENSBURG, J. B. J. & VAN DEN BERG, J. 2009. Perspective on the development of stem borer resistance to *Bt* maize and refuge compliance at the Vaalharts irrigation scheme in South Africa. *Crop Prot,* 28**,** 684-9.

KUHN-NENTWIG, L., BÜCHELER, A., STUDER, A. & NENTWIG, W. 1998. Taurine and histamine: low molecular compounds in prey hemolymph

increase the killing power of spider venom. *Naturwissenschaften,* 85**,** 136-8.

KUNIMI, Y., FUXA, J. R. & HAMMOCK, B. D. 1996. Comparison of wild type and genetically engineered nuclear polyhedrosis viruses of *Autographa californica* for mortality, virus replication and polyhedra production in *Trichoplusia ni* larvae. *Entomol Exp Appl,* 81**,** 251-7.

LACEY, L. A., FRUTOS, R., KAYA, H. K. & VAIL, P. 2001. Insect pathogens as biological control agents: Do they have a future? *Biol Contr,* 21**,** 230-48.

LALLAS, P. L. 2001. The Stockholm Convention on persistent organic pollutants. *Am J Int Law,* 95**,** 692-708.

LAPIED, B., LE CORRONC, H. & HUE, B. 1990. Sensitive nicotinic and mixed nicotinic-muscarinic receptors in insect neurosecretory cells. *Brain Res,* 533**,** 132-6.

LEÃO, R. M., CRUZ, J. S., DINIZ, C. R., CORDEIRO, M. N. & BEIRÃO, P. S. L. 2000. Inhibition of neuronal high-voltage activated calcium channels by the ω-*Phoneutria nigriventer* Tx3-3 peptide toxin. *Neuropharmacology,* 39**,** 1756-67.

LEWIS, R. J. & GARCIA, M. L. 2003. Therapeutic potential of venom peptides. *Nat Rev Drug Discov,* 2**,** 790-802.

LEWIS, R. J., NIELSEN, K. J., CRAIK, D. J., LOUGHNAN, M. L., ADAMS, D. A., SHARPE, I. A., T., L., ADAMS, D. J., BOND, T., THOMAS, L., JONES, A., MATHESON, J., DRINKWATER, R., ANDREWS, P. R. & ALEWOOD, P. F. 2000. Novel ω-conotoxins from *Conus catus* discriminate among neuronal calcium channel subtypes. *J Biol Chem,* 275**,** 35335-44.

LITTLE, M. J., WILSON, H., ZAPPIA, C., CESTELE, S., TYLER, M. I., MARTIN-EAUCLAIRE, M. F., GORDON, D. & NICHOLSON, G. M. 1998. δ-Atracotoxins from Australian funnel-web spiders compete with scorpion α-toxin binding on both rat brain and insect sodium channels. *FEBS Lett,* 439**,** 246-52.

LITTLETON, J. T. & GANETZKY, B. 2000. Ion channels and synaptic organisation: analysis of the *Drosophila* genome. *Neuron,* 26**,** 35-43.

LORD, J. C. 2005. From Metchnikoff to Monsanto and beyond: the path of microbial control. *J Invertebr Pathol,* 89**,** 19-29.

LOUNIBOS, L. P. 2002. Invasions by insect vectors of human disease. *Annu Rev Entomol,* 47**,** 233-66.

LUDY, C. & LANG, A. 2006. A 3-year field-scale monitoring of foliage-dwelling spiders (Araneae) in transgenic *Bt* maize fields and adjacent field margins. *Biol Contr,* 38**,** 314-24.

MACKENZIE, J. S., GUBLER, D. J. & PETERSEN, L. R. 2004. Emerging flaviviruses: the spread and resurgence of Japanese encephalitis, West Nile and dengue viruses. *Nat Med,* 10**,** S98-109.

MAIN, B. Y. 1984. *Spiders,* Sydney, William Collins Pty Ltd.

MATTHIAS, L. J., YAM, P. T., JIANG, X. M., VANDEGRAAFF, N., LI, P., POUMBOURIOS, P., DONOGHUE, N. & HOGG, P. J. 2002. Disulfide exchange in domain 2 of CD4 is required for entry of HIV-1. *Nat Immunol,* 3**,** 727-32.

MCCUTCHEN, B. F., CHOUDARY, P. V., CRENSHAW, R., MADDOX, D., KAMITA, S. G., PALEKAR, N., VOLRATH, S., FOWLER, E., HAMMOCK, B. D. & MAEDA, S. 1991. Development of a recombinant

baculovirus expressing an insect-selective neurotoxin: potential for pest control. *Nat Biotechnol,* 9**,** 848-52.

MCDONOUGH, S. I., MINTZ, I. M. & BEAN, B. P. 1997. Alteration of P-type calcium channel gating by the spider toxin ω-Aga-IVA. *Biophy J,* 72**,** 2117-28.

MCDONOUGH, S. I., BOLAND, L. M., MINTZ, I. M. & BEAN, B. P. 2002. Interactions among toxins that inhibit N-type and P-type calcium channels. *J Gen Physiol,* 119**,** 313-28.

MCKINNEY, M. T., SCHOCH, R. M. & YONAVJAK, L. 2007. *Environmental science: systems and solutions,* Sudbury, Jones and Bartlett.

MCMICHAEL, A. J. 2001. Impact of climatic and other environmental changes on food production and population health in the coming decades. *Proc Nutr Soc,* 60**,** 195-201.

MEBS, D. 2001. Toxicity in animals. Trends in evolution? *Toxicon,* 39**,** 87-96.

MERRITT, J. E., ARMSTRONG, W. P., BENHAM, C. D., HALLAM, T. J., R., J., JAXA-CHAMIEC, A., LEIGH, B. K., MCCARTHY, S. A., MOORES, K. E. & RINK, T. J. 1990. SK&F 96365, a novel inhibitor of receptor-mediated calcium entry. *Biochem J,* 271**,** 515-22.

MESSUTAT, S., HEINE, M. & WICHER, D. 2001. Calcium-induced calcium release in neurosecretory insect neurons: fast and slow responses. *Cell Calcium,* 30**,** 199-211.

MILLER, L. K. 1995. Genetically engineered insect virus pesticides: present and future. *J Invertebr Pathol,* 65**,** 211-6.

MILLER, M. K., WHYTE, I. M., WHITE, J. & KEIR, P. M. 2000. Clinical features and management of *Hadronyche* envenomation in man. *Toxicon,* 38**,** 409-27.

MILLS, J. D. & PITMAN, R. M. 1997. Electrical properties of a cockroach motor neuron soma depend on different characteristics of individual Ca components. *J Neurophysiol,* 78**,** 2455-66.

MINTZ, I.M., VENEMA, V.J., SWIDEREK, K.M., LEE, T.D., BEAN, B.P., ADAMS, M.E., 1992. P-type calcium channels blocked by the spider toxin ω-Aga-IVA. *Nature* 355**,** 827–9.

MOBLI, M., DE ARAÚJO, A. D., LAMBERT, L. K., PIERENS, G. K., WINDLEY, M. J., NICHOLSON, G. M., ALEWOOD, P. F. & KING, G. F. 2009. Direct visualization of disulfide bonds through diselenide proxies using [77]Se NRM spectroscopy. *Angew Chem Int Ed Engl,* 48**,** 9312-4.

MOLINSKI, T. F., DALISAY, D. S., LIEVENS, S. L. & SALUDES, J. P. 2009. Drug development from marine natural products. *Nat Rev Drug Discov,* 8**,** 69-85.

MOORE, J. W., NARAHASHI, T., ANDERSON, N. C., BLAUSTEIN, M. P., WATANABE, A., TASAKI, I., SINGER, I. & LERMAN, L. 1967. Tetrodotoxin: comments on effects on squid axons. *Science,* 157**,** 220-1.

MORIN, S., BIGGS, R. W., SISTERSON, M. S., SHRIVER, L., ELLERS-KIRK, C., HIGGINSON, D., HOLLEY, D., GAHAN, L. J., HECKEL, D. G., CARRIERE, Y., DENNEHY, T. J., BROWN, J. K. & TABASHNIK, B. E. 2003. Three cadherin alleles associated with resistance to *Bacillus thuringiensis* in pink bollworm. *Proc Natl Acad Sci U S A,* 100**,** 5004-9.

MOSBAH, A., KHARRAT, R., FAJLOUN, Z., RENISIO, J., BLANC, E., SABATIER, J., EL AYEB, M. & DARBON, H. 2000. A new fold in the

scorpion toxin family, associated with an activity on a ryanodine-sensitive calcium channel. *Proteins,* 40**,** 436-42.

MOSCARDI, F. 1999. Assessment of the application of baculoviruses for control of *Lepidoptera. Annu Rev Entomol,* 44**,** 257-89.

MOUHAT, S., JOUIROU, B., MOSBAH, A., DE WAARD, M. & SABATIER, J. 2004. Diversity of folds in animal toxins acting on ion channels. *Biochem J,* 378**,** 717-26.

MUKHERJEE, A. K., SOLLOD, B. L., WIKEL, S. K. & KING, G. F. 2006. Orally active acaricidal peptide toxins from spider venom. *Toxicon,* 47**,** 182-7.

MUTH, J. N., VARADI, G. & SCHWARTZ, A. 2001. Use of transgenic mice to study voltage-dependent Ca^{2+} channels. *Trends Pharmacol Sci,* 22**,** 526-32.

NARAHASHI, T. 1996. Neuronal ion channels as the target sites of insecticides. *Pharmacol Toxicol,* 78**,** 1-14.

NARAHASHI, T., ROY, M. L. & GINSBURG, K. S. 1994. Recent advances in the study of mechanism of action of marine neurotoxins. *Neurotoxicology,* 15**,** 545-54.

NASSEL, D. R. 1996. Neuropeptides, amines and amino acids in an elementary insect ganglion: functional and chemical anatomy of the unfused abdominal ganglion. *Prog Neurobiol,* 48**,** 325-420.

NATION, J. L. 2002. *Insect physiology annd biochemistry,* London, CRC Press.

NAUEN, R. 2006. Insecticide mode of action: return of the ryanodine receptor. *Pest Manag Sci,* 62**,** 690-2.

NAUEN, R. 2007. Insecticide resistance in disease vectors of public health importance. *Pest Manag Sci,* 63**,** 628-33.

NICHOLSON, G. M. 2007a. Fighting the global pest problem: preface to the special Toxicon issue on insecticidal toxins and their potential for insect pest control. *Toxicon,* 49**,** 413-22.

NICHOLSON, G. M. 2007b. Insect-selective spider toxins targeting voltage-gated sodium channels. *Toxicon,* 49**,** 490-512.

NICHOLSON, G. M. & GRAUDINS, A. 2002. Spiders of medical importance in the Asia-Pacific: atracotoxin, latrotoxin and related spider neurotoxins. *Clin Exp Pharmacol Physiol,* 29**,** 785-94.

NICHOLSON, G. M., GRAUDINS, A., WILSON, H. I., LITTLE, M. & BROADY, K. W. 2006. Arachnid toxinology in Australia: from clinical toxicology to potential applications. *Toxicon,* 48**,** 872-98.

NICHOLSON, G. M., LITTLE, M. J. & BIRINYI-STRACHAN, L. C. 2004. Structure and function of δ-atracotoxins: lethal neurotoxins targeting the voltage-gated sodium channel. *Toxicon,* 43**,** 587-99.

NICHOLSON, G. M., WALSH, R., LITTLE, M. J. & TYLER, M. I. 1998. Characterisation of the effects of robustoxin, the lethal neurotoxin from the Sydney funnel-web spider *Atrax robustus*, on sodium channel activation and inactivation. *Pflügers Arch,* 436**,** 117-26.

NICHOLSON, G. M., WILLOW, M., HOWDEN, M. E. & NARAHASHI, T. 1994. Modification of sodium channel gating and kinetics by versutoxin from the Australian funnel-web spider *Hadronyche versuta. Pflügers Arch,* 428**,** 400-9.

NORTON, R. S. & PALLAGHY, P. K. 1998. The cystine knot structure of ion channel toxins and related polypeptides. *Toxicon,* 36**,** 1573-83.

NOWYCKY, M. C., FOX, A. P. & TSIEN, R. W. 1985. Three types of neuronal calcium channel with different calcium agonist sensitivity. *Nature,* 316**,** 440-3.

NRC 2000. *The future role of pesticides in US agriculture,* Washington, D.C., National Research Council.

OERKE, E. C. & DEHNE, H. W. 2004. Safeguarding production-losses in major crops and the role of crop protection. *Crop Protection,* 23**,** 275-85.

OLIVERA, B. M. 2002. *Conus* venom peptides: reflections from the biology of clades and species. *Annu Rev Ecol System,* 33**,** 25-47.

OLIVERA, B. M., CRUZ, L. J., DE SANTOS, V., LECHEMINANT, G. W., GRIFFIN, D., ZEIKUS, R., MCINTOSH, J. M., GALYEAN, R., VARGA, J., GRAY, W. R. & ET AL. 1987. Neuronal calcium channel antagonists. Discrimination between calcium channel subtypes using ω-conotoxin from *Conus magus* venom. *Biochemistry,* 26**,** 2086-90.

OLIVERA, B. M., MCINTOSH, J. M., CRUZ, L. J., LUQUE, F. A. & GRAY, W. R. 1984. Purification and sequence of a presynaptic peptide toxin from *Conus geographus* venom. *Biochemistry,* 23**,** 5087-90.

PALLAGHY, P. K., NIELSEN, K. J., CRAIK, D. J. & NORTON, R. S. 1994. A common structural motif incorporating a cystine knot and a triple-stranded β-sheet in toxic and inhibitory polypeptides. *Protein Sci,* 3**,** 1833-9.

PAROLA, P. & RAOULT, D. 2001. Ticks and tickborne bacterial diseases in humans: an emerging infectious threat. *Clin Infect Dis,* 32**,** 897-928.

PATZ, J. A., CAMPBELL-LENDRUM, D., HOLLOWAY, T. & FOLEY, J. A. 2005. Impact of regional climate change on human health. *Nature,* 438**,** 310-7.

PATZ, J. A. & REISEN, W. K. 2001. Immunology, climate change and vector-borne diseases. *Trends Immunol,* 22**,** 171-2.

PEARCE, F. 2002. US millers fight for banned pesticide. *New Scientist.*

PEARCE, F. 2003. Pesticide industry won't pay its dues. *New Scientist.*

PETERSEN, L. R. & ROEHRIG, J. T. 2001. West Nile virus: a reemerging global pathogen. *Emerg Infect Dis,* 7**,** 611-4.

PFLUGER, H. J. & WATSON, A. H. 1988. Structure and distribution of dorsal unpaired median (DUM) neurones in the abdominal nerve cord of male and female locusts. *J Comp Neurol,* 268**,** 329-45.

PHAM TRUNG, N., FITCHES, E. & GATEHOUSE, J. A. 2006. A fusion protein containing a lepidopteran-specific toxin from the South Indian red scorpion (*Mesobuthus tamulus*) and snowdrop lectin shows oral toxicity to target insects. *BMC Biotechnol,* 6**,** 18.

PIMENTA, A. M. & DE LIMA, M. E. 2005. Small peptides, big world: biotechnological potential in neglected bioactive peptides from arthropod venoms. *J Pept Sci,* 11**,** 670-6.

PINNOCK, R. D. & SATTELLE, D. B. 1987. Dissociation and maintenance in vitro of neurones from adult cockroach (*Periplaneta americana*) and housefly (*Musca domestica*). *J Neurosci Methods,* 20**,** 195-202.

PINTO, J., LYND, A., ELISSA, N., DONNELLY, M. J., COSTA, C., GENTILE, G., CACCONE, A. & DO ROSARIO, V. E. 2006. Co-occurrence of East and West African kdr mutations suggests high levels of resistance to pyrethroid insecticides in *Anopheles gambiae* from Libreville, Gabon. *Med Vet Entomol,* 20**,** 27-32.

PLATNICK, N. 1993. Advances in spider taxonomy, 1988-1991. *The New York Entomological Society, New York*.

PLATNICK, N. 1995. An Abundance of Spiders. *Natural History,* 104**,** 50-3.

PLATNICK, N. I. 2011. *The World Spider Catalog, Version 12.0* [Online]. Available: http://research.amnh.org/iz/spiders/catalog/ [Accessed 6 July 2011].

PLOTNIKOVA, S. N. 1969. Effector neurons with several axons in the ventral nerve cord of the Asian grasshopper, *Locusta migratoria*. *J Evol Biochem Physiol,* 5**,** 276-8.

POPHAM, H. J., LI, Y. & MILLER, L. K. 1997. Genetic improvement of *Helicoverpa zea* nuclear polyhedrosis virus as a pesticide. *Biol Contr,* 10**,** 83-91.

PRENTICE, M. B. & RAHALISON, L. 2007. Plague. *Lancet,* 369**,** 1196-207.

PRIKHOD'KO, G. G., POPHAM, H. J., FELCETTO, T. J., OSTLIND, D. A., WARREN, V. A., SMITH, M. M., GARSKY, V. M., WARMKE, J. W., COHEN, C. J. & MILLER, L. K. 1998. Effects of simultaneous expression of two sodium channel toxin genes on the properties of baculoviruses as biopesticides. *Biol Contr,* 12**,** 66-78.

PRIKHOD'KO, G. G., ROBSON, M., WARMKE, J. W., COHEN, C. J., SMITH, M. M., WANG, P., WARREN, V., KACZOROWSKI, G., VAN DER PLOEG, L. H. & MILLER, L. K. 1996. Properties of three baculovirus-expressing genes that encode insect-selective toxins: μ-Aga-IV, As II, and Sh I. *Biol Contr,* 7**,** 236-44.

RABENSTEIN, D. L. & WEAVER, K. H. 1996. Kinetics and equilibria of the thiol/disulfide exchange reactions of somatostatin with glutathione. *J Org Chem,* 61**,** 7391-7.

RANDALL, A. & TSIEN, R. W. 1995. Pharmacological dissection of multiple types of Ca^{2+} channel currents in rat cerebellar granule neurones. *J Neuroscience,* 15**,** 2995-3012.

RANSON, H., CLAUDIANOS, C., ORTELLI, F., ABGRALL, C., HEMINGWAY, J., SHARAKHOVA, M. V., UNGER, M. F., COLLINS, F. H. & FEYEREISEN, R. 2002. Evolution of supergene families associated with insecticide resistance. *Science,* 298**,** 179-81.

RASH, L. D., BIRINYI-STRACHAN, L. C., NICHOLSON, G. M. & HODGSON, W. C. 2000. Neurotoxic activity of venom from the Australian eastern mouse spider (*Missulena bradleyi*) involves modulation of sodium channel gating. *Br J Pharmacol,* 130**,** 1817-24.

RASH, L. D. & HODGSON, W. C. 2002. Pharmacology and biochemistry of spider venoms. *Toxicon,* 40**,** 225-54.

RAVEN, R. J., BAEHR, B. C. & HARVEY, M. S. 2002. Spiders of Australia: interactive identification to subfamily. Collingwood Victoria: CSIRO.

RAYMOND-DELPECH, V., MATSUDA, K., SATTELLE, B. M., RAUH, J. J. & SATTELLE, D. B. 2005. Ion channels: molecular targets of neuroactive insecticides. *Invert Neurosci,* 5**,** 119-33.

REGEV, A., RIVKIN, H., INCEOGLU, B., GERSHBURG, E., HAMMOCK, B. D., GUREVITZ, M. & CHEJANOVSKY, N. 2003. Further enhancement of baculovirus insecticidal efficacy with scorpion toxins that interact cooperatively. *FEBS Lett,* 537**,** 106-10.

RICHARDS, A., MATTHEWS, M. & CHRISTIAN, P. 1998. Ecological considerations for the environmental impact evaluation of recombinant baculovirus insecticides. *Annu Rev Entomol,* 43**,** 493-517.

RUDY, B. & IVERSON, L. E. 1997. *Ion Channels*, Elsevier Science.

SAEZ, N. J., SENFF, S., JENSEN, J. E., ER, S. Y., HERZIG, V., RASH, L. D. & KING, G. F. 2010. Spider-venom peptides as therapeutics. *Toxins,* 2**,** 2851-71.

SATTENSPIEL, L. 2000. Tropical environments, human activities, and the transmission of infectious diseases. *Am J Phys Anthropol,* Suppl 31**,** 3-31.

SCHNÖLZER, M., ALEWOOD, P., JONES, A., ALEWOOD, D. & KENT, S. 1992. *In situ* neutralization in Boc-chemistry solid phase peptide synthesis: Rapid, high yield assembly of difficult sequences. *Int J Pept Protein Res,* 40**,** 180-93.

SEVILLA, P., BRUIX, M., SANTORO, J., GAGO, F., GARCIA, A. G. & RICO, M. 1993. Three-dimensional structure of ω-conotoxin GVIA determined by ^{1}H NMR. *Biochem Biophys Res Commun,* 192**,** 1238-44.

SHELTON, A. M., TANG, J. D., ROUSH, R. T., METZ, T. D. & EARLE, E. D. 2000. Field tests on managing resistance to *Bt*-engineered plants. *Nat Biotechnol,* 18**,** 339-42.

SHELTON, A. M., ZHAO, J. & ROUSH, R. T. 2002. Economic, ecological, food safety, and social consequences of the deployment of *Bt* transgenic plants. *Annu Rev Entomol,* 47**,** 845-81.

SINAKEVITCH, I. G., GEFFARD, M., PELHATE, M. & LAPIED, B. 1996. Anatomy and targets of dorsal unpaired median neurones in the terminal abdominal ganglion of the male cockroach *Periplaneta americana* L. *J Comp Neurol,* 367**,** 147-63.

SINGH, A., HILDEBRAND, M. E., GARCIA, E. & SNUTCH, T. P. 2010. The transient receptor potential channel antagonist SKF96365 is a potent blocker of low-voltage-activated T-type calcium channels. *Br J Pharmacol,* 160**,** 1464-75.

SMITH, L. A., PEIXOTO, A. A., KRAMER, E. M., VILLELLA, A. & HALL, J. C. 1998. Courtship and visual defects of cacophony mutants reveal functional complexity of a calcium-channel α1 subunit in *Drosophila*. *Genetics,* 149**,** 1407-26.

SMITH, P. K., KROHN, R.I., HERMANSON, G.T., MALLIA, A.K., GARTNER, F.H., PROVENZANO, M.D., FUJIMOTO, E.K., GOEKE, N.M., OLSON, B.J., KLENK, D.C. 1985. Measurement of protein using bicinchoninic acid. *Anal Biochem,* 150**,** 76-85.

SNUTCH, T. P., SUTTON, K. G. & ZAMPONI, G. W. 2001. Voltage-dependent calcium channels-beyond dihydropyridine antagonists. *Curr Opin Pharmacol,* 1**,** 11-6.

SOLLOD, B. L., WILSON, D., ZHAXYBAYEVA, O., GOGARTEN, J. P., DRINKWATER, R. & KING, G. F. 2005. Were arachnids the first to use combinatorial peptide libraries? *Peptides,* 26**,** 131-9.

SOLOMON, T. & MALLEWA, M. 2001. Dengue and other emerging flaviviruses. *J Infect,* 42**,** 104-15.

SOONG, T. W., STEA, A., HODSON, C. D., DUBEL, S. J., VINCENT, S. R. & SNUTCH, T. P. 1993. Structure and functional expression of a member of the low voltage-activated calcium channel family. *Science,* 260**,** 1133-6.

STADTMAN, T. C. 1996. Selenocysteine. *Annu Rev Biochem,* 65**,** 83-100.

STEVENSON, P. A. & SPORHASE-EICHMANN, U. 1995. Localisation of octopaminergic neurones in insects. *Comp Biochem Physiol A Physiol,* 110**,** 203-15.

STEWART, L. M., HIRST, M. L., FERBER, M. L., MERRYWEATHER, A. T., CAYLEY, P. J. & POSSEE, R. D. 1991. Construction of an improved baculovirus insecticide containing an insect-specific toxin gene. *Nature,* 352**,** 85-8.

STONE, K. & WILLIAMS, K. 1996. Reverse-phase HPLC separation of enzymatic digests of proteins. *In:* WALKER, J. (ed.) *The protein protocols handbook.* New Jersey: Humana Press.

STORER, N. P., BABCOCK, J. M., SCHLENZ, M., MEADE, T., THOMPSON, G. D., BING, J. W. & HUCKABA, R. M. 2010. Discovery and characterization of field resistance to *Bt* maize: *Spodoptera frugiperda* (Lepidoptera: Noctuidae) in Puerto Rico. *J Econ Entomol,* 103**,** 1031-8.

SUN, X., CHEN, X., ZHANG, Z., WANG, H., BIANCHI, F. J., PENG, H., VLAK, J. M. & HU, Z. 2002. Bollworm responses to release of genetically modified *Helicoverpa armigera* nucleopolyhedroviruses in cotton. *J Invertebr Pathol,* 81**,** 63-9.

SUTHERLAND, S. K. 1980. Antivenom to the venom of the male Sydney funnel-web spider *Atrax robustus*: preliminary report. *Med J Aust,* 2**,** 437-41.

SUTHERLAND, S. K. 1983. Genus *Atrax* Cambridge, the funnel-web spiders. *In:* SUTHERLAND, S. K. (ed.) *Australian Animal Toxins.* Melbourne: Oxford University Press.

SUTHERLAND, S. K. & TIBBALLS, J. 2001. The genera *Atrax* and *Hadronyche*, funnel web spiders. *In:* SUTHERLAND, S. K. & TIBBALLS, J. (eds.) *Australian Animal Toxins: the creatures, their toxins and care of the poisoned patient.* Melbourne: Oxford University Press.

SUTHERST, R. W. 2004. Global change and human vulnerability to vector-borne diseases. *Clin Microbiol Rev,* 17**,** 136-73.

SWARTZ, K. J. & MACKINNON, R. 1995. An inhibitor of the $K_v2.1$ potassium channel isolated from the venom of a Chilean tarantula. *Neuron,* 15**,** 941-9.

SWARTZ, K. J. & MACKINNON, R. 1997a. Hanatoxin modifies the gating of a voltage-dependent K^+ channel through multiple binding sites. *Neuron,* 18**,** 665-73.

SWARTZ, K. J. & MACKINNON, R. 1997b. Mapping the receptor site for hanatoxin, a gating modifier of voltage-dependent K^+ channels. *Neuron,* 18**,** 675-82.

SZEWCZYK, B., HOYOS-CARVAJAL, L., PALUSZEK, M., SKRZECZ, I. & LOBO DE SOUZA, M. 2006. Baculoviruses- re-emerging biopesticides. *Biotechnol Adv,* 24**,** 143-60.

TABASHNIK, B. E., CARRIERE, Y., DENNEHY, T. J., MORIN, S., SISTERSON, M. S., ROUSH, R. T., SHELTON, A. M. & ZHAO, J. Z. 2003. Insect resistance to transgenic *Bt* crops: lessons from the laboratory and field. *J Econ Entomol,* 96**,** 1031-8.

TABASHNIK, B. E., SISTERSON, M. S., ELLSWORTH, P. C., DENNEHY, T. J., ANTILLA, L., LIESNER, L., WHITLOW, M., STATEN, R. T., FABRICK, J. A., UNNITHAN, G. C., YELICH, A. J., ELLERS-KIRK, C., HARPOLD, V. S., LI, X. & CARRIERE, Y. 2010. Suppressing

resistance to *Bt* cotton with sterile insect releases. *Nat Biotechnol,* 28**,** 1304-7.

TABASHNIK, B. E., VAN RENSBURG, J. B. & CARRIERE, Y. 2009. Field-evolved insect resistance to *Bt* crops: definition, theory, and data. *J Econ Entomol,* 102**,** 2011-25.

TALEKAR, N. S. & SHELTON, A. M. 1993. Biology, ecology and management of the diamondback moth. *Annu Rev Entomol,* 38**,** 275-301.

TEDFORD, H. W., FLETCHER, J. I. & KING, G. F. 2001. Functional significance of the β hairpin in the insecticidal neurotoxin ω-atracotoxin-Hv1a. *J Biol Chem,* 276**,** 26568-76.

TEDFORD, H. W., GILLES, N., MENEZ, A., DOERING, C. J., ZAMPONI, G. W. & KING, G. F. 2004a. Scanning mutagenesis of ω-atracotoxin-Hv1a reveals a spatially restricted epitope that confers selective activity against insect calcium channels. *J Biol Chem,* 279**,** 44133-40.

TEDFORD, H. W., SOLLOD, B. L., MAGGIO, F. & KING, G. F. 2004b. Australian funnel-web spiders: master insecticide chemists. *Toxicon,* 43**,** 601-18.

THOMAS, A. 2001. Spider boom puzzles experts. Available: http://www.abc.net.au/science/news/stories/s249734.htm [Accessed 7th March 2008].

TILMAN, D., CASSMAN, K. G., MATSON, P. A., NAYLOR, R. & POLASKY, S. 2002. Agricultural sustainability and intensive production practices. *Nature,* 418**,** 671-7.

TOENNIESSEN, G. H., O'TOOLE, J. C. & DEVRIES, J. 2003. Advances in plant biotechnology and its adoption in developing countries. *Curr Opin Plant Biol,* 6**,** 191-8.

TOMALSKI, M. D. & MILLER, L. K. 1991. Insect paralysis by baculovirus-mediated expression of a mite neurotoxin gene. *Nature,* 352**,** 82-5.

UCHIDA, K., SAITO, K., KITAJIMA, T. & KAMIKAWA, Y. 2000. Effects of Ba^{2+} on SK&F 96365-sensitive sustained contraction of rat pulmonary artery. *J Pharm Pharmacol,* 52**,** 1513-8.

UEBERHEIDE, B. M., FENYO, D., ALEWOOD, P. F. & CHAIT, B. T. 2009. Rapid sensitive analysis of cysteine rich peptide venom components. *Proc Natl Acad Sci U S A,* 106**,** 6910-5.

UN 2009. World Population Prospects: The 2008 revision, Highlights. Working Paper No ESA/P/WP.210. United Nations, Department of Economic and Social Affairs Population Division.

UNDERHILL, D. 1987. Unwelcome stranger. In: Sutherland S.K. (Ed) Australia's Dangerous Creatures. *Readers Digest.*

USEPA. 2011. *What are biopesticides?* [Online]. United States Environmental http://www.epa.gov/opp00001/biopesticides/whatarebiopesticides.htm [Accessed 3 July 2011].

VAN BEEK, N. A. M. & HUGHES, P. R. 1998. The response time of insect larvae infected with recombinant baculoviruses. *J Invertebr Pathol,* 72**,** 338-47.

VASSILEVSKI, A. A., KOZLOV, S. A. & GRISHIN, E. V. 2009. Molecular diversity of spider venom. *Biochemistry (Mosc),* 74**,** 1505-34.

VEDANARAYANAN, V., SOREY, W. H. & SUBRAMONY, S. H. 2004. Tick paralysis. *Semin Neurol,* 24**,** 181-4.

VERNICK, K. D. & WATERS, A. P. 2004. Genomics and malaria control. *N Engl J Med,* 351**,** 1901-4.

VETTER, I., DAVIS, J. L., RASH, L. D., ANANGI, R., MOBLI, M., ALEWOOD, P. F., LEWIS, R. J. & KING, G. F. 2011. Venomics: a new paradigm for natural products-based drug discovery. *Amino Acids,* 40**,** 15-28.

VETTER, R. S. & ISBISTER, G. K. 2008. Medical aspects of spider bites. *Annu Rev Entomol,* 53**,** 409-29.

WAITE, J. H. & TANZER, M. L. 1981. Polyphenolic substance of *Mytilus edulis*: novel adhesive containing L-dopa and hydroxyproline. *Science,* 212**,** 1038-40.

WANG, X., SMITH, R., FLETCHER, J. I., WILSON, H., WOOD, C. J., HOWDEN, M. E. & KING, G. F. 1999. Structure-function studies of ω-atracotoxin, a potent antagonist of insect voltage-gated calcium channels. *Eur J Biochem,* 264**,** 488-94.

WARE, G. W. & WHITACRE, D. M. 2004. *The Pesticide Book,* Willoughby, MeisterPro Information Resources.

WHALON, M. E., MOTA-SANCHEZ, D. & HOLLINGWORTH, R. M. 2008. *Global pesticide resistance in arthropods,* Wallingford, CABI.

WHEELER, W. B. 2002. Role of research and regulation in 50 years of pest management in agriculture. Prepared for the 50th anniversary of the Journal of Agricultural and Food Chemistry. *J Agric Food Chem,* 50**,** 4151-5.

WHETSTONE, P. A. & HAMMOCK, B. D. 2007. Delivery methods for peptide and protein toxins in insect control. *Toxicon,* 49**,** 576-96.

WHITE, J. 2010. Venomous animals: clinical toxinology. *EXS,* 100**,** 233-91.

WHITE, J., CARDOSO, J. L. & HUI, W. F. 1995. Clinical toxicology of spider bites. *In:* MEIER, J. & WHITE, J. (eds.) *Handbook of Clinical Toxicology of Animal Venoms and Poisons.* Boca Raton: CRC Press.

WHO 1992. Vector resistance to insecticides. 15th report of the WHO Expert Committee on Vector Biology and Control. *World Health Org. Tech. Rep. Ser.,* 818**,** 1-62.

WHO 2007. International Travel and Health. Geneva: World Health Organisation.

WICHER, D. & PENZLIN, H. 1997. Ca^{2+} currents in central insect neurons: electrophysiological and pharmacological properties. *J Neurophysiol,* 77**,** 186-99.

WICHER, D., WALTHER, C. & PENZLIN, H. 1994. Neurohormone D induces ionic current changes in cockroach central neurones. *J Comp Physiol A,* 174**,** 507-15.

WICHER, D., WALTHER, C. & WICHER, C. 2001. Non-synaptic ion channels in insects-basic properties of currents and their modulation in neurons and skeletal muscles. *Prog Neurobiol,* 64**,** 431-525.

WILSON, D. & ALEWOOD, P. F. 2004. Australian funnel-web spider venom analysed with on-line RP-HPLC techniques. *In:* AGUILAR, M. (ed.) *HPLC of peptides and proteins: meethods and protocols.* New Jersey: Humana Press.

WITTMANN, E. J. & BAYLIS, M. 2000. Climate change: effects on culicoides-transmitted viruses and implications for the UK. *Vet J,* 160**,** 107-17.

WOOD, D. L., MILJENOVIC, T., CAI, S., RAVEN, R. J., KAAS, Q., ESCOUBAS, P., HERZIG, V., WILSON, D. & KING, G. F. 2009. ArachnoServer: a database of protein toxins from spiders. *BMC Genomics,* 10**,** 375.

WOOD, H. A. & GRANADOS, R. R. 1991. Genetically engineered baculoviruses as agents for pest control. *Annu Rev Microbiol,* 45**,** 69-87.

WU, C. F., SUZUKI, N. & POO, M. M. 1983. Dissociated neurons from normal and mutant *Drosophila* larval central nervous system in cell culture. *J Neurosci,* 3**,** 1888-99.

WU, C. H., HSIEH, M. J., HUANG, J. H. & LUO, S. F. 1996. Identification of low molecular weight allergens of American cockroach and production of monoclonal antibodies. *Ann Allergy Asthma Immunol,* 76**,** 195-203.

YUDELMAN, M., RATTA, A., NYGAARD, D. F., INTERNATIONAL FOOD POLICY RESEARCH INSTITUTE. & INTERNATIONAL DEVELOPMENT RESEARCH CENTRE (CANADA) 1998. *Pest management and food production : looking to the future,* Washington, D.C., U.S.A., International Food Policy Research Institute.

ZAIM, M. & GUILLET, P. 2002. Alternative insecticides: an urgent need. *Trends Parasitol,* 18**,** 161-3.

ZILBERMAN, D., SCHMITZ, A., CASTERLINE, G., LICHTENBERG, E. & SIEBERT, J. B. 1991. The economics of pesticide use and regulation. *Science,* 253**,** 518-22.

ZLOTKIN, E. 1991. Venom neurotoxins - models for insecticides. *Phytoparasitica,* 19**,** 177-182.

ZLOTKIN, E., FISHMAN, Y. & ELAZAR, M. 2000. AaIT: from neurotoxin to insecticide. *Biochimie,* 82, 869-81.